General Disclaimer

One or more of the Following Statements may affect this Document

- This document has been reproduced from the best copy furnished by the organizational source. It is being released in the interest of making available as much information as possible.

- This document may contain data, which exceeds the sheet parameters. It was furnished in this condition by the organizational source and is the best copy available.

- This document may contain tone-on-tone or color graphs, charts and/or pictures, which have been reproduced in black and white.

- This document is paginated as submitted by the original source.

- Portions of this document are not fully legible due to the historical nature of some of the material. However, it is the best reproduction available from the original submission.

Produced by the NASA Center for Aerospace Information (CASI)

07

"Made available under NASA sponsorship
in the interest of early and wide dissemination of Earth Resources Survey
Program information and without liability
for any use made thereof."

SR-0577

E76-10424
CR-148300

MONITORING THE GROWTH OR DECLINE OF VEGETATION ON MINE DUMPS

RECEIVED BY
NASA STI FACILITY
DATE: 2/30/76
DCAF NO. 01/2830
PROCESSED BY
☒ NASA STI FACILITY
☐ ESA-SDS ☐ AIAA

B.P. GILBERTSON

SPECTRAL AFRICA (PTY) LIMITED
P.O. BOX 2
RANDFONTEIN Tvl.
Republic of South Africa

(E76-10424) MONITORING THE GROWTH OR DECLINE OF VEGETATION ON MINE DUMPS Final Report, Jun. 1972 - Dec. 1975 (Spectral Africa (Pty) Ltd., Randfontein) 144 p HC $6.00 CSCL 08F G3/43

N76-28601

Unclas
00424

DECEMBER, 1975.

TYPE III REPORT - FINAL

Original photography may be purchased from:
EROS Data Center
10th and Dakota Avenue
Sioux Falls, SD 57198

ORIGINAL CONTAINS
COLOR ILLUSTRATIONS

COUNCIL FOR SCIENTIFIC AND INDUSTRIAL RESEARCH
P.O. BOX 395
PRETORIA Tvl.
Republic of South Africa.

1577A

RECEIVED
JUN 30 1976
SIS/902.6

1. SR No. 0577	2. Type of Report TYPE III - FINAL	3. Recipient's Catalog No.
4. Title MONITORING THE GROWTH OR DECLINE OF VEGETATION ON MINE DUMPS		5. Report Date DECEMBER, 1975 6. Period Covered JUNE, 1972 TO DECEMBER, 1975
7. Principal Investigator B.P. GILBERTSON		8. No. of Pages
9. Name and Address of Principal Investigator's Organization SPECTRAL AFRICA (PTY) LIMITED P.O. BOX 2 RANDFONTEIN. Transvaal Republic of South Africa.		10. Principal Investig.Rept.No. 74/1 11. GSFC Technical Monitor MR. GEORGE ENSOR
12. Sponsoring Agency Name and Address COUNCIL FOR SCIENTIFIC AND INDUSTRIAL RESEARCH P.O. BOX 395 PRETORIA. Transvaal Republic of South Africa.		13. Key Words (Selected by Principal Investigator) REFLECTANCE MINE DUMPS COMPUTERISED INTERPRETATION MULTISPECTRAL PATTERN RECOGNITION

14. Supplementary Notes

The Principal Investigator is indebted to his co-investigators, and especially to Mr. T.G. Longshaw, for support throughout the project period. He is also indebted to Mr. D.T. Williamson and Mr. T. Williams who contributed significantly to the project, although not formally involved as co-investigators.

15. Abstract

It has been established that particular mine dumps can be detected and identified on ERTS-1 imagery, and that patterns of vegetative growth on the dumps can be recognized from a simple visual analysis of photographic images. Because vegetation tends to occur in patches on many mine dumps, it is unsatisfactory to classify complete dumps into categories of percentage vegetative cover. A more desirable approach is to classify the patches of vegetation themselves. The coarse resolution of conventional densitometers restrict the accuracy of this procedure, and consequently a direct analysis of ERTS CCT's is preferred.

The application of multispectral pattern recognition techniques to the CCT data showed that well vegetated areas could be distinguished from unvegetated areas with high accuracy. However, the classification accuracy was much lower where the CCT resolution element was larger than the dimensions of "target uniformity" i.e. for areas that are partially vegetated. Further study is required when repetitive and seasonal coverage in CCT form becomes available.

TABLE OF CONTENTS

NO.	DESCRIPTION	PAGE
1	INTRODUCTION	1
2	BACKGROUND TO THE PROJECT	2
3	OBJECTIVES OF THE PROJECT	6
4	GROUND TRUTH DATA GATHERED BY PROJECT TEAM	8
5	DATA RECEIVED FROM NASA	9
6	TECHNIQUES FOR ANALYSIS	12
7	ANALYSIS AND RESULTS	13
8	CONCLUSIONS	32
9	REFERENCES	33
	APPENDIX 'A'	34
	APPENDIX 'B'	35
	APPENDIX 'C'	36
	APPENDIX 'D'	37
	APPENDIX 'E'	38
	APPENDIX 'F'	39
	APPENDIX 'G'	40
	APPENDIX 'H'	41

1. INTRODUCTION

This report has been prepared in accordance with section 2, phase 3, paragraph (e) of the "Provisions for Participation in the NASA Earth Resources Technology Satellite - A (ERTS-1) Project". As such it is the Type III Final Report, and documents the history, findings and techniques of the research project carried out as ERTS-1 investigation bearing MMC number SR-0577 and GSFC user ID F0023.

This project was concerned with evaluating the utility of ERTS-1 data in monitoring the growth and decline of vegetation on mine dumps in the Republic of South Africa.

In addition to this research, scientists working with the Principal and co-investigators evaluated the utility of ERTS imagery in a number of other fields of application. This work resulted in seven papers that were read at the second and third ERTS investigator meetings. Abstracts of these papers appear in Appendix A. Furthermore, a separate report on the geological applications of the ERTS images was prepared and a reproduction of the resulting publication appears in Appendix B.

This report describes only the analysis of the mine dump imagery in terms of project SR-0577. Chapter 2 describes the background to the project, and chapter 3 defines the specific objectives. Chapters 4 and 5 describe respectively the ground truth gathered by the project team in the course of the investigation, and the ERTS-1 data provided by NASA. Chapter 6 outlines the techniques used for analysis, while chapter 7 presents the analysis itself, and the results obtained. Chapter 8 summarises the main conclusions.

2. BACKGROUND TO THE PROJECT

2.1 The Extent of Mining Activities in South Africa

Mining has been the germinal industry in the growth of South Africa's economy. It has expanded phenomenally since the discovery of diamonds near Kimberley in the 1860's, and is today carried out on a large scale in different parts of the country.

South Africa's major mining area, the Witwatersrand, is the largest and richest mining region in the world. The 40 mines along the 300 km perimeter of the Witwatersrand basin mill about 250 000 tons of rock ore per day. These operations generate huge quantities of waste material, as almost all of this milled tonnage must be disposed of as tailings. Disposal is by means of slimes dams which presently cover an area of 150 km^2 and provide for the disposal of 3×10^9 tons of slimes.

This large scale disposal of industrial waste has to be effected in a relatively densely populated region that is served and drained by only one large river, the Vaal. The inevitable environmental hazards of the operation are thus aggravated by proximity to large population centres and vital water resources.

2.2 The Environmental Effect of Slimes Disposal

The environmental effects of slimes disposal can conveniently be classified as primary and secondary.

The primary effect is simply the obliteration of whatever natural community exists on the site of the disposal dump. There is

nothing that can be done to directly alter this effect, although its impact can be reduced by judicious siting of new dumps.

Secondary effects result from structural or surface instability of completed disposal dumps. The most serious of these are structural failure resulting in collapse or subsidence, water erosion which pollutes the water shed and spreads waste materials, and wind erosion which cause air pollution and the spread of fine materials.

Structural stability depends, in the first instance, on engineering design to adequate factors of safety. In practice structural failure is a minor problem, with slow spreading of the basal perimeter the only cause for concern.

The extent and seriousness of water erosion is seldom realised. It has been estimated that an average rate of rainwater erosion of completed slimes dam walls is 0,1m per annum. In the case of a typical unprotected dam with an area of 50 ha and a mean height of 20m, this results in an annual loss of some 30 000 tons of wall material. Having regard to the fact that there are some 300 slimes dams in the Witwatersrand basin, it can be appreciated that the loss of waste material from erosion is potentially very great. The di placement of waste material is in itself a nuisance and its pollution of the important Vaal river catchment area is a serious problem.

A further loss of material from slimes dams is caused by the action of wind on dry surfaces. No reliable data are available

on the rate of wind erosion of slimes dam tops but it may apparently be of the order of tens of millimeters. This amounts to hundreds of tons per hectare per annum, and gives rise to dust pollution in the vicinity of the dumps and for considerable distances down wind.

2.3 Controlling the Environmental Effects of Slimes Disposal

Control of the environmental hazards of slimes disposal is not only desirable but also a legal obligation in terms of a number of statutory enactments. To avoid the problems of slope instability and stream pollution created by slimes dam erosion it is necessary to reduce considerably the velocity of rain water run-off from the walls. This is achieved by reducing slope angles, by finishing slopes to a smooth instead of a stepped surface and by planting vegetation. Vegetation is also established on the tops of dams to control wind erosion and consequent air pollution by dust.

In practice, planting vegetation is the primary means of promoting the structural and surface stability of slimes dams. Vegetation is also used to stabilise the sand dumps which are by-products of older methods of ore treatment.

2.4 Management of Vegetation on Slimes Dams and Sand Dumps

Slime residues consist of very finely ground silicious rock. From a botanical point of view these slimes, which are cyanided during treatment processes, are initially noxious but with weathering the noxious properties disappear. However, the ores from which the slimes are derived contain pyrite which, with weathering, tends to produce acid conditions on the dump.

Establishment of vegetation on these dams requires the removal of acidity produced by pyrite oxidation within the first 1 to 2 meters of slimes surface to which air has access. It has been found that the most effective means of removing this acidity is to leach the acid into the alkaline material within the dams. To avoid evaporative conditions during which acidity rises to the surface, leaching conditions must be maintained as continuously as possible. Permeability of the slimes is low (20 - 40 mm per day), and continuous leaching must be maintained for periods of 6 weeks or more. This is best achieved by low rates of water application with fine sprays. Leached conditions are subsequently maintained by mulching and by the construction of reed barriers which prevent exposure of unoxidised slimes by water and wind erosion.

Vegetation is established by seeding, fertilization and irrigation of the prepared slimes surfaces. Thereafter vegetation is fertilized and irrigated as required.

The sand dumps from older methods of ore treatment are more easily vegetated than slimes dams. They are composed of finely crushed rock material from which the minerals in time leach out leaving no binding properties. The resulting material becomes similar to river sand and with no nutrient value is an inert and inhospitable medium for plant growth. Its deficiencies are, however, fairly readily overcome by fertilization and irrigation and the provision of protective reed barriers against water and wind erosion.

ORIGINAL PAGE IS
OF POOR QUALITY

A large scale mine dam vegetation programme has been implemented by the Vegetation Unit of the Chamber of Mines, and independent mines have adopted similar programs.

2.5 Monitoring Condition of Mine Dump Vegetation

The growth or decline of vegetative cover on mine dumps has been monitored by both aerial photography and site visits. Site visits are normally preferred because they are more accurate and less expensive than aerial photography. However, because of the geographic separation of mine dumps (see fig. 5.1) site visits can be laborious and difficult to co-ordinate. This project was designed to investigate the feasibility of using ERTS-1 data to carry out the monitoring process.

3. OBJECTIVES OF THE PROJECT

ERTS-1 project SR-0577 had the broad objective of evaluating the utility of ERTS-1 data in monitoring the growth or decline of vegetation on mine dumps. Two specific short-term objectives were formulated, viz.

(a) To determine whether ERTS imagery can be used to distinguish mine dumps with vegetative cover from mine dumps without vegetative cover at 3 monthly intervals throughout the year.

(b) To ascertain whether the percentage of mine dump area that is covered by vegetation can be determined at 3 monthly intervals throughout the year.

Two sub-objectives were also formulated in the original proposal, namely

(c) To determine whether the pollution of rivers from mine dumps can be detected.

(d) To provide management data to the mining authorities with respect to the state of vegetative cover of all the mine dumps in the Republic.

However, the revised Data Handling plan recommended discarding these two sub-objectives. It was recommended that (c) be discarded since the ground resolution of the imagery does not allow a study of spatial detail in the typically narrow South African rivers. It was recommended that (d) be discarded due to the time limit placed by NASA on the program. Since ERTS is an experimental satellite, management data could not be provided on a continuing basis. It was therefore proposed that the techniques developed in terms of the main objectives be made available to the mining authorities for use when a space sensing system operating on a continuing basis is available.

4. GROUND TRUTH DATA GATHERED BY PROJECT TEAM

The original proposal and revised data handling plan forsaw the need for ground truth information for the evaluation of the ERTS-1 data. Accordingly two types of ground truth data were collected, namely field reflectance measurements, and aircraft overflight imagery.

4.1 In Situ Spectral Measurements

A spectroradiometric system housed in a mobile laboratory was used to measure the bivariate reflectance properties of natural objects comprising the surface of a number of selected target mine dumps. The system allowed spectral reflectance measurements to be made in the spectral region 400 nm to 1 000 nm, and has been described elsewhere (Longshaw, 1974).

The results of the spectral reflectance measurements carried out on mine dumps, sand and vegetation during the course of this project are discussed and analysed in detail in Appendix C.

4.2 Aircraft Overflight Imagery

Aircraft overflight imagery was gathered during the course of the project using SDC Mk II multispectral camera (four-lens) and a Wild RC-10 camera. Narrow and broad band multispectral imagery as well as conventional colour and false colour imagery were obtained at different scales and seasons. A record of this photography is presented in Appendix D.

5. DATA RECEIVED FROM NASA

Two types of product have been received from NASA, namely 70 mm positive and negative transparencies, and computer compatible tapes (CCT's). The test area for this investigation is shown in figure 5.1.

Figure 5.1.

All imagery received was catalogued and indexed, and figure 5.1 records the photographic products received from NASA for the mine-dump test area. The data of figure 5.1 are tabulated in appendix E.

It has already been explained that the Witwatersrand is South Africa's major mining area. The minedumps along the Witwatersrand have been subjected to the most systematic vegetation program, and extensive ground truth is available. Accordingly the Witwatersrand complex was selected for the most intensive study under this project. Table 5.1 list the photographic images received of this area, while table 5.2 lists the three CCT's received. The CCT of frame 1006-16504 was used to establish the computer programs discussed in appendix G. The other two frames were used for the mine dump analysis described in sub-chapter 7.6.

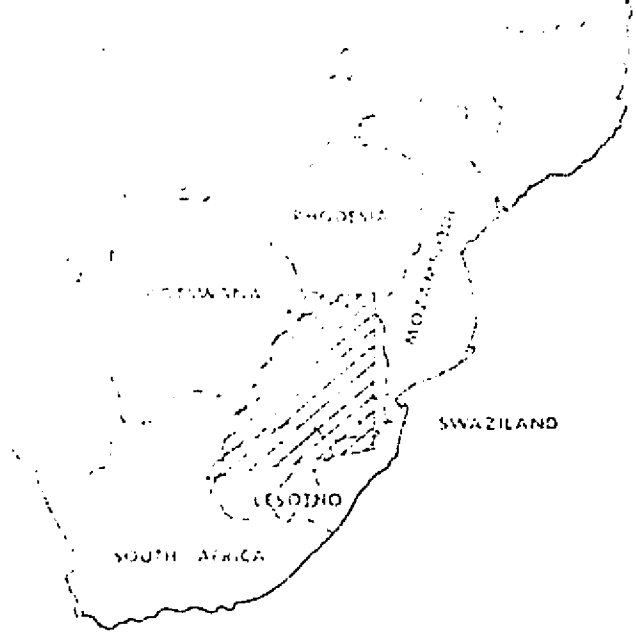

LOCATION MAP

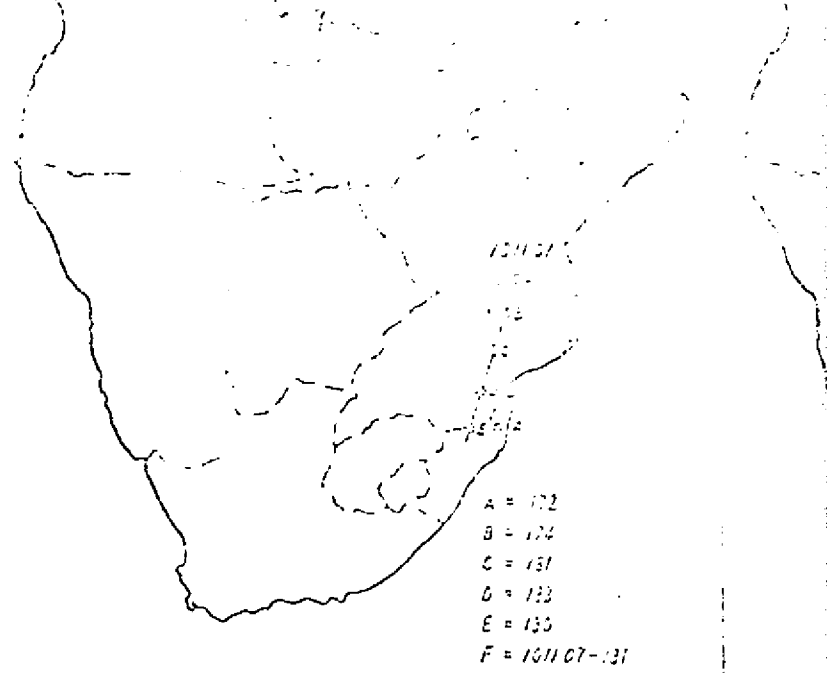

CYCLE № 1

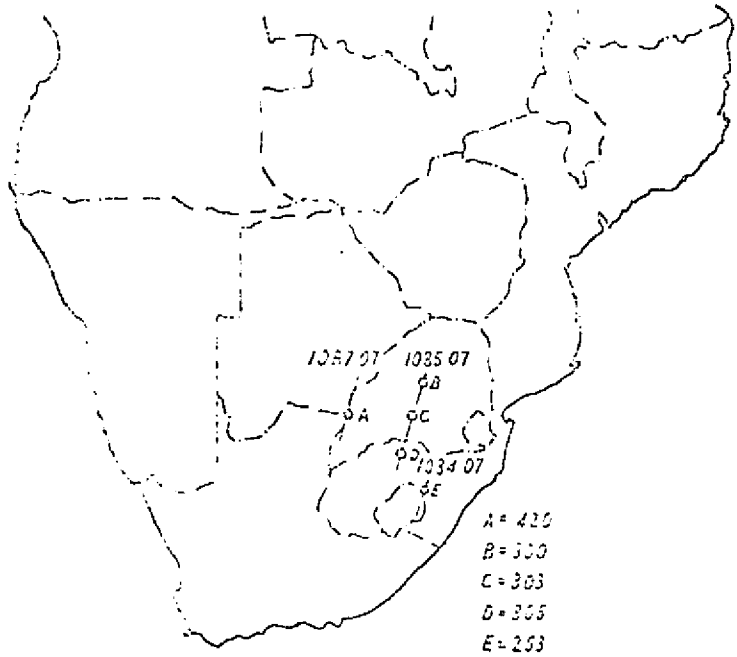

CYCLE № 5

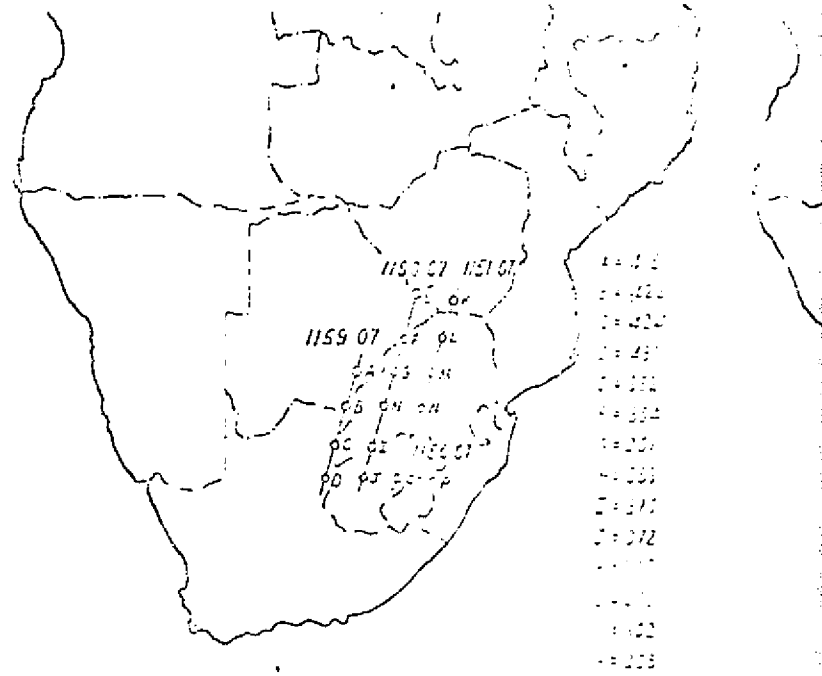

CYCLE № 3

ORIGINAL PAGE IS
OF POOR QUALITY

FOLDOUT FRAME 1

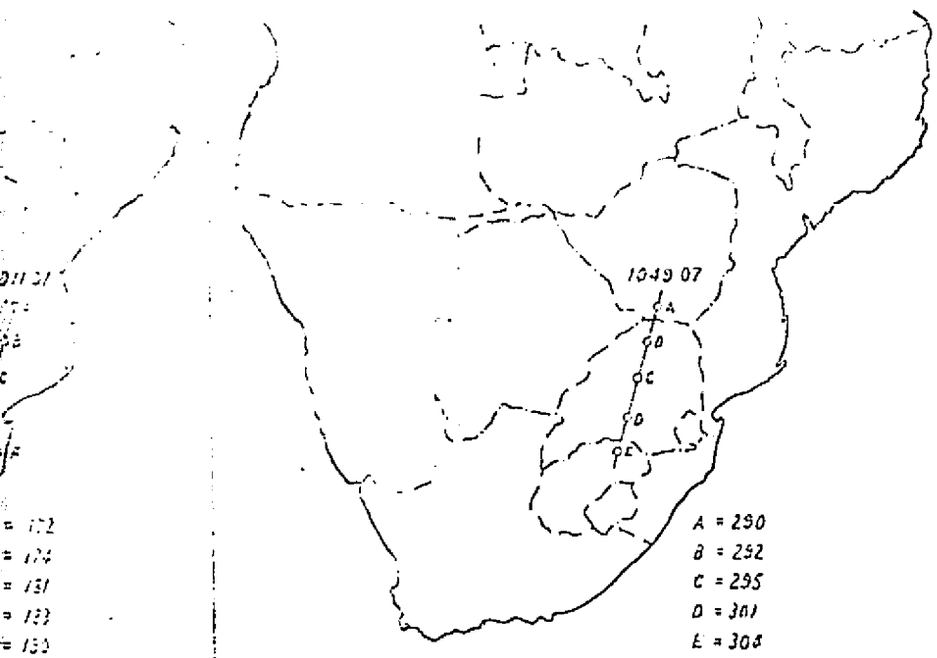

CYCLE Nº2

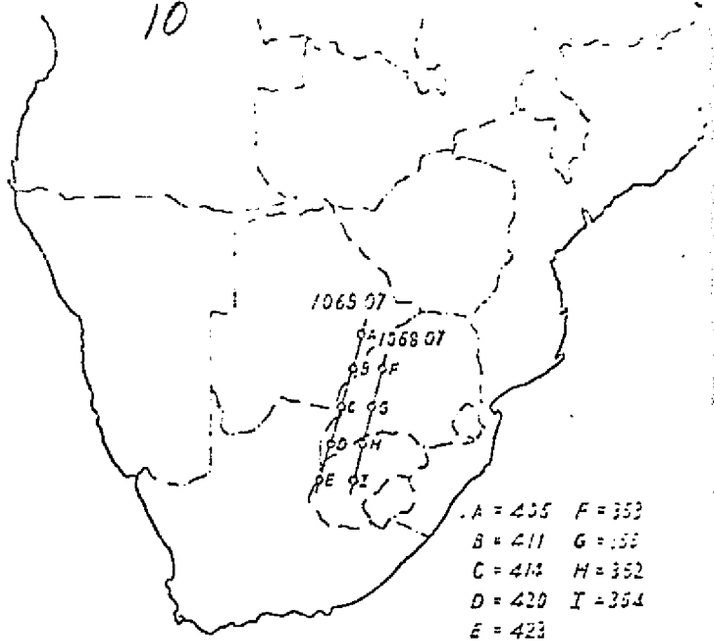

CYCLE Nº 4

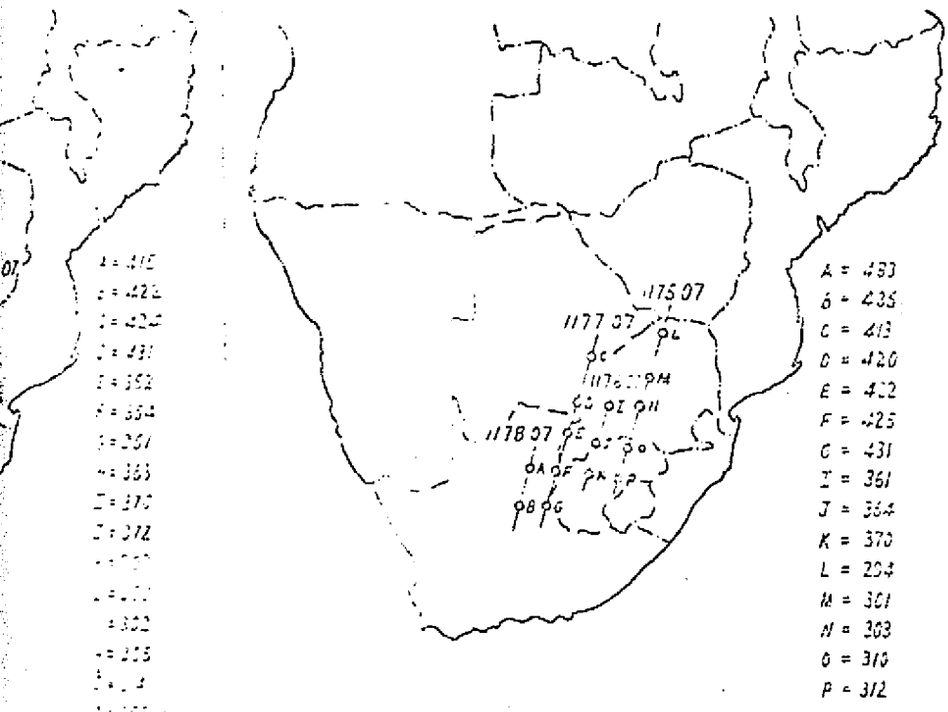

CYCLE Nº 10

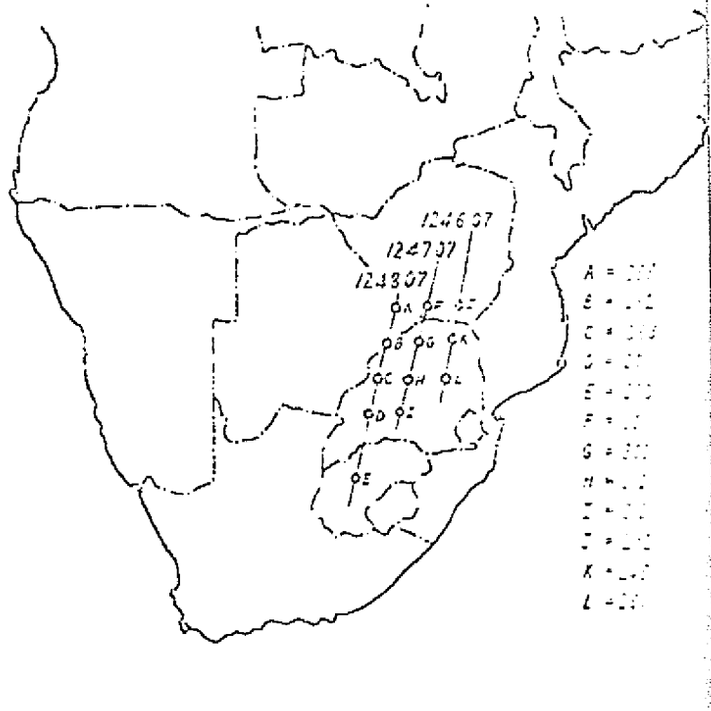

CYCLE Nº 14

FIGURE 5.1

FOLDOUT FRAME 2

TABLE 5.1

ERTS-1 IMAGES OF THE WITWATERSRAND COMPLEX

IMAGE NO.	AREA	DATE	SEASON	CLOUD COVER %	QUAL-ITY	COMMENTS
1049-07301	Entire Witwatersrand	10SEP72	Winter	0	GGGG	Smog obscures many mine dumps. West Witwatersrand clear.
1068-07355	West Witwatersrand	29SEP72	Winter	10	GGGG	Cloud shadow obscures a number of mine dumps.
1085-07303	Entire Witwatersrand	16OCT72	Spring	10	GGGG	Good.
1157-07305	Entire Witwatersrand	27DEC72	Summer	40	GGGG	Clouds cover entire mine dump area.
1158-07363	West Witwatersrand	28DEC72	Summer	0	PPPP	Good.
1175-07303	Entire Witwatersrand	14JAN73	Summer	20	GGGG	Scattered cloud obscures number of mine dumps.
1176-07361	West Witwatersrand	15JAN73	Summer	40	PPPP	Cloud obscures number of mine dumps.
1247-07312	Entire Witwatersrand	27MAR73	Summer	20	GGGG	Cloud obscures most mine dumps.
1248-07371	West Witwatersrand	28MAR73	Summer	10	GGGG	Cloud obscures number of mine dumps.

TABLE 5.2

IMAGE NO.	SENSOR	AREA	CLOUD COVERAGE
1006-16504	RBV	Kansas Area	10%
1049-07301	MSS	Entire Witwatersrand	20% Haze
1175-07303	MSS	Entire Witwatersrand	20% Cloud

6. TECHNIQUES FOR ANALYSIS

Two techniques were established for the analysis of the ERTS-data, namely photographic and automatic. These are discussed below.

6.1 Photographic

The analysis of photographic products required in the first place the preparation of later generation imagery from the 70 mm transparencies received from NASA. A well-equipped photographic laboratory was available for this purpose. Black and white imagery was prepared using conventional photolaboratory techniques; colour composite imagery by following the procedures outlined in Appendix F. These were interpreted mainly by using conventional photointerpretation techniques.

6.2 Automatic

In order to provide an automatic interpretative capability a set of computer programs were established to allow the reading and manipulation of ERTS-1 CCT-data. These programs are described in Appendix G, and in sub-chapters 7.7 and 7.8.

7. ANALYSIS AND RESULTS

7.1 Recognition of mine dumps

A mosaic of the Witwatersrand Mine Dump Complex was prepared from black and white prints of colour photography obtained during the ground truth missions (see sub-chapter 4.2). This mosaic was rephotographed at a scale of 1:250 000, and is shown in figure 7.1.

Figure 7.1

Colour composites prepared from ERTS images 1049-07301 and 1175-07303 are shown in figure 7.2 and 7.3 respectively. These colour composites were prepared by printing MSS band 4, 5 and 7 in blue, green and red respectively. Essentially all of the mine dumps present in the aerial photography mosaic can be detected and identified on these ERTS-1 images.

Figures 7.2 and 7.3

7.2 Location of the Mine Dumps

Although the greatest concentration of mine dumps occur along the Witwatersrand basin, others are widely dispersed throughout

ORIGINAL PAGE IS
OF POOR QUALITY

Figure 7.1 : Reduction to 1:250 000 of aerial photography mosaic

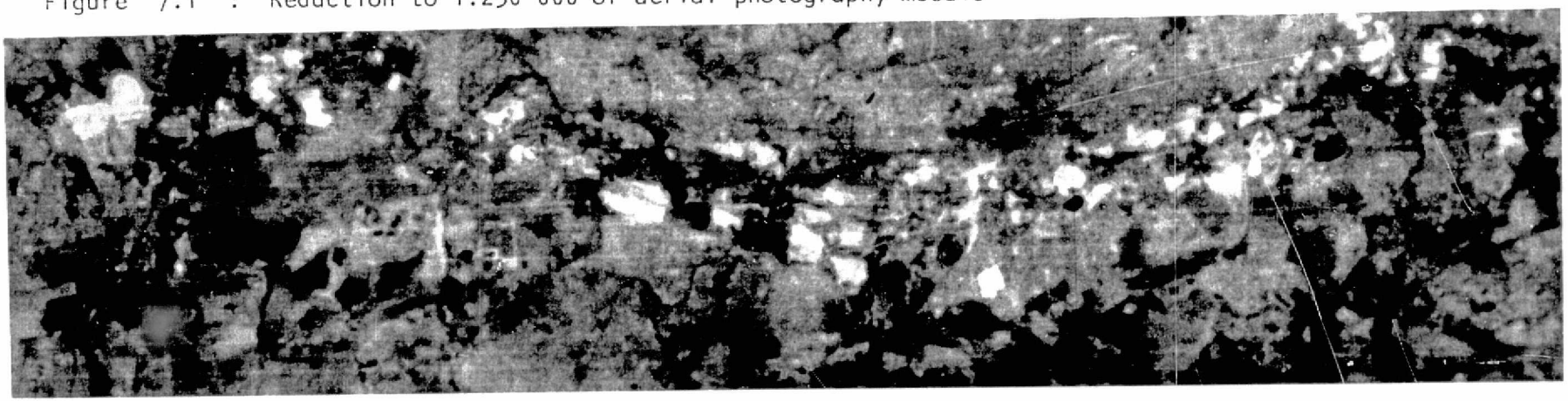

Figure 7.2 : ERTS-1 image 1049-07301 at scale of 1:250 000

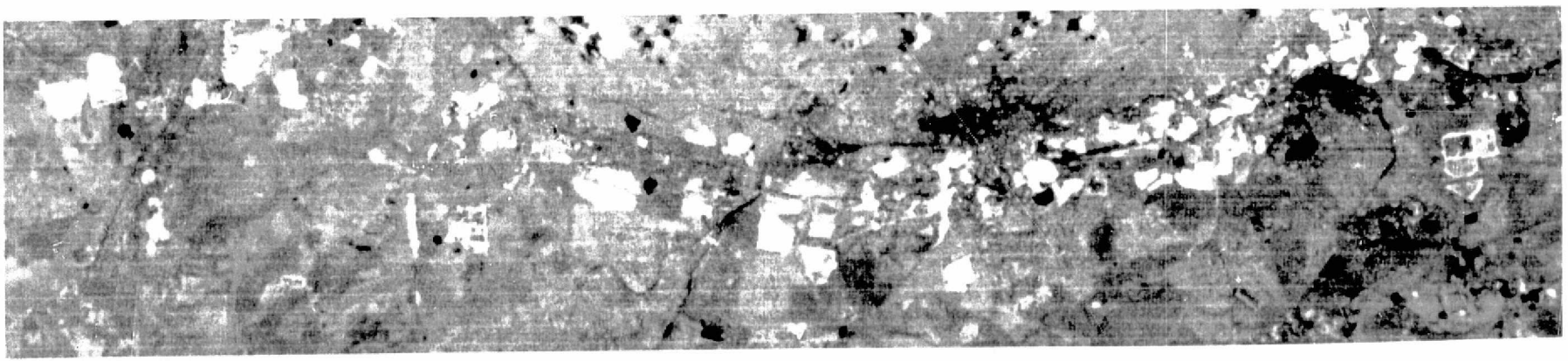

Figure 7.3 : ERTS-1 image 1175-07303 at scale of 1:250 000

the Republic. Most are contained in the test area shown in figure 5.1. All of the major mine dumps in this area, and even some of the minor ones, can be detected and identified on ERTS-1 imagery. This is shown in table 7.1.

TABLE 7.1

RECOGNITION OF MINE DUMPS IN TEST AREA, EXCLUDING WITWATERSRAND COMPLEX

MINE DUMP OF:	VISIBLE ON IMAGE NUMBER
Messina copper mines	1049-07290
Consolidated Murchison at Grootvlei	1138-07243
Phalaborwa	1138-07243
New Consort and other Barberton mines	1047-07184
Swaziland Iron ore mines	1047-07184
Premier Diamond Mine	1049-07301
Rustenburg Platinum mines	1050-07355
Impala Platinum mines	1050-07355
Kimberley Diamond mines	1177-07425

7.3 Recognition of vegetation via qualitative analysis

As part of the ground truth program target mine dumps were selected and classified on the basis of differential vegetative cover. Five categories were established, ranging from bare slime exposure to self-sustaining, 100% vegetative cover. These categories are shown in table 7.2.

TABLE 7.2

CATEGORIES OF MINE DUMP VEGETATION

Vegetation Category	Description of Degree of Vegetative Cover	Example of dump in this Category
0	No vegetation cover	5/L/29 3/L/5 (East side)
1	A very small plant community, usually constantly "farmed" by fertilizing, water spraying and "ploughing".	3/L/5(West side)
2	A poor cover of plants requiring continuous attention. Extensive "soil" exposure.	6/L/20
3	A reasonable cover of vegetation requiring occasional attention and fertilizing with a number of "soil" exposures on small areas of high acidity.	7/L/1
4	A good cover of vegetation, probably self-sustaining, with only a few "soil" exposures on small areas of locally high acidity.	1/L/40 1/L/41
5	A self-sustaining plant and tree community over 100% of the dump surface.	1/A/20

ERTS-1 imagery was then analysed qualitatively in an attempt to establish a relationship between percentage of mine dump covered by vegetation and image density and/or colour.

The qualitative analysis was performed using mainly a colour composite print prepared of image 1049-07301 with MSS bands 4, 5, and 7 shown in

blue, green and red respectively. Similar results can be obtained by using the other non-cloud covered images of table 5.1.

A good qualitative relationship was found to exist between the categories of table 7.2 and the mine dump images in figure 7.2, with the more densely vegetated dumps (i.e. those falling in categories 4 and 5) appearing darker than the unvegetated dumps (those falling in categories 0 and 1). In addition, vegetation patterns are visible on the ERTS-1 imagery which are in good agreement with ground truth, i.e. with patterns observed on aircraft overflight photography. This can be seen by comparing figures 7.4a and 7.4b.

Figures 7.4a and 7.4b.

This qualitative analysis showed that the five vegetative categories could be distinguished within mine dumps appearing on the ERTS imagery, particularly in the dry season. However, discrimination between the different categories may be impeded by artificial irrigation or fertilization which induce vigorous growth and give small plant communities an appearance that is misleading when considered in relation to untended but better established and larger plant communities.

7.4 Identification of Seasonal Trends

Table 5.1 shows that the imagery available for this project has covered 3 seasons, i.e. the end of the dry winter season, the

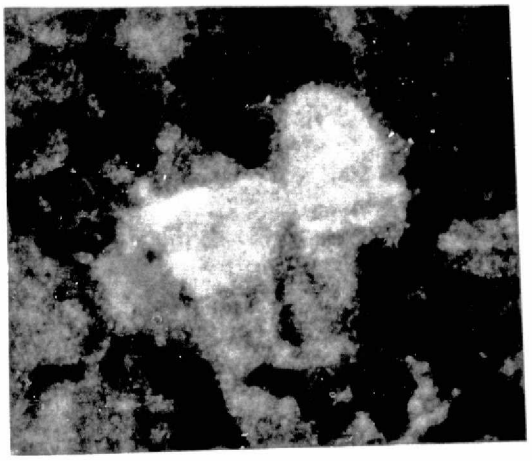

Figure 7.4a : Enlargement from colour composite of ERTS-image 1049-07301

Figure 7.4b : Aircraft overflight imagery using EK 2443

ORIGINAL PAGE IS
OF POOR QUALITY

spring, and the middle of the wet summer season. This seasonal coverage has enabled the detection of a distinct seasonal trend in the vegetative cover of the selected dumps, with an increase in the vigour and density of the vegetative cover apparent on the summer imagery. This can be seen by preparing colour composite of the winter (1049-07301) and summer (1175-07303) imagery, as shown in figures 7.2 and 7.3.

7.5 Quantitative analysis

Quantitative analysis was originally carried out by making densitometric measurements on black and white negatives enlarged to 1:160 000 scale of various mine dumps on the ERTS-1 image. Plots of image density versus wavelength (i.e. ERTS-1 band number) were then prepared for different vegetation categories of table 7.2. These plots showed a good separation between the density readings for vegetation categories 0,1,4 and 5 and consequently it was anticipated that mine dumps falling into these categories would be identifiable. However, a number of anomalies were observed, particularly for the vegetation categories 2 and 3. Some of these anomalies were explained by an investigation into the records for the Chamber of Mines Vegetation Program, which revealed that irrigation had been carried out on some of the dumps prior to the date on which the ERTS-imagery was gathered. The reflectance properties of these dumps were consequently changed quite markedly by the resulting vigorous growth of vegetation. This analysis has been reported (Gilbertson, 1973).

ORIGINAL PAGE IS
OF POOR QUALITY

Subsequent quantitative investigation has shown a major problem to be the non-uniformity of vegetative cover on any given mine dump. It can be clearly seen from figure 7.4 that a mine dump in a given vegetation category can have a high vegetative density in some areas and a low vegetative density in other areas. Accordingly it is inaccurate to classify a whole mine dump in a single vegetative density. Furthermore since the density measurements are made using a 1 mm diameter stop*, the density recorded is invariably an average over a number of localised vegetation categories. Accordingly, the attempt to obtain a quantitative densitometric relationship between mine dumps categorised according to table 6.2 was abandoned. Efforts were subsequently concentrated on direct quantitative analysis from the ERTS CCT's which allowed a much higher resolution than did the 1 mm aperture of the densitometer. This analysis is described in sub-chapter 7.6 below.

7.6 Initial Computer Analysis

Subsequent to the realisation that the vegetation categories of table 7.2 were applicable to localised areas on mine dumps, rather than to mine dumps as a whole (see sub-chapter 7.5) it became apparent that the 1 mm resolution of the densitometer aperture was inadequate. The best resolution obtainable existed on the CCT's. However, the original statement to NASA of the data requirements for this project made no mention of the need for CCT's, and accordingly delays occurred while a request for

---

* Macbeth Quantalog Densitometer with 1 mm aperture.

the new data format was authorised. The first ERTS-1 CCT's of the test area were received in the latter half of November, 1973. A set of computer programs to perform the data reading and manipulating functions required for basic CCT analysis were established, and are discussed in Appendix F. All subsequent quantitative analysis was carried out on the digital data.

Preliminary work investigated the resolution of the CCT's. The area of the Witwatersrand mine dump complex was stripped from the two CCT's of ERTS frames 1049-07301 and 1175-07303, and dumped onto a line printer. The format was convenient in that 64 characters were available on the printer to represent each of the 64 MSS levels. A matrix of characters was thus produced from a mosaic of the line printer pages. Sections of this mosaic were then decoded from the character printout onto a grid of interval 5,9 mm horizontally and 7,9 mm vertically. This gave a 1:10 000 scale pixel grid. The corresponding multispectral band from the aircraft underflight was superimposed on this grid. The photographic overlay was then adjusted to give a "best fit" of pixel radiance levels and film density. The CCT pixel grid was thus accorded a geographic reference grid so that any point on the ground could be spatially located in the CCT matrix. The grid and overlay image are shown in figure 7.5.

It can be seen that the ERTS resolution elements are smaller than the large continuous patches of vegetation, and accordingly it should be possible to monitor such patches. However, in areas where the vegetation is less well established, the size of the

resolution elements is of the same order or larger than that of the target dimensions, and accordingly recognition difficulties could be anticipated.

The ensuing work was aimed at applying multispectral pattern recognition techniques to the CCT data, and is detailed in sub-chapters 7.7 and 7.8 below.

7.7 Improving CCT Locational Accuracy

The majority of South African mine dumps, and certainly all of the major dumps in the Witwatersrand area, are identified on maps issued by the Surveyor-General. Therefore, no difficulty exists in locating these dumps, nor in defining their boundaries using the South African National Co-ordinate System. However, in order to study the spectral features of the dumps from the CCT's, it is important that the CCT digital picture element (pixel) corresponding to given point on the ground be accurately located in the South African National Co-ordinate System, and vice versa. This locational accuracy is dependent on the degree to which sensor attitude and positional errors are corrected within the NDPF Processing Subsystems. For Bulk data, these errors are only partially corrected and the root mean square average deviation of a point on the ground from the calculated projected location of its imaged pixel is of the order of 700 meters.

Location accuracy can be improved by relating tonal features within CCT image to corresponding ground features. These common features can be used as control points to set up transformation equations whereby pixels corresponding to specific ground points can be located within the CCT matrix. This mathematical correspondence is

readily stablished via an Affine Transformation that takes the form of two polynomial equations of the same order, and that relates coordinates in the skew pseudo-perspective of the CCT data to coordinates in the conformal projection of the base maps.

Two computer sub-routines were established to apply this transformation. The one, suitable for use over relatively small geographical areas such as the Witwatersrand mine dump region, utilized a linear transformation. The other, intended for use over the full CCT frame, was based on a second order transformation. The functioning and evaluation of these sub-routines are detailed in Appendix H. It will be seen that these programs improved image location accuracy to the order of 40 meters rms for small areas (500 Km^2) and 120 meters rms over the full frame (area > 25 000 Km^2).

The use of these subroutines allowed particular CCT pixels to be accessed and utilised in the multispectral pattern recognition program described in sub-chapter 7.8 below.

7.8 Multispectral Pattern Recognition

A special purpose computer program was written to classify pixels into ground object categories on the basis of the spectral radiance information contained in the CCT data. This program performed a maximum likelihood decision, given the assumption that the probability densities of the various object classes could be approximated by multivariate Gaussian distributions. This program is executed on a Data General Nova Eclipse, and is of general application in a wide variety of multispectral pattern recognition problems.

Its application to the identification of mine dump vegetation categories proceeded as follows.

Four mine dump vegetation classes were established as set out in table 7.3.

TABLE 7.3. : MINE DUMP VEGETATION CLASSES

CLASS NUMBER	PERCENTAGE OF PIXEL AREA COVERED BY VEGETATION
1	Less than 25%
2	Between 25% and 50%
3	Between 50% and 75%
4	Greater than 75%

Detailed ground truth information as per table 7.3. was tabulated for a total of 619 pixels corresponding to the mine dumps 1/L/40, 1/L/41, 3/L/4, 3/L/5 and 3/L/6. Approximately one third of these "classified" pixels (427 in all), selected so as to be representative of all 5 dumps, were used as training sample to estimate the mean vectors and variance- covariance matices for each of the 4 classes. Table 7.4 shows these results for classes 1 and 4, and will be seen to confirm in a general manner the results of the in situ spectral reflectance measurements. Thus the mean radiance of the slimes (class 1) is higher in all bands than that of the vegetation (class 4). Furthermore, the variation in the slime radiance is greater than that in the vegetation radiance. This is a consequence of the non-uniformity of the slimes, due to contamination, varying composition, water pools etc. The vegetation of class 4 on the other hand, is generally of a uniform appearance.

TABLE 7.4 : ESTIMATED PARAMETERS FOR 2 CLASSES

	CLASS 1				CLASS 4			
Mean Vector	79,50	92,72	89,66	38,16	55,21	61,15	63,58	28,48
Covariance Matrix	428,5				130,7			
	508,1	613,6			163,8	214,8		
	385,2	461,1	353,3		120,2	160,7	129,2	
	135,1	162,2	123,6	44,7	34,6	49,4	42,4	16,1

Generally speaking, it may be concluded from table 7.4 that there is a reasonable separation between the estimated parameters of classes 1 and 4. However, a similar comparison with the estimated parameters of classes 2 and 3 (not tabulated here) shows a much greater overlap, as may be expected.

The estimated population parameters for each of the 4 classes, were then used in the maximum likelihood classifier to assign each of the remaining ground truth coded pixels to one of the 4 ground truth categories. A quantitative comparison was made between this classification and the ground truth data. The results are summarised in table 7.5.

TABLE 7.5 : COMPARISON OF CLASSIFICATION RESULTS AND GROUND TRUTH

MAXIMUM LIKELIHOOD CLASSIFICATION	GROUND TRUTH CLASSIFICATION			
	CLASS 1	CLASS 2	CLASS 3	CLASS 4
Class 1	72	10	15	6
Class 2	15	31	47	8
Class 3	5	27	84	18
Class 4	2	16	43	28
Total Number of Pixels	72	84	189	60
% Correctly Classified	76%	37%	44%	47%
% Correctly Classified to within 1 class	93%	81%	92%	90%

The main points to be noted in table 7.5 are as follows:

(a) The highest recognition accuracy was achieved for class 1, where more than 75% of the pixels were correctly classified.

(b) Less than 50% of the pixels in the remaining 3 classes were correctly classified. However, the classifications were generally in error by only one class, so that less than 10% of the pixels classified as belonging to class 1, 3 and 4 deviated from their ground truth classification by more than 1 class. The corresponding percentage for class 2 is 20%.

(c) A consequence of (b) above is that pixels from ground truth classes 1 and 4 were rarely confused. This confirms the anticipations of section 7.6 above and is in agreement with the estimated population parameters of table 7.4.

A number of further studies were carried out to investigate the sensitivity of the classification accuracies to different methods of selecting the training sample. It was found that the classification accuracy decreased sharply when non-representative training sets were used, and in particular when training sets comprised of pixels of one mine dump were used to classify another dump. This result, although not completely unexpected, does emphasise the differences that exist between mine dumps and the need for caution in extrapolating signatures between dumps. It would seem that this problem could be overcome by establishing individual signatures for each dump, perhaps even on a pixel-by-pixel basis. However such work would require repetitive coverage of the same dumps, and this is currently not available to us in CCT form.

Our overall conclusions from this work may be formulated as follows:

(a) The application of multispectral pattern recognition techniques has allowed well vegetated areas of the mine dumps studied to be distinguished from unvegetated areas with high accuracy.

(b) Classification accuracies are much lower for areas that are partially vegetated, or phrased alternatively, for areas in which the size of the CCT resolution element is greater than that of the physical area over which the target is uniform. In such areas a problem of "mixed signatures" occurs, and this requires further investigation.

(c) On the basis of (a) above it would seem likely that the growth and/or decline of mine dump vegetation could be detected when such changes had reached an advanced stage, and had

spread over areas larger than the CCT resolution element. Conclusion (b) above indicates that early detection of such changes would be much more difficult with the present system resolution. However this problem requires further study, particularly with regard to the use of repetitive and seasonal coverage (currently not available in CCT form) for the establishment of the various target signatures.

7.9 Radiometric Analysis

In addition to the recognition studies on mine dump vegetation, an attempt was made to establish a radiometric relationship between the "in-situ" reflective measurements and the radiance recorded by the MSS.

From the field reflectance data shown in Appendix B, typical spectral reflectance values for slime exposure, Eragrostis curvula and Acacia cyclopsis were tabulated. The annotation data of ERTS frame 1049-07301 gave a solar elevation of 41° from which a total solar irradiance value at the time of MSS imaging was calculated using published local data (Kok, 1972). Thus, a reflected radiance from the three dam surface vegetation categories could be calcu-

lated for correlation with the MSS measured radiances.

A numerical integration yielded the radiances L_{N_T} reflected directly from the surfaces, where L_{N_T} is given by

$$L_{N_T} = \int_0^\infty \frac{1}{\pi} . \rho_T(\theta_r,\phi_r).\Phi_s(\theta_s).R_N(\lambda). \, d\lambda$$

Here $\rho\ (\theta_r,\phi_r)$ = target bivariate reflectance normalized to a Lambertian standard.

$\Phi_s(\theta_s)$ = solar irradiance at the time of MSS imaging for solar elevation θ_s.

$R_N\ (\lambda)$ = responsivity for each band and

L_{N_T} = radiance value for each target T in each band N.

This integration procedure was carried out for the three vegetation cover categories using the data recorded on the CCT frame 1049-07301, and the calculated radiances are shown in table 7.4 in the columns headed "GROUND".

A pixel grid at 1:10 000 scale was then produced from the CCT (see sub-chapter 7.7) for the area covering slimes dams 1/L/38,39, 40 and 41. Multispectral aerial photography using passbands similar to those of the MSS sensors (see section 4.2) was then overlaid on the pixel grid at the same scale and its superposition adjusted until photographic density and MSS sensor levels gave a "best fit". Pixels covering uniform areas corresponding most closely to the three vegetative categories were selected and their MSS reflected radiance values compared with those calculated. The results are shown in table 7.6 in the columns headed "CCT".

TABLE 7.6

CALCULATED AND CCT MEASURED RADIANCES FOR GROUND OBJECT CATEGORIES IN W. Cm^{-2}. Sr^{-1}.

	BAND 1		BAND 2		BAND 3		BAND 4	
GROUND OBJECT CATEGORY	GROUND	CCT	GROUND	CCT	GROUND	CCT	GROUND	CCT
SLIME	2,2	2,2	1,7	1,6	1,6	1,7	1,6	2,0
ERAGROSTIS CURVULA	0,5	1,5	0,4	1,4	0,5	1,1	0,7	1,5
MESOPHYTIC VEGETATION	0,3	0,9	0,2	0,6	0,8	0,8	1,2	1,1

Table 7.6 shows the differences between calculated and measured radiances as a percentage of measured radiance. The agreement obtained for measurements on the most uniform target, viz. slimes (differences not more than 20%) is surprisingly good in view of the fact that the calculations took no account of parameters such as scattering and absorption that degrade the radiometric fidelity.

TABLE 7.7

PERCENTAGE DIFFERENCE BETWEEN GROUND CALCULATED AND MSS OBSERVED RADIANCES

$$\frac{\text{CCT - GROUND}}{\text{CCT}} \times 100$$

BAND	1	2	3	4
SLIME	0	- 6	+ 6	+20
ERAGROSTIS CURVULA	+67	+72	+55	+53
MESOPHYTIC VEGETATION	+67	+67	0	- 9
ROGERS*	-10	-18	-20	-23

(* Calculated from Rogers et al, 1973)

The last row of table 7.7 shows the results of similar calculations carried out by other investigators over test areas in the U.S.A. (Rogers, 1973). These do not differ significantly in magnitude, although they show a more regular trend.

The radiance calculations and measurements carried out on Eragrostis curvula and mesophytic vegetation show much larger differences. This is not entirely unexpected since these two ground object categories, when imaged in given pixels, always contained small areas of slime exposure, (see section 7.6 above) and consequently would exhibit higher radiances. This data of table 7.7 support this supposition except for the case of mesophytic vegetation in band 4. No explanation has yet been found for this anomaly.

Furthermore, it is suspected that the relatively high CCT values are not completely explained by the partial vegetation coverage, since in general the exposed areas were only a small proportion of the selected pixels. A more extensive comparison in other areas and for other times is required, as is an atmospheric absorption/scattering model.

8. CONCLUSIONS

This document has reported on the application of ERTS type data to the process of monitoring the growth and decline of vegetation on mine dumps. It has been established that particular mine dumps throughout the entire test area can be detected and identified. It has also been established that patterns of vegetative growth on the mine dumps can be recognised from a simple visual analysis of photographic images. Because vegetation tends to occur in patches on many mine dumps, it is unsatisfactory to classify complete dumps into categories of percentage vegetative cover. A more desirable approach is to classify the patches of vegetation themselves. The coarse resolution of conventional densitometers restrict the accuracy of this procedure, and consequently a direct analysis of ERTS CCT's is preferred.

A set of computer programs were therefore written to perform the data reading and manipulating functions required for basic CCT analysis. More advanced programs were then written to improve the CCT locational accuracy (via an Affine Transformation) and to implement multispectral pattern recognition techniques (based on a maximum likelihood decision rule).

Application of these procedures to the problem of classifying mine dump vegetation showed that well vegetated areas could be distinguished from unvegetated areas with high accuracy. However the classification accuracy was much lower

ORIGINAL PAGE IS
OF POOR QUALITY

for partially vegetated areas, i.e. for areas where the CCT resolution element was larger than area of "target uniformity". It thus seems likely that the growth and/or decline of mine dump vegetation can be monitored once it has spread over areas larger than the CCT resolution element, but that early stages of such changes would be much more difficult to detect. This aspect should be further studied when repetitive and seasonal coverage of the mine dumps becomes available, and it is anticipated that further improvements in the classification accuracies will then be achieved.

9. REFERENCES

Gilbertson, B
Monitoring vegetation cover on mine dumps with ERTS-1 imagery : some initial results
NASA Symposium on Significant Results obtained from the Earth Resources Technology Satellite - 1
Goddard Space Flight Center, March 5 - 9, 1973, pg. 577.

Kok, C.J.
Spectral irradiance of daylight at Pretoria
J. Phys. D : Appl. Phys., Vol. 5, 1972, pg. 1513.

Longshaw, T.G.
Field spectroscopy for multispectral remote sensing : an analytical approach
Applied Optics, Vol. 13, pg. 1487. 1974.

Rogers, Robert H; Peacock, Keith; and Shah, Navine
Techniques for correcting ERTS data for solar and atmospheric effects
(Abstract only available at present time)
Paper I 7 presented at
NASA Third ERTS Symposium, December 10 - 14, 1973.

APPENDIX 'A'

ABSTRACTS OF SIGNIFICANT RESULTS REPORTED AT ERTS-1 SYMPOSIA

MONITORING VEGETATION COVER ON MINE DUMPS WITH ERTS-1 IMAGERY : SOME INITIAL RESULTS

Brian Gilbertson, Spectral Africa (Pty) Limited, P.O. Box 2, Randfontein, Republic of South Africa.

ABSTRACT

One of the aftermaths of mining activities in South Africa has been the development and growth of mine tailings dumps. Environmental pollution from these dumps may be largely prevented by ensuring that a vegetative growth covers the entire dump and to this end the Chamber of Mines incurs annual expenses in excess of $1 000 000. The growth or decline of this vegetative cover is monitored by both aerial photography and site visits.

ERTS-1 imagery is being used in an attempt to differentiate between mine dumps having varying degrees of vegetative cover. Two ERTS-1 images that cover part of the main mine dump area have been received to date, and have been analysed both qualitatively and quantitatively.

It has been found that the various mine dumps can be located and identified. Differences in vegetative cover can be seen and measured. Patterns of vegetative growth, some characteristic of particular dumps, can also be seen. It is therefore tentatively concluded that mine dumps can be differentiated with respect to their vegetative cover on these initial images. Subsequent imagery showing seasonal variations should facilitate the program.

It is anticipated that such ERTS-type imagery could ultimately be used to provide management data to the mining authorities with respect to the state of vegetative cover of all the major mine dumps in the Republic.

+ + + + + + +

ORIGINAL PAGE IS
OF POOR QUALITY

ERTS IMAGERY AS A SOURCE OF ENVIRONMENTAL INFORMATION FOR SOUTHERN AFRICA

Douglas T. Williamson and Brian Gilbertson, (Spectral Africa, P.O. Box 2, Randfontein. Republic of South Africa).

ABSTRACT

Southern Africa is faced with a variety of environmental problems that reflect the different states of development of countries in the region. The task of the environmental planner is in many instances complicated by a lack of basic resource information. The acquisition of the necessary data is often impeded by shortage of trained personnel and lack of funds, particularly in developing nations of the region.

This paper describes the range of environmental problems in Southern Africa and shows specific examples of how ERTS type imagery can materially assist in solving these problems. These examples demonstrate that ERTS type data will be of substantial value to both the industrialized and the developing nations of Southern Africa, provided that problems of availability and user education are overcome.

+ + + + + + +

APPLICATION OF ERTS IMAGERY IN ESTIMATING THE ENVIRONMENTAL IMPACT OF A FREEWAY THROUGH THE KNYSNA AREA OF SOUTH AFRICA

Douglas T. Williamson and Brian Gilbertson (Spectral Africa, P.O. Box 2, Randfontein. Republic of South Africa).

ABSTRACT

In the coastal areas north-east and south-west of Knysna, South Africa lie natural forests, lakes and lagoons highly regarded by many for their aesthetic and ecological richness. A freeway construction project has given rise to fears

of the degradation or destruction of these natural features.

We investigated the possibility of using ERTS imagery to estimate the environmental impact of the freeway and found that

(a) All threatened features could readily be identified on the imagery and their position in relation to the proposed freeway route was immediately obvious.

(b) It was possible within a short time to provide an area estimate of damage to indigenous forest which matched official estimates based on more protracted studies.

(c) In several important respects the imagery has advantages over maps and aerial photos for this type of work.

(d) The imagery will enable monitoring of the actual environmental impact of the freeway when completed.

We concluded that ERTS imagery, with its regional coverage, ease and speed of interpretation, will streamline environmental impact studies of this scope with likely economic benefits.

+ + + + + + +

VEGETATION MAPPING FROM ERTS IMAGERY OF THE OKAVANGO DELTA

Douglas T. Williamson (Spectral Africa (Pty) Limited, P.O. Box 2, Randfontein, Republic of South Africa.

ABSTRACT

The Okavango is Botswana's major water resource. As yet it is essentially undeveloped and supports large wild life populations both within the system itself

and in the adjacent semi-arid areas. Development of the delta for its water resources and recreational potential is inevitable and imminent. Much basic resources data is urgently required to facilitate sound planning.

Other workers have studied ERTS imagery of the delta from a geological and hydrological perspective. The present study has been specifically directed at mapping vegetation types within the delta and generally concerned with finding what information of value to plant and animal ecologists could be extracted from the imagery. To date it has been found that

(i) It is possible to map broad vegetation types from the imagery. This has enabled preparation of a vegetation map of the delta which considerably refines existing maps.

(ii) Imagery of the delta records the state of the system in a manner which will facilitate long-term studies of plant succession.

(iii) Phenological events can be detected. This may allow inferences to be drawn about seasonal movements of animal populations.

(iv) The imagery can be used to detect and map wild fires. This will be useful in determining the role of fire in the ecology of the region.

Using the imagery it is thus possible to map existing vegetation and monitor both short and long-term changes.

These results have been obtained after a few months of work using only colour composites of the delta and without sophisticated, automated techniques of data extraction and analysis. They demonstrate that ERTS type imagery can be

a valuable tool to those responsible for planning and managing the exploitation of natural resources in the developing world.

+ + + + + + +

THE INFLUENCE OF SEASONAL FACTORS ON THE RECOGNITION OF SURFACE LITHOLOGIES FROM ERTS-IMAGERY OF THE WESTERN TRANSVAAL

Jan Grootenboer (Spectral Africa (Pty) Limited, P.O. Box 2, Randfontein, Republic of South Africa).

ABSTRACT

The value to geological studies of repetitive ERTS-imagery was investigated by comparing two images gathered during different seasons over an area in the western Transvaal Province of the Republic of South Africa.

The first of the two images (1050-07355) was gathered on September 11th., 1972, co-inciding with the end of the dry winter season. The second image (1158-07363) was gathered in the middle of the summer rainfall season on December 28th., 1972.

A comparison of the two images reveals striking differences in the amount of reconizable geological detail. The most pronounced difference is the marked enhancement on the December image of tonal variations associated with individual surface lithologies. This contrast in tonal values is evident in all four spectral bands, though particular bands emphasize individual lithologies more clearly than others. Basic igneous rocks of the Bushveld Complex, for instance, are most clearly defined on bands 6 and 7, while certain areas underlain by granite are distinguishable only on band 4.

ORIGINAL PAGE IS
OF POOR QUALITY

Tonal variations on the September image permit recognition of the major lithological units to a degree which is slightly inferior to that displayed by a 1:1 000 000 scale geological map. The very marked tonal differences displayed by the December image, however, permit recognition of detailed lithological units compatible with published geological maps at 1:250 000 scale. In addition, this image reveals the presence of distinct stratigraphic subdivisions within the previously undifferentiated Dolomite Series of the Transvaal System.

The differences exhibited by the two images clearly demonstrate the importance of repetitive ERTS coverage in geological investigations, particularly in areas of marked seasonal variations. In the present case variations in soil moisture content and atmospheric haze appear to constitute the most important factors exerting an influence on the tonal characteristic of different surface lithologies and consequently on the ease of recognition of such lithologies. Under different conditions, however, other seasonal factors may be of equal or greater importance.

+ + + + + + +

STRATIGRAPHIC SUBDIVISION OF THE TRANSVAAL DOLOMITE FROM ERTS IMAGERY

Jan Grootenboer (Spectral Africa (Pty) Limited, P.O. Box 2, Randfontein, Republic of South Africa); Ken Eriksson, John Truswell (Department of Geology, University of the Witwatersrand, Jan Smuts Avenue, Johannesburg, Republic of South Africa).

ABSTRACT

ERTS imagery has revealed the presence of broad stratigraphic subdivisions in the previously undifferentiated Transvaal Dolomite of the western Transvaal, Republic of South Africa.

While detailed field mapping in areas of good outcrop, as well as borehole logging has recently led to the recognition of a stratigraphy in the Transvaal Dolomite of the central Transvaal, poor outcrop in the western Transvaal has to date prevented this. The ERTS-imagery, however, clearly reveals the presence of six, and in the far west seven, distinct stratigraphic zones extending along strike for a distance of at least 200 km. Ground truth selected on the basis of ERTS imagery, identified these zones as corresponding to alternating units of dark-grey, chert-poor and light-grey relatively chert-rich carbonates. With an appreciation of the defined stratigraphy of the central Transvaal, the detailed geology mapped along the traverses was readily related to the zones evident on the imagery, extending the established stratigraphic subdivision of the carbonate sequence over an area of some 4000 sq. km.

The investigation clearly demonstrates the potential applications of ERTS-imagery in geological studies, even in a country where the geology is supposedly well known.

+ + + + + + +

ERTS-1 IMAGERY AS AN AID TO THE DEFINITION OF THE GEOTECTONIC DOMAINS OF THE SOUTHERN AFRICAN CRYSTALLINE SHIELD

Morris J. Viljoen, Geological Research Department, Johannesburg Consolidated Investment Company Limited, P.O. Box 2, Randfontein, Republic of South Africa.

ABSTRACT

The ancient granite-greenstone cratons and the metamorphic mobile belts are two major geotectonic units of the Southern African Crystalline Shield. Each has its own distinctive geotectonic style. The granite-greenstone cratons

are characterised by arcuate vulcano-sedimentary belts encircling or partially encircling diapirically intrusive gneissic tonalitic batholiths. These rocks, with their well defined structural imprint, are sharply transgressed by younger, more potash-rich granites. The metamorphic mobile belts, on the other hand, are characterised by paragneisses and rocks of amphibolite and granulite facies metamorphic grade. Plastic flowage folding phenomena involving complex refolding and the development of basin and dome structures are the most diagnostic features.

Portions of these two geotectonic environments have been studied on ERTS-1 imagery. It was found that the broad synoptic view provided by this imagery is ideally suited to a study of the diagnostic macro-structures, and that the different geotectonic styles could be clearly recognized. ERTS-1 imagery thus allows a more accurate definition than exists at present of the contact zones of the two domains. This may be of considerable economic importance, since basic/ultrabasic rocks containing some of the worlds largest metal deposits have been emplaced along similar contact regions within the Canadian Shield.

These initial results warrant a more detailed study and form the basis of a proposal submitted for the ERTS-B program. The proposal involves a study of the granite-greenstone cratons and encircling mobile belts with a view to gaining an insight into the relevance of plate tectonics of Precambrian times. It has been suggested that the mobile metamorphic belts could represent the root zones of mountain systems and, therefore, the sites of possible subduction zones for plates of early Archaean earth crust. The greenstone belts have often been equated with island arc systems and as such could themselves represent ancient subduction zones.

ORIGINAL PAGE IS
OF POOR QUALITY

APPENDIX 'B'

35a

R. P. VILJOEN M.Sc., Ph.D., M. J. VILJOEN M.Sc., Ph.D.,
J.C.I. Fundamental Geological Research Department, P.O. Box 2, Randfontein, 1760, South Africa.

J. GROOTENBOER B.Sc. (Hons.), Ph.D. and T. G. LONGSHAW B.Sc. (Hons.)
Spectral Africa (Pty) Limited, P.O. Box 2, Randfontein, 1760, South Africa.

ERTS-1 IMAGERY: AN APPRAISAL OF APPLICATIONS IN GEOLOGY AND MINERAL EXPLORATION

SYNOPSIS

Since its launching in July, 1972, the ERTS-1 satellite has acquired some 150 000 images of the Earth's surface, so that at the present time good cloud free imagery of over 90 per cent of land areas is readily available. These images are finding an ever-increasing application in a number of scientific disciplines amongst which the earth sciences figure prominently. Eearly investigations have been primarily of a scientific nature but the stage has now been reached where most of the possible applications have been outlined and the imagery is beginning to find routine application in mineral exploration and related geological fields.

This paper briefly describes the technology of the ERTS satellite and the sensing systems on board. The processes involved in producing photographic imagery and in particular false colour composite images are outlined while the potential of the computer-compatible tapes in automated data processing is indicated.

Factors influencing the geological data content of the imagery and the value of synoptic coverage are discussed and it is shown that under suitable conditions the imagery has important applications in the fields of regional tectonics, structural analysis, geological mapping, and mineral exploration. Detailed studies are presented to illustrate the application of ERTS in each of these fields. These are mainly drawn from Southern Africa and Western Australia where some of the finest ERTS imagery to date, has been obtained.

A critical analysis of ERTS as compared to other geological techniques is presented and anticipated future developments in the remote sensing of earth resources from space platforms is outlined.

It is concluded that ERTS imagery forms a valuable new geological tool that, if applied correctly and in conjunction with other geological techniques under appropriate conditions, can effect considerable saving of time and money in a number of geological disciplines, notably in mineral exploration.

INTRODUCTION

The first Earth Resources Technology Satellite, ERTS-1, which was launched by NASA on July 23, 1972, marked the beginning of a completely new era in the approach to the study of a number of scientific disciplines including geology and earth resources. Although the spacecraft and its ground-support facilities drew upon the extensive expertise developed by NASA, observers expressed scepticism on whether the satellite payload would live up to expectations. This payload consisted of three Return Beam Vidicon (RBV) cameras, a Multispectral Scanner (MSS), and a Data Collection System (DCS). Although the RBV cameras failed

Dr R. P. Viljoen obtained his degrees in geology from the University of Witwatersrand. In 1962 he joined the Economic Geology Research of this University where he studied various aspects of the mineralogy and petrology of Witwatersrand gold ores. After obtaining an M.Sc degree from the results of this study he worked for the mining industry for two years. From 1965-1969 Dr Viljoen was employed by the C.S.I.R. carrying out geological research in the Barberton Mountain Land, as part of South Africa's contribution to the International Upper Mantle Project, obtaining his Ph.D degree from the results of this investigation in 1970. During the same year he joined the Johannesburg Consolidated Investment Company Limited where, together with Dr M. J. Viljoen he started the newly created Fundamental Geological Research Department. His work has been primarily concerned with mineral exploration, target selection and the development of models of various types of mineralization based on studies carried out both in Southern Africa and overseas. In 1974 he was appointed head of the Fundamental Research Department of J.C.I. where his main interest has been the development of remote sensing methods for future routine use in mineral exploration.

Dr M. J. Viljoen obtained his degrees in geology from the University of Witwatersrand. He received an M.Sc degree in 1963 through the Economic Geology Research Unit for work on various aspects of gold mineralization in the Barberton Mountain Land. After a spell of two years with the mining industry he joined the C.S.I.R. in 1965 and until 1969 was concerned with further research work in the Barberton Mountain Land, which formed part of South Africa's contribution to the International Upper Mantle Project. After obtaining a Ph.D degree from these studies in 1970, he joined the Johannesburg Consolidated Investment Company Limited where together with his brother, Dr R. P. Viljoen, started the newly created Fundamental Geological Research Department of the company. He has been primarily concerned with the development of models for various types of mineralization based on extensive geological mapping and geochemical studies in Southern Africa. Dr Viljoen has also studied numerous mineral occurrences in overseas countries. He is still involved with this work and in the application of remote sensing techniques to mineral exploration.

Mr T. G. Longshaw obtained a B.Sc (Hons.) degree in physics and mathematics at the University of East Anglia in 1968. After two years research in such diverse fields as nuclear physics, solid state physics, and geophysics, he turned to the science of remote sensing in 1970 by joining the newly formed Johannesburg Consolidated Investment Company Limited subsidiary, Spectral Africa (Pty) Limited. For the last four years he has been closely involved in the research and development of new remote sensing exploration techniques from aircraft and satellites. He has been a NASA ERTS-1 co-investigator for the past three years.

Dr J. Grootenboer graduated from the University of the Witwatersrand with a B.Sc degree in physics and geology in 1963 and a B.Sc. (Hons.) in Economic Geology in 1965. He worked as an exploration geologist with the Johannesburg Consolidated Investment Company Limited before going to Canada where he obtained a Ph.D for research work in the field of sulphur isotope geochemistry. He joined the International Division of Cominco in 1970 and was engaged in base metal exploration in Canada, Southern Africa, Australia, and Greenland. He took up his present position of senior geologist with Spectral Africa in 1973 and is currently engaged in developing new remote-sensing techniques and investigating their applicability to geological problems.

soon after launch, after, in fact, having performed much to the sceptic's predictions, the MSS has provided high-quality synoptic imagery beyond even the optimist's expectations. This has been particularly the case in the geological disciplines and many earth scientists throughout the world are now realizing the tremendous potential of NASA's generously shared technology.

Many articles have been published on the findings of ERTS-1 geological studies of which initial results were limited to general observations ('gee-whizz' claims as Americans described them) and reiteration of the potential of the imagery. At this early stage tangible benefits, in the form of improved geological mapping as an aid to mineral exploration, for example, were still rather obscure. Opinions as to the effectiveness of the technique thus varied between that of traditionalists who viewed new methods with cautious conservatism to the wild claims of the popular press who suggested that individual ore bodies could and actually had been located solely from the study of ERTS-1 imagery. In practical terms, the role of ERTS imagery lies somewhere between the two but not until recently have more critical analyses been able to dismiss speculation and clearly state the new information value of ERTS imagery in realistic geological terms.

Perhaps the most significant results from these assessments have been the identification of large-scale geological features, many of which are of a tectonic nature and that had previously been unknown even from detailed geological mapping. In addition, stratigraphic information has been enhanced in numerous cases, even in areas where outcrops are not present. On this firm factual footing, ERTS imagery has established a position as a valuable regional mapping tool. Although it is too early yet to appreciate the full implications of these findings, it is becoming increasingly clear that,when used together with other data in a multi-disciplinary approach, ERTS imagery should play a major role in helping to unravel the problems of regional ore emplacement.

The introductory section of this paper summarizes the data acquisition aspect of the ERTS programme and describes two different methods of producing imagery. The first method involves standard photographic techniques to produce colour composite images from NASA 70 mm transparencies and the second, the production of high resolution black-and-white and colour composite displays from Computer Compatible Tapes (CCT's). The paper then provides a review of the use of the imagery by way of examples in a number of facets of geology. Finally, two case histories, which attempt to illustrate the practical benefit of ERTS imagery in current mineral exploration programmes, are presented.

THE ERTS-1 SATELLITE

The ERTS-1 satellite revolves around the earth at an altitude of 900 kilometres in a circular sun-synchronous orbit, systematically covering the Earth's surface every 18 days. This cycle of complete global coverage allows the onboard sensor system to acquire repetitive imagery under constant observation conditions of any area from 81° north to 81° south latitude according to commands issued from NASA's Operation Control Centre.

The acquisition of this MSS data takes place in four spectral bands through the same optical system. Two of these bands (numbers 4 and 5) have wavelength ranges from 0,5 to 0,6 and 0,6 to 0,7 micrometres, corresponding to the green-yellow and the red regions respectively of the visible electromagnetic spectrum. The other two bands (numbers 6 and 7) have wavelength ranges from 0,7 to 0,8 and 0,8 to 1,1 micrometres respectively, corresponding to near infrared regions of the spectrum. The MSS scans crosstrack swaths 185 km wide with twenty-four detectors (6 for each spectral band), by way of an oscillating mirror. Each detector observes a spot on the ground nominally 79 metres square, which is swept (roughly west to east) over an angle from ± 2,88 about the vertical. As there are six detectors in each band, a strip 474 metres wide is scanned per mirror oscillation. In the 73,42 milliseconds taken for one scan to be completed and the mirror to oscillate back to its 'scan-start' position, the spacecraft (travelling roughly south) has advanced 474 metres along track and the next six-scan sweep begins. This scanning mode is described as contiguous, i.e. no spaces exist between scan lines and no area is covered more than once. The series of scan signals thus produced by the detectors is then multiplexed and encoded to give a digital bit stream. This bit stream is either recorded on one of the satellite's wide band tape recorders and subsequently telemetered to a ground receiving station or directly telemetered as it is produced if the satellite is within range of a ground receiving station.

As no receiving station in South Africa is suitable for ERTS video data reception, users in this country receive MSS imagery by the indirect method via NASA's National Data Processing Facility (NDPF). NDPF apply radiometric and geometric corrections to the data and issue scene-corrected imagery in the form of photographic products or Computer Compatible Tapes (CCT's) to approved users. Of these products, 70 mm transparencies are the most convenient to the user from which he can make black-and-white enlargements via standard photographic procedures, or, if he has the facilities, can produce composite colour prints to enhance spectral information.

The CCT's, however, require specialized equipment to extract the image data. As their name

implies, they contain the video data comprising an MSS image in a form suitable for processing by computer. Automatic interpretation techniques have been discussed elsewhere[1,2,3,4,5] and it is outside the scope of this paper to deal with this extensive field. What will be discussed in this paper is an aspect of CCT's that is tangible to the geologist, namely a photographic display of processed CCT data. This method of producing imagery involves the use of a mini-computer with a digital-to-analogue conversion facility and a linescan film recorder.

An earth scientist, therefore, has a wide selection of methods at his disposal to extract resource information from ERTS imagery. Geological photo-interpretation of any country that has signed an ERTS agreement may be carried out depending only on image availability, coverage, and facilities for producing imagery in a suitable format.

Over the three years of operation of ERTS-1 (now renamed LANDSAT-1) the MSS has provided extensive coverage of the world's land masses. In many cases, however, sub-optimum quality or cloud cover has detracted from the usefulness of the imagery in regional geological studies. In Southern Africa, for example, this has led to the situation that no area has cloud-free coverage over all four seasons. This has limited the comprehensive study of some areas as seasonal coverage has been found to be an important aspect of geological interpretations in several areas[6].

Despite this limitation, substantial progress has been made in regional mapping of the African subcontinent of which this paper presents several examples as well as describing a study in Western Australia.

PRINTING OF MSS IMAGES

The production of MSS black-and-white prints is relatively straightforward. Using the four NASA 70 mm negatives (1 : 3 369 000 scale) comprising the four spectral bands of an MSS frame, enlargements are made to 1:1 000 000 scale using Kodak 2420, a fine grained duplicating material. From these working negatives, any number of black-and-white prints can be made with scales from 1:1 000 000 to 1 : 250 000.

Colour compositioning several bands is more involved, however, and requires the three chosen bands (usually bands 4, 5, and 7) to be produced as separations in exact spatial register. These separations, once registered, are punched in this position, placed on register pins overlying Kodak 4109 Print Film on a photographic enlarger base platform, and exposed sequentially through Wratten 98, 99, or 29 filters, depending on whether the separation images are required to appear as blue, green, or red in the final colour print. Standard colour-processing of the print film gives a master negative from which colour prints can be conventionally produced.

A promising new technique that should find widespread application is the preparation of diazo colour composite images[7]. Using a routine ammonia printing process coloured diazo transparent contact prints are prepared from 230 mm negatives of individual MSS bands obtained from NASA. Superposition of three such transparencies produces a transparent colour composite ERTS image at 1:1 000 000 scale. Although theoretical considerations would imply diazo colour composites to be on a par with their photographic counterparts, empirically, it has been noted that image definition is inferior to the photographic composite.

CCT photographic displays are printed similarly, although the format size and scale is somewhat different. As contrast is high in these displays, low-contrast duplicating materials are used in the intermediate stages, although the final colour print material is the same.

GEOLOGICAL APPLICATIONS OF ERTS IMAGERY

The representation of geological features on ERTS depends on a large number of factors and varies considerably from one area of the World to another. In general, imagery of the drier areas of the globe has a higher geological content, particularly where well exposed, and where young surficial deposits are absent.

Some of the best imagery has been obtained over Southern Africa where a combination of favourable geological, climatic, and physiographic conditions has resulted in ERTS imagery unequalled anywhere for its wealth of geologic information.

The most important of these conditions are:

- favourable arid climate and resulting sparse vegetation over large areas,
- geological stability of the African shield, which has produced extensive and relatively undeformed rock sequences since early Proterozoic times,
- mature topography with a close relationship between geology and surface features,
- thin residual soil cover.

Climatic conditions constitute the single most important control. The desert and semi-desert areas of Angola, South West Africa, Botswana, and South Africa produce excellent ERTS images. These images show great geological detail particularly where large outcrops are exposed along the Atlantic scarp and in entrenched river valleys. Elsewhere within the desert zone, in areas of thin sand cover, it may be possible to trace sporadic outcrops of resistant formations. The same holds for the surrounding steppe zone, which is frequently covered by a surficial layer of calcrete, marl, or clay.

The intermediate climatic zones of Southern Africa all exhibit a very close relationship between

surface features and underlying geology, producing many excellent ERTS images. The strong seasonal climatic variations experienced over most of this area result in marked variations in the amount of geological detail represented on images gathered at different seasons[6].

In the Savanna-thornbush climatic zone, deeper weathering obscures the detailed geological features of the underlying bedrock geology but unless the soils reach a substantial thickness, it is still possible to discern much of the regional geology and structure.

In the tropical rain forest zone a combination of dense vegetation together with thick soil cover greatly reduce the value of the imagery, though a great deal of structural information can still be deduced from geomorphological evidence.

One of the most useful features of ERTS imagery is the unique synoptic view it provides of large portions of the Earth's surface. This, in conjunction with the planimetric nature of the imagery and almost total lack of distortion that makes it possible to join images together into mosaics of uniform tonal quality, has added a new dimension to regional geological and structural mapping. The mosaics greatly increase the synoptic properties of the imagery and are invaluable in that they provide a regional representation of the interrelationships of various rock units and give a totally new indication of the extent of major geological structures. This in turn broadens the scale of geological thinking, so that instead of considering areas of only a few hundred or at most a few thousand square miles, as is normal with conventional field mapping and photogeological techniques, the ERTS investigator is dealing with entire countries and even sub-continents. This leads to the investigations of other continents, thereby greatly extending the experience of an individual geologist, expanding his knowledge, and eliminating local prejudices. It is probable that the greatest advantage of the ERTS programme will eventually lie in this broadening of geological knowledge and in the correlation between distinctive geological domains on a World-wide basis and the standardization of geological terminology, the lack of which has been one of the big drawbacks of the science.

The applications of ERTS imagery to geology are essentially similar to those of conventional aerial photography. Important advantages relative to the latter lie in the synoptic view provided, the uniform illumination and tonal quality, the multispectral nature of the imagery, the repetitive coverage, the digital computerized output, the ready availability, and the relatively low cost. The relative lack of resolution (approximately 80 M), however, is a notable drawback compared to aerial photography.

Aerial photography has been extensively used for the production of detailed geological maps and provides much information not apparent from ERTS imagery. On the other hand ERTS imagery illustrates many regional aspects of geology often not indicated on even the best available geological maps. The technique can therefore be regarded as complimentary to aerial photography with the same applications as the latter but on a different scale.

The immediate application of the imagery is of course most striking in under-developed countries where little or no reliable mapping is present[8]. Figure 1A illustrates the availability of published geological maps of Southern Africa while figure 1B depicts three broad zones from which different amounts of geological data are obtainable from ERTS imagery. When studied in conjunction with figure 1A, it is clear that ERTS imagery is capable of providing significant amounts of new geological data for large portions of the African sub-continent.

ERTS imagery has found ready application in several fields in the earth sciences[1,2,3]. Some of the most important are illustrated by means of a number of examples, mainly from Southern Africa.

The main fields discussed include:

- structural geology,
- lithological identification and regional stratigraphic mapping,
- recognition of geotectonic domains,
- mineral exploration.

STRUCTURAL GEOLOGY

ERTS imagery is of exceptional value in displaying the extended large-scale structural elements of large regions. Such elements include the tectonic style, regional joint patterns, and major fracture systems as well as individual structural features such as faults, anticlines, domes, etc. Frequently, because of their breadth and continuity many of these features have been overlooked on the ground or on aerial photographs where the small and localized effects of a segment exposed discontinuously from one outcrop to the next were insufficient to allow identification.

The synoptic nature of the imagery also frequently enhances the appearance of major structural features owing to the interplay between underlying structure, topography, vegetational distribution, and solar illumination.

Examples of the use of ERTS imagery in following major linear features as well as in the synoptic study of folded regions, are given below.

Linears

Up until the present time one of the main features of geological ERTS interpretation has been the recognition of linear features varying in length from a few kilometres to hundreds of kilometres. Such features are generally a manifestation of a variety of surface features including slight tonal differences in areas of rock outcrop, sand, soil or

vegetation cover, alignment of topographic forms, drainage patterns, and vegetation.

Linear features of this type can generally be equated with structural elements such as faults, joints, or fractures. In certain instances, however, they may be coincidental or of an artificial origin (e.g. roads, fence lines, etc.) and Short and Lowman[9] have proposed the non-genetic term linear for all such features prior to their verification from ground investigations.

In any given area it is invariably possible to recognize considerably more linears than are shown on even detailed geological maps. Minor linear features, however, such as small-scale faults and joints, are often not apparant on the imagery because of limitations of resolution.

Okavango faults

Good examples of linear features are illustrated by image number 1054-07571 (Figure 2), which covers the south-western portion of the Okavango Delta of Botswana.

Two remarkably straight and continuous, major NE-SW trending regional lineaments indicated in red on the overlay to Figure 2, constitute striking features. They represent the traces of major fault zones that clearly control the distal portion of the Okavango Delta, thereby enhancing their linearity. One of these features follows the Thamalakane river and portions of the Nhabe river passing almost through the town of Maun, while the other follows the Kunyere river passing through Toteng and controlling the limits of the south-eastern shore line of lake Ngami.

A number of lineaments of almost the same extent and parallel to the major ones described above are also to be seen on the image. These are particularly clear in the outcrop area to the east and south east of lake Ngami. Outcrops in this area represent rocks of the Karroo super group, the Ghanzi formation, and the Kgwebe formation. Components of all three of these geological entities can be distinguished and the linears represent the manifestation of fault traces that have given rise to a number of graben and horst blocks in post-Karroo times.

A number of less obvious linears are also to be seen on the image and include possible second-order faults that branch from the two main faults described above, especially in the vicinity of the Thamalakane and Kunyere rivers.

The major zone of NE-SW faults seen on this image is of considerable importance, as a study of adjoining images indicates that they may represent a south-westerly branch of the East African Rift system, possibly extending as far to the south-west as the Windhoek area of central South West Africa. Seismic evidence suggests that movement is still taking place along these fault zones as indicated by concentrations of earthquake epicentres and by reversals in the flow of water in the complicated waterways at the distal portion of the Delta.

In addition to the purely geological information obtainable from the image, it also contains a wealth of information relating to water resources, range resources and ecology[10].

Tantalite Valley fault zone

Another example of a major linear fault zone of somewhat different character to the Okavango faults described above, is the so-called Tantalite Valley fault zone in the N.W. Cape Province and southern S.W.A. The presence of this mega-structural dislocation of sub-continental dimensions was totally unknown from any available published information prior to the acquisition of satellite imagery for the area. Figure 3 shows the linear structure where it transects the Bushmanland Metamorphic Sequence in the vicinity of the Orange river.

It appears to take the form of a major wrench dislocation with a right lateral sense of movement as is clearly revealed by drag in the Bushmanland sequence rocks. The linear aspect of this structure is marked by a well-defined zone of shearing indicated in red on the overlay (Figure 3). This shear zone can be traced for a distance of 450 kilometres along strike before its effects are dissipated into splay faults. Although the lineament is not immediately apparent to the south-east of the zone of splay faults, shown in Figure 3, examination of the ERTS mosaic of the N.W. Cape (Figure 11) shows a 60 km long zone of superficial deposits lying above rocks of the Karroo system north of Vanwyksvlei and indicated on the 1:1 000 000 geological map of the Republic of South Africa. This zone almost certainly represents the surface manifestation of the south-easterly extension of the Tantalite Valley fault zone.

A number of large intrusive mafic bodies as well as numerous smaller bodies have been emplaced along this structural dislocation. According to Joubert[11], continued movement after the emplacement of the mafic bodies is indicated by the conversion of most of the intrusives to amphibolites. Three such bodies are seen on the ERTS image, which also indicates a progressive swing of their direction of elongation from roughly east/west to north/south as one proceeds in an easterly direction (Figure 3).

Wrench faults of this nature are also referred to as transcurrent or transform faults, and are of

FIGURE 1 (a) Top. Available published geological maps of Southern Africa.

FIGURE 1 (b) Bottom. Subdivision of Southern Africa according to amount of geological information evident from ERTS imagery relative to that obtainable from published geological maps. Contours depicting mean annual rainfall are superimposed.

35F

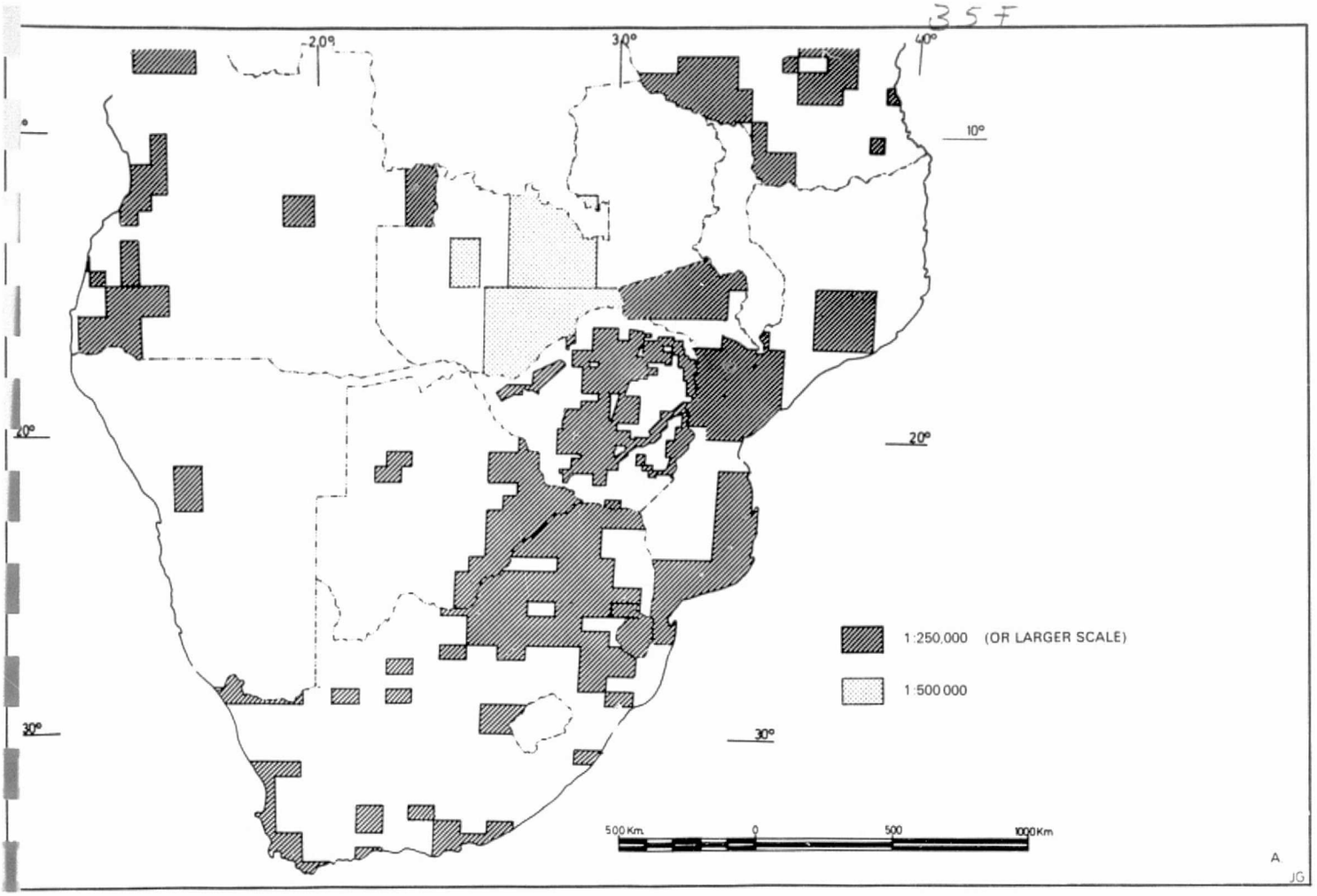

20°
30°
40°
10°
20°
30°
1:250,000 (OR LARGER SCALE)
1:500 000
500 Km
0
500
1000 Km
A
JG

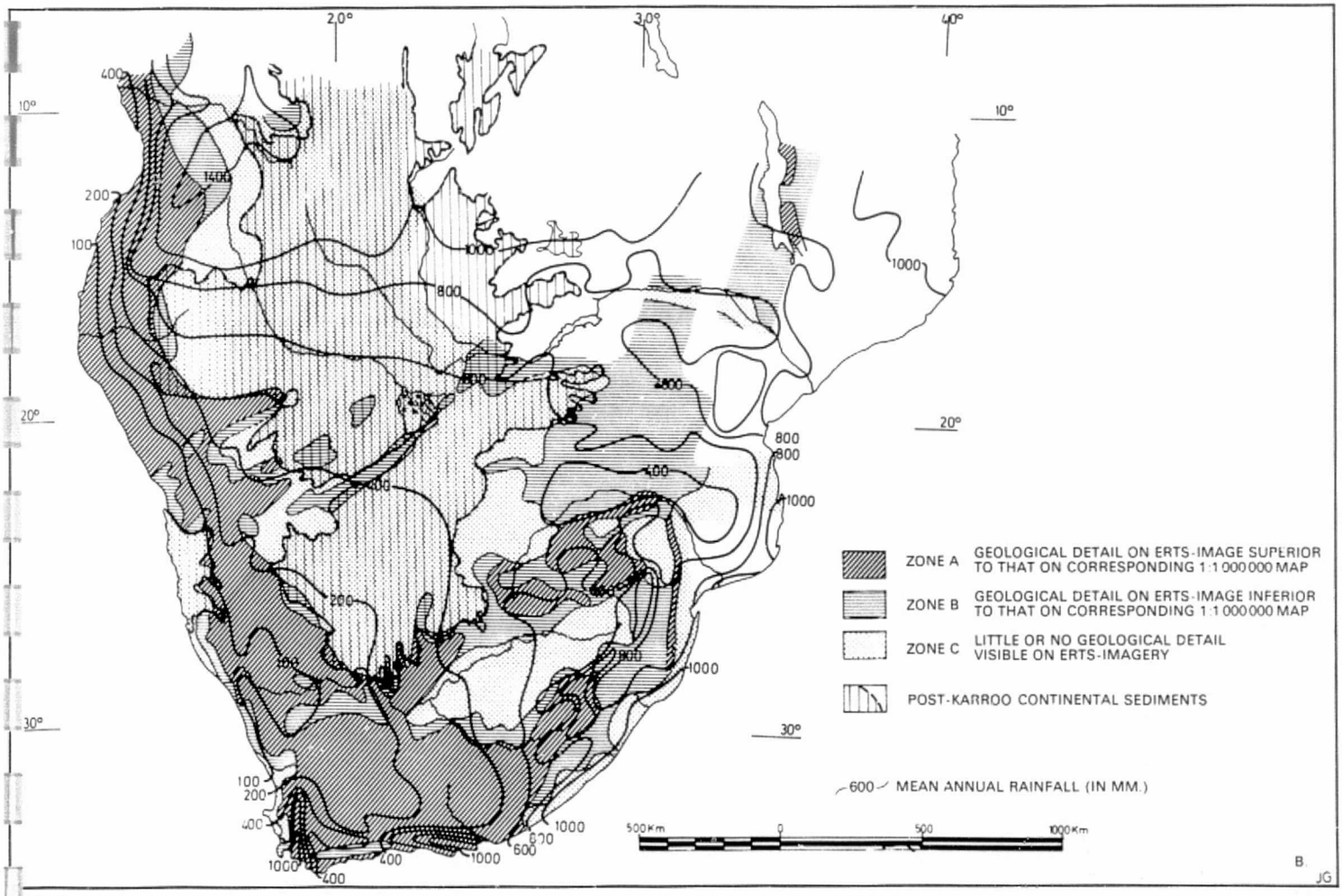

20°
30°
40°
10°
20°
30°
400
200
100
1400
1000
800
1000
800
800
400
1000
200
1000
100
200
400
1000
400
1000
600
800
1000
ZONE A GEOLOGICAL DETAIL ON ERTS-IMAGE SUPERIOR TO THAT ON CORRESPONDING 1:1 000 000 MAP
ZONE B GEOLOGICAL DETAIL ON ERTS-IMAGE INFERIOR TO THAT ON CORRESPONDING 1:1 000 000 MAP
ZONE C LITTLE OR NO GEOLOGICAL DETAIL VISIBLE ON ERTS-IMAGERY
POST-KARROO CONTINENTAL SEDIMENTS
600 MEAN ANNUAL RAINFALL (IN MM.)
500 Km
0
500
1000 Km
B
JG

considerable importance with respect to plate tectonics. The synoptic picture that ERTS provides of such features indicates the potential of the imagery in the study of continental and even global tectonics.

Folding

Many different styles of folding on several scales have been discerned on ERTS imagery, which, in many areas, is capable of affording an unparalleled view of small, intricate fold patterns in relation to much broader fold patterns. The imagery is well suited to the study of regional deformation and in particular the style of folding in the great younger fold mountain belts of the World. These fold belts are often characterized by good outcrop and are difficult of access. Although many such mountain ranges may be covered by a thick mantle of vegetation over large parts, major structure beneath such cover is frequently revealed.

ERTS imagery, once again by the continuity of structural information that it affords, is providing a unique new approach to the understanding of the broad tectonic pattern and structural complexities of such belts.

Cape fold belt

As an example of the above, Figure 4 portrays part of an ERTS image covering a small portion of the east-west trending Cape fold belt of South Africa in a region to the N.E. of Cape Town. The most conspicuous features are resistant masses of the essentially quartzitic sediments of the Table Mountain Series of the Cape System. These quartzites occupy the cores of anticlinal structures and are readily distinguishable by their dark maroon colour tone on the colour composite image and their generally massive nature. In the south-western part of the area a fairly resistant dark mass with a dendritic drainage pattern represents a block of Nama shales and quartzites. The more subdued pattern of the Witteberg quartzites and shales is also fairly distinctive.

The best indication as to the folding patterns and styles in the area are afforded by the more argillaceous rock units. In particular the folding style in the Bokkeveld shales is strikingly demonstrated where the contrast between reddish grey and almost white stratigraphic horizons gives a good indication of the minute details of the fold pattern. A number of axial plane faults are associated with these folds (Figure 4). Similar fold patterns are to be seen in the Dwyka, Ecca, and Beaufort sediments along the north margin of the fold belt in the upper part of the image. In this area individual stratigraphic units can be traced for long distances and constitute components of extensive elongate fold structures. The contact between the Dwyka and the Ecca series can be readily mapped and the important white-band marker horizon of the upper Dwyka series is clearly seen.

The tone and texture of Cretaceous sediments along the southern border of the image are also distinctive.

LITHOLOGICAL IDENTIFICATION AND MAPPING

The recognition of different rock types from ERTS imagery is difficult at times but under certain conditions it is possible, in conjunction with a limited amount of field work, to identify and trace broad stratigraphic zones.

Once a correlation has been established between distinctive zones present on the ERTS imagery and the particular stratigraphic unit on the ground, such units are readily traceable over large distances and across several ERTS scenes.

Stratigraphy of the Transvaal dolomite

Figure 5 illustrates the value of repetitive ERTS imagery in lithological studies by comparing two images gathered during different seasons over an area in the Western Transvaal. For comparison the most detailed available map of the Transvaal Dolomite is indicated in Figure 5C.

The images cover flat-lying, gently undulating country and have been described in detail by Grootenboer *et al*[12]. The first image (Figure 5A) was gathered in September, 1972, at the end of the dry winter season when most of the vegetation is light brown in colour and the indigenous trees are leafless. Slight tonal variations are apparent within the dolomite sequence suggesting a number of hitherto unmapped stratigraphic components.

The second image (Figure 5B) was gathered during December, 1972, at the height of the rainy summer season with the country now being covered by green grassland and with the indigenous vegetation in full leaf. This image, in contrast to the winter equivalent, shows strong tonal variations that definitely appear to be related to stratigraphic components within the Dolomite series. Such stratigraphic units had not previously been recognized from this area (compare Figures 5A and 5C).

The difference in tonal contrast between the two images is probably the result of variations in soil moisture content, atmospheric haze, and the association of characteristic vegetation with underlying geology on the summer image. All three of these factors are directly related to the rainfall cycle[6].

The conformable nature of the colour tones seen on the ERTS image, which extend over a strike length of some 200 km, suggest that they are a manifestation of broad stratigraphic units. This was

FIGURE 2. ERTS image No. 1054-07571, September, 1972, covering the southern portion of the Okavango Delta of Botswana and indicating the presence of a number of regional NE – SW trending linear features representing faults, which clearly control the distal-portion of the delta. Scale of imagery 1:1 000 000.

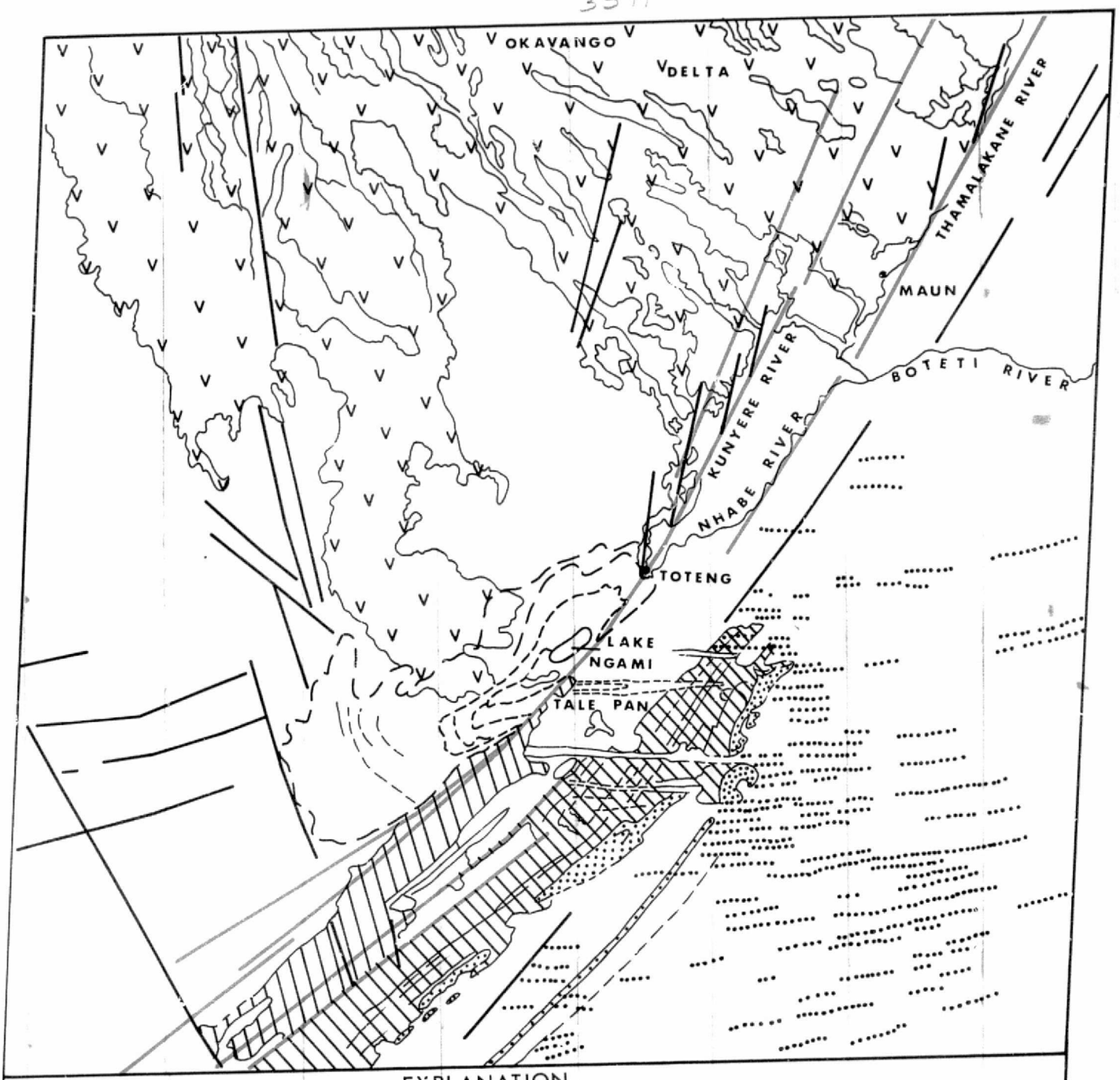

EXPLANATION

SCALE 1:1000 000

- MAJOR REGIONAL LINEAMENTS
- LINEAMENTS
- LINEAR SAND DUNES
- PREVIOUS POSITIONS OF LAKE NGAMI SHORE LINE
- KARROO BASALT AND SANDSTONE PLUS GHANZI FORMATION
- GHANZI FORMATION
- PORPHYRY AND ASSOCIATED ROCKS OF KGWEBE FORMATION
- MAINLY INDURATED SEASONAL SWAMP OF OKAVANGO DELTA BUT INCLUDING DRY SEASONAL SWAMP

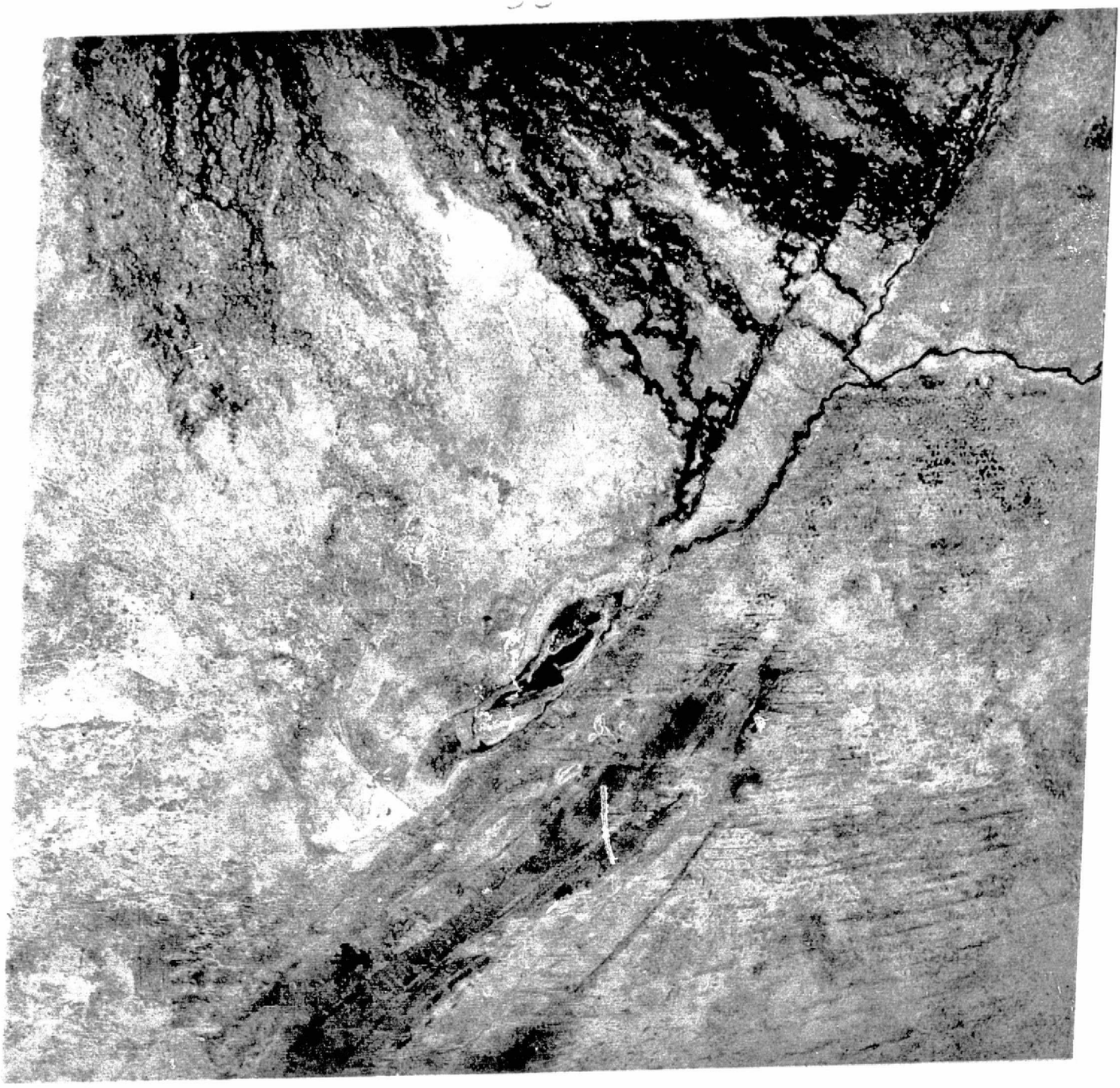

confirmed by ground traverses that identified the dark-light tonal areas as reflecting major alternating zones of dark grey, chert-poor dolomite and light grey, chert-rich dolomite. These zones can be directly equated to broad stratigraphic zones established in the well-exposed Zwartkops area some distance to the east of the area covered by the image depicted in Figure 5.

Thus, despite a long history of geological activity, no stratigraphic subdivisions of the dolomite in this poorly exposed area had been established and this investigation has clearly demonstrated the usefulness of ERTS imagery as a rapid mapping technique in addition to providing data, probably unattainable by any other method.

The Nama Sediments of South West Africa

Figure 6 illustrates the application of ERTS imagery as a geological mapping tool. The image covers semi-arid, sparsely vegetated terrain in the vicinity of Mariental in South West Africa, an area where the annual rainfall amounts to less than 200 mm. Geological formations present in the area include Archaean basement, a folded sequence of arenaceous and argillaceous sediments belonging to the Proterozoic Tsumis Formation, and younger undeformed cover rocks consisting of horizontally disposed shallow-water sediments of the early Paleozoic Nama Group overlain by flat-lying sediments and volcanics of the Upper Carboniferous–Permian Karroo System. These rocks are covered by a number of surficial deposits including river alluvium, calcrete, and windblown sand, ranging in age from Tertiary to Recent. Soil cover over most of the area is thin and in the areas where surficial deposits are absent outcrop conditions are often very good.

The main interest in this image lies in the vividness with which the stratigraphy of the Nama Group is displayed. In this area the Group consists of a basal limestone sequence of the Kuibis formation, overlain by the Schwarzrand formation of greenish shales with sandstone intercalations that, in turn, is overlain by a monotonous succession of reddish argillaceous sandstone and arenaceous mudstones belonging to the Fish River formation.

The basal Kuibis limestones are clearly distinguishable by their grey colour tone and dendritic drainage pattern in the south-western portion of the image where they are relatively flat lying, dipping some 5 degrees to the northeast. In the north-western portion of the image, however, where they have been folded and are more steeply dipping, their representation on the image is no longer as distinct.

In contrast to previous work[13], the ERTS image clearly reveals a two-fold division of the Schwarzrand formation. A lower unit is represented as an area of complexly interbanded lighter and darker olive colour tones. The lighter units correspond to reddish argillaceous sandstones while the darker units represent greenish shales. The sequence dips eastwards at a low angle and the apparent interbanding merely reflects variations in topography with the sandstones being more resistant and capping low hills. Dark bluish and brown colour tones represent an upper unit consisting predominantly of greenish shales with only minor argillaceous sandstones.

The upper Fish River formation of the Nama Group consists of a thick monotonous succession of reddish, shallow-water sediments gradational between argillaceous sandstones and arenaceous mudstones. Because of the small gradational variations in lithology, this unit had never previously been sub-divided stratigraphically. On the ERTS image, however, a number of broad stratigraphic subdivisions are clearly evident, characterized by zones of varying colour tone. The colour tone is directly related to the lithology, becoming progressively darker with increasing content of argillaceous material so that the lightest units correspond to sandstones and the darkest to mudstones with a complete range of intermediate varieties. The Fish River formation, therefore, can be broadly subdivided into three 'sandstone' units, with three interbedded 'mudstone' units.

The Karroo System is represented by sediments of the Dwyka Tillite formation and volcanics of the Stormberg series. The volcanics are characterized by a vivid blue colour tone on ERTS, the result of their dark-brown colour and excellent outcrop. The Dwyka sediments are distinguished by a lighter bluish-grey colour tone.

Surficial deposits are clearly evident on the image and the various types can be readily distinguished on the basis of distribution pattern, texture, and colour tone. Alluvial deposits show a very white colour tone. Calcrete is characterized by a light-brown tone, often with a characteristic pitted texture, while deposits of wind-blown desert sand show up yellow with the larger dunes clearly distinguishable as linear features.

The image clearly reveals the unrivalled applicability of ERTS imagery as a geological mapping tool, particularly in arid climatic regions and in dealing with extensive monotonous sequences of relatively undeformed formations.

Recent deposits in Western Australia

As another example of the use of ERTS in regional mapping problems, a portion of the east Pilbara region of Western Australia has been used.

FIGURE 3. Portion of ERTS image No. 1055-08053, September, 1972, illustrating a linear shear zone that represents a wrench fault of sub-continental dimensions displaying right lateral movement. Most of the rocks that are involved in this structure belong to the Bushmanland sequence of the Namaqualand Metamorphic Complex of the N.W. Cape Province of South Africa and portions of southern South West Africa. Scale of imagery approximately 1:500 000.

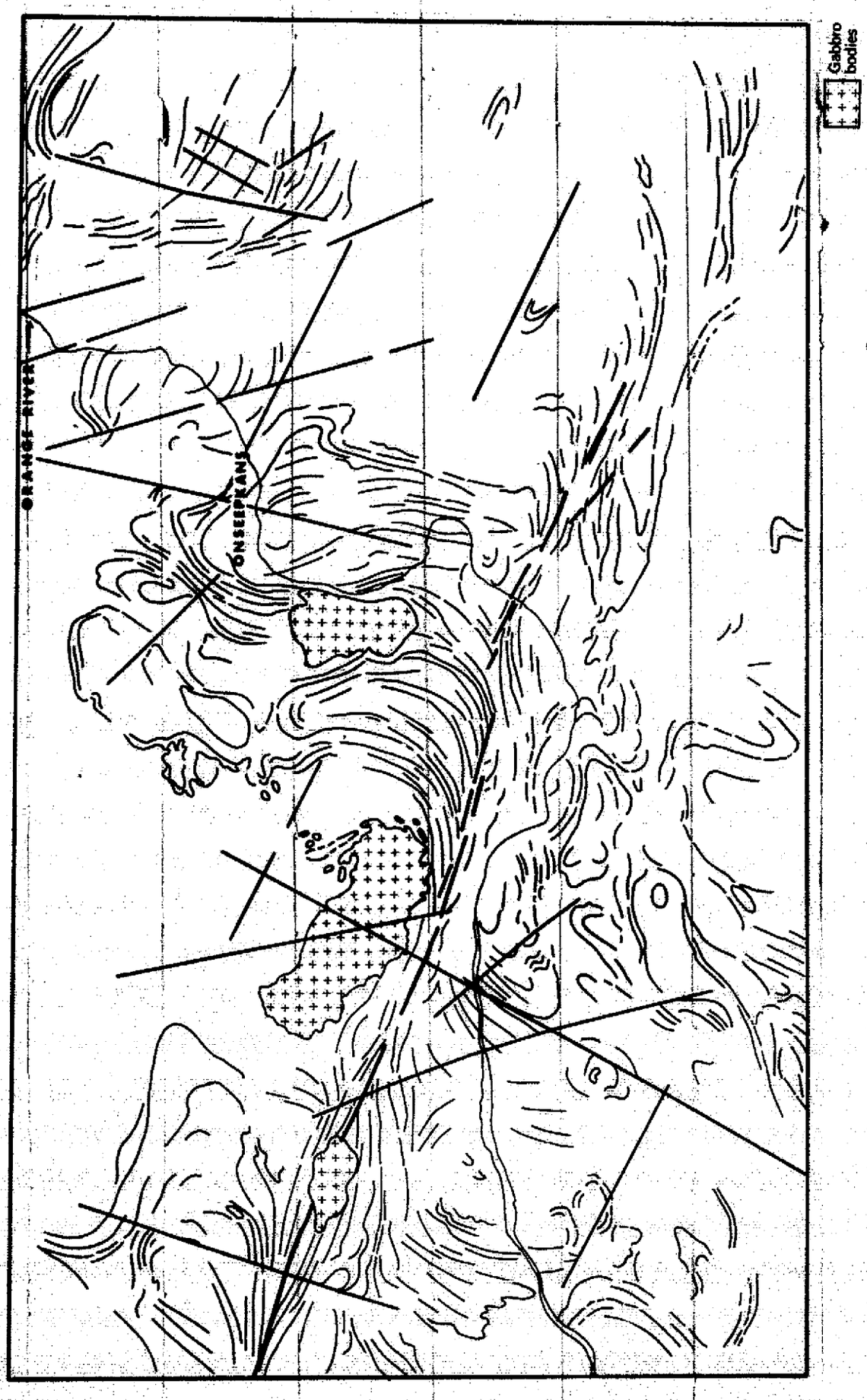
ORANGE RIVER
ONSEEPKANS
Gabbro bodies

In this area younger Proterozoic and Cainozoic formations overlie an archaean granite-greenstone-terrain, a discussion of which is presented later. The illustration (Figure 7) represents an enlargement of the south-eastern portion of ERTS image number 1148-01282.

A remarkable range of colour tones representing varied lithologies, and particularly the more recent Cainozoic sediments, is evident. 1:250 000 Geological Survey maps of Western Australia were used as a general guide to the interpretation, which was significantly aided by regional helicopter reconnaissance traverses in the region.

Younger, generally flat-lying volcanics and sediments of the Fortescue Group unconformably overlie the granite greenstone terrain along the southern side of the image. Several classes of much more recent Cainozoic deposits, related mainly to the recent drainage systems of the Fortescue river and the Noreena and Kulkinbah creeks, as well as to the Tertiary lateritic Hammersly surface, are superimposed onto the Fortescue stratigraphy.

The layered stratigraphy of the Fortescue group is best developed towards the west where a conspicuous tongue protrudes northwards immediately to the west of the town of Nullagine and covers older rocks of the granite-greenstone basement. A distinctive massive porphyry is present at the base of this elongate Proterozoic basin and is readily identifiable by its greenish-yellow tone and joint pattern. In a complex structure along the west of this basin the lowermost Mount Roe basalt of the Fortescue group (identifiable by its darker green tone) is exposed. This is followed by a broad basin of the Hardy sandstone assemblage, the distinctive arkoses yielding a light yellowish-brown tone while some of the shaly varieties give somewhat darker colour tones.

The sandstones are overlain to the south by an assemblage characterized by yellowish-green and bluish-green tones, representing essentially a volcanic stratigraphy of the Fortescue group with interlayered siltstones, shales, tuffs, etc. Several stratigraphic zones with differing colour tones can be traced within this succession. Some of the broader lava horizons are characterized by the development of scattered patches of fairly deep, lateritic residual soils.

The top of the Fortescue group is marked by scattered small outcrops of the Roy Hill shale member, a generally leached white-and-grey sediment giving rise to a distinctive white signature on the image.

Immediately south of the above occurs a persistent and resistant horizon known as the Marra Mamba iron formation. This chert and jaspilitic iron formation constitutes the base of the overlying Hammersly group and can be continuously traced virtually across the entire southern part of the image. It has a dark grey-green tone and is marked along its south side by patches of extremely dark-green material representing residual red cappings of hematitic and canga iron deposits.

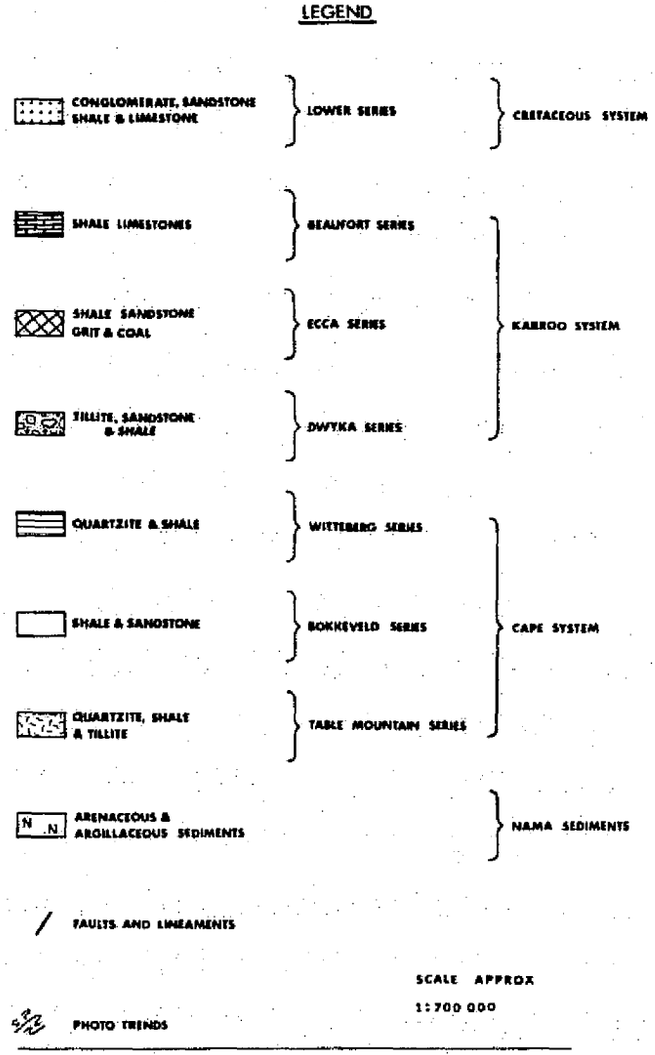

Other ferruginous deposits in the area also have a dark-green false colour signature and appear to be related largely to the present drainage system. Extensive lateritic and ferricrete deposits are associated with many of the tributaries of the Noreena and Kulkinbah Creeks. In part these probably also represent ferruginized shaly and cherty materials within the Fortescue group.

Extremely dark, narrow, bluish-green patches are strung out along the head-water tributaries of the Nullagine and Shaw rivers. These represent the ferruginized remnants of ancient river terraces.

Several distinctive classes of recent deposit are clearly revealed by colour tone and texture along the

FIGURE 4. Portion of ERTS image No. 1143-07560, December, 1972, showing details of fold patterns and other structure in the Cape fold belt of the southern Cape Province of South Africa. Scale of imagery approximately 1:700 000.

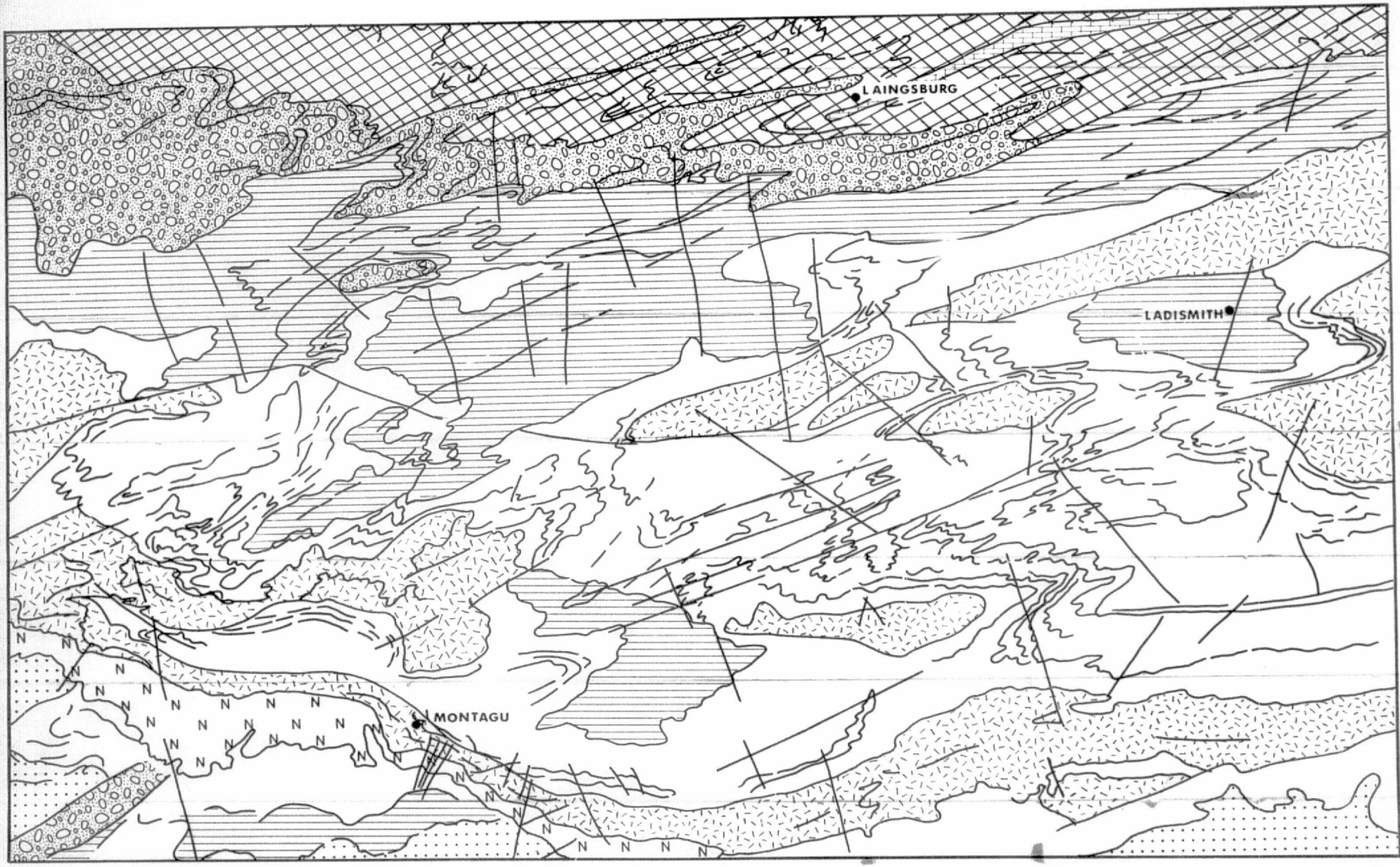
LAINGSBURG
LADISMITH
MONTAGU

Fortescue river in the south-western part of the image. Braided outwash fans and talus deposits are developed on either side of the broad flat valley of the river and are clearly recognizable because of texture and colour. To the north of the river these deposits consist largely of banded chert and iron formation fragments and are derived mainly from the Marra Mamba formation. In the extreme south west similar deposits are derived largely from the Brockman iron formation (not seen on the image).

A subtle zonation is apparant within the alluvial fans with a zone of darker green, probably more iron-rich material, for example, clearly covering the distal (southern) part of the braided talus deposits derived from the Marra Mamba iron formation.

A zone of light, pinky-grey material on the flats of the Fortescue river plain constitutes the virtually horizontal, distal parts of both alluvial fans. These deposits are considered to represent chemical precipitates, forming at the present time in the distal portions of the fans. They consist largely of limestones and some calcareous gravels with opaline silica and terminate abruptly against the recent alluvial river deposits of the broad, flat Fortescue river plain. The latter have light-yellowish-grey tones. Minor patches of probable chemical sediments can also be observed within these alluvial beds.

Light, pinky-grey limestone and opaline silica deposits are well developed and clearly discernible along the Noreena Creek. In places they pass through a bright green-coloured transitional zone of fine outwash material and chemical sediment to the broad orange coloured interfluvial sand flats.

Along the north western tributary of Noreena Creek, limestone deposits occur in direct contact with the interfluvial sand flats. Several different tones, ranging from orange to yellow, probably indicate different textures and particle sizes of outwash and interfluvial sand accumulations.

DEFINITION OF GEOTECTONIC DOMAINS

The broad synoptic view provided by ERTS imagery is ideally suited to a study of the diagnostic macrostructures of different geotectonic domains. In the crystalline basement terrains of the earth's shield areas, the two most important geotectonic entities are the so-called granite/greenstone cratons and the metamorphic mobile belts. In several instances ERTS-1 imagery has allowed for a more accurate definition than exists at present of the contact zones between these two geological entities as well as for a perspective and new synoptic view of the important diagnostic macrostructures within the two domains[14].

The Granite-Greenstone and Mobile Belt Pattern

The archaean granite-greenstone terrains appear to be remarkably similar in all of the better known shield areas of the world. Volcano-sedimentary sequences known as greenstone belts are the most distinctive features of these terrains and represent the remnants of previously more extensive accumulations of volcanic and sedimentary rocks. The greenstone belts in their present form appear to 'float' in the form of deformed synclinal 'keels' or 'rafts' in complex granite terrains[15].

Most belts have been subjected to strong structural deformation that is responsible for their characteristic form. Narrow, arcuate schist belts trending at various angles from the main belt are particularly important as are large-scale isoclinal folds with axes more or less parallel to the regional grain of the belt.

The lowermost volcanic assemblage of most greenstone belts commences with a suite of ultramafic and related rocks, intermediate to acid tuffs and magnesium-rich basalts. Some of the ultramafics represent sub-aqueous peridotite lavas while others form part of layered intrusive ultramafic complexes. The lowermost volcanic succession is overlain largely by metatholeiitic basalts (greenstones) with narrow interlayers of acid lava and chert. Shales, greywackes, and quartzites form the uppermost stratigraphic assemblages of most belts.

Several different types of granitic rock, each with its own tectonic style, are generally present. The oldest are invariably gneisses of tonalitic composition, and often intrude the lowermost volcanics in the form of diapiric domes. The arcuate schist belts tend to drape around these domes, which are responsible for the distinctive greenstone pattern noted earlier. Younger potassium-rich granites tend to sharply transgress earlier structural trends.

Surrounding and dividing the cratonic nuclei are a series of metamorphic mobile belts. Such belts are essentially linear zones of high-grade metamorphism and granitization and show evidence of plastic flowage folding with the development of a complex pattern of re-folded folds. Major linear zones of transcurrent dislocation are common, particularly along the marginal zones of the mobile belts and there is usually evidence of repeated fault movement. From the above it is clear that the major structures typical of these belts are very different from those encountered in greenstone

FIGURE 5 (a). Portion of ERTS image No. 1050-07355, September, 1972, showing the extent of the Dolomite Group of the Transvaal Sequence with certain elements of the dolomite stratigraphy being discernible. Scale of imagery approximately 1:800 000.

FIGURE 5 (b). Portion of ERTS image No. 1158-07363, December, 1972, covering the same area as 5 (a) but with a number of stratigraphic components within the Dolomite Sequence being clearly discernible. Scale of imagery approximately 1:800 000.

FIGURE 5 (c). Extent of the Dolomite Group in the same area obtained from the best available published geological maps. Scale of map 1:800 000.

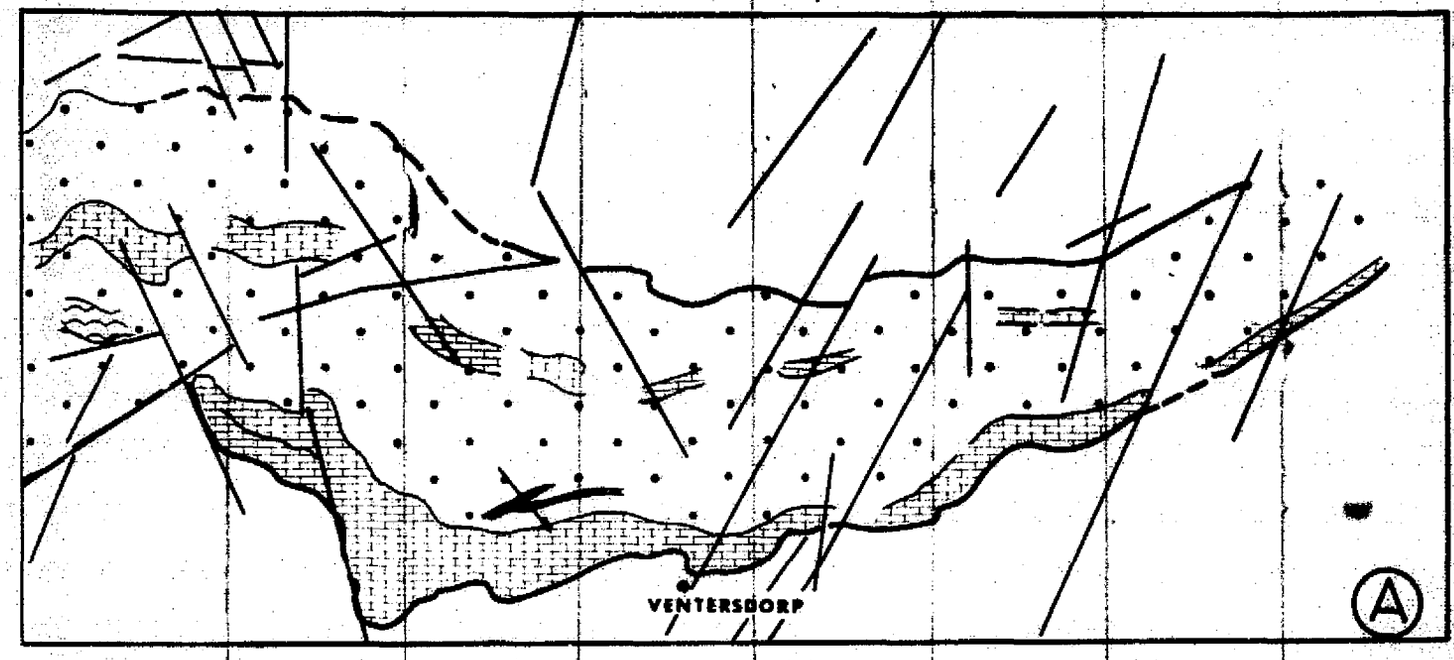

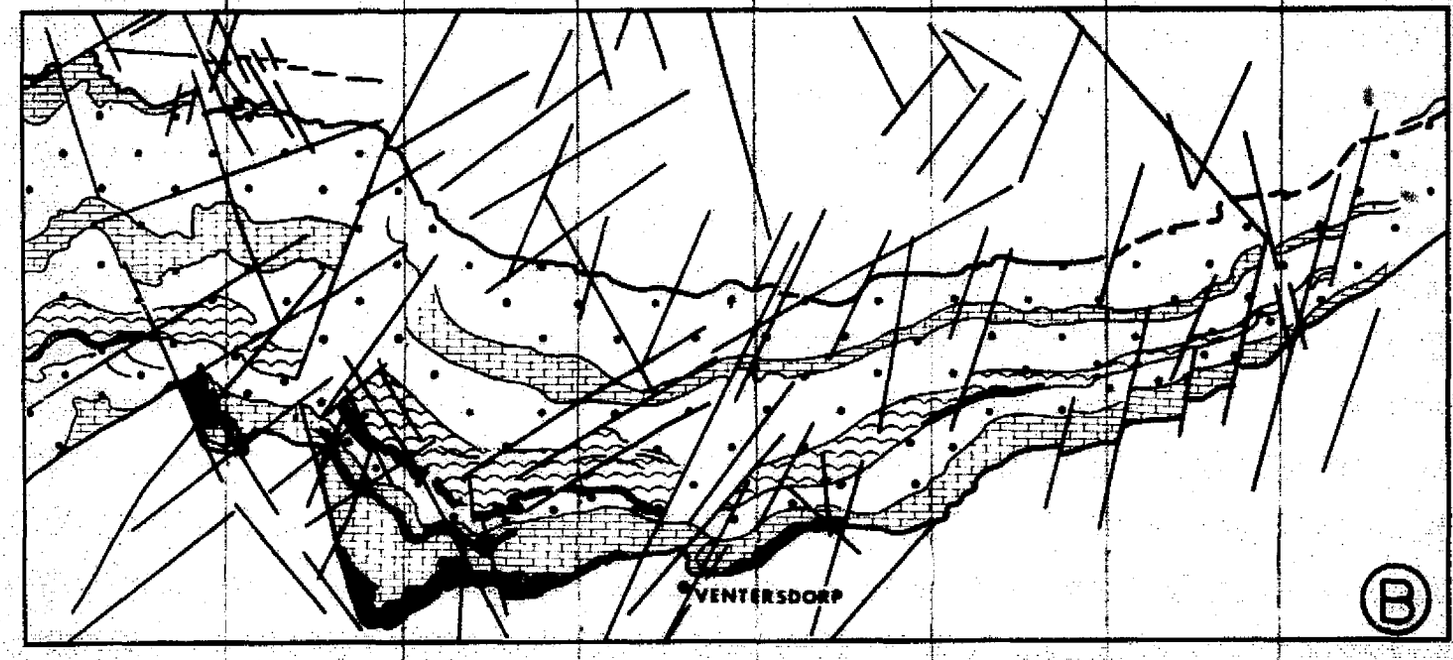

LEGEND

ESTABLISHED LIMITS OF TRANSVAAL DOLOMITE

INTERPOLATED CONTACT OF TRANSVAAL DOLOMITE

DOMINANTLY LIGHT, CHERT-RICH DOLOMITE, NOT DIFFERENTIATED IN C

STRATIGRAPHIC ZONES COMPRISED MAINLY OF DARK, CHERT-POOR DOLOMITE

AS ABOVE BUT NARROWER AND AT TIMES WITH DARKER TONES REPRESENTING DARK, CHERT-POOR DOLOMITE

ZONE COMPRISED OF ALTERNATING DARK, CHERT-POOR DOLOMITE AND LIGHT, CHERT-RICH DOLOMITE

ERTS LINEAMENTS REPRESENTING FAULTS AND JOINTS

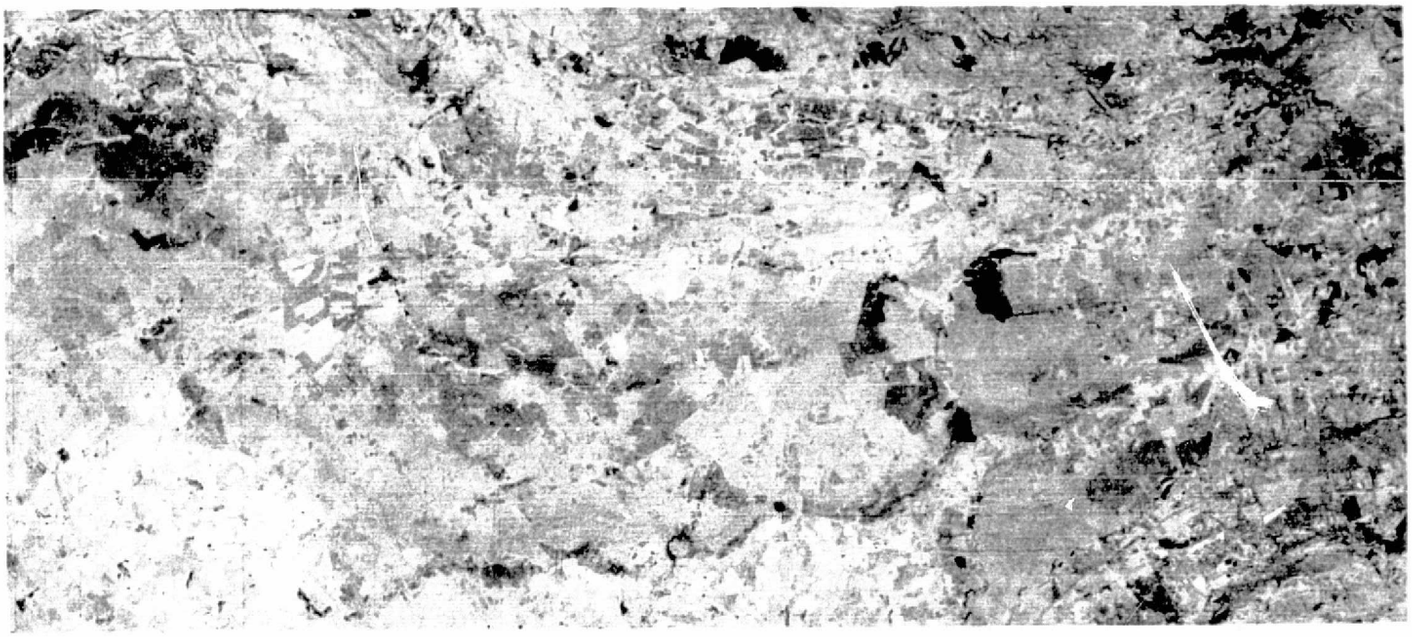

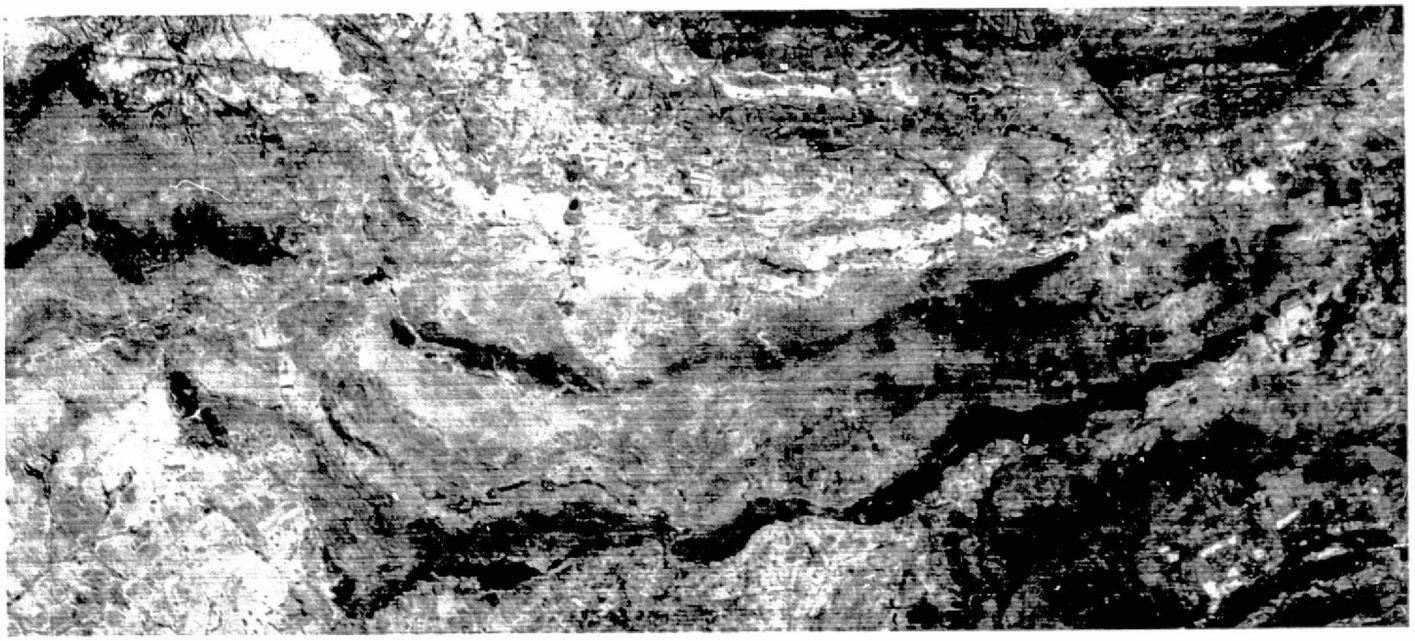

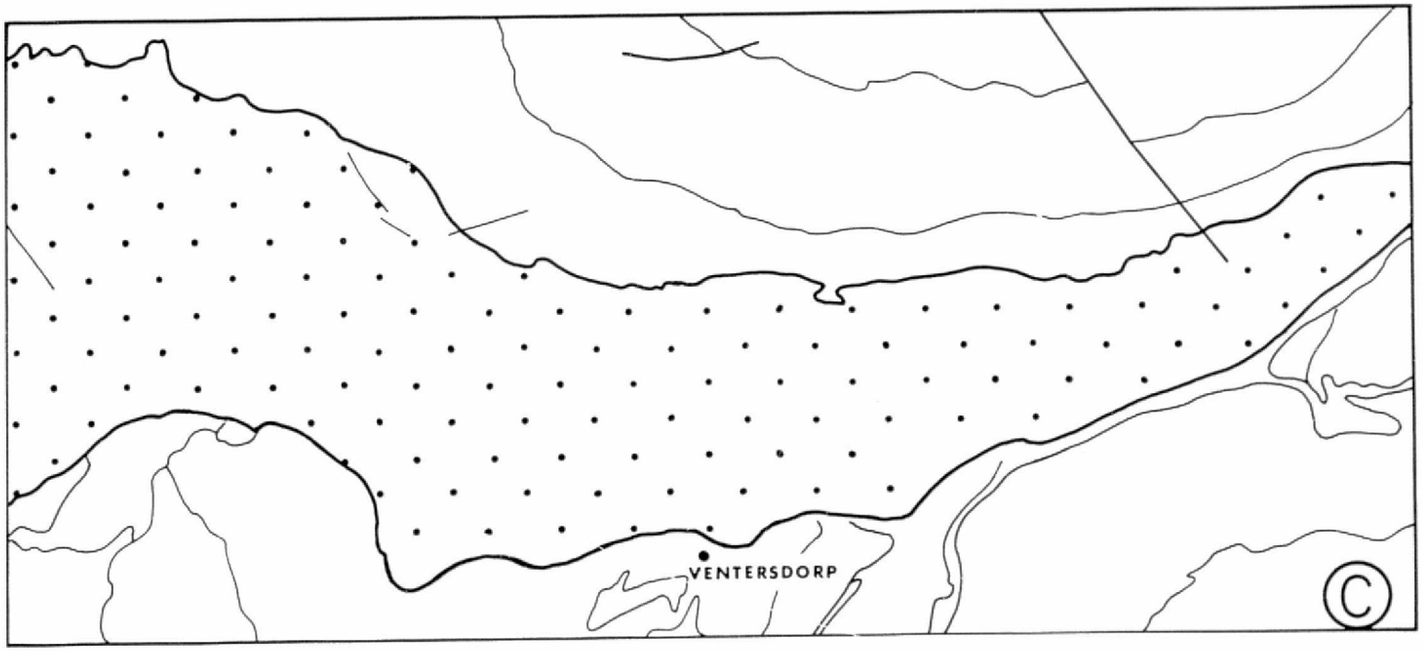
VENTERSDORP
©

belts and they reflect fundamental differences in the geotectonic setting of the two environments.

The Granite-Greenstone terrain of Southern Rhodesia

ERTS-1 image number 1103-07291 covers part of the southern sector of the Rhodesian craton and a portion of the linear north marginal zone of the Limpopo mobile belt (Figure 8). All of the greenstone belts have been mapped by the Rhodesian Geological Survey, but the geology of much of the granite terrain and the mobile belt is poorly understood with available data being mainly from photogeological interpretation.

The Great Dyke is seen in the central part of the image and is the most clearly defined feature. The bulk of the Dyke is ultramafic in nature (grey-blue on the colour composite image) but contains very well-defined (heavily vegetated) layers and canoe-shaped remnants of gabbro that give an exceptionally clear view of the internal structure of the body.

All the features of the granite-greenstone environment are clearly visible. These include the arcuate schist belt slivers that are striking features in the case of the Buhwa, Gwanda, and Filabusi belts. Certain of the stratigraphic components of the greenstone belts are also distinguishable, particularly in the case of the Shangani belt where the lowermost stratigraphic assemblage comprised of a resistant layered ultramafic body along the north margin and banded ironstones and magnesium metabasalts along the east margin, form conspicuous features. This zone, clearly distinguished by dark grey colour tones, can be traced southwards where it appears to swing to the south-east and continues along the northern flank of the Filabusi belt. A layered body similar to the Shangani body is also developed in this area. The Shabani and Mashaba ultramafic complexes are clearly visible and the waste dumps from asbestos mining operations are conspicuous. The younger intrusive nature of the Mashaba ultramafic body is clearly demonstrated by the western limb of the intrusive, which is superimposed on a north-south stratigraphy consisting of greenstone belt slivers lying within tonalitic gneisses.

In all cases the internal structure (mainly folding) and the gross stratigraphy of the greenstone belts is discernible. In addition all the major mines in the area are clearly recognized by their waste dumps, which generally have white-to-blue tones.

The distinctive geotectonic styles of the various cratonic granites are also to be seen. The generally featureless terrain, which gives rise to lighter colour tones, is underlain by the tonalitic gneiss assemblage. Arcuate greenstone-belt tongues protrude into this material and probably define or partly define individual diapiric tonalitic batholiths. Numerous cross-cutting, potassium-rich granite bodies occur in the area and as a result of their somewhat more resistant and jointed nature have greater water-holding properties. This has resulted in a more luxuriant plant growth that clearly defines such bodies.

The most well defined of these bodies intrudes the Shangani belt causing abrupt truncation of all the stratigraphic trends. In addition, several other similar but somewhat smaller bodies are also discernible in the western sector of the image. An extensive and as yet unmapped elongated zone of potassium-rich granite has recently been identified by the Rhodesian Geological Survey in the zone between the Shabani and Buhwa greenstone belts. The contacts of this granite (termed the Chibi batholith), which might be a marginal manifestation of the Limpopo metamorphic mobile belt, can be mapped with remarkable accuracy from the image. The body is characterized by a spectacular joint and/or fault system normal to the contact of the mobile belt. The jointing has led to the development of numerous component granite domes that are surrounded by thick vegetation.

Besides the Great Dyke, two narrow but well-defined parallel satellite dykes are also conspicuous features of the image. These, together with a number of other dykes that are also clearly seen, give a good indication of the type and extent of faulting that appears to have right lateral movement.

Part of the north marginal zone of the Limpopo mobile belt occupies the S.E. part of Figure 8 and is discussed later in the section on the mobile metamorphic belt environment.

The Granite-Greenstone terrain of the East Pilbara region – Western Australia

Part of the East Pilbara granite-greenstone terrain of Western Australia is shown in Figure 9. This is perhaps one of the most spectacular ERTS images known of a granite-greenstone area in which the distinctive geotectonic pattern is remarkably clear. Up until recently the only available geological map of this area was a broad reconnaissance one on which many of the features discernible on the ERTS image were not depicted. More detailed but uncoloured maps of this area have recently been published but do not afford quite the same regional insight into the area.

Several diapiric tonalitic batholiths form the most striking features of the area and these are encircled by narrow arcuate greenstone belts. Although the granite greenstone contacts appear to be regionally conformable, numerous areas of local transgression are evident and in many instances

FIGURE 6. ERTS image No. 1147-08163, December, 1972, illustrating the enhancement of hitherto-unmapped stratigraphic components of flat-lying strata of the Nama system in southern South West Africa. Scale of imagery 1:1 000 000.

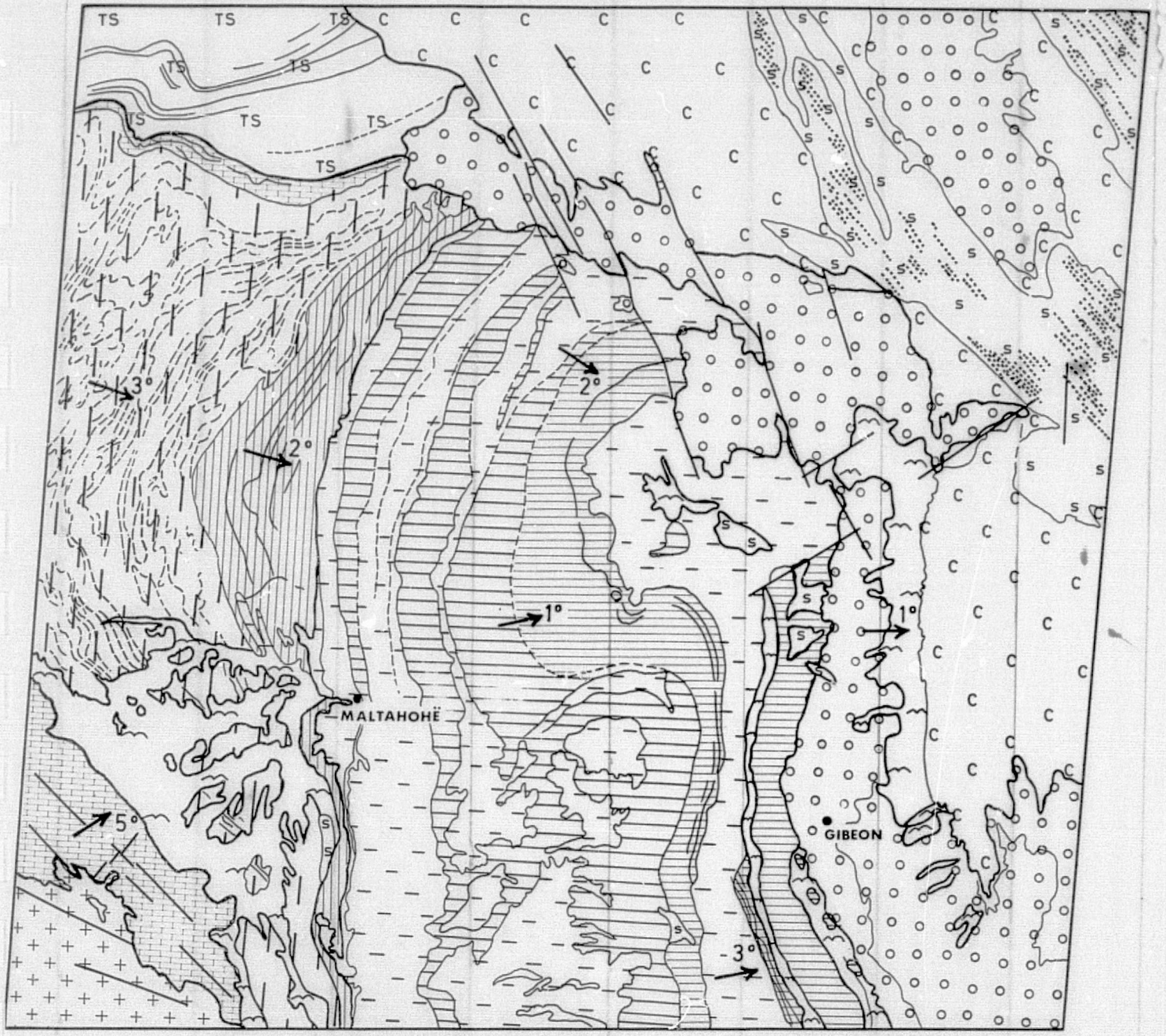

EXPLANATION

SCALE 1:1 000 000

- WINDBLOWN SAND INCLUDING DUNES
- CALCRETE
- ALLUVIUM
- SEDIMENTS AND VOLCANICS – KARROO
- TS — TSUMIS FORMATION
- BASEMENT
- RED ARGILLACEOUS SANDSTONE
- RED QUARTZITIC MUDSTONE
- RED MUDSTONE
  - } FISH RIVER FM.
- GREEN SANDSTONE AND SHALE
- GREEN SHALE INTERBEDDED WITH GREY QUARTZITE
  - } SCHWARZ RAND FM.
- BLACK LIMESTONE
  - } KUIBIS FM.
- } NAMA GROUP
- TRENDS
- ERTS LINEARS

35 V

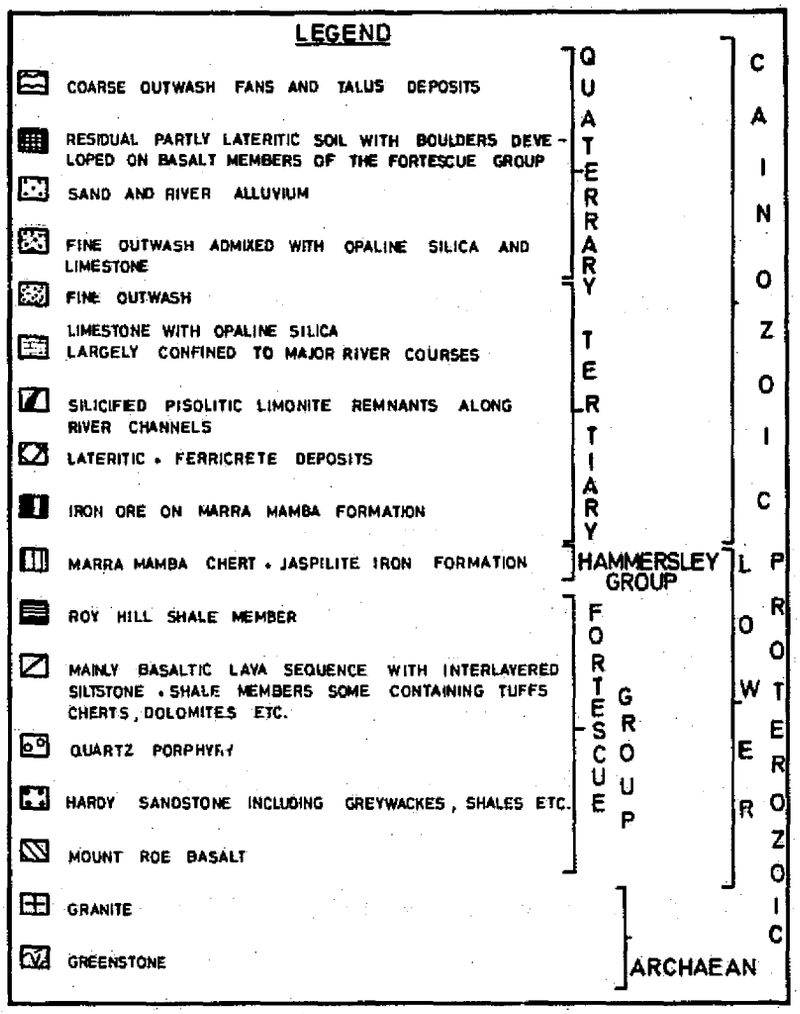

narrow tongues of greenstone material protrude into the granite and appear to become largely granitized. The above evidence supports a largely magmatic intrusive origin for much of the granitic material. Several different zones can be seen within the granite bodies including some characterized by a linear fabric generally parallel to the greenstone contact as well as coarser textured more resistant areas. The former represent areas of strongly foliated and banded gneisses as well as areas of granitization and hybridization of the greenstones, while the latter areas probably represent more resistant potassium-rich granites. A classical disharmonic fold structure (features common in greenstone terrains) can be seen in the bi-cuspate region between adjoining granite domes towards the central part of the image.

A layered stratigraphy is evident within the greenstone belts consisting of lighter and darker bands, the former representing essentially acid volcanic and related rocks and the latter basic volcanics. Some of the larger chert bands associated with the terminal phase of acid volcanic cycles can clearly be traced and are particularly clear in the area immediately west of Marble Bar. Virtually the whole greenstone assemblage, locally known as the Warrawoona, can be equated with the Mafic to Felsic Unit, an ubiquitous feature of most other greenstone belts[15].

Towards the east central part of the area a distinctive package of rocks with a light tone and with a finely banded linear trend can be discerned. This is known as the Mosquito Creek group and represents a distinctive assemblage of sediments in the form of greywackes, subgreywackes, shales, and quartzites. Some mafic volcanics in contact with granite, occur along the south flank of this sequence.

The mobile metamorphic belt environment

Features considered to be typical of the mobile

FIGURE 7. Enlarged portion of ERTS image No. 1148-01282, December, 1972, covering part of the east Pilbara area of Western Australia and showing the distribution of Cainozoic and Proterozoic cover formations, various components of which can clearly be distinguished by distinctive colour tones. Scale of imagery approximately 1:500 000.

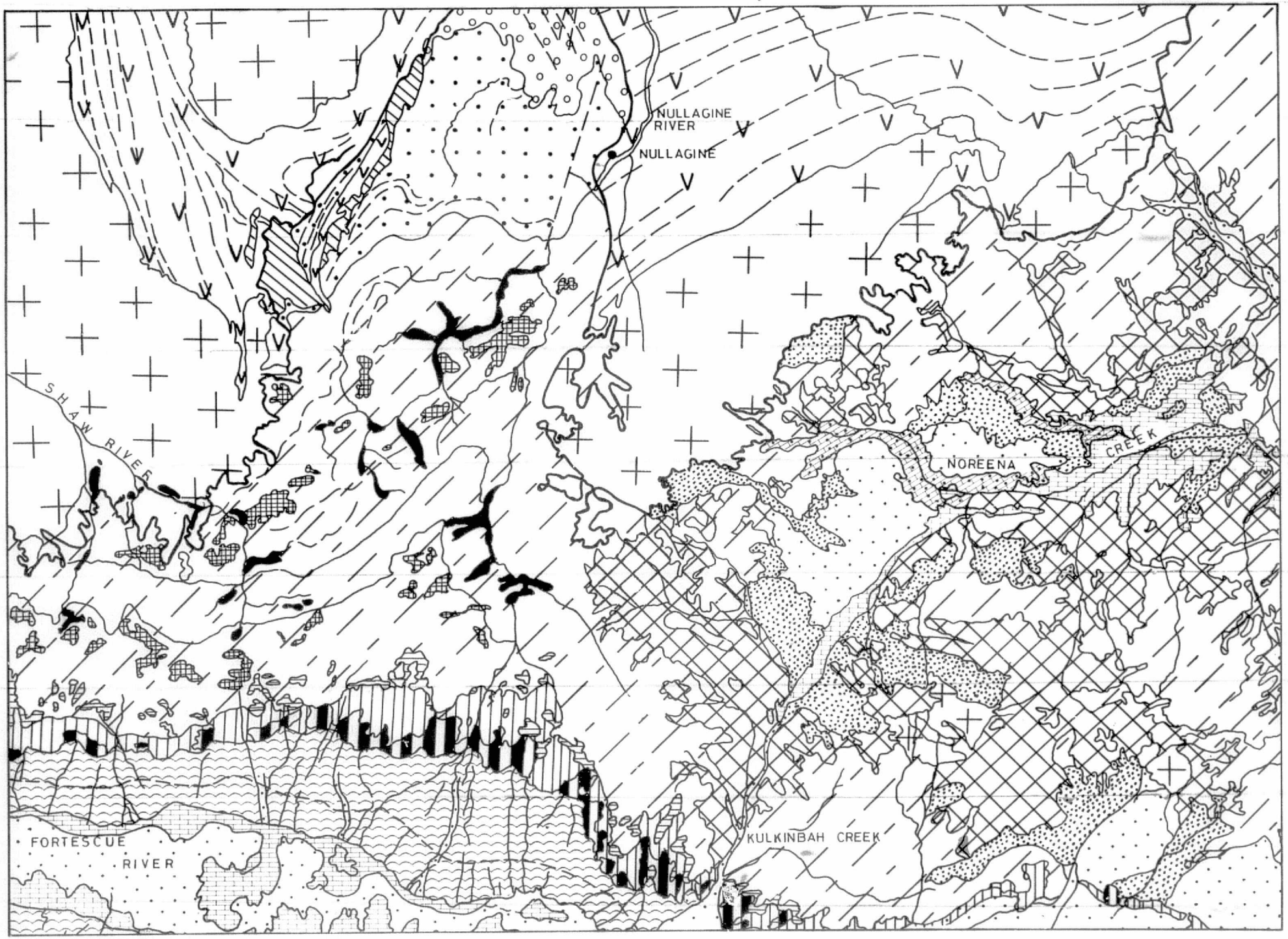
NULLAGINE RIVER
NULLAGINE
SHAW RIVER
NOREENA CREEK
FORTESCUE RIVER
KULKINBAH CREEK

metamorphic belt environment, and particularly the pattern of complex folding, are clearly seen on imagery covering the Namaqualand belt of the N.W. Cape. Figure 11, to be discussed later, is an ERTS mosaic of this region, and Figure 3, discussed earlier, is an enlargement of part of this high-grade metamorphic terrain along part of the Tantalite Valley fault zone.

Part of the north marginal zone of the Limpopo mobile belt occupies the S.E. part of Figure 8 and although lacking the large-scale flowage folding features, present only in the central part of the belt, the distinctive linear grain, tonal difference, and absence of arcuate forms readily distinguishes this terrain from the granite-greenstone terrain to the north. The strong linearity of trends along the north margin is due to tectonic overprinting in the form of shearing and major transcurrent dislocation.

Another example of a metamorphic mobile belt environment is provided by the central zone of the Damara geosyncline of S.W.A. Granite intrusion and high-grade metamorphism have resulted in a complex fold pattern that is very distinctive and readily distinguishable from the pattern in the Khomas schists to the south (Figure 13). These schists have suffered only greenschist facies metamorphism and retain a characteristic linear trend lacking the more intricate pattern of the high-grade metamorphites.

From the above examples it is the writers' opinion that the broad synoptic view provided by the imagery is ideally suited to a study of the diagnostic macrostructures of major geotectonic domains. ERTS-1 imagery should, for example, allow for a better understanding and for a more accurate definition than exists at present of the contact zones between the granite greenstone and metamorphic mobile belt environments. This may be of considerable economic importance since basic/ultrabasic rocks containing some of the world's largest nickel deposits have been emplaced along similar contact regions within the Canadian Shield. These include the Thompson belt deposits at the junction of the Superior Craton with the Churchill mobile belt and the Sudbury nickel irruptive lying within the contact region of the Grenville front (mobile belt) and the Superior granite-greenstone province.

MINERAL EXPLORATION

It is the authors' contention that ERTS imagery will play an ever-increasing role in mineral exploration if used for specific problems in the various facets of exploration and in conjunction with other exploration techniques. The practical use of ERTS in mineral exploration can be defined as follows.

- Defines areas of regional interest and sometimes focusses on specific structures and other surface anomalies as possible exploration targets. Eliminates large areas of little or no mineral potential, particularly in those regions where geological knowledge is limited.
- Provides important information necessary for planning practical aspects of an exploration programme, including exploration techniques, and reduces the time in reaching decisions on setting up a programme.
- Provides better geological maps than those available in many regions of the world. Occasionally ERTS provides unique geological information not obtainable through other methods.
- Assists geoscientists in gaining a better understanding of regional geological factors, results in a broadening of geological knowledge, and aids in inspiring more imaginative overviews.
- Saves time and money.

The most important use of the method undoubtedly lies in the early phases of regional exploration programmes when it is imperative to gain regional geological maps to evaluate the relationship between known mineralization and the regional geological framework of a particular area. An understanding of this type is, and will become more and more critical in future exploration programmes particularly in little known and poorly mapped terrain as it enables geologists to select 'target areas' for more detailed follow-up work by conventional exploration techniques. This is particularly important in South Africa where mineral rights are generally in private hands and the acquisition of options can be costly.

As pointed out by Grootenboer *et al*[16], the most important application of ERTS by exploration companies lies in the field of geological mapping, structural analysis, and the identification of geotectonic domains, aspects discussed previously in this paper.

It should be stressed, however, that ERTS data only supplement rather than supplant existing exploration techniques. Other methods will be employed much as they have been, especially for deeper mineral deposits. The sequence of exploration remains: (1) data compilation, (2) selection of target areas, (3) basic mapping, (4) selective geophysical and geochemical prospecting, and (5) drilling to determine the amount and extent of the deposit. ERTS' contributions are orientated towards phase (2) above and, to a lesser extent, phase (3).

Exaggerated claims have been made about the ability of ERTS to locate new mineral deposits but

FIGURE 8. ERTS image No. 1049-07290, September, 1972, covering part of the southern portion of Rhodesia and showing the contrasting tectonic styles illustrated by the Rhodesian granite-greenstone craton and the north marginal zone of the Limpopo Mobile Belt. Scale of imagery 1:1 000 000.

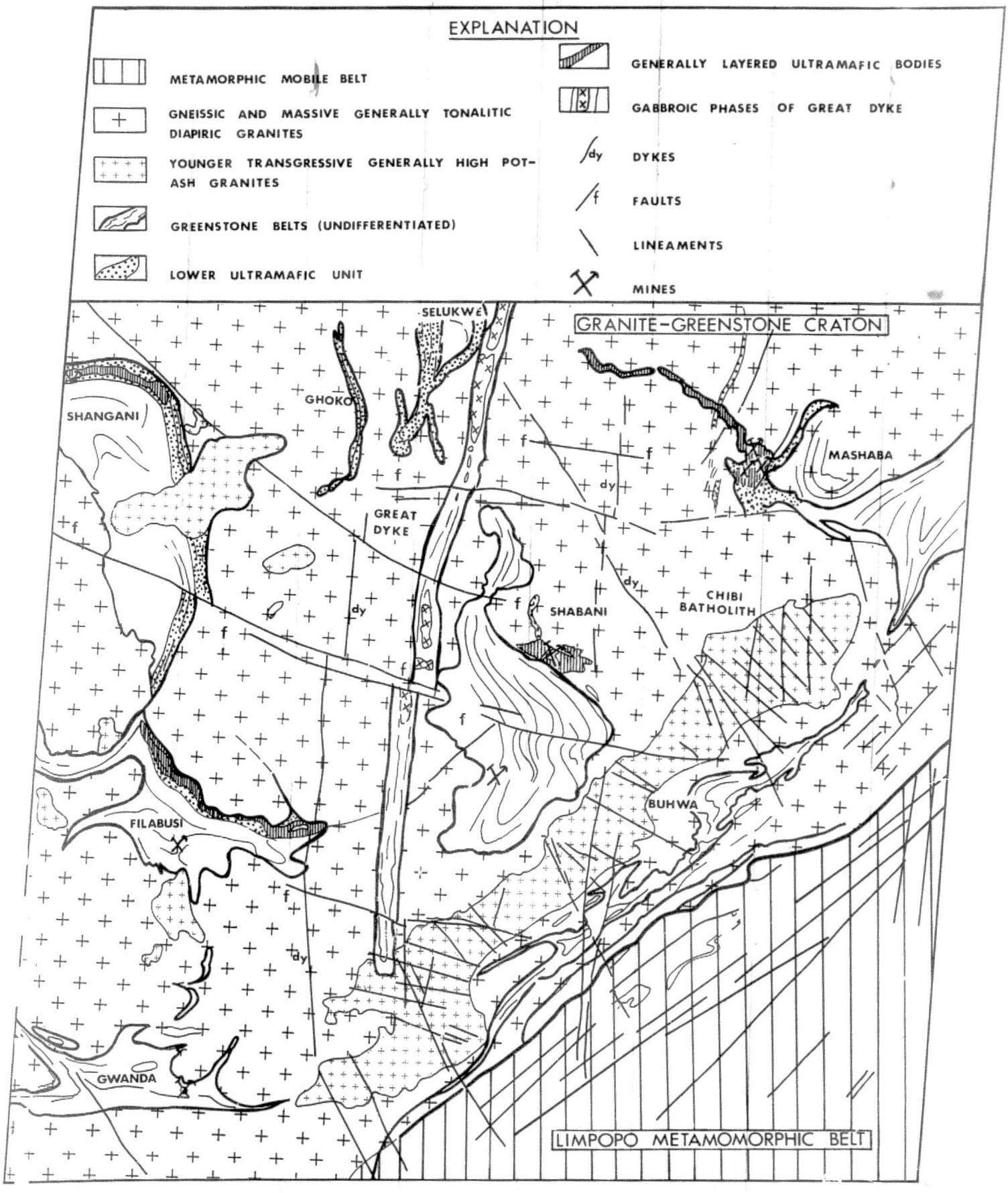
EXPLANATION
METAMORPHIC MOBILE BELT
GNEISSIC AND MASSIVE GENERALLY TONALITIC DIAPIRIC GRANITES
YOUNGER TRANSGRESSIVE GENERALLY HIGH POTASH GRANITES
GREENSTONE BELTS (UNDIFFERENTIATED)
LOWER ULTRAMAFIC UNIT
GENERALLY LAYERED ULTRAMAFIC BODIES
GABBROIC PHASES OF GREAT DYKE
dy DYKES
f FAULTS
LINEAMENTS
MINES
GRANITE-GREENSTONE CRATON
SELUKWE
GHOKO
SHANGANI
MASHABA
GREAT DYKE
SHABANI
CHIBI BATHOLITH
BUHWA
FILABUSI
GWANDA
LIMPOPO METAMOMORPHIC BELT

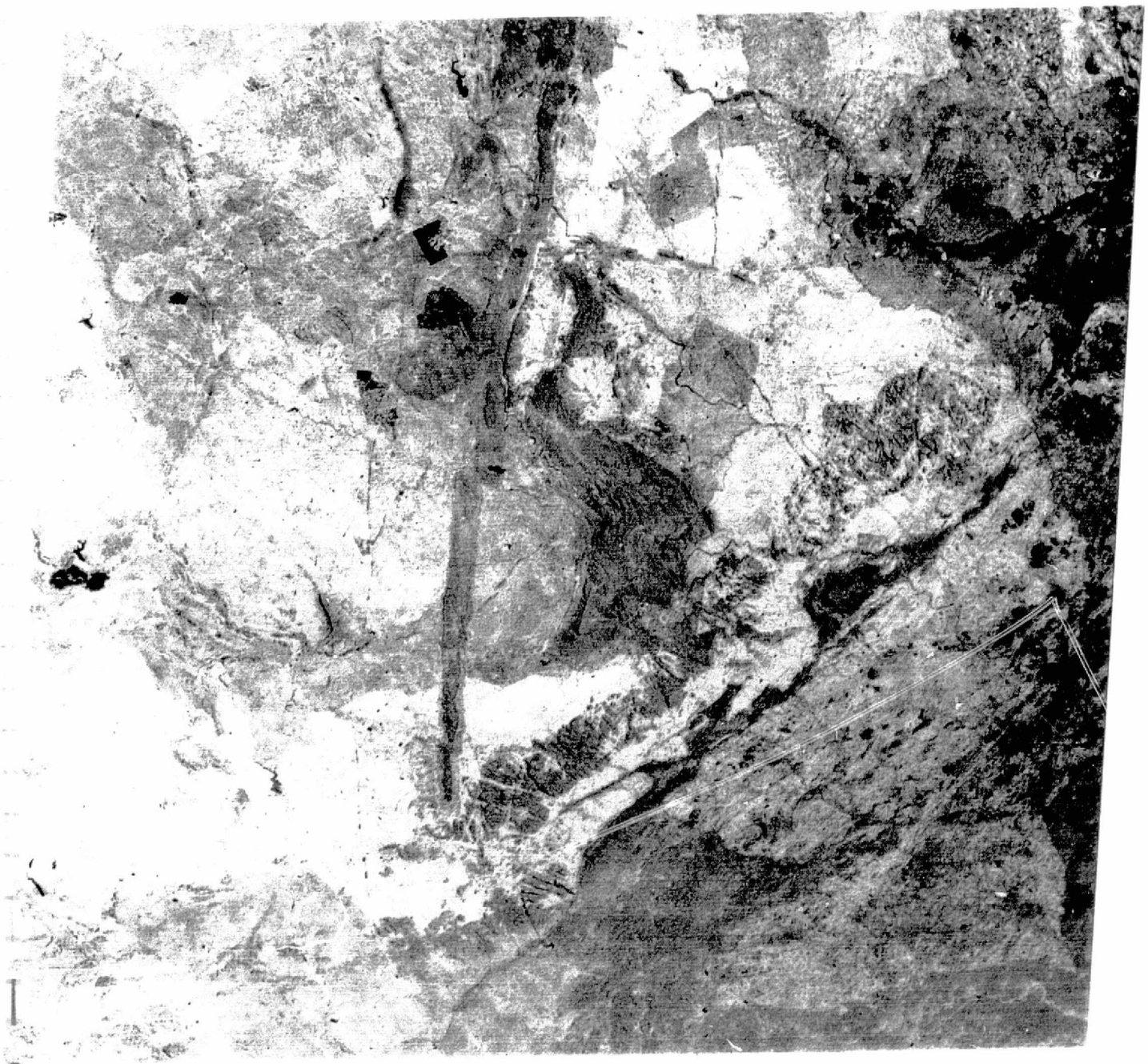

to date there have been no verified reports of ore bodies discovered exclusively from the use of ERTS imagery. Under appropriate conditions, however, mineral deposits that extend to the surface may be characterized by distinctive surface manifestations such as gossans or zones of alteration. If these surface products cover large enough areas and have distinctive spectral properties then they should, theoretically at least, be detectable from ERTS imagery.

Goetz and Rowan (referred to by Short and Lowman[9]) have reported encouraging results in this connexion in so far as limonite appears to give a spectral response that is quite different from other common minerals and that with suitable processing of computer compatible tapes it might become possible to enhance areas of limonitic enrichment.

Two case histories serve to demonstrate the use of ERTS imagery in mineral exploration programmes in Southern Africa.

Case history no 1

The N.W. Cape Province

The N.W. Cape Province of South Africa provides a good example of the practical advantage of ERTS-1 imagery in providing a regional geological framework as a guide to a mineral exploration programme in a largely unmapped terrain[17]. Available geological maps of this area at the time of the discovery of a number of base-metal deposits only covered a strip of country along the south bank of the Orange river and a region to the west and south of the Springbok-Okiep copper mining area (Figure 10).

From the point of view of competitive mineral exploration it was essential that an insight into the regional geological controls of the base metal mineralization of the area be obtained as rapidly as possible. Conventional methods of producing suitable regional geological maps were considered to be too time-consuming and the region therefore provided an excellent test of the use of ERTS-1 imagery in mineral exploration.

Eight ERTS-1 colour composite images enlarged to a scale of 1:500 000 were used in the compilation of a regional geological map and a mosaic constructed from these images has been reduced to a scale of approximately 1:2 000 000 (Figure 11).

Before any interpretation was carried out, a detailed study of all the available published maps was made in order to correlate the expression of various formations with features seen on the ERTS images.

Reconnaissance road traverses were undertaken in both the mapped and unmapped areas to establish ground truth. Final interpretation was carried out after a certain amount of mapping had been done directly on the images, correlating geological features from a light aircraft flying at an altitude of about 3 000 metres above ground level. These data were then plotted onto 1:500 000 topographic sheets, somewhat simplified and finally reduced to a scale of approximately 1:2 000 000 (Figure 12).

General geology

The area under consideration is divisible into four main geological entities, the most important of which is an extensive 1 000-million-years-old, metamorphic gneiss terrain, the Namaqualand Metamorphic Complex, which is well exposed in the valley of the Orange River. The metamorphic terrain is terminated to the east of Upington by a major NNW–SSE trending zone of dislocation (the Brakbos fault zone). This fault zone separates the metamorphites from a very much older granite-greenstone terrain lying to the east and known as the Kaapvaal craton. In the area under consideration, the Kaapvaal craton is, for the most part, largely covered by relatively unmetamorphosed, predominantly sedimentary rocks, belonging to a series of extensive proterozoic basins. Geochronological studies indicate that most of the basement granites of the Kaapvaal craton have ages in excess of 2 500 million years.

In the western portion of the area, in a region known as the Richtersveld (Figure 12), the structural style and the grade of metamorphism changes and a series of vulcano-sedimentary formations striking roughly north-south are associated with granite (the Vioolsdrift granite), which has an age of about 1 800 million years. In the north and south central portions of the area the Bushmanland metamorphites are overlain by much younger flat-lying sedimentary formations belonging to the Nama and Karroo systems. Each of these major geological entities will be described in turn with reference to their expression on ERTS-1 imagery.

Sedimentary formations of the Kaapvaal craton

One of the most striking features seen on the ERTS images is the spectacular discontinuity (the Brakbos fault zone) that separates the Kaapvaal craton in the east from the Bushmanland Metamorphic Complex in the west. The interface between the two structural provinces is not clearly defined in the field and had previously been drawn along the Doornberg lineament some 30 kilometres to the east of, and parallel to the Brakbos zone. The true position of the contact was first established by Pretorius[18] on the basis of results of a trend surface analysis of the regional gravity field. ERTS imagery, which became available after completion of the gravity study, clearly confirms the existence of the Brakbos fault zone and reveals all other structural

FIGURE 9. ERTS image No. 1148-01282, December, 1972, showing the granite-greenstone geotectonic pattern illustrated by the east Pilbara region of Western Australia. Note younger Proterozoic and Cainozoic cover rocks to the south. Scale of imagery 1:1 000 000.

3523

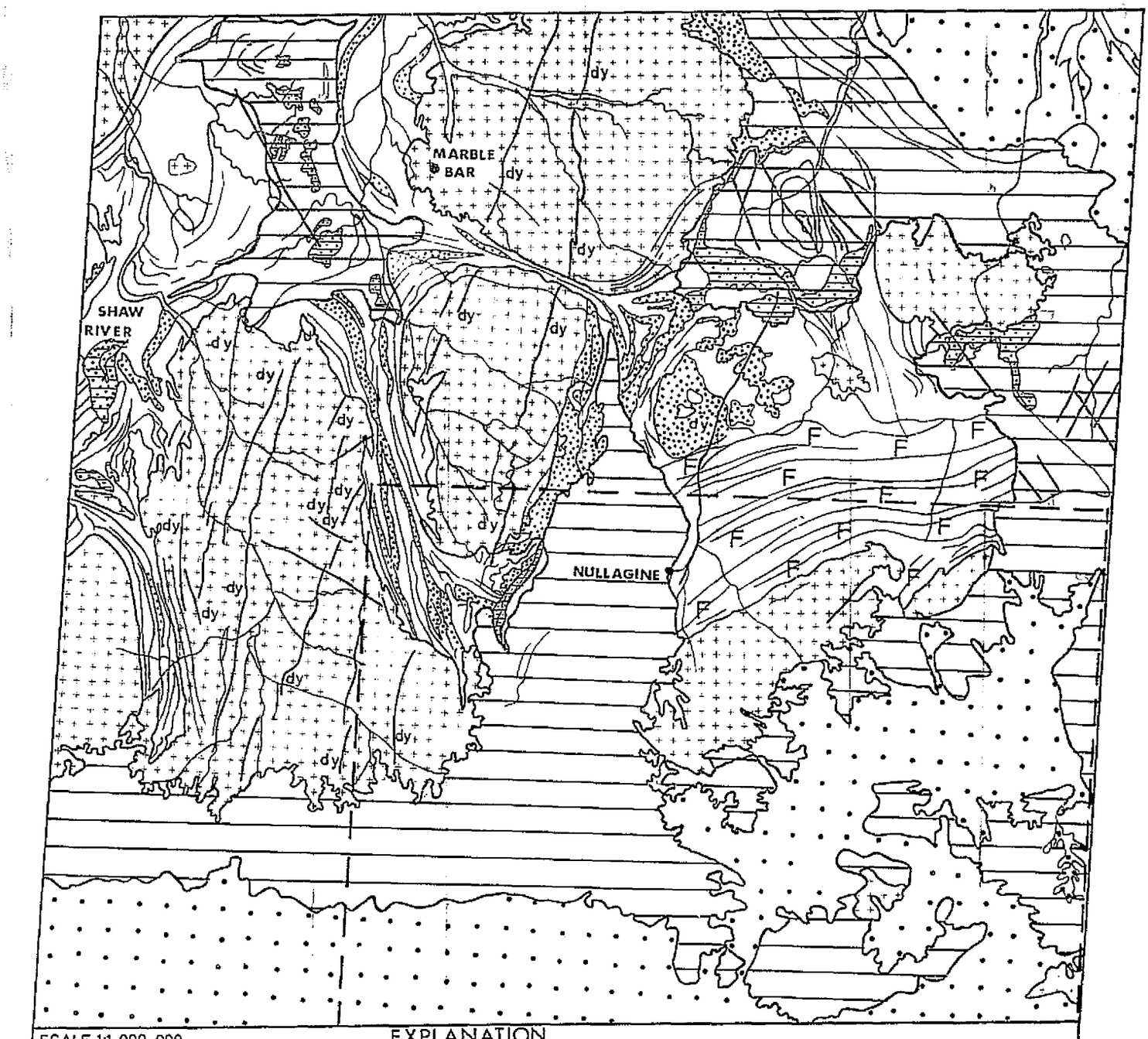

SCALE 1:1 000 000

EXPLANATION

- MAINLY CAINOZOIC COVER
- LARGELY INTERMEDIATE TO BASIC VOLCANICS — PROTEROZOIC
- LARGELY SEDIMENTS — PROTEROZOIC
- DIAPIRIC GRANITIC PLUTONS — ARCHAEAN
- SEDIMENTS OF THE MOSQUITO CREEK — ARCHAEAN
- MAINLY BASIC TO ULTRABASIC LAVAS — GREENSTONES — ARCHAEAN
- MAINLY ACID VOLCANICS + VOLCANOCLASTIC SEDIMENTS — GREENSTONES — ARCHAEAN
- dy MAJOR DYKES
- FAULTS & ERTS LINEAMENTS
- AREA COVERED BY MORE DETAILED INTERPRETATION (FIGURE 7)

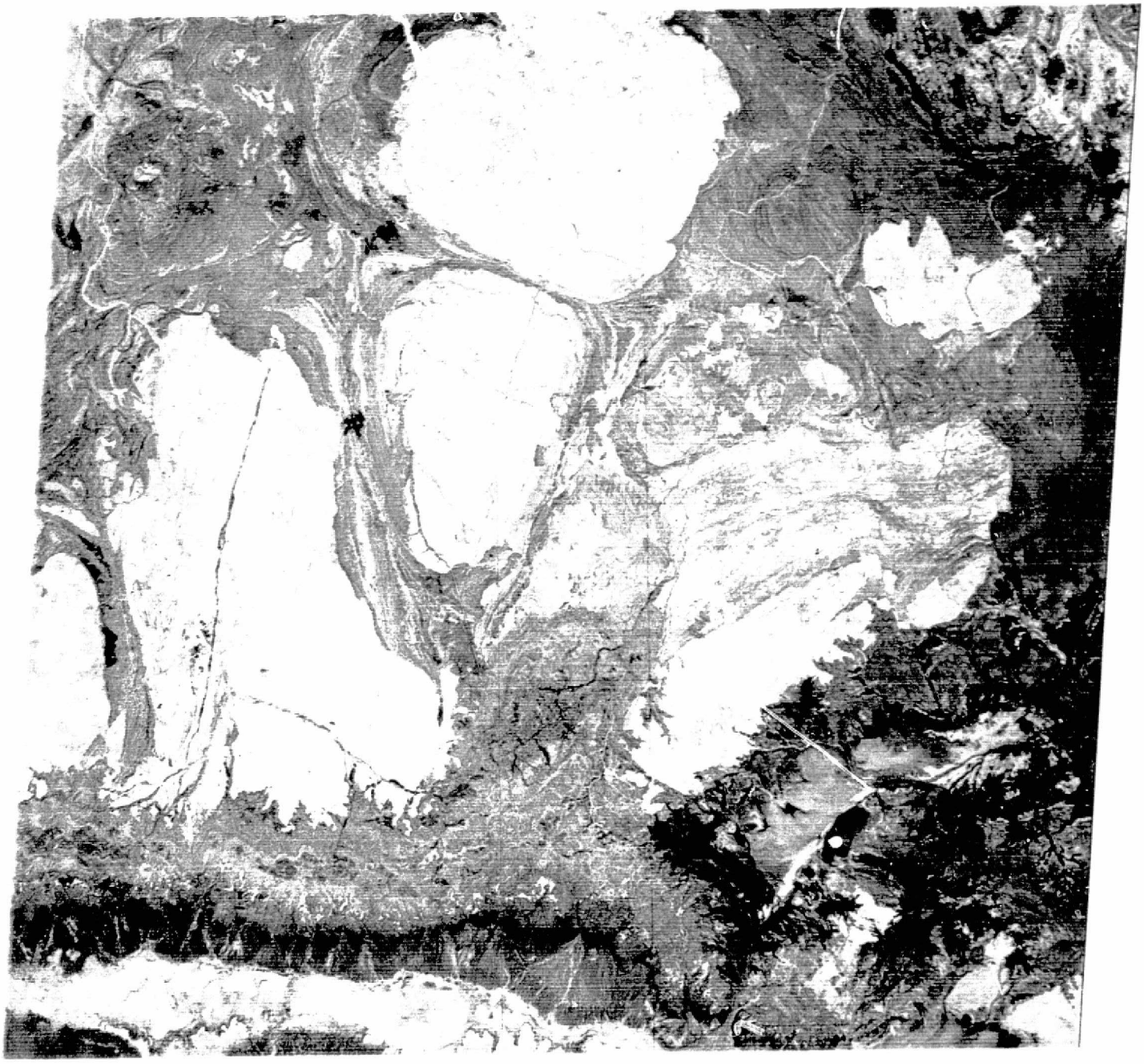

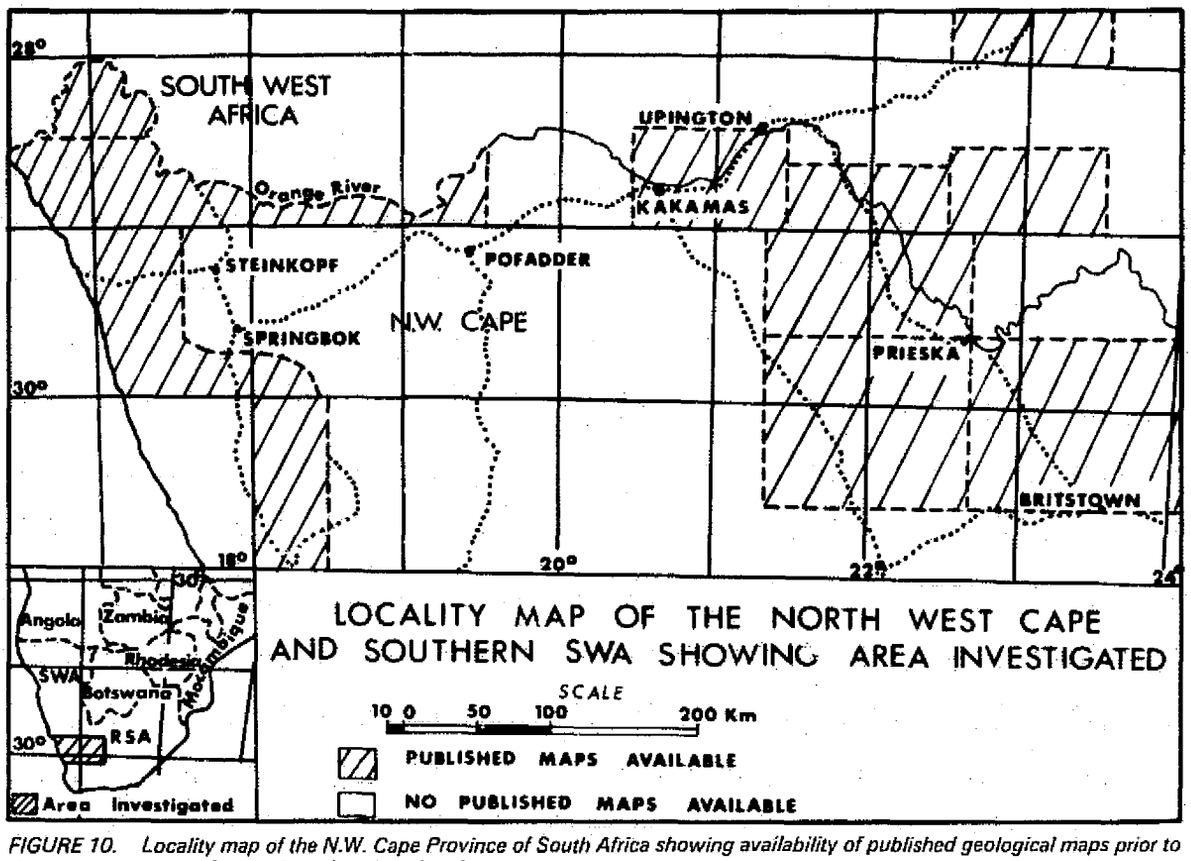

FIGURE 10. Locality map of the N.W. Cape Province of South Africa showing availability of published geological maps prior to the commencement of extensive mineral exploration programmes.

features deduced from the geophysical investigations. These include:

- ☆ a number of major faults parallel to and lying east of the Brakbos fault zone, clearly discernible in the country immediately west of the town of Prieska,
- ☆ intense deformation mainly in the form of folding of the north-south striking Proterozoic sedimentary formations as they approach the Brakbos fault zone from the north east,
- ☆ abrupt truncation of all Proterozoic sedimentary formations by the Brakbos fault zone with no evidence of them straddling this discontinuity and thus being represented within the Namaqualand Metamorphic Complex as has been suggested.

Pretorius[18] concluded that the earlier availability of the imagery would have rendered the re-assessment of the gravity field unnecessary.

Newly discovered Cu mineralization occurs along the Brakbos fault zone and the ease with which the zone can be traced on ERTS underlines the important contribution that the imagery can make in mineral exploration in terrain where conventional aerial photography had previously failed to disclose the presence of regional controlling structures.

Flat-lying sedimentary cover rocks

The imagery clearly reveals the distribution pattern of flat-lying sedimentary beds belonging to the Karroo and Nama systems that formerly covered most of the Namaqualand Metamorphic Complex. This pattern indicates both the erosive action of the Orange river and its tributaries and yields information regarding the underlying basement structure *(see later)*. Of particular interest are two fault-bounded blocks of Nama sediments extending from a point some 30 kilometres to the west of the Springbok-Okiep mining area towards the Orange river. The distinctive brownish colour tones of these Nama rocks, locally referred to as the Nient-Nababeep plateau, are clearly seen on ERTS imagery (Figures 11 and 12).

The Karroo sediments are characterized on ERTS by grey and dark grey colours. Areas of thick and thin Karroo cover are also apparent, expecially in the region to the south of Pofadder in the south-central portion of the mosaic (Figure 12). In addition dolerite dykes and sills within this formation can be mapped in great detail from the images and in many instances appear to be partly controlled by major linear features as in the area to the southwest of Kenhardt (see Figures 11

3526

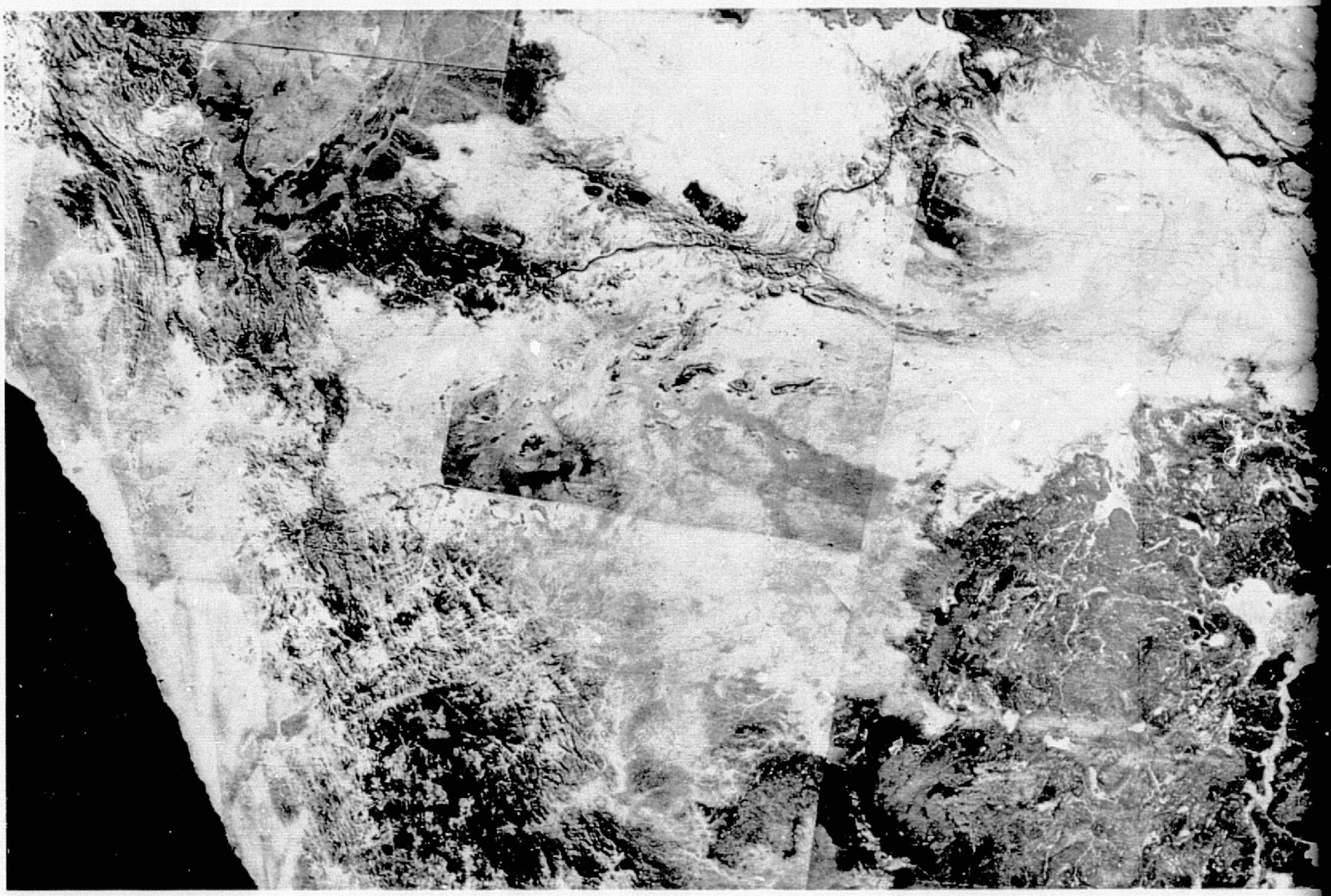

and 12). The location of numerous salt pans, especially in the area to the south of Kenhardt, is even more strongly controlled by these linear features (Figure 11).

Older vulcano-sedimentary formations of the west coast

Elements of the geology of the north-south trending vulcano-sedimentary formations of the Richtersveld area of the west coast are distinguishable on the imagery. In particular, the contacts of the Stinkfontein formation, which comprises one of the most important components of the geology, can be clearly demarcated. These rocks have not been involved in the 1 000 million year old metamorphic overprinting of the Namaqualand metamorphic event and have been intruded by granites that have radiometric ages of approximately 1 800 million years. Thus although the contact with the higher grade metamorphites to the east is not readily apparent from the imagery, the tectonic style of the vulcano-sedimentary formations is clearly different to the pattern displayed by rocks of the Bushmanland sequence, which have been involved in the thermal event referred to above.

The geology and structure of the Namaqualand metamorphic complex

The Namaqualand metamorphic complex forms part of a more extensive belt of 1 000-million-years-old metamorphic rocks that extends across the southern portion of South Africa and includes both basement and supracrustal rocks. Rock types encountered in the latter group are of considerable importance from an economic point of view and comprise a large variety of quartzofelspathic gneisses with variable amounts of biotite and muscovite, banded amphibolitic and calc silicate assemblages, and a variety of quartzitic rocks. The basement upon which they rest is ill-defined but is probably represented mainly by porphyroblastic augen gneisses.

The entire assemblage has undergone intense deformation and several periods of folding have

FOLDOUT FRAME

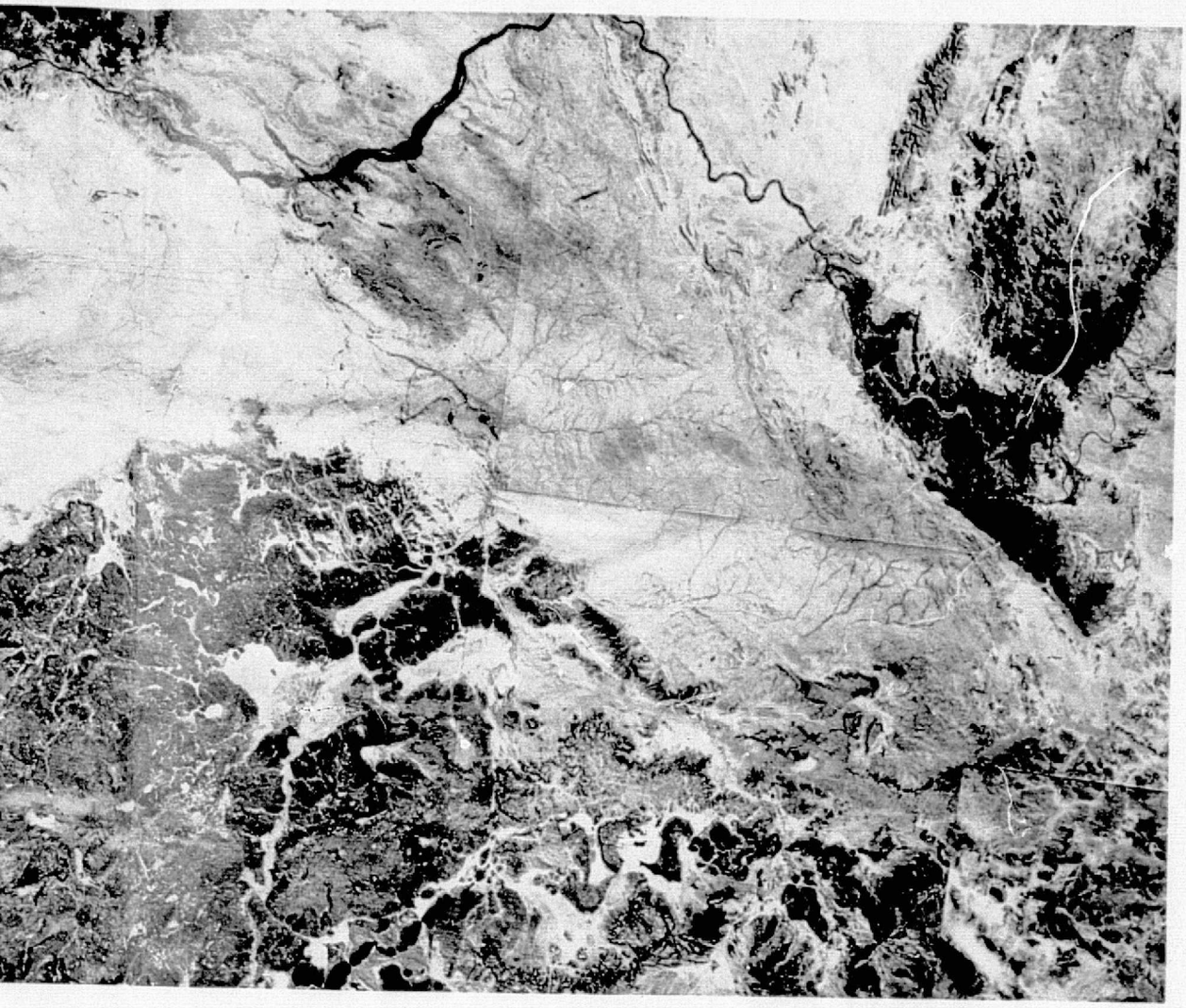

FIGURE 11. ERTS mosaic of the N.W. Cape Province of South Africa produced from 8 colour composite prints and reduced to a scale of approximately 1:1 850 000.

FOLDOUT FRAME 2

been described by Joubert[19] from the area to the west and south of the Springbok-Okiep mining district. Numerous fault zones and lineaments also feature prominently and have played an important part in the overall tectonic framework of the region.

Various components of the supracrustal sequence, which has been subdivided into three general groups, have been recognized from a point some 30 kilometres from the west coast extending in an easterly direction towards a major zone of dislocation (the Tantalite Valley fault zone) situated a short distance to the north of the town of Pofadder and trending NW–SE (see Figures 11 and 12 and earlier description, Figure 3).

As each major sequence of east-west striking rocks crosses this zone of dislocation it is deflected to form large refolded lobate structures on the north-eastern side. The latter structures have a general north-south strike but are themselves deformed by younger folds with axes trending parallel to the Tantalite valley fault zone. This phenomenon is well illustrated in the area immediately north of the Orange river by the sequence of rocks that commences in the Goodhouse area. It is also shown by the sequence portrayed by the black ornament that commences in the region to the north west of the Springbok-Okiep mining district and strikes in an overall east-west direction towards the town of Pofadder. Some distance to the east of the town the assemblage swings northwards and then north west culminating at a point to the west of Kakamas on the Orange river (Figure 12).

The stratigraphic sequence lying to the south of the Springbok-Okiep mining district also strikes east-west but is covered as one proceeds east, firstly by sand and then by younger flat lying sediments of the Karroo system. When these rocks again make their appearance from under the Karroo in the vicinity of Kenhardt, they strike in a generally north west direction from this town to Kakamas on the Orange river (Figures 11 and 12). These outcrop trends reflect the interplay of a number of different fold directions which give rise to a typical interference pattern.

One of the most prominent structures seen on the mosaic is the Pypklip anticline (see Figure 12), which represents one of the last episodes of plastic deformation of the Bushmanland sequence. The fold axis trends WNW–ESE and is parallel to the Tantalite valley wrench fault (described earlier) as well as a number of other linears. Computer processing of regional gravity data by Pretorius[18] has shown the existence of a major gravity low in an area lying to the south-west of Kakamas and referred to as the Pypklip-anomaly. This feature lies directly on the Pypklip anticlinal axis and is elongated in the same direction as the latter, thus confirming the existence of this structure.

Earlier fold episodes can also be seen from the imagery for example at Gams and Aggenys and by plotting all these features it is possible to indicate up to three periods of deformation. These episodes correspond closely to the sequence of deformation established by Joubert[20] in parts of the N.W. Cape after several years of detailed study.

The relationship between mineral deposits and various stratigraphic components of the Bushmanland Sequence, established from the imagery is of great importance as many of the occurrences appear to be of the stratiform type: taking structure into account as well, it has been possible to select target areas for more detailed exploration.

Faults and linear features

Numerous well-defined linear features, some of them undoubtedly representing faults and in most cases not mapped previously, constitute conspicuous features on the imagery. A number of prominent directions have been defined from the study of ERTS and represent various phases of brittle deformation that have affected the terrain.

NNW–SSE direction

A very strong set of fractures conforming to this direction, which parallels the west coast, occur in a strip of country occupying the coastal region for a distance of some 120 kilometres inland. Features such as the termination of younger cover sequences at this point, the preservation of remnants of cover sequence rocks in a NNW–SSE trending belt between the eastern Richtersveld and th Springbok-Okiep mining area, the north-south trending zones of older vulcano-sedimentary rocks in the Richtersveld and the general attenuation of the Bushmanland supracrustal rocks in this area, suggest that the entire coastal strip has been an area of active uplift with attendent horst and graben faulting that has preserved both younger and older sedimentary sequences in the area.

This direction of fracturing becomes less intense further east but is again manifested by the large fault zone to the east of Goodhouse, which clearly controls the distribution pattern of the younger flat-lying cover sequences (see Figures 11 and 12). Features with the same direction are also clearly to be seen in the area to the north-east of Pofadder and to the south-west and north-west of Kenhardt, and the Brakbos fault zone itself with subsidiary faults further east, constitutes a spectacular expression of this direction.

The latter zone with its associated parallel faults also represents a zone of relative uplift as is manifested by the southward swing of the outcrop pattern of younger cover rocks between Kenhardt and Prieska (in the Copperton area) and the northward swing of similar rocks to the north of Upington.

35 2 8

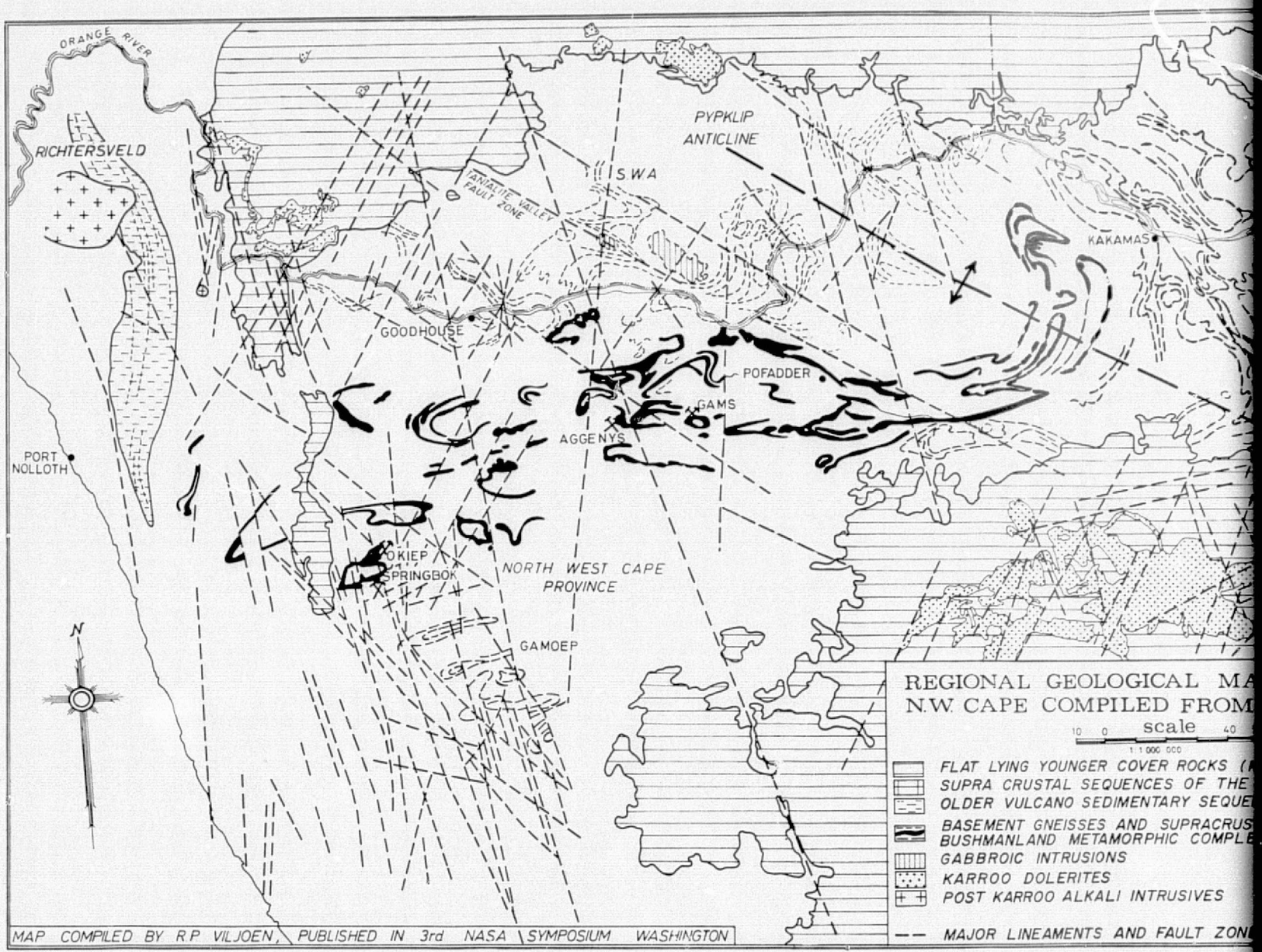

NW–SE direction

The Tantalite Valley fault zone is the most important linear feature conforming to this direction and can clearly be traced through Karroo cover in the area to the south-east of Kenhardt. This fault zone has acted as the basis for the intrusion of gabbro plugs in the area to the north west of Pofadder (see Figure 3 and earlier description). Parallel linear features are to be seen to the north and south west of Pofadder and in the area surrounding the Springbok-Okiep copper mining district.

NE–SW direction

Linear features conforming to this direction are well developed along the west coast zone particularly between the Richtersveld and the Springbok-Okiep area. The intersection of these with the other fracture directions described, probably acted as the locus for the emplacement of younger igneous rocks including post-Karroo alkaline intrusives of the Richtersveld. Two of these, *viz.* the Kuboos pluton and the Rooiberg ring structure can be seen on the imagery (Figures 11 and 12).

Conclusions

ERTS imagery has been an important aid to mineral exploration programmes in the N.W. Cape Province of South Africa. A regional geological map produced from the imagery has proved invaluable in channeling exploration efforts into promising areas. The use of the method in largely

FOLDOUT FRAME 1

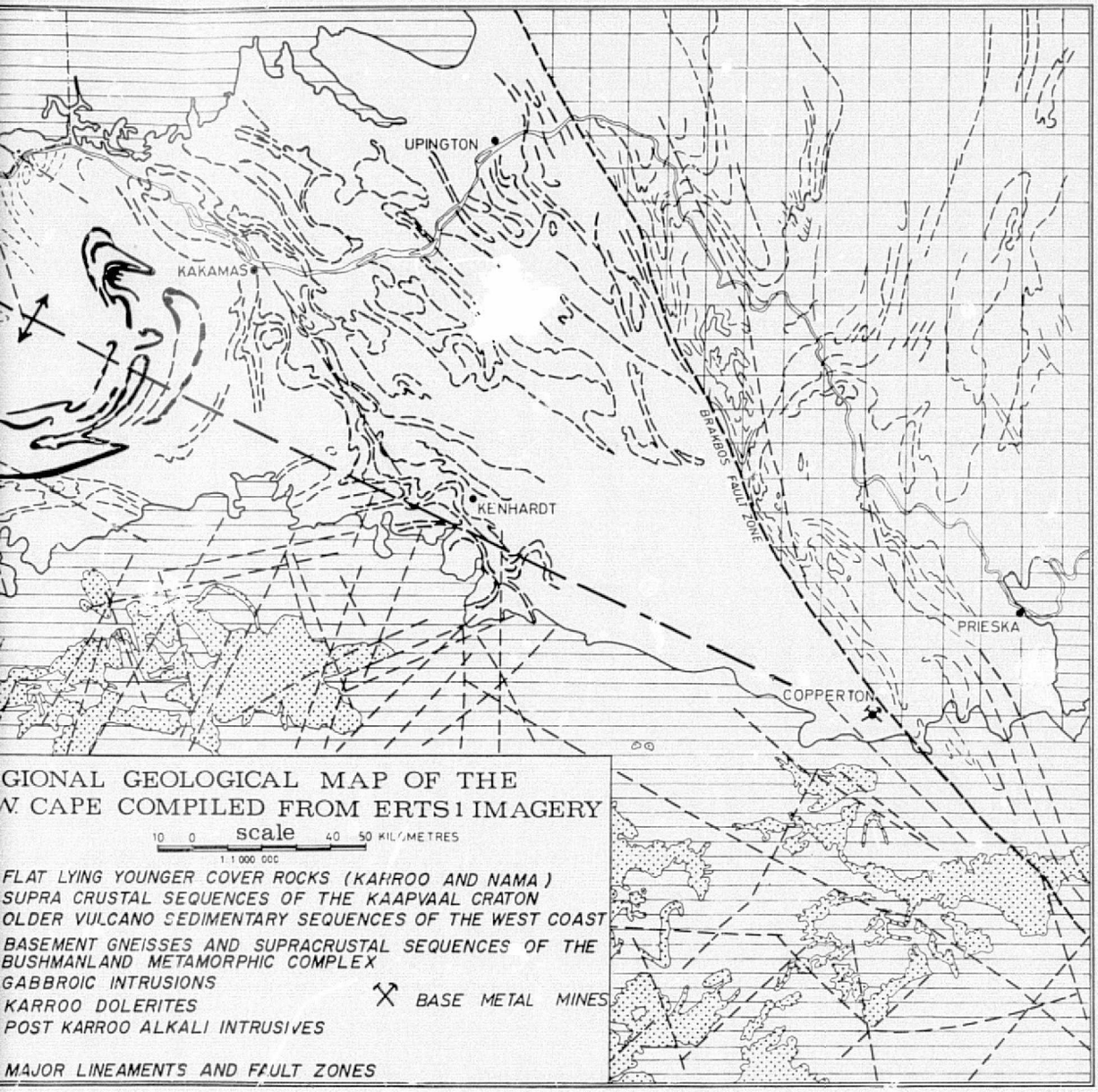

FIGURE 12.

ok-
the
cted
ous
s of
oos
een

l to
ape
ical
in-
nto
gely

FOLDOUT FRAME 2

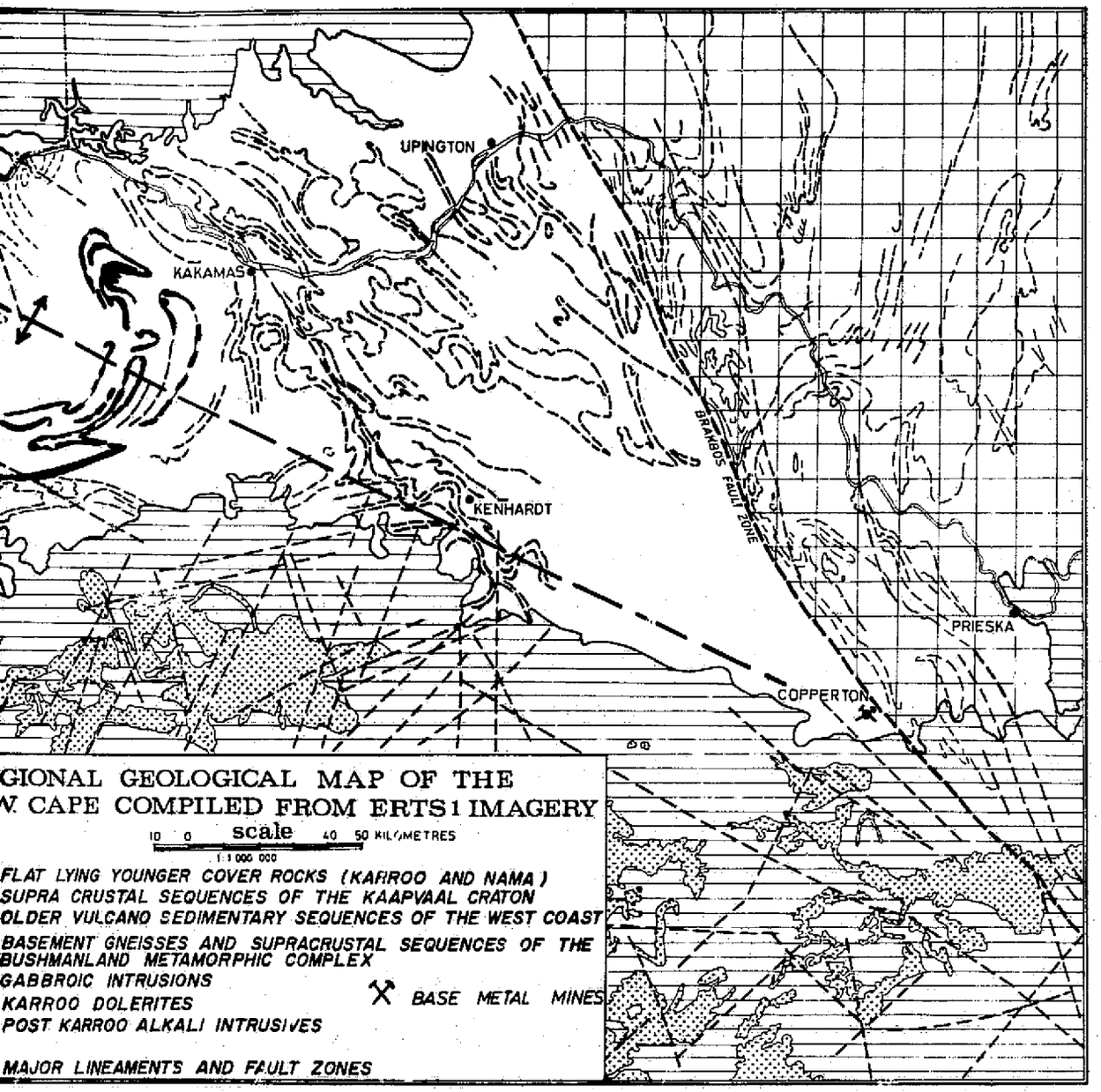

FIGURE 12.

ok-
the
ted
ous
s of
pos
een

to
ape
ical
in-
nto
gely

157

ROLLOUT FRAME 2

3527

unmapped or poorly mapped arid areas such as the N.W. Cape, is unrivalled. Techniques developed during this study are acting as the framework for similar investigations in other regions and are expected to become a routine preliminary stage in future mineral exploration programmes.

Case history no 2

The Matchless Amphibolite Belt, S.W.A.

Introduction

Attention has recently been focussed on the Matchless amphibolite belt of central South West Africa because of the occurrence of a number of base-metal deposits along its strike.

The belt constitutes a distinctive and well-demarcated stratigraphic component of the Khomas Series, which forms part of the ENE–WSW trending Damara geosyncline of central South West Africa. Field investigations have indicated that the belt of amphibolite extends for a distance of some 350 kilometres, commencing in the vicinity of the Kuiseb river in the WSW, to a point some 125 kilometres ENE of the city of Windhoek, where it disappears under Kalahari sand cover. Several interesting base-metal occurrences are located in close proximity to the amphibolite, which therefore acts as an ideal regional geological marker horizon for mineral exploration.

The old Gorob and Hope mines, which have been known for some time, are situated at the folded WSW extremity of the belt within the Namib desert park and just north of the Kuiseb river. The Matchless mine lies some 30 kilometres WSW of Windhoek, while the newly discovered Otjihase, Ongeama, and Ongombo West Group of deposits are situated approximately 30 kilometres ENE of Windhoek.

Three ERTS-1 colour composite prints were used in the compilation of a regional geological map of the central portion of the Damara geosyncline as an aid to an extensive mineral exploration programme, the main aims being to ascertain the following:

- whether the amphibolite belt could be traced from ERTS imagery,
- whether structural complexities along the belt could be seen on the imagery and whether there was any relationship between these and the base-metal mineralization,
- whether the extent and distinctive characteristics of the Khomas series in relation to other geological components of the Damara geosyncline could be recognized.

Interpretation of ERTS imagery

The three ERTS images used in the interpretation have been reduced to a scale of approximately 1:1 400 000 and are portrayed in mosaic form in Figure 13. Owing to a number of factors, the most important of which is the arid nature of the region, this mosaic provides a remarkable picture of the regional structure of a large portion of the Damara geosyncline (Figure 13).

The Matchless belt is clearly visible as a well-defined narrow black line along most of its strike length between the Hope mine and Windhoek, although in the former area two discrete amphibolite zones are apparent in an area where the belt appears to terminate in the form of a large fold. Some distance to the east of the Gorob mine and lying immediately south of the main amphibolite zone are a number of graphitic schist horizons. These are clearly discernible as greyish coloured bands on the imagery. Still further east the amphibolite belt disappears for a distance of several kilometres but reappears to the east becoming progressively thicker towards the Matchless mine where it appears to thicken even more. To the east of the mine more than one amphibolitic horizon can be seen but these become fainter towards Windhoek and are discernible only for a short distance to the east of the city. No clear indication of the possible extension of the amphibolite belt to the east of this point can be obtained from the 1:1 400 000 scale imagery portrayed in Figure 13, mainly owing to structural complexities in the area and this region was consequently studied using CCT photographic products *(see later)*.

Regionally the Khomas Series can be readily distinguished from other units of the Damara belt by its structural style. It is comprised of a monotonous sequence of quartz-felspar-biotite schists derived essentially from greywackes, sub-greywackes, and shales. These schists give rise to large areas of continuous outcrop and comprise the Khomas Highlands of central South West Africa. A number of graphitic schist horizons developed mainly towards the north, as well as the amphibolite belt itself, are the only recognizable stratigraphic units within the Khomas Series. Most of these can be seen on the ERTS imagery, a distinctive feature being their strong linearity in an ENE – WSW direction with very little indication of open folding. This pattern is in marked contrast to the tectonic style of the central portion of the Damara belt that lies to the north of the Khomas Series and that is characterized by numerous eye-type folds in an area of higher grade metamorphism and intrusive anatectic granites. In a similar fashion rocks lying to the south of the Khomas Series have also been complexly folded, the resultant structures being somewhat different to those encountered in the northern zone mentioned above, and easily distinguishable from the Khomas Series.

A characteristic of both the northern and

FIGURE 13. ERTS mosaic of the Central portion of the Damara geosyncline of central South West Africa showing the distribution of a number of base-metal occurrences in relation to the Matchless Amphibolite Belt and the Khomas Series. Scale of imagery approximately 1:1 400 000.

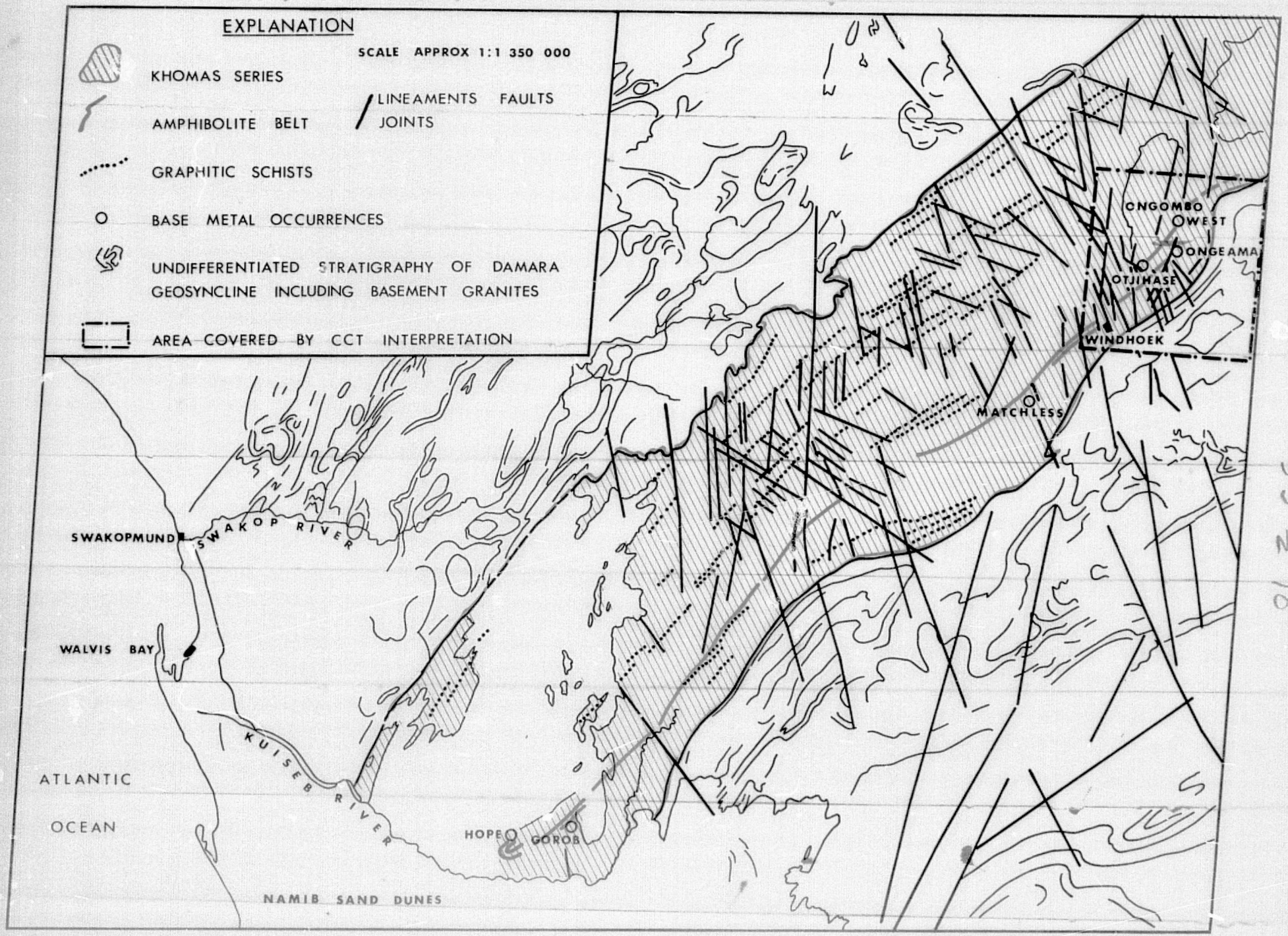
EXPLANATION
SCALE APPROX 1:1 350 000
KHOMAS SERIES
AMPHIBOLITE BELT
GRAPHITIC SCHISTS
BASE METAL OCCURRENCES
UNDIFFERENTIATED STRATIGRAPHY OF DAMARA GEOSYNCLINE INCLUDING BASEMENT GRANITES
AREA COVERED BY CCT INTERPRETATION
LINEAMENTS FAULTS JOINTS
ONGOMBO WEST
ONGEAMA
OTJIHASE
WINDHOEK
MATCHLESS
SWAKOPMUND
SWAKOP RIVER
WALVIS BAY
KUISEB RIVER
ATLANTIC OCEAN
HOPE
GOROB
NAMIB SAND DUNES

35 N 10

35 2 11

35 2 12

FIGURE 14 (a). Print from CCT photographic display (Band 5)

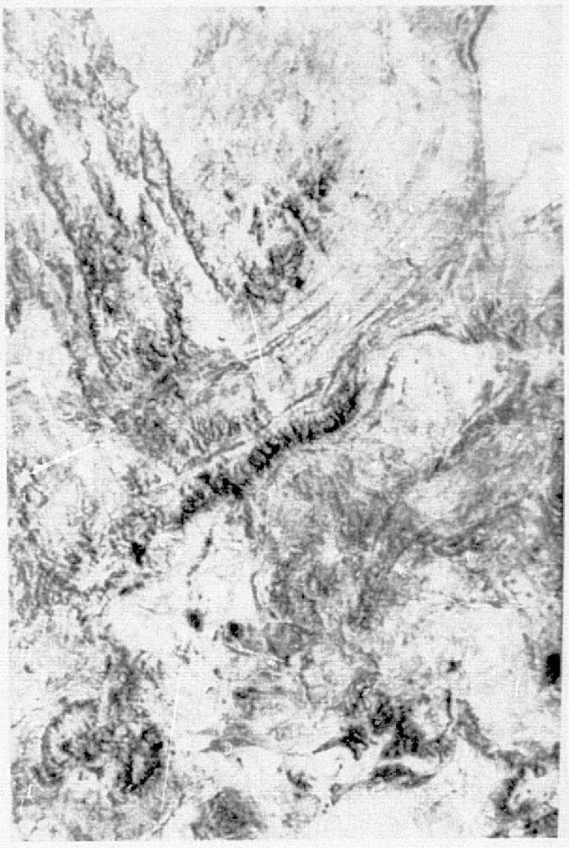

FIGURE 14 (b). Print from CCT photographic display (Band 7)

REPRODUCIBILITY OF THE
ORIGINAL PAGE IS POOR

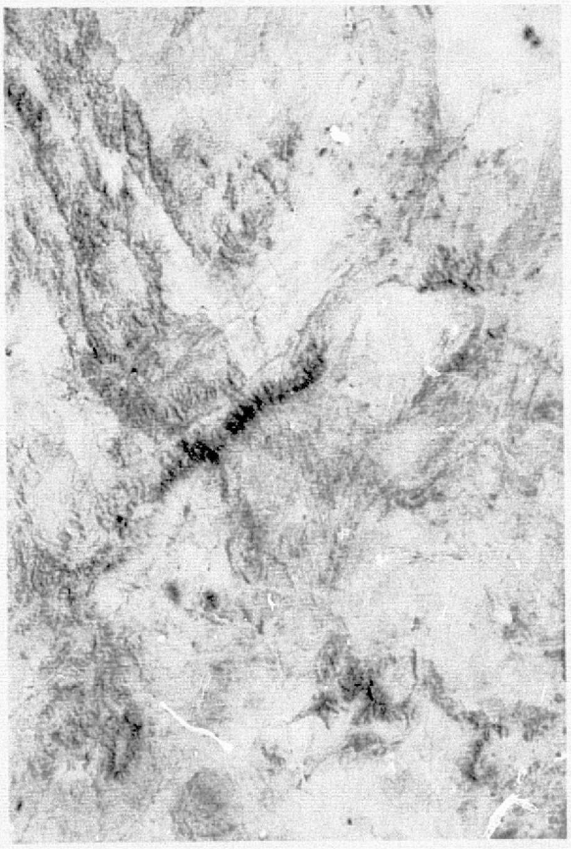

FIGURE 14 (c). Print from a section of a NASA 70 mm negative (Band 5)

FIGURE 14 (d). Print from a section of a NASA 70 mm negative (Band 7)

southern zones is the presence of granitic rocks representing both basement and anatectic varieties. These are not represented in the Khomas Series, which suggests that the meta-greywackes and associated rocks which constitute the latter, form part of a deep, elongated trough of sediments and volcanics of probable eugeosynclinal type and confined by regional tectonic basement highs lying to the north and south. This tectonic setting might explain the linearity in the structural style revealed by these rocks on ERTS imagery.

Numerous linears are clearly visible from the mosaic, a feature being the confinement of many of them (especially the shorter ones) to the Khomas Series (see Figure 13). Most of the less extensive linears probably represent joints and also enhance the differences between the Khomas Series and the structural domains to the north and south of it. Some of the linears, and particularly the longer ones do, however, represent faults. A strong NW – SE set for example occupies a zone between Windhoek and the Otjihase mine (Figure 13). Some of these faults afford the control for a number of hot springs that occur in the vicinity of the city.

Computer Compatible Tapes

In an endeavour to enhance and possibly trace the amphibolite belt to the east of Windhoek and to obtain a better understanding of the complicated regional structure in the Otjihase area, use was made of Computer Compatible Tapes obtained directly from EROS. The area investigated by this method is shown in Figure 13, and before the results are described it is pertinent to present a brief outline of the advantages of the tapes relative to standard photographic products and the methods used to present this data in a form that can be used by the geologist.

Apart from photographic products, NASA issue ERTS-1 imagery in the form of Computer Compatible Tapes (CCT's). This alternative product, as its name implies, contains the video data comprising an MSS image in a form suitable for processing by computer. CCT's offer a flexible tool by which imagery can be analysed using the well-established principles of computer data processing. Although more convenient to use, NASA photographic products are inferior to Bulk CCT's in their spatial and radiometric qualities. In fact the bulk CCT 'represents the resolution of the sensor itself, or, the performance of the system, were there no degradation due to subsequent spacecraft and ground processing' (NASA[20]). However, an ERTS frame in CCT form is made up of 24 million bytes of video data and presentation of processed picture elements (pixels) on standard computer peripherals can produce voluminous handcopy. As 'packing' video information on film is considerably more efficient than normal computer output methods, it is desirable to combine this advantage of the NASA photographic product with the image fidelity of the CCT.

In the examples presented here, this was achieved by decoding the digital CCT video data using a computer and employing a digital-to-analogue converter to produce a voltage value for each pixel. These analogue voltages were then recorded on an FM tape recorder and were simultaneously displayed on an oscilloscope to produce a waveform for each MSS scan line. This recorded information was then exposed onto film by effectively photographing a 'television' image of the video using a linescan film recorder.

This technique is not limited to the display of individual bands but can be extended to produce a high-resolution image of any pointwise computation of the interleaved spectral bands from an MSS frame. For illustrative purposes, however, examples of this display technique in the present paper have been limited to individual bands, of which bands 5 and 7 are shown in Figure 14(a) and (b) respectively.

For comparative purposes, prints of band 5 and 7 from the NASA 70 mm negative are shown as Figures 14(c) and 14(d) respectively. From this comparison at a scale of 1:660 000, it can be seen that considerably more structural information is present in the CCT displays than in the conventional NASA photographic format. Although gross tectonic features are similarly represented in both forms of imagery, smaller scale geological features are much more apparent in the CCT display. A colour composite of CCT-displayed bands 4, 5, and 7 is also compared to its equivalent colour composite derived from NASA 70 mm negatives. In these images, shown here at a scale of 1:240 000 (Figure 15(a) and 15(b)) spectral differences between bands are seen more distinctively in the CCT display (Figure 15(a)) than in the comparative NASA product (Figure 15(b)). Cultural features such as rivers, agricultural areas (seen as red), and in particular, the city of Windhoek (seen as blue-lower left of images) are clearly identified.

Interpretation of CCT data

Figure 16(b) is a geological and structural interpretation of the country around the Otjihase group of occurrences, based on the interpretation of bands 4, 5, and 7 from CCT photography, displayed on a scale of 1:240 000. An illustration of one of the CCT bands used (band 4) is shown in Figure 16(a) for comparative purposes.

Examination of this image indicates that the amphibolite belt, which in this instance consists of a number of individual units, can be traced to the east of Windhoek but disappears in the vicinity of the Ongeama gossan. (Individual gossans cannot at this stage be recognized from the imagery owing to their limited size, but their positions have been

35 2 14

indicated on the interpretation to facilitate description.)

Although not as clear, the amphibolite belt can again be seen to the east of the Otjihase gossan and towards the Ongombo West occurrence, disappearing in an easterly direction. The entire Belt between Otjihase and Ongombo west and further east therefore appears to have been displaced to the north. No other continuous stratigraphic components can be recognized within the Khomas schists themselves, but stratigraphic components of the more quartzitic Aus member of the Khomas series can be clearly distinguished as a well-defined belt to the south-east. Most of the rocks consist of felspathic quartzites but amphibolitic components of this stratigraphy are clearly discerned on the imagery by their darker tones. Major structural disturbances in these stratigraphic trends, taking the form of a sharp swing north accompanied by folding with possible truncation, is seen in a zone to the south of the white Nossob river (see Figures 16(a) and 16(b)). To the north, fairly regular trends are once more encountered and there is a strong suggestion of one or more zones of major structural disturbance running approximately along the course of the Otjihase river.

Two domes of reactivated basement granite are clearly discernible by their lighter colour tones on the right hand side of the image and are separated by a zone of intense deformation of supracrustal rocks that include certain components of the Aus series (see Figure 16(b)).

The imagery provides a large amount of unique regional structural information, the zone of faulting between Windhoek and Otjihase being particularly clear. Although the dominant fault direction is NNW–SSE, there are also strong N.W. and N.E. components as well. Some of these faults clearly displace the amphibolite belt apparently by an echelon movement in the region to the east of Windhoek. Numerous other faults are also apparent, particularly in the area to the south east of the Otjihase gossan (see Figure 16(b)). While most of the fault traces appear to form fairly high angles with the schistosity of the Khomas Series and have in many instances been accentuated by the drainage pattern, other evidence suggests the presence of a number of older fault zones, probably in the form of wrench or thrust faulting with the fault traces being close to the schistosity of the Khomas schists and therefore not as readily apparent.

Of particular interest is the evidence for one or more major early thrust or wrench faults with left lateral movement and with attendant minor folding (referred to above), which were responsible for the probable displacement seen in the Aus series and in the displacement of the amphibolite belt. One branch of this system of early faulting appears to follow the Otjihase river while the other, which has been displaced in part by the younger faults, occupies a zone more or less between the Otjihase and Ongeama gossans continuing in an easterly direction, and merging with the fault described above.

Further evidence for the presence of this zone of dislocation is provided by a zone of good outcrop with dark tones and conspicuous, linears, within the Khomas Series and lying to the south-east of the Otjihase gossan (see Figure 16(a)). The same tone is to be seen to the north between the Otjihase and White Nossob rivers and this distribution pattern suggests displacement of some type of stratigraphic component within the Khomas Series by the wrench faulting referred to earlier.

In order to analyse the structural pattern obtained from the CCT imagery in more detail, a regional geological map (Figure 17) of the country around the Otjihase Ongeama and Ongombo West occurrences was re-examined.

This mapping, which was carried out by the Fundamental Geological Research Department of the Johannesburg Consolidated Investment Company Limited to aid mineral exploration along the amphibolite belt, indicates the zone of amphibolite that is traceable from Windhoek, petering out in the vicinity of the Ongeama gossan. No amphibolites have been located to the east of Ongeama along strike (see Figure 17). A northern belt of amphibolite is also present commencing just east of the Otjihase gossan where it is associated with a number of distinctive talc, chlorite-carbonate rocks, and continuing as a zone of discontinuous and scattered amphibolite lenses that can be traced further east and that occur in more or less the same stratigraphic zone as the Ongombo West occurrence, which straddles the White Nossob river (see Figure 16(a) and 16(b)). The amphibolite belt is again traceable to the east of the latter occurrence. Other features recorded during the mapping programme were the distribution of vein quartz outcrops and deflation residues of vein quartz rubble mainly on the higher areas adjacent to streams. Most of the vein quartz material indicated on the map represents the latter material.

Some of the major ERTS lineaments obtained from the CCT interpretation have been plotted onto this map and confirm a number of structures that were not apparent even from the fairly detailed geological mapping. The interpretation strongly suggests that the duplication of the amphibolite belt is due to the zone of thrust faulting deduced from the interpretation of the CCT products.

Conclusions

If used in the correct context and in specific areas where information regarding regional structure and stratigraphy is required in a particular exploration or geological problem, CCT-produced imagery

35 z 15

FIGURE 15 (a). Colour composite from CCT photographic displays printing Bands 4, 5 and 7 in blue, green and red respectively.

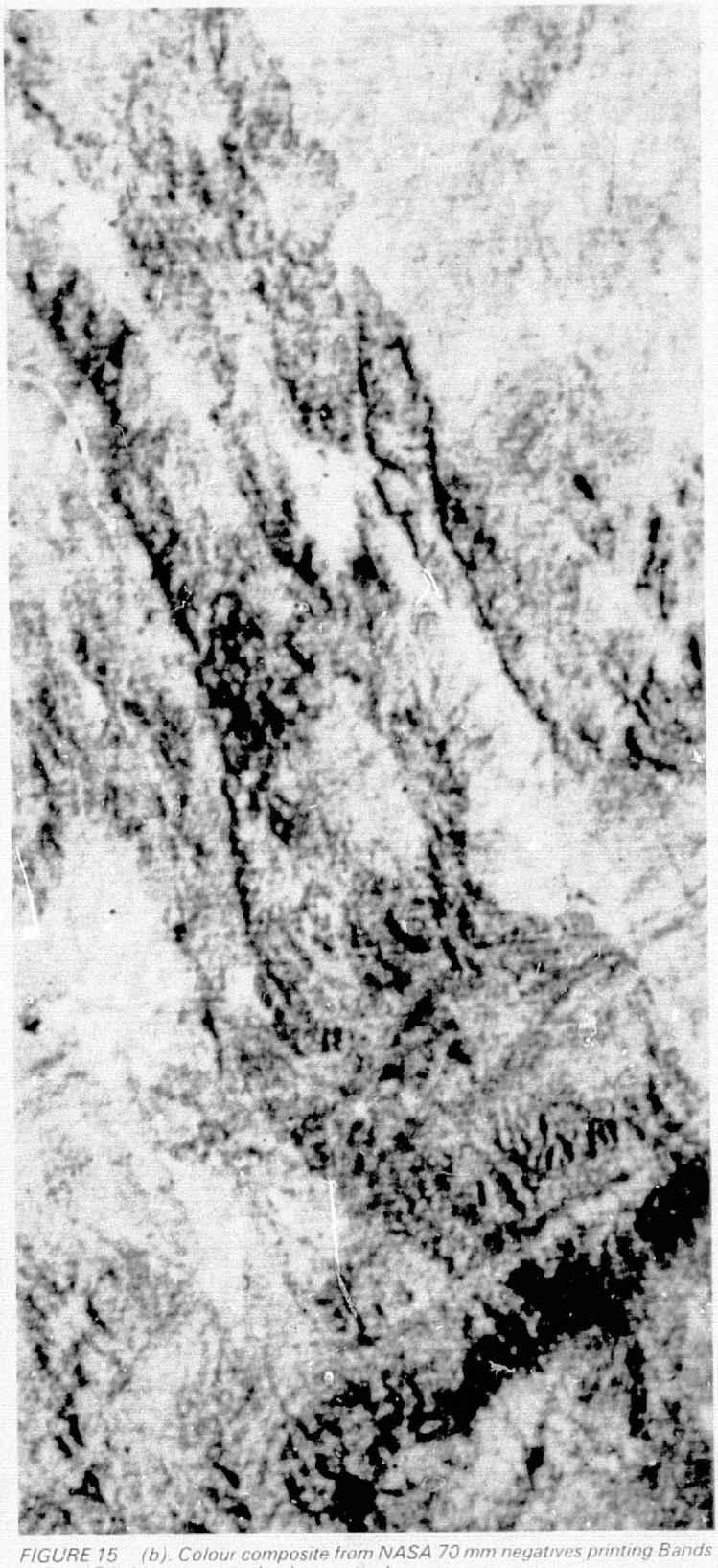

FIGURE 15 (b). Colour composite from NASA 70 mm negatives printing Bands 4, 5 and 7 in blue, green and red respectively.

will certainly become a more and more useful tool. If the method can be developed on a routine basis, then it will be possible to gain a quick regional geological understanding of numerous prospect areas in a very short period of time thus conceivably avoiding a number of unnecessary steps, and hence expenditure, in future exploration programmes.

FUTURE DEVELOPMENT

A satisfying aspect of ERTS has been the amount and quality of geological information present in the imagery and digital data even though the ground resolution is 10 to 100 times lower than normal for conventional aerial photography. The tradeoff of reduced resolution for increased area of synoptic coverage has not cost as much as some critics had predicted. Nevertheless, resolutions from satellite imagery must improve by estimated factors of 2 to 10 if certain applications in geology are to become feasible. Such increases in resolution would bring about significant improvements in identifying and mapping lithologic and stratigraphic units, in recognizing lower orders or faulting and jointing and in picking out the smaller (and more numerous) patches of surface mineral alteration. It seems safe to predict that synoptic imagery from satellites will compete with or supplant aerial photography for most applications when resolutions of 10 to 30 feet are achieved. This might be partially achieved by LANDSAT 3 where it is planned to increase the resolution fairly considerably.

Alternate directions of solar illumination are of importance in the enhancement of relief, in the reduction of possible bias in orientation of linears and in permitting accurate recording of colour and brightness differences. This can be accomplished either by a succession of sun-synchronous satellites operating at different pass times or by high resolution pointable geosynchronous satellites that observe the same area as it undergoes daily and seasonal lighting changes.

It is not clear whether broadening the range of spectral coverage and/or decreasing the band widths and/or increasing the number of channels or bands will aid materially in identifying rock types or composition. Nor has it been demonstrated that automated spectral recognition of lithologies is a practical possibility.

Perhaps the most significant new advances in geologic applications from space observations will come from new imaging and digital data processing techniques not yet developed or proved. So far, very little of positive value to geologic studies has emerged from the use of colour-additive viewers or electronic enhancement devices such as those which convert grey levels or density steps in a black-and-white image to a colour-coded rendition on a TV screen. However, these instruments have worked mainly on 'raw' or unprocessed images. Scenes produced through computer reprocessing often reveal previously hidden information when graphically displayed and manipulated on an image console. Fourier analysis, either with optical filters or by computer, promises to be a powerful technique for systematically measuring directional trends and extents of linear features and other non-randomly distributed spatial elements on the ground.

If some or all of the abovementioned aspects could be instituted, the quality and hence data applicability of ERTS imagery could be considerably improved providing not only a supplementary aid for aerial photography, but adding significant and in many cases unique detailed and regional data, unobtainable from any other method.

CONCLUSIONS

Remote sensing from space platforms is neither a panacea nor an all-purpose black-box system that will revolutionize the geological sciences. It is merely another tool available to geologists to study certain problems. In perspective, ERTS, its predecessors and follow-on spacecraft, Skylab and LANDSAT 2, are essentially only sophisticated extensions of aerial remote-sensing systems.

These satellites comprise a new, useful component in a multi-level system for observing the Earth over a range of 'magnifications'. Like aerial photography, space imagery has its own sets of limitations and special advantages coupled to the particular problems addressed. Space imagery is particularly suited to the study of large-scale geological features many of which could prove to be of fundamental importance to the study of global tectonics and regional processes of ore emplacement.

Other important advantages are associated with the synoptic nature of the ERTS imagery, the uniform illumination, lack of distortion, and repetitive coverage. In future the amenability of multispectral scanner imagery to specialized automated processing techniques may be an important advantage.

The impact of ERTS is reflected by the fact that three NASA Symposia devoted solely to results of ERTS investigations have been held since the launching of the satellite. At these a total of some 350 papers were presented in the fields of agriculture, forestry, range resources, environmental studies, oceanography, earth sciences, land use, and mapping and interpretation techniques.

FIGURE 16 (a). Photographically produced CCT imagery (band 4) of the country around the Otjihase copper deposits of South West Africa. Scale of imagery approximately 1:300 000.

FIGURE 16 (b). Composite geological and structural map of the same area compiled from the interpretation of bands 4, 5, and 7 of photographically produced CCT imagery. Scale of map approximately 1:300 000.

35 z 17

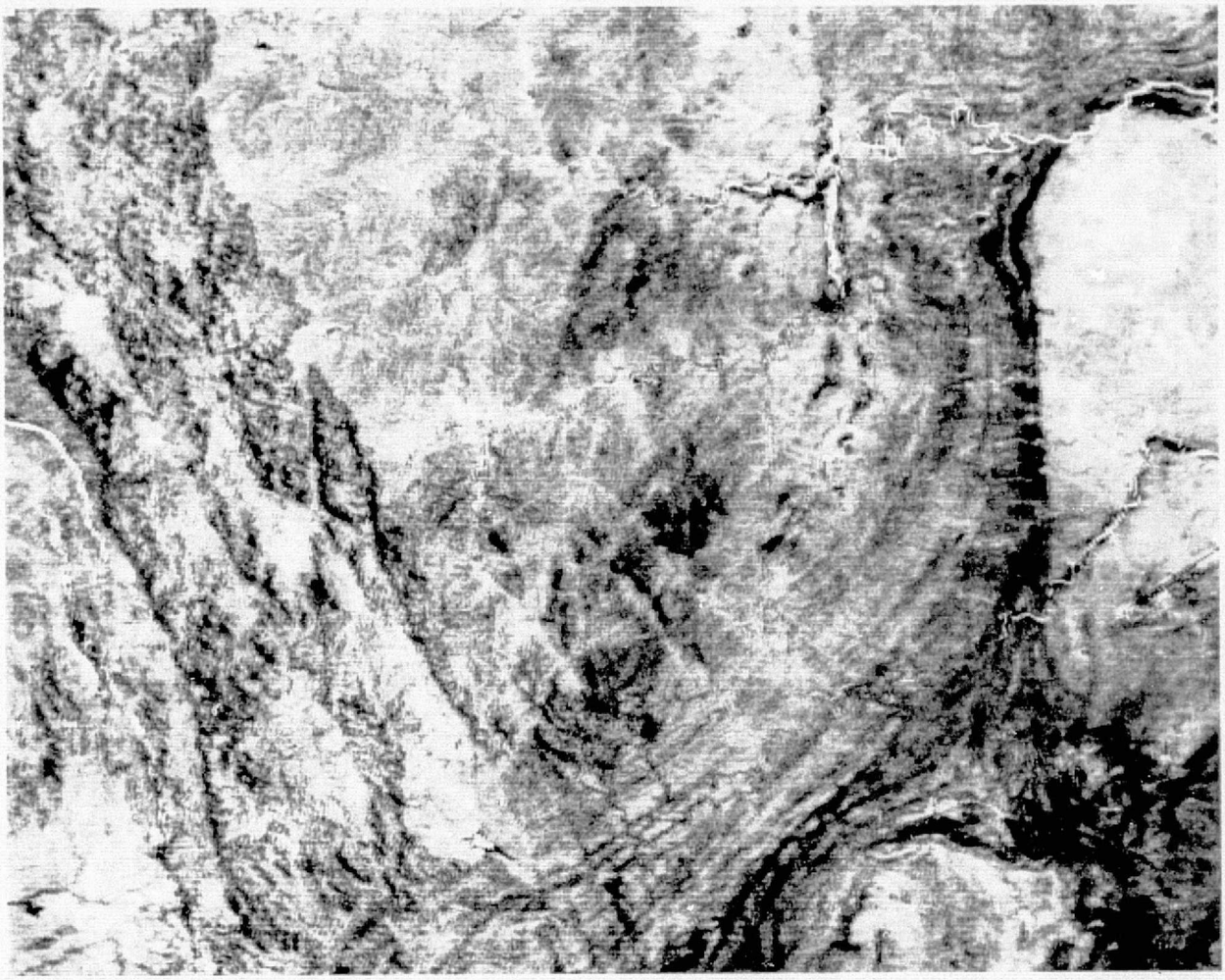

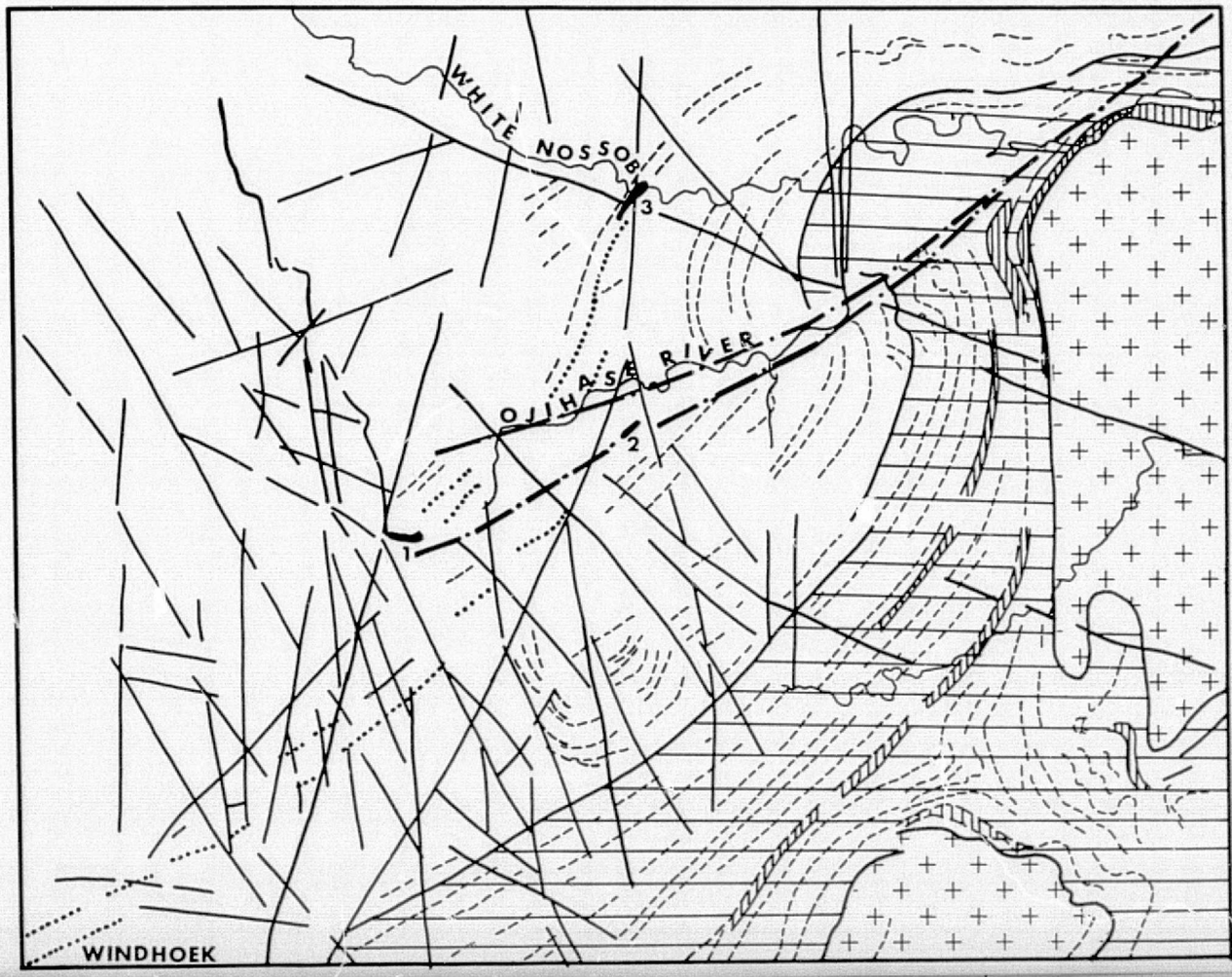

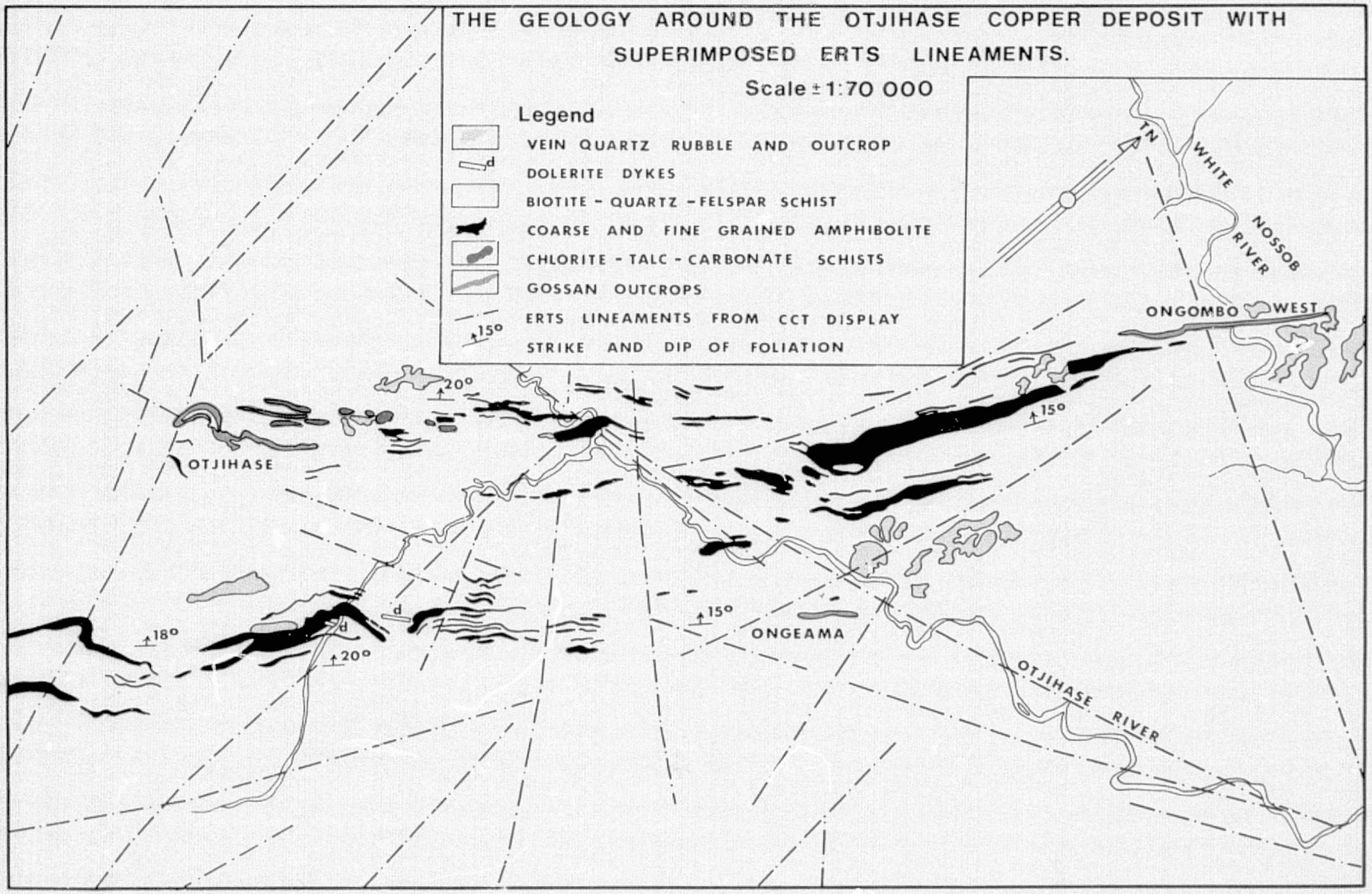

FIGURE 17. Geological map of the country around the Otjihase, Ongeama and Ongombo West base metal occurrences of central South West Africa. Some of the more important lineaments obtained from photographically produced CCT imagery are superimposed to aid in the understanding of the regional structure of the area

35-2-18

The particular suitability of ERTS to the earth sciences is illustrated by the fact that this category has always attracted the largest number of papers. In addition numerous other papers dealing with geological ERTS investigations have been presented or published within the past three years. (C.S.I.R.[21], Cospar[22,23]).

The results of these findings have been so encouraging that a second ERTS satellite (LANDSAT 2) the launch of which was initially in doubt, was placed into orbit on the 22nd January, 1975, and a 3rd is tentatively planned for 1977. Besides the ERTS-receiving station in the United States of America similar stations are operating in Brazil and Canada and one is planned for Zaire in the near future. Applications have been made for similar facilities in Italy and Iran and many scientists feel the need for a similar station in South Africa.

Since imagery first became available, a rapid shift in the Earth sciences from the initial show-and-tell stage to investigations of a purely scientific nature and now to an emphasis on effective applications of direct economic benefit in the fields of mineral exploration and national mineral resource evaluation has occurred. The present paper has outlined the important practical contribution that the imagery can make in a number of geological applications under favourable conditions. It has been demonstrated that ERTS can often yield certain types of geological information more efficiently than other methods and occasionally can even provide unique information not obtainable otherwise.

ERTS was conceived primarily as an experimental research programme. The extent to which similar future satellite systems will find large-scale routine application will depend on a careful evaluation of the results of the ERTS programme. Despite the value of repetitive coverage, it is likely that most geological applications can be accomplished with currently available images, with the promise that future technological improvements, particularly as far as resolution is concerned, will add important dimensions to our interpretative capability. There are enough tasks arising from available ERTS data to keep many geologists busy extracting and applying relevant data for many years.

ACKNOWLEDGEMENTS

All aspects of this study have been made possible by the generosity and far-sightedness of the management of the Johannesburg Consolidated Investment Company Limited. The facilities provided by the establishment of a Fundamental Geological Research Department, Spectral Africa (Pty) Limited, together with the efforts of ERTS-1 principal investigator, Mr B. P. Gilbertson, has laid the foundations for investigations of the type described in this paper. All the images studied, which rank amongst the best produced anywhere in the world, were obtained from Spectral Africa (Pty) Limited and Drs R. P. and M. J. Viljoen have worked closely with Dr J. Grootenboer and Mr T. G. Longshaw in this project to ensure the correct balance between the technological side of the imagery and image production and the practical applications in problems of geology and mineral exploration.

Three of the authors, namely Drs R. P. Viljoen, M. J. Viljoen, and J. Grootenboer have attended NASA Symposia in Washington that have dealt with the applications of ERTS-1 imagery in various scientific desciplines. The funding for these trips was provided by the Johannesburg Consolidated Investment Company Limited and Spectral Africa (Pty) Limited and is gratefully acknowledged.

The assistance of NASA, from whom the negatives and CCT tapes were obtained, is gratefully acknowledged. The generous facilities that NASA has put at the disposal of earth scientists all over the world has been invaluable.

REFERENCES

1. NATIONAL AERONAUTICS AND SPACE ADMINISTRATION. *1st Earth Resources Technology Satellite symposium, Washington, Sep. 1972.* Washington, NASA, 1972.
2. NATIONAL AERONAUTICS AND SPACE ADMINISTRATION. *2nd Earth Resources Technology Satellite symposium, Washington, Mar. 1973.* Washington, NASA, 1973.
3. NATIONAL AERONAUTICS AND SPACE ADMINISTRATION. *3rd Earth Resources Technology Satellite symposium, Washington, Dec. 1973.* Washington, NASA, 1973.
4. LONGSHAW, T. G., and GILBERTSON, B. Computerised interpretation of ERTS-1 data in South Africa. *S. Afr. J. Sci.*, vol. 70, 1974, pp. 114-117.
5. LONGSHAW, T. G. Photographic imaging of ERTS-1 CCT data for high resolution display. *2nd symposium on remote sensing – ERTS-1, – Grahamstown, Jul. 1974.* Pretoria, Council for Scientific and Industrial Research, 1974.
6. GROOTENBOER, J. The influence of seasonal factors on the recognition of surface lithologies from ERTS imagery of the Western Transvaal. *3rd Earth Resources Technology Satellite symposium, Washington, Dec. 1973.* Washington, NASA, 1973.
7. MALAN, O. G. Diazo colour composites of ERTS images. *2nd Symposium on remote sensing – ERTS-1, Grahamstown, Jul. 1974.* Pretoria, Council for Scientific and Industrial Research, 1974.
8. GROOTENBOER, J., and GILBERTSON, B. ERTS imagery as an aid to geological mapping and mineral exploration in Southern Africa. *Cospar seminar on space applications of direct interest to developing countries, Sao José dos Campos, Jun. 1974.* Paris, COSPAR, 1974.
9. SHORT, N. M., and LOWMAN, P. D. Earth observations from space – outlook for the geological sciences. New York, Goddard Space Flight Centre, *Report X-650-73-316*, 1973.
10. WILLIAMSON, D. T. Vegetation mapping from ERTS imagery of the Okavango delta. *Third Earth Resources Technology Satellite symposium, Washington, Dec. 1973.* Washington, NASA, 1973.
11. JOUBERT, P. Wrench-fault tectonics in the Namaqualand metamorphic complex. Cape Town, University of Cape Town, *Precambrian Research Unit Bulletin 15*, 1974.
12. GROOTENBOER, J., ERIKSON, K., and TRUSWELL, J. Stratigraphic subdivision of the Transvaal dolomite from ERTS imagery. *3rd Earth Resources Technology Satellite symposium, Washington, Dec. 1973.* Washington, NASA, 1973.

35 z 20

13. GERMS, G. J. B. The stratigraphy and palaeontology of the Lower Nama group, South West Africa. Cape Town, University of Cape Town, *Precambrian Research Unit Bulletin 12*, 1972.
14. VILJOEN, M. J., and VILJOEN, R. P. ERTS-1 imagery as an aid to the definition of the geotectonic domains of the Southern African Crystalline Shield. Washington, NASA, *Report SP-327*. 1973.
15. VILJOEN, M. J., and VILJOEN, R. P. A reappraisal of granite-greenstone terrains of shield areas based on the Barberton model. *Upper Mantle Project*. Johannesburg. Geological Society of South Africa, 1969. *Geological Society of South Africa, Special Publication no. 2*. pp. 245-274.
16. GROOTENBOER, J., VILJOEN, R. P., and VILJOEN, M. J. ERTS imagery and mineral exploration in Southern Africa. *2nd symposium on remote sensing – ERTS-1, Grahamstown, Jul. 1974*. Pretoria, Council for Scientific and Industrial Research, 1974.
17. VILJOEN, R. P. ERTS-1 imagery as an aid to the understanding of the regional setting of base metal deposits in the North West Cape Province, South Africa. *3rd Earth Resources Technology Satellite symposium, Washington, Dec. 1973*. Washington, NASA, 1973.
18. PRETORIUS, D. A. The structural boundary between the Kaapvaal and Sonama crustal provinces. Johannesburg, University of the Witwatersrand, Economic Geology Research Unit, *Information Circular 88*, 1974.
19. JOUBERT, P. The regional tectonism of the gneisses of part of Namaqualand. Cape Town, University of Cape Town, *Precambrian Research Unit Bulletin 10*. 1971.
20. NATIONAL AERONAUTICS AND SPACE ADMINISTRATION. Data users handbook – Nasa earth resources technology satellite. Washington, NASA, *Document 71SD4249*. 1971.
21. COUNCIL FOR SCIENTIFIC AND INDUSTRIAL RESEARCH. *2nd symposium on remote sensing – ERTS-1, Grahamstown, Jul. 1974*. Pretoria, The Council, 1974.
22. COSPAR. *Symposium on the approaches to Earth survey problems through use of space techniques, Constance, May 1973*. Paris, COSPAR, 1973.
23. COSPAR. *Seminar on space applications of direct interest to developing countries*, Sao José dos Campos, Jun. 1974. Paris, COSPAR, 1974.

APPENDIX 'C'

PRECEDING PAGE BLANK NOT FILMED

APPENDIX C : IN SITU SPECTRAL REFLECTANCE MEASUREMENTS

The initial program for interpretation of ERTS-1 imagery was based on the comparative technique of comparing all dumps discernible on the imagery to preselected test dumps of known vegetative cover. Optimum sensors that could be employed to carry out this operation were specified from ground reflectance measurements and small scale aerial photography. Multispectral imagery from aircraft underflights were examined on the basis of ground truth. Subsequently the categorization of slimes dams from imagery was carried out from both the photographic and CCT product.

SELECTION OF "CALIBRATION" MINE DUMPS

The selection of "calibration" mine dumps was tentatively made from existing aerial photography. A short list of dumps that would best be resolved on the ERTS-1 imagery was compiled. Ground observation of a selection of these dumps was then undertaken and a vegetation cover classification assigned. The vegetation scale specified in the proposal, namely "completely vegetated", "partially vegetated" and "completely barren", was found to be inappropriate. A more meaningful classification was found to be as shown in table 7.2 of the main text. On this scale one "calibration" dump of each category was selected on the basis of size (large as possible), homogeneity (vegetation distribution even over the top surface), and contrast (with its adjacent environment).

THE REFLECTANCE MEASUREMENT PROGRAM

Choice of Measurement Targets: In order to specify optical filters for the multispectral aerial camera system, in situ spectral reflectance measurements[2] were taken on plant species and "soil" exposures (slime) for slimes dams 1/L/40, 5/L/31, and 5/L/29. These represented the 4, 2, and 0 vegetation levels (see table 7.2 of the main text) respectively.

Of the various plant species initially sown on a dump as a seed mix Eragrostis curvula usually predominates as the species best adapted to the slimes dam environment. Sand dumps are vegetated similarly but were not measured for the following reasons.

(a) Generally the sand dumps were small in relation to the resolution of ERTS-1 imagery (1/A/20 is an exception) and have much smaller lateral extent than slimes dams.

(b) Slimes dams are more numerous in the Witwatersrand area.

(c) Due to the small particle size of the slimes dam, the pollution problem is greater than for the sand dump.

(d) A number of sand dumps have reached stage 5 and no longer present a pollution problem.

Consequently the essential spectral reflectance characteristics required for the project were exhibited by:

(A) Slime exposure (soil)

(B) Eragrostis (grass)

(C) Partial cover Eragrostis/Slime exposure (soil/grass)

(D) Miscellaneous slimes dam plant species (e.g. clover, pampas grass, trees).

The miscellaneous plants of (D) were the more mesophytic species and were also representative of vegetation on stage 5 sand dumps.

Spectral Reflectance Measurements on slimes dam 1/L/40: During the period 1st February, 1972 to 4th February, 1972, spectral reflectance measurements were carried out on slimes dam 1/L/40. All four target categories stated above as

(A) to (D) were present on the dam surface and the chemical composition and physical properties of the slime were typical of slimes dams in the Witwatersrand area. The results were therefore considered to give a good indication of the anticipated reflectance of all dumps in the classification 1 to 5. Measurements were carried out on the targets shown in table A.1.

TABLE A.1

Target Number	Description of Area	Classification	Field of View Coverage (f.o.v.)
1	Good grass cover	B	100% Eragrostis Curvula
2	Partial grass cover	C	Eragrostis/slime exposure
3	Partial grass cover	C	Eragrostis/slime exposure
4	Partial grass cover	C	Eragrostis/slime exposure
5	Slime exposure	A	100% white slime
6	Clover	D	100% clover (Medilago Sativa)
7	Clover	D	80% clover/20% Eragrostis
8	Pampas Grass	D	60% leaf/40% flower (Cortaderia Seloana)
9	Pampas grass	D	60% leaf/40% flower (Cortaderia Seloana)
10	"Fort Jackson"	D	100% leaf (Acacia Cyclopis)
11	Silver Wattle	D	100% leaf (Acacia Baileyana)

The curves on figures A1 and A2 are the bivariate reflectances calculated by computer analysis of the spectroradiometer measurements. These curves demonstrate the substantial difference between slime, Eragrostis and more mesophytic plant species.

The reflectance curve of a vigorous growth Eragrostis (fig. A1) exhibits the characteristic chlorophyll absorption regions (400 nm to 500 nm and 600 nm to 700 nm). This selective absorption is seen to a much greater degree for more

FIGURE A1

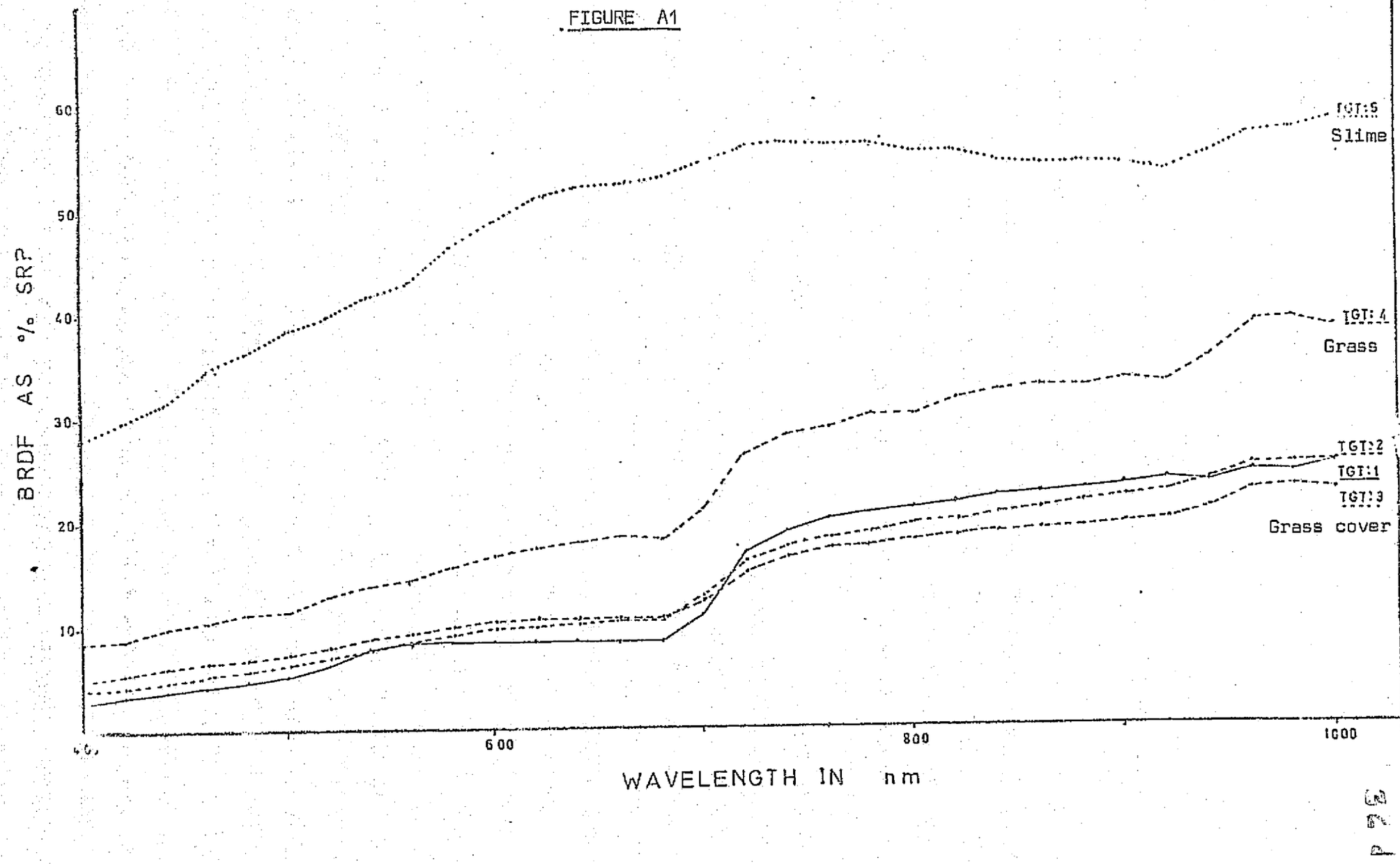
BRDF AS % SRP
60
50
40
30
20
10
600
800
1000
WAVELENGTH IN nm
TGT:5
Slime
TGT:4
Grass
TGT:2
TGT:1
TGT:3
Grass cover

mesophytic vegetation (see fig. A2) due to the greater chlorophyll content of the leaves. The comparatively low infrared reflectance of Eragrostis in the condition it generally exhibits on slime (fig. A1) is indicative of its low water requirements and hardy nature. This low water requirement and tenacity of the species have afforded the plant its importance in the slime dam vegetation program.

The partial Eragrostis/slime exposure BRDF's of targets 2 and 3 (figure A1) exhibit proportionally higher values in the chlorophyll absorption regions. Target 4 has a greater proportion of slime in the f.o.v. and gives an intermediate BRDF. Targets 6 to 11 were of the minority species growing where environmental conditions were comparatively good. Water conditions and slime compaction were more favourable for plant growth in these areas so that these species could be established in order to act as wind breaks for the more open areas of the dam. The BRDF's shown in figure A2 demonstrate the vigour of targets 6 to 11 in their strong chlorophyll absorption regions and high reflectance in the infra-red indicative of a healthy water content in the leaf.

Spectral Reflectance Measurements on Slimes Dams 5/L/29 and 5/L/31 : During the mid-winter period 28th June, 1972, to 6th July, 1972, further reflectance measurements were carried out on slimes dams 5/L/29 (classification 0) and 5/L/31 (classification 2). This completed the preliminary measurement program and gave data on the seasonal variation of the Eragrostis and further slime exposure reflectance values, as described in table A.2.

FIGURE A2

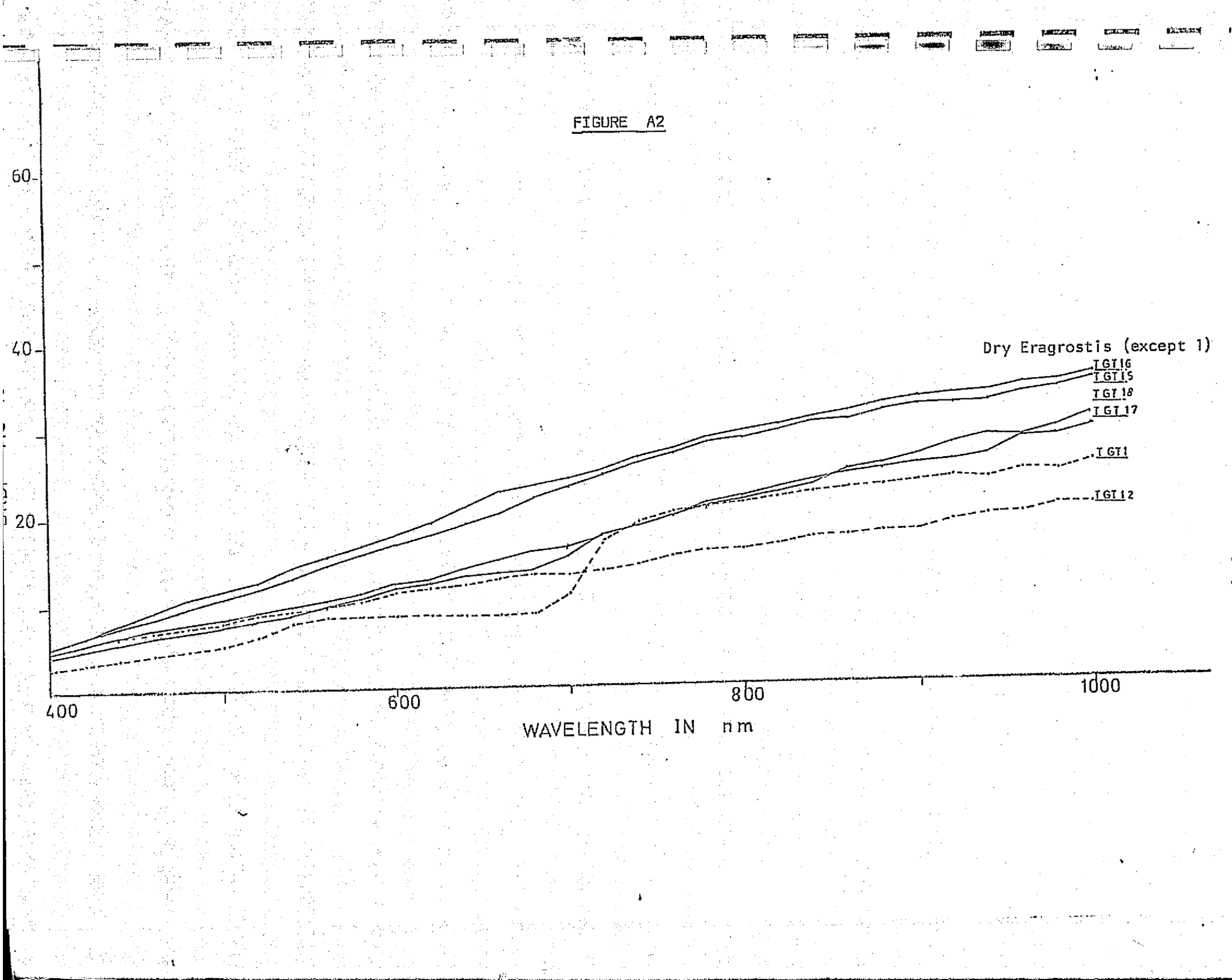
60
40
20
400
600
800
1000
WAVELENGTH IN nm
Dry Eragrostis (except 1)
TGT16
TGT15
TGT18
TGT17
TGT1
TGT12

TABLE A.2

Target Number	Description of Area	Classification	Field of View Coverage
12	Good grass cover	B	100% Eragrostis Curvula (Dry condition)
13	Slime exposure	A	100% white slime
14	Slime exposure	A	100% white slime
15	Good grass cover	B	100% Eragrostis Curvula (Dry condition)
16	Good grass cover	B	100% Eragrostis Curvula (Dry condition)
17	Good grass cover	B	100% Eragrostis Curvula (Dry condition)
18	Good grass cover	B	100% Eragrostis Curvula (Dry condition)

This reflectance data is shown in figs. A3 and A4 respectively. The slime BRDF of 5/L/29 is seen to be very similar to that of 1/L/40. The Eragrostis, however, exhibited a distinct lack of chlorophyl absorption. As this 600 nm to 700 nm band appeared to contrast favourably the winter and summer reflectances of the species, it was concluded that a multispectral filter in this region was most relevant for monitoring seasonal variation.

CONCLUSIONS

From observations of a number of slimes dams, it was apparent that the majority of vegetation patterns could be resolved on a grid basis into elements comprised of the target categories (A) to (D). The initial measurements were considered sufficient to determine the regions of the spectrum most suitable for mine dump vegetation monitoring and multispectral photography was planned on the resulting data. It was required that differences in the vegetative cover definitions of table 7.2 of the main text be maximised in the multispectral imagery so that the categories could be photographically defined. From the above observations of figures A2 to A4 and the available filters, it was concluded that filters desig-

FIGURE / A3

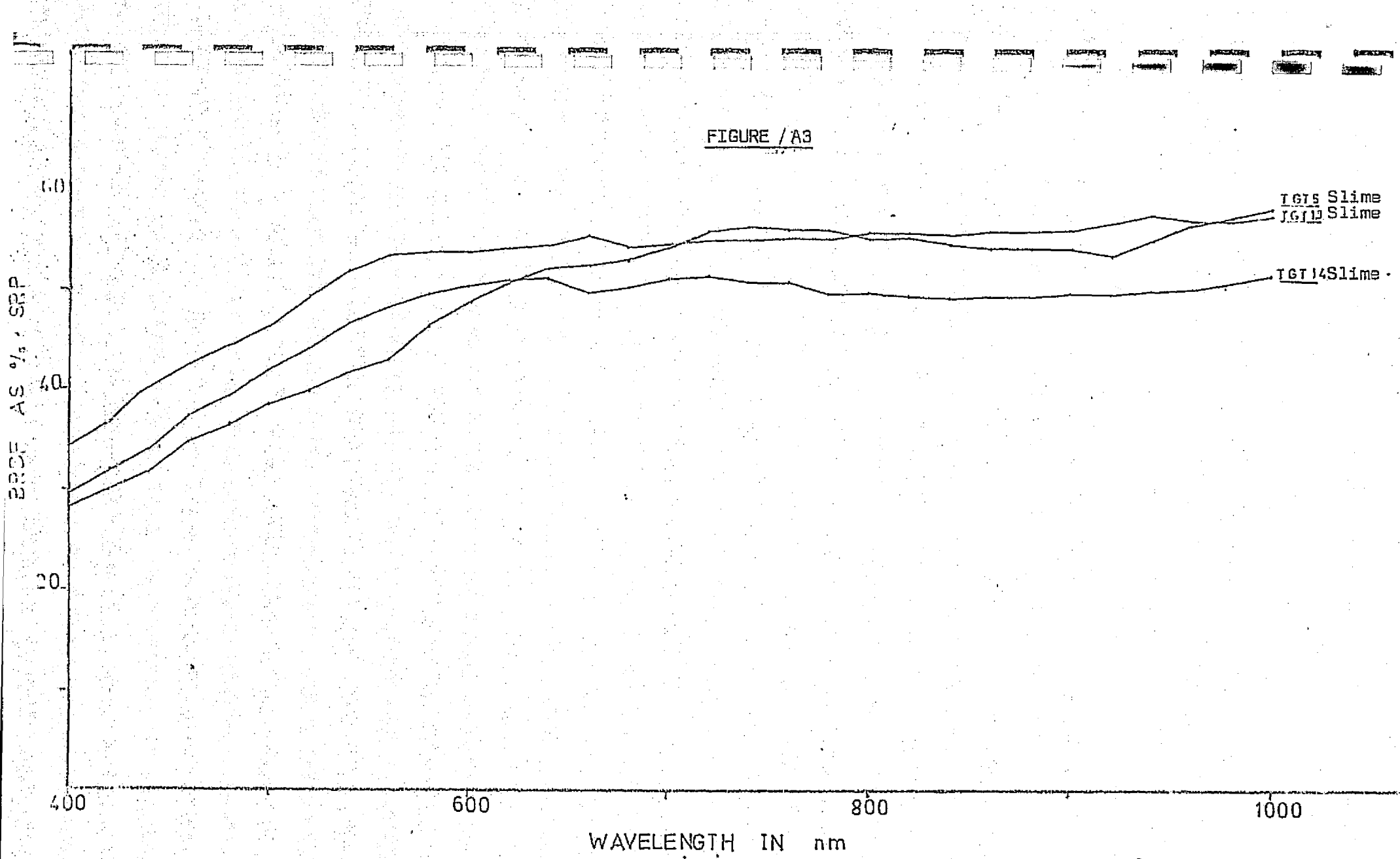
60
40
20
400
600
800
1000
WAVELENGTH IN nm
TGT5 Slime
TGT10 Slime
TGT14Slime

FIGURE A4

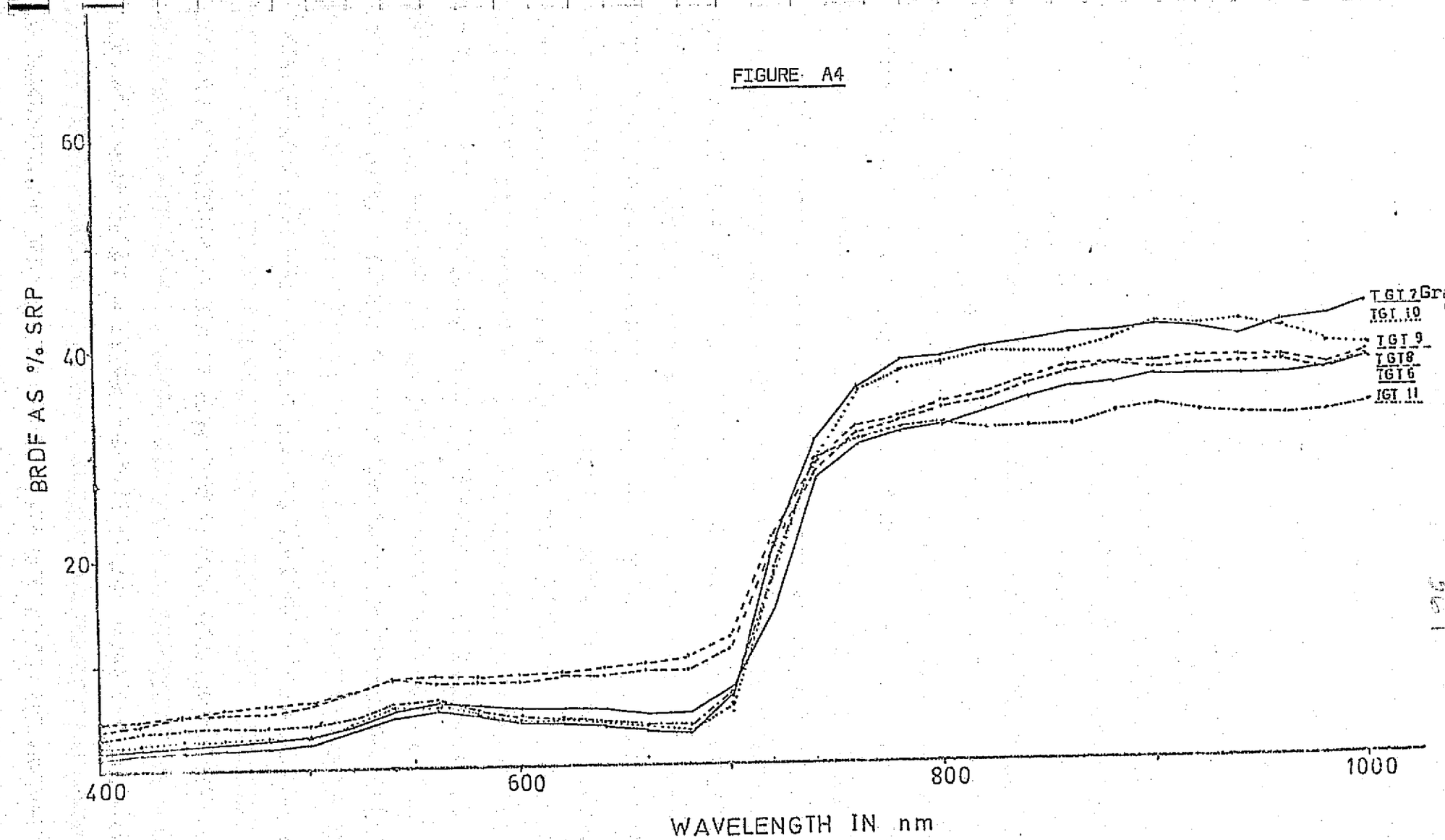
60
40
20
BRDF AS % SRP
400
600
800
1000
WAVELENGTH IN nm
TGT 7 Gr
TGT 10
TGT 9
TGT 8
TGT 6
TGT 11

nated I, L, M and Q (see figures A5 and A6), were most suitable for the recording of mine dump vegetation cover with maximum contrast between categories. Of these, filter M was most suitable for observing the season variation of Eragrostis attributed to leaf chlorophyll and water content fluctuation. This filter corresponded approximately to MSS band 5.

The passbands of the RBV and MSS of the ERTS-1 satellite are shown in fig. A7. MSS imagery appears most suitable for vegetation contrast due to the narrow passband specifications and out-off. In order to simulate these, an underflight of the multispectral aerial camera was scheduled for filters F, N, G and Q.

FIGURE A5

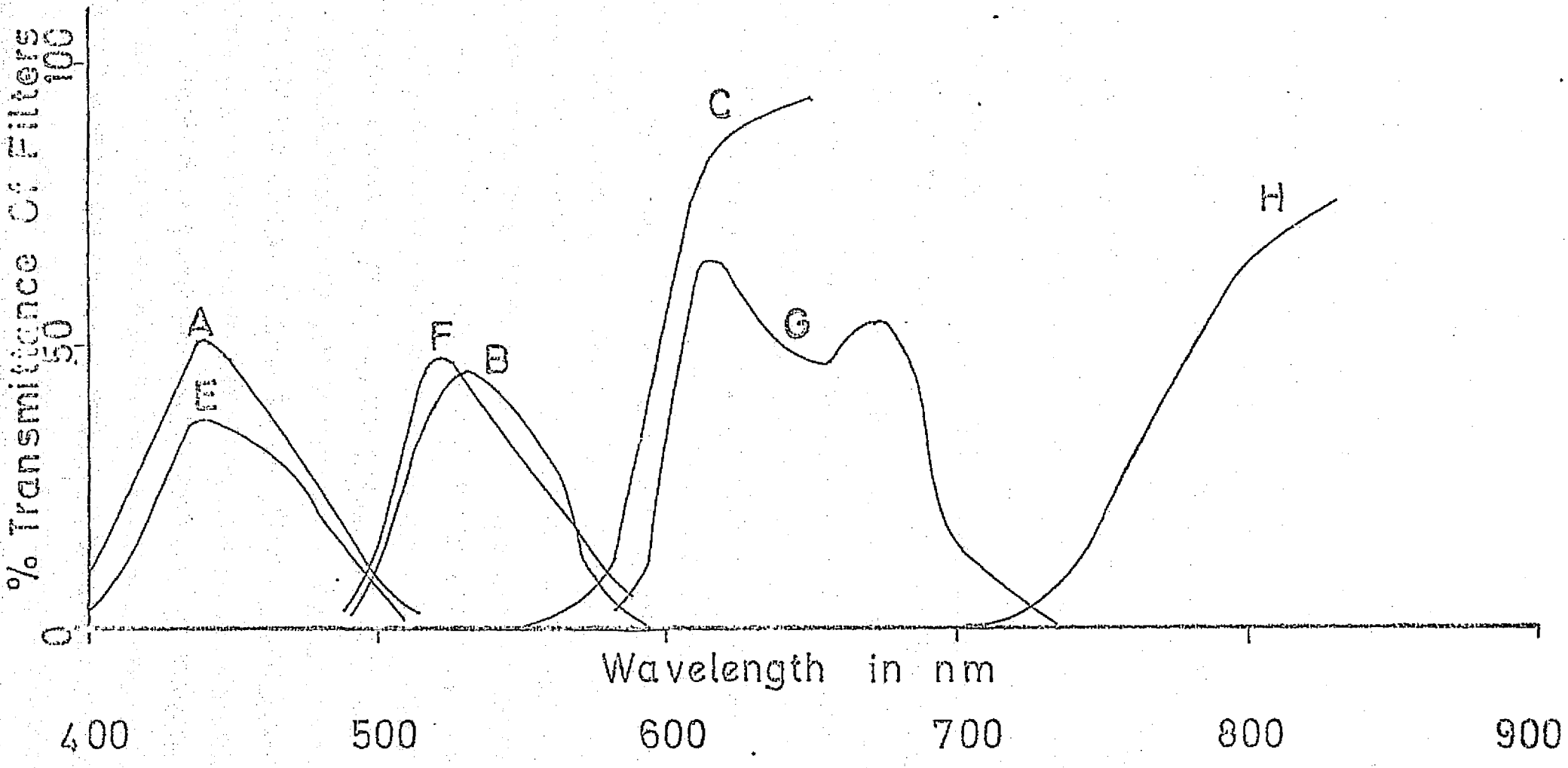
% Transmittance of Filters
100
50
0
A
E
F
B
C
G
H
Wavelength in nm
400
500
600
700
800
900

FIGURE A6

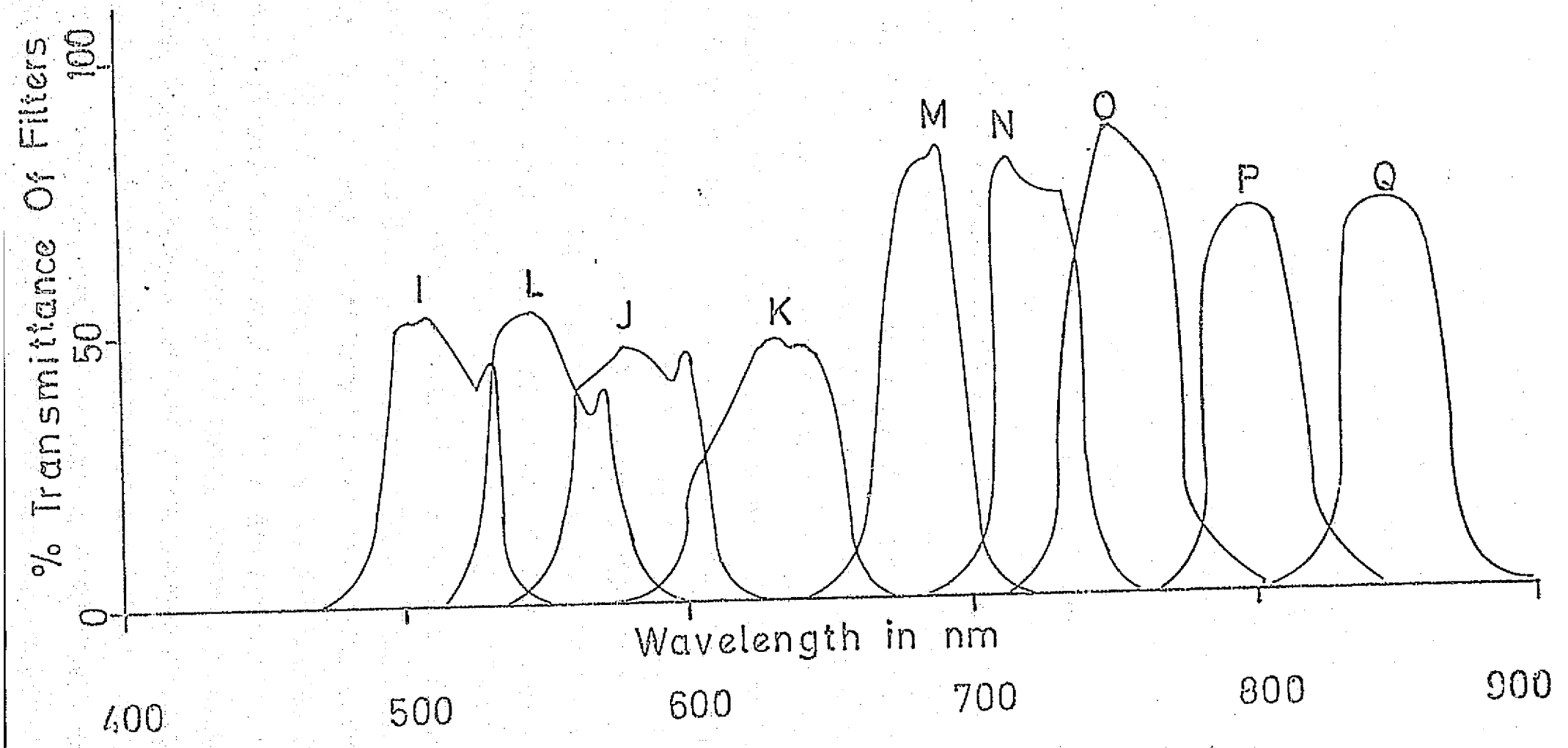
% Transmittance Of Filters
100
50
0
I
L
J
K
M
N
O
P
Q
Wavelength in nm
400
500
600
700
800
900

FIGURE A7

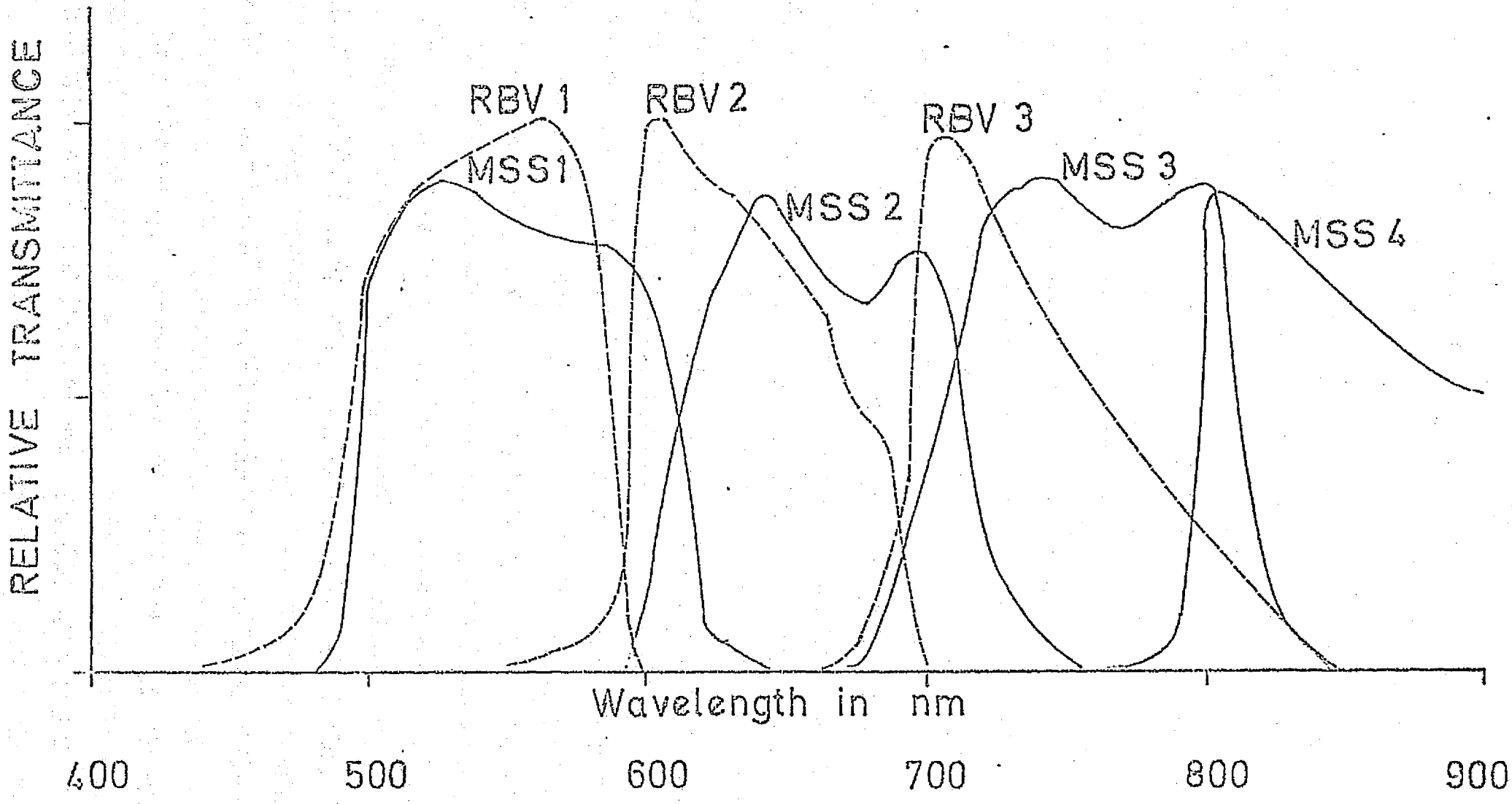
RELATIVE TRANSMITTANCE
RBV 1
RBV 2
RBV 3
MSS 1
MSS 2
MSS 3
MSS 4
Wavelength in nm
400
500
600
700
800
900

APPENDIX 'D'

INDEX OF

SOME WITWATERSRAND MINE DUMPS

RELATING TO

ERTS 1 PROGRAM SR 0577

No.	Chamber of Mines Index No.	Mine	Group
1	1/L/41	Randfontein Estates G.M.Co.	J.C.I
2	1/L/40	" " " "	"
3	1/L/39	" " " "	"
4	1/L/38	" " " "	"
5	1/L/37	" " " "	"
6	1/A/20	" " " "	"
7	1/L/22	West Rand Consolidated Mines	General Mining
8	1/L/24	" " " "	" "
9	1/L/26	" " " "	" "
10	2/L/11	Rand Leases Gold Mines	Anglo Vaal
11	2/L/9	" " " "	" "
12	3/L/4	Crown Mines	Independent.
13	3/L/6	" "	"
14	3/L/5	" "	"
15	5/L/29	Van Dyk Consolidated Mines	Union Corp.
16	5/L/31	South African Land & Exp.Co.	Anglo American
17	6/L/17	Grootvlei Pty. Mines	Union Corp.
18	7/L/1	Daggafontein Mines	Anglo American
19	7/L/2	East Daggafontein	" "
20	7/L/4	Vogelstruisbult Gold Mine	Goldfields of S.A.

INDEX OF

9 FLIGHT INDECES

OF

SOME WITWATERSRAND MINE DUMPS

RELATING TO

ERTS 1 PROGRAM SR 0577

SHEET NO.	SENSOR	SEASON	SCALE OF PHOTOGRAPHY
1	S.D.C. MULTI-SPECTRAL	WINTER	1 : 40 000 APPROX.
2	WILD RC10, UAg/COLOUR NEG.	WINTER	1 : 45 000 APPROX.
3	WILD RC10, SAg/PAN. NEG.	SUMMER	1 : 70 000 APPROX.
4	WILD RC10, SAg/COLOUR NEG.	SUMMER	1 : 70 000 APPROX.
5	WILD RC10, UAg/I-R COLOUR POS.	SUMMER	1 : 20 000 APPROX.
6	WILD RC10, UAg/COLOUR NEG.	SUMMER	1 : 20 000 APPROX.
7	S.D.C. MULTI-SPECTRAL	SUMMER	1 : 40 000 APPROX.
8	WILD RC10, SAg/COLOUR NEG.	WINTER	1 : 70 000 APPROX.
9	WILD RC10, SAg/I-R COLOUR POS.	WINTER	1 : 70 000 APPROX.

FLIGHT INDEX
OF
SOME WITWATERSRAND MINE DU
RELATING TO
ERTS I PROGRAM SR 0577

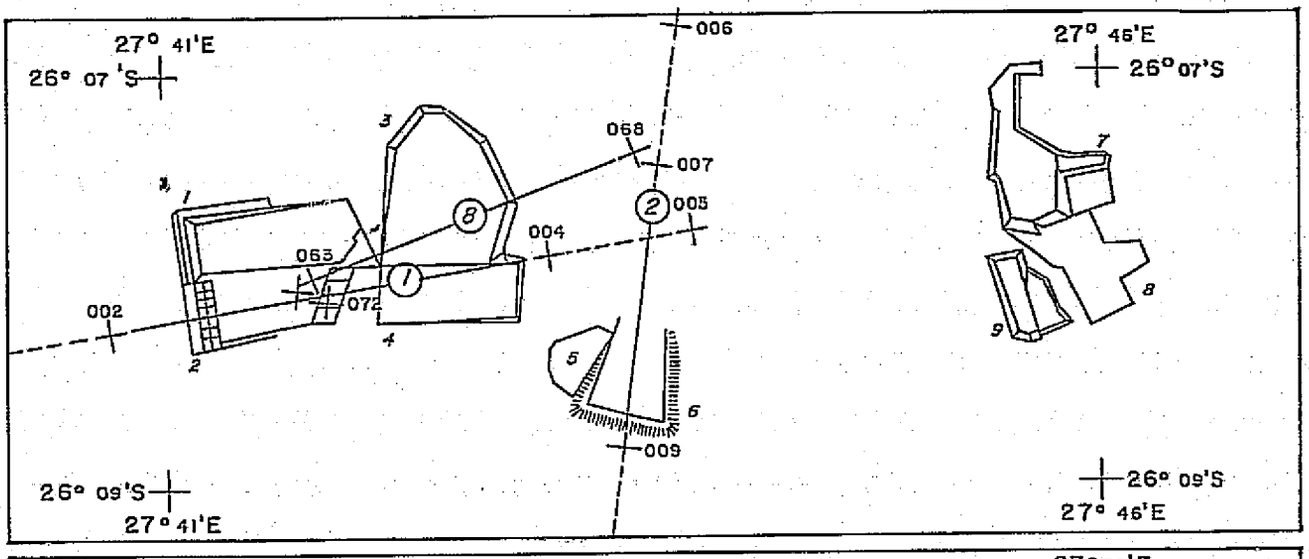

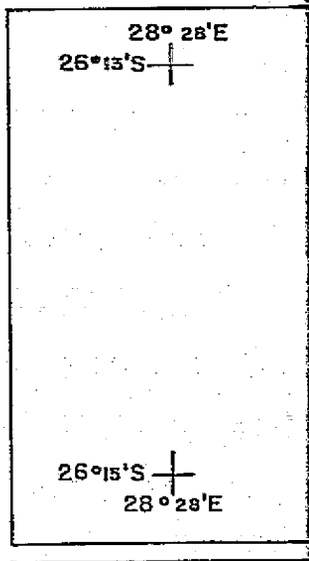

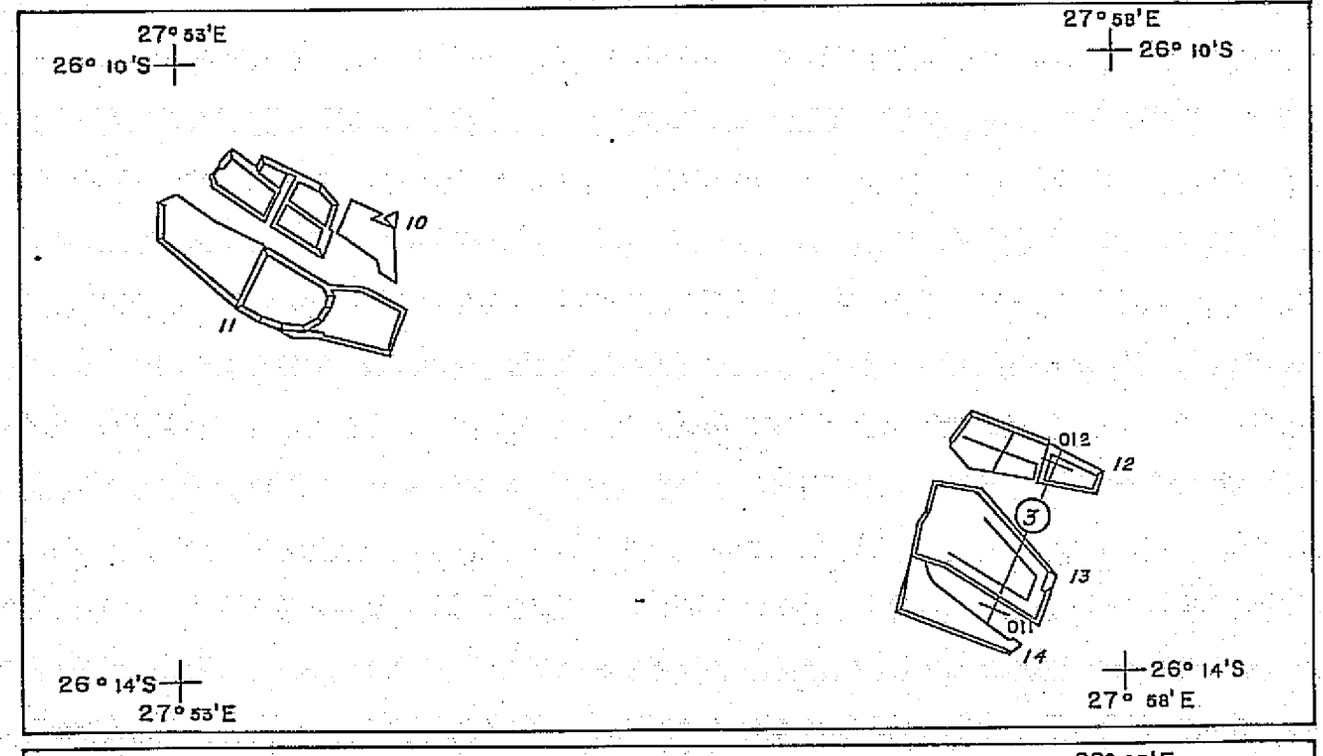

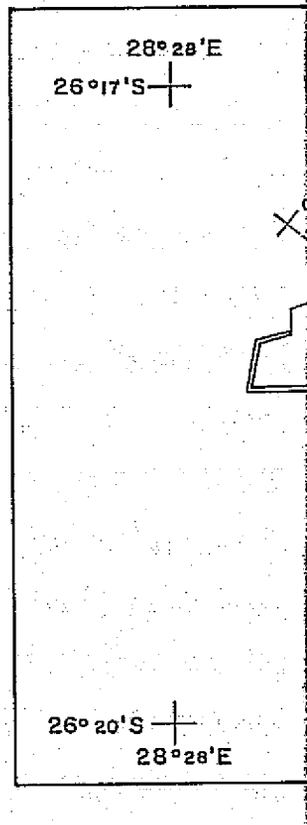

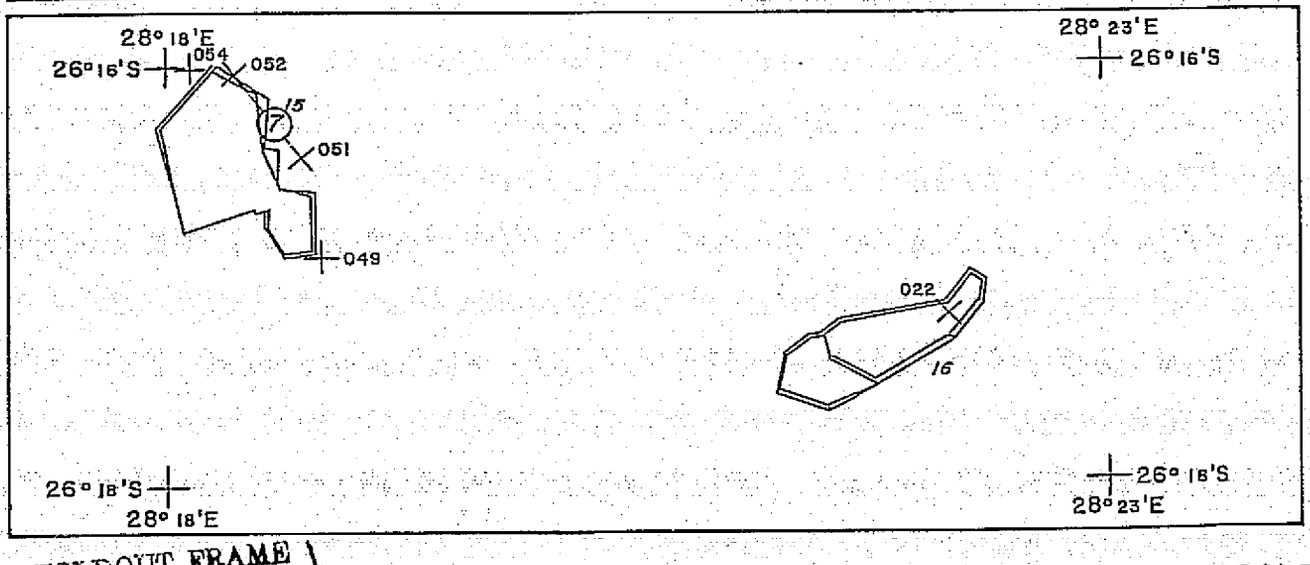

JOB No;
CAMERA;
LENS/ES;
FOCAL LENG
FILTER/S;
FILMS;
SCALES &
STRIP
1
2
3
4
5
6
7
8

FOLDOUT FRAME 1

SCALE 1 : 75 000

FLIGHT INDEX
OF
E WITWATERSRAND MINE DUMPS
RELATING TO
ERTS I PROGRAM SR 0577

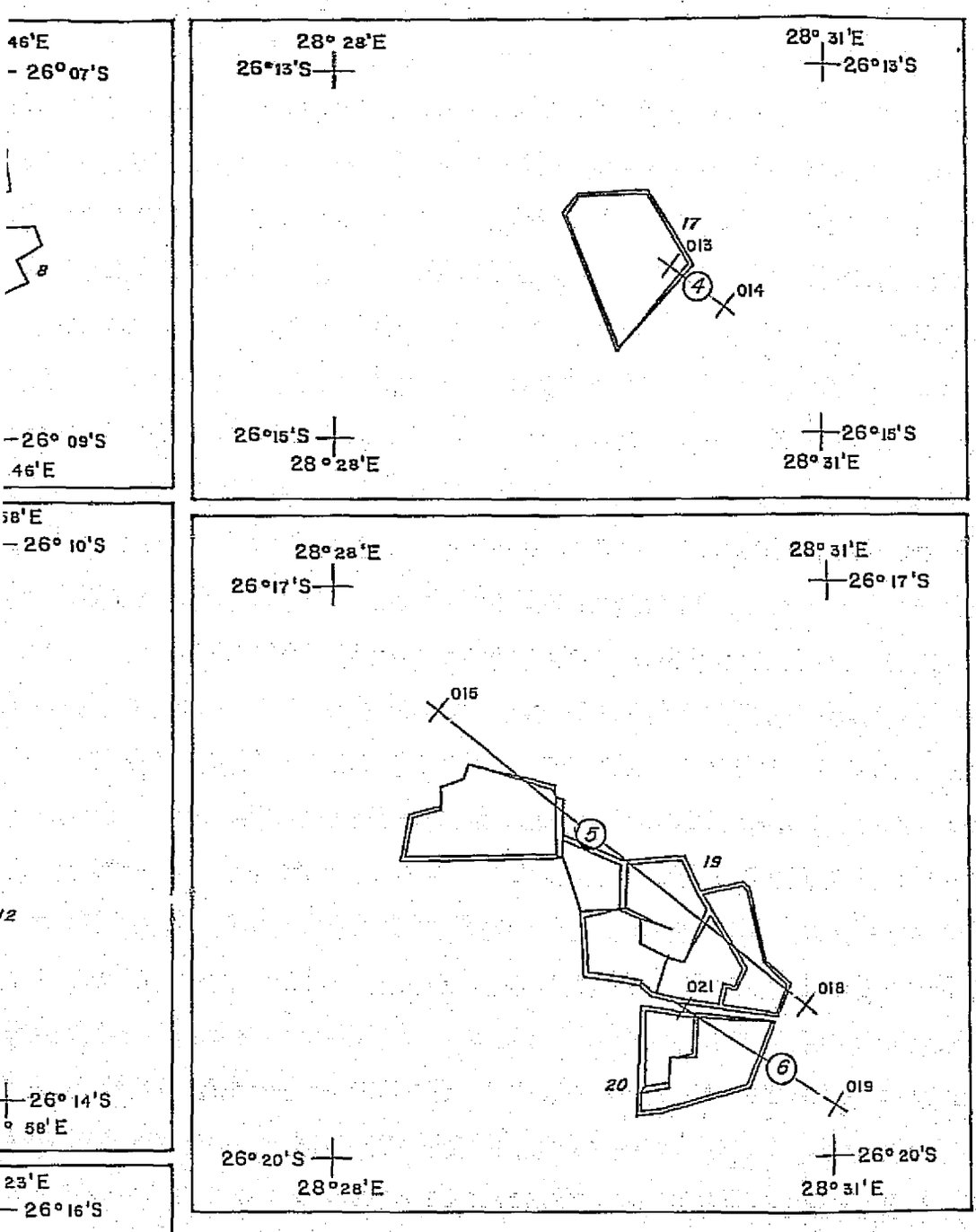

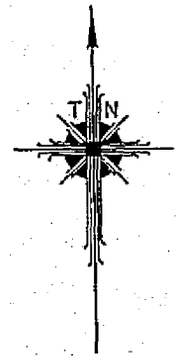

JOB No; 71 / 14
CAMERA; SDC MULTI-SPECTRAL (TYPE K22 MOD)
LENS/ES; 4 x SCHIENDER - KREUZNACH XENOTAR 1:2,8
FOCAL LENGTH; 150mm, No1,10-801-925; No 2,10-801-912; No 3,10-801-899; No 4, 10-801-913
FILTER/S; Q/Q* N/M * G/E * F/L *
FILMS; KODAK 2424 (B & W I R NEG.)
SCALES & DATES OF PHOTOGRAPHY;

STRIP No.	SCALE	No's	DATE
1	1:40,000	003 - 005	26 th JUL 72
2	"	006 - 010	"
3	"	011 - 012	"
4	"	013 - 014	"
5	"	015 - 018	"
6	"	019 - 021	"
-	"	022	"
-	"	049	"
7	"	051 - 052	"
-	"	054	"
*8	1:20000	063 - 068	"
*	1:10 000	070	"
*	1: 5 000	072	"

SPECTRAL AFRICA (PTY.) LTD.
PO.BOX 2, RANDFONTEIN.
TEL. 663 3687
TELEX. J/7614

SCALE 1 : 75 000

FOLDOUT FRAME 2

RJ.S. 26.1.74

FLIGHT INDEX
OF
SOME WITWATERSRAND MINE DUM
RELATING TO
ERTS I PROGRAM SR 0577

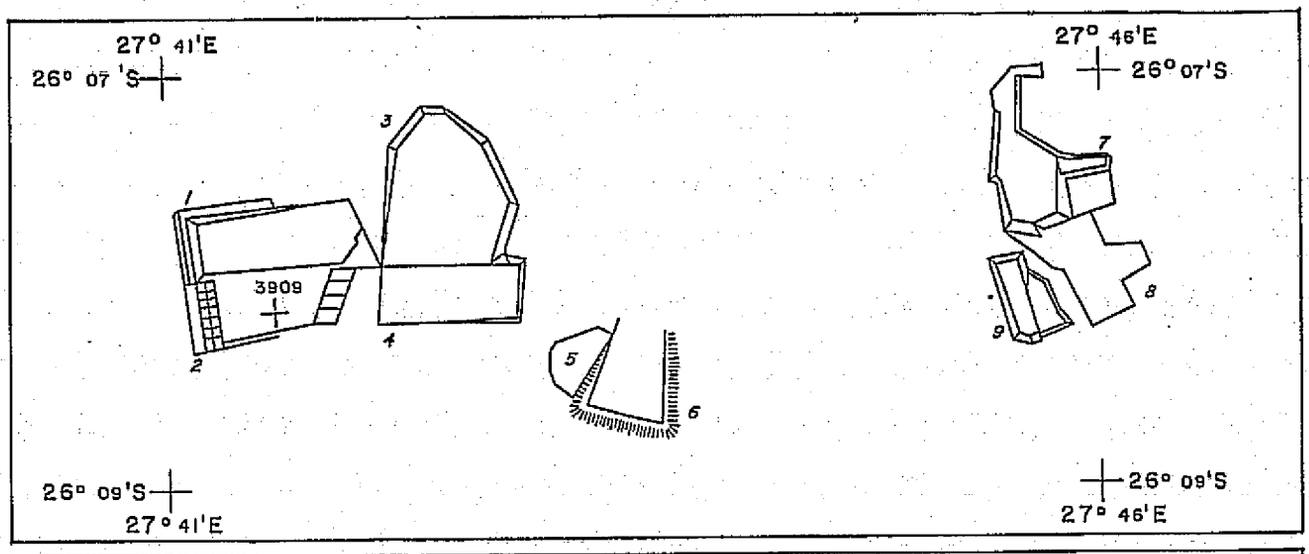

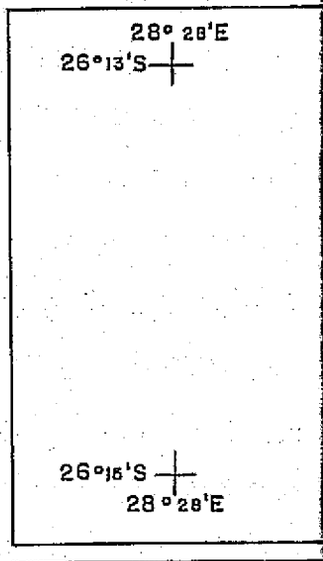

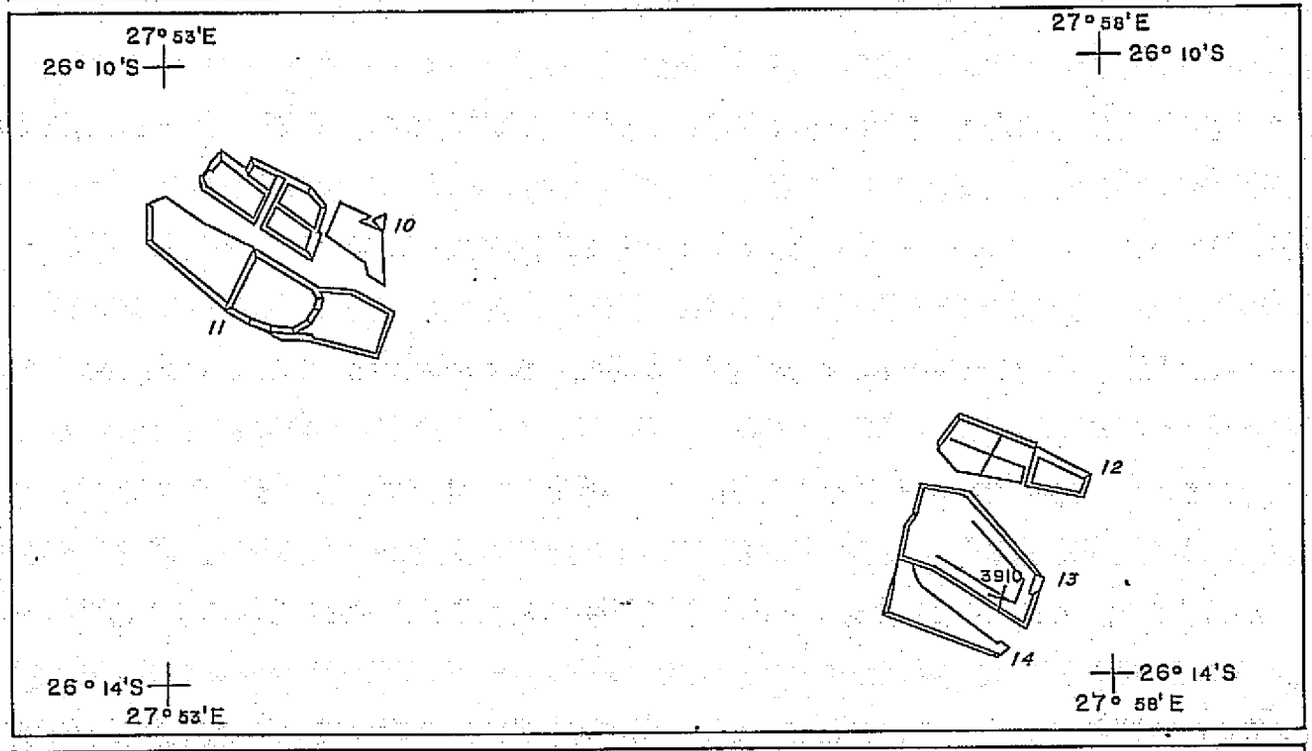

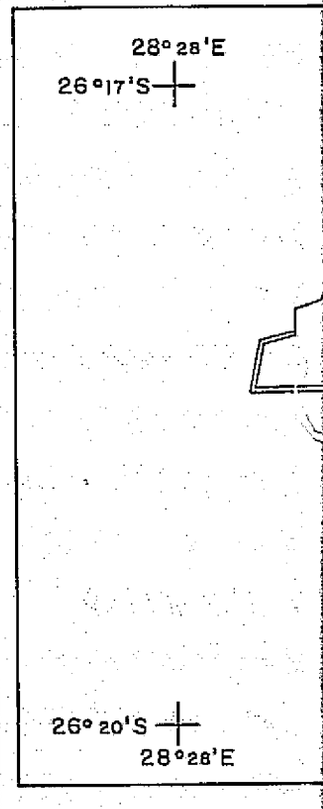

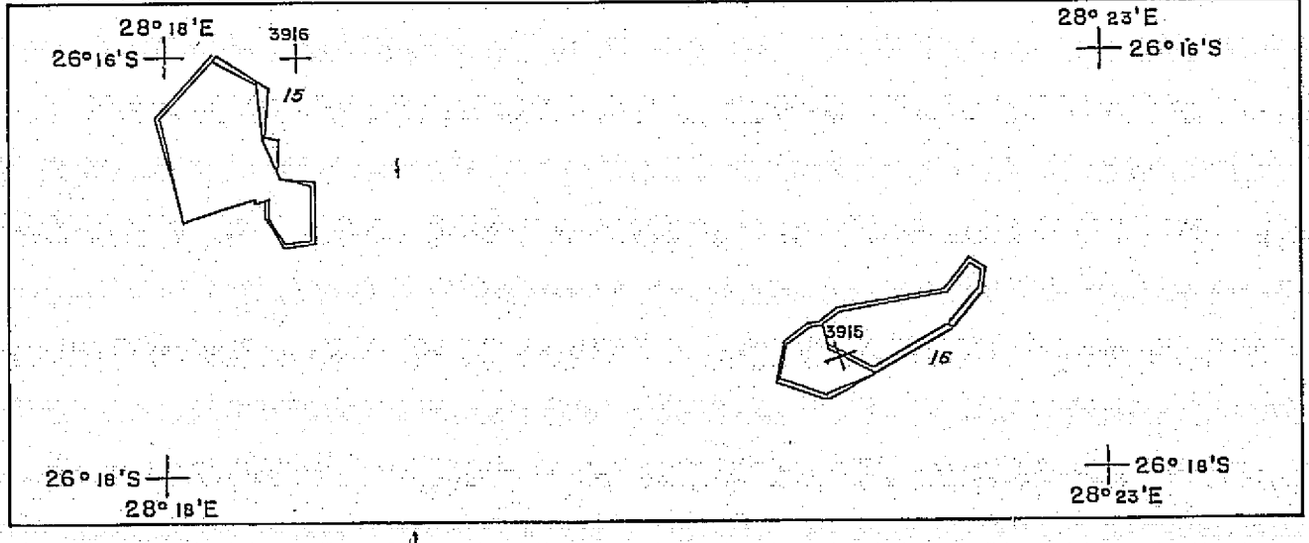

JOB No;
CAMERA;
LENS/ES;
FOCAL LENGT
FILTER/S;
FILMS;
SCALES & D
STRIP N

FOLDOUT FRAME 1

SCALE 1 : 75 000

FLIGHT INDEX
OF

ME WITWATERSRAND MINE DUMPS
RELATING TO
ERTS I PROGRAM SR 0577

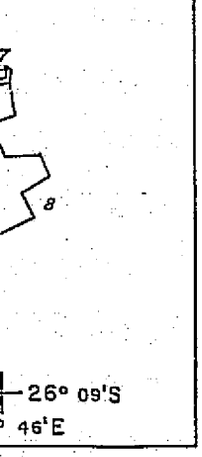

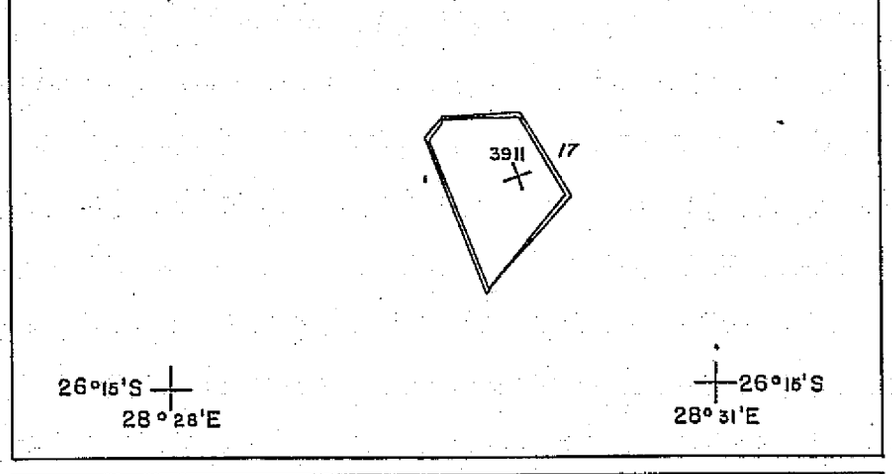

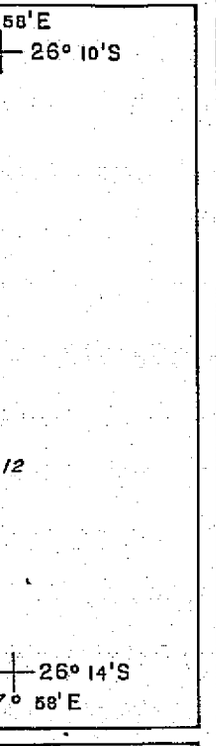

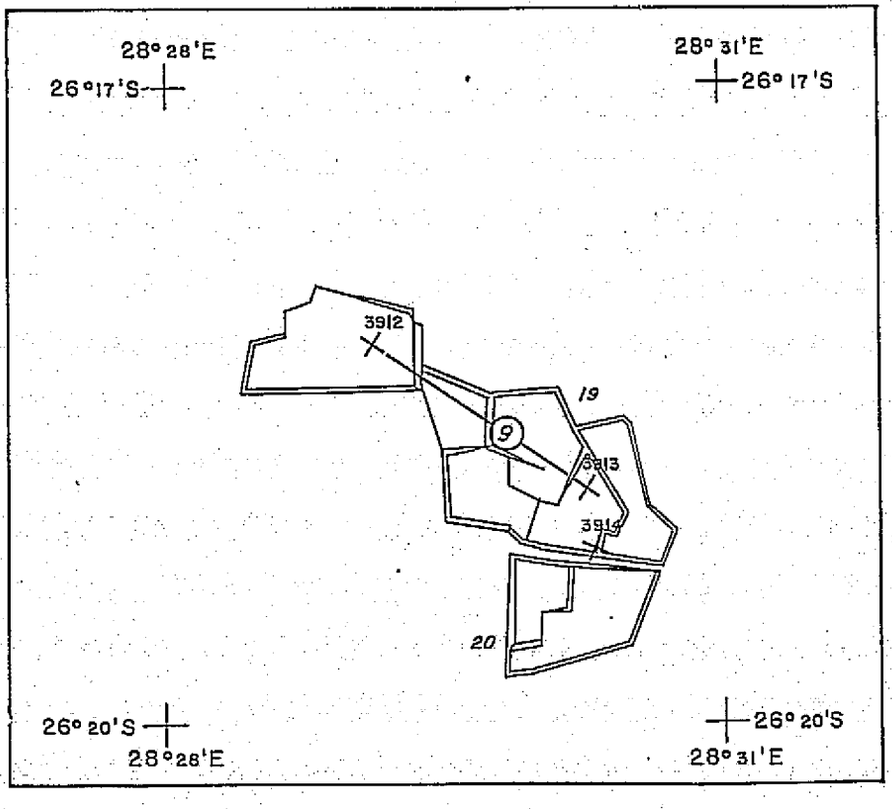

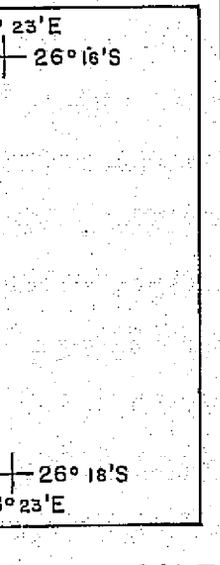

JOB No;	71 / 14
CAMERA;	WILD RC10, No. 1346
LENS/ES;	UAg, No 1016.
FOCAL LENGTH;	151, 45mm.
FILTER/S;	—
FILMS;	KODAK AEROCHROME 2445 (NEG.)

SCALES & DATES OF PHOTOGRAPHY;

STRIP No.	SCALE	No's	DATE
-	1:45000 APPROX.	3909	26th. JUL. 72
-	"	3910	" "
-	"	3911	" "
9	"	3912 - 3913	" "
-	"	3914	" "
-	"	3915	" "
-	"	3916	" "

SPECTRAL AFRICA (PTY.) LTD.
P.O. BOX 2, RANDFONTEIN.
TEL. 663 3687
TELEX. J/7614

SCALE 1 : 75 000

R.J.S. 26.1.74

FRAME 2

SOME WITWATERSRAND MINE DU
RELATING TO
ERTS I PROGRAM SR 0577

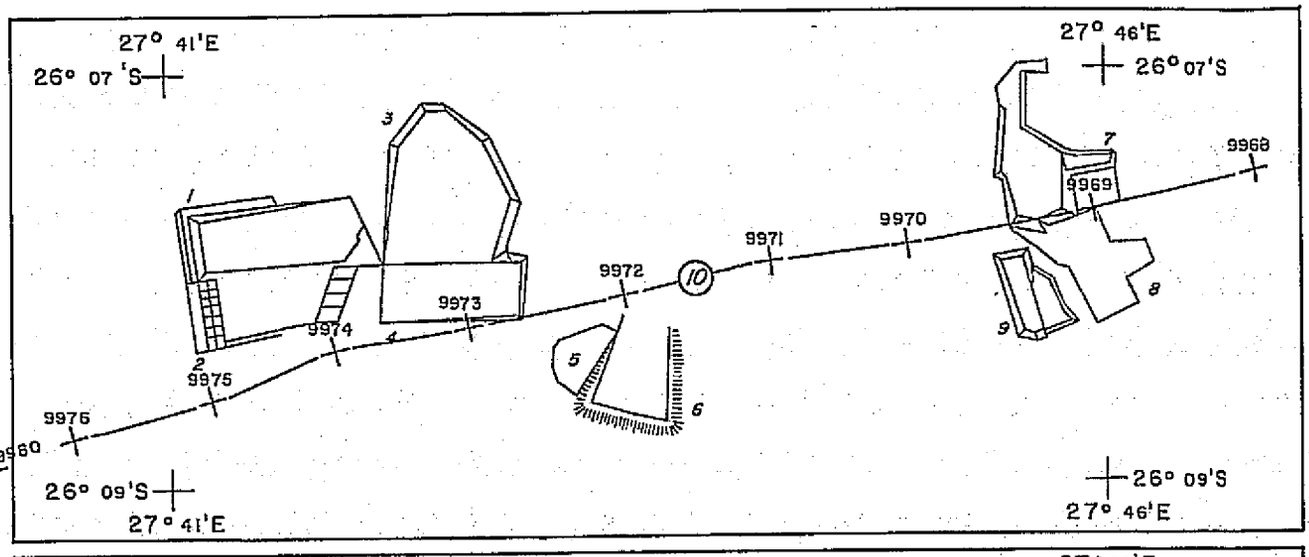

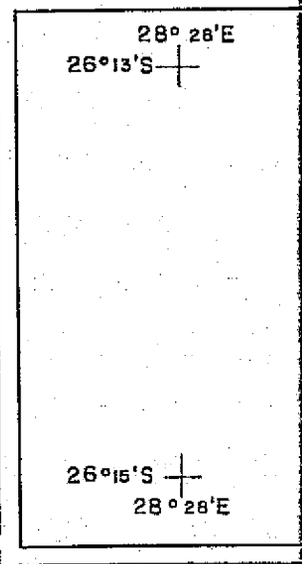

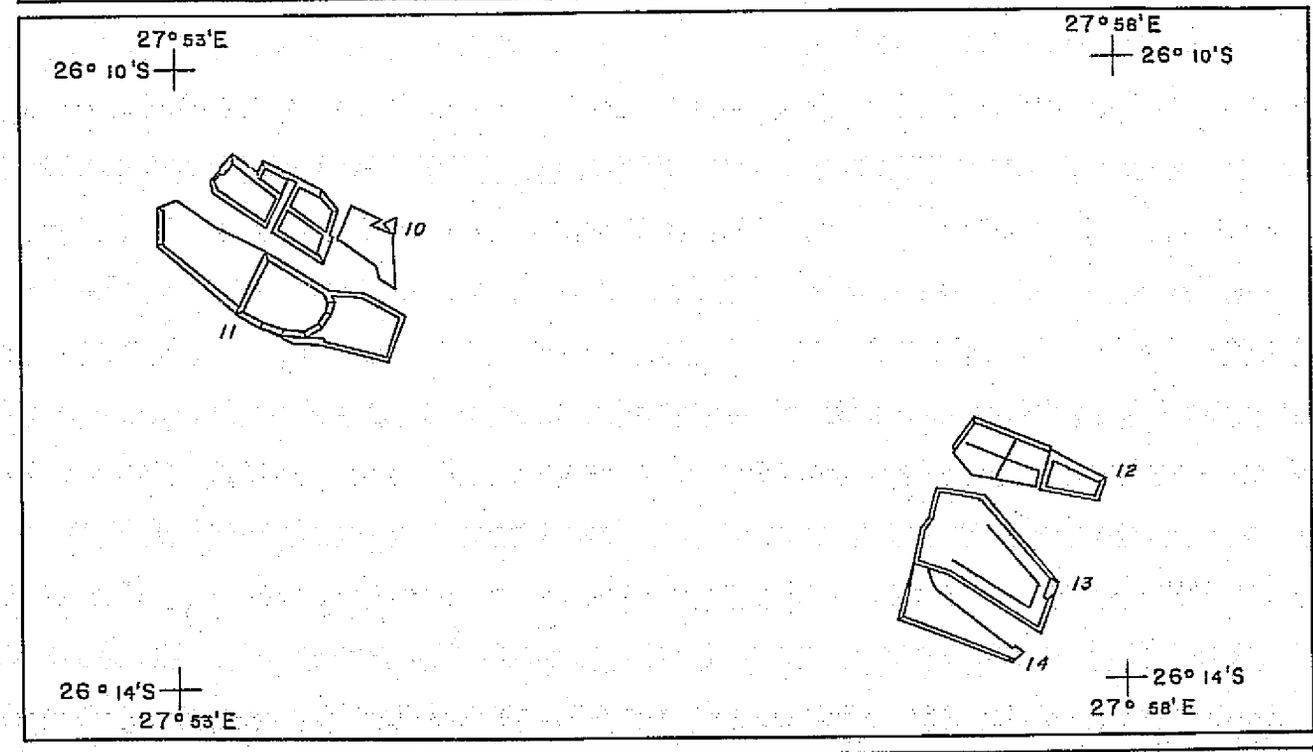

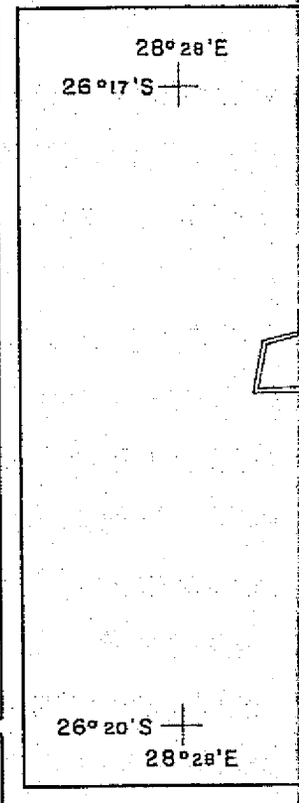

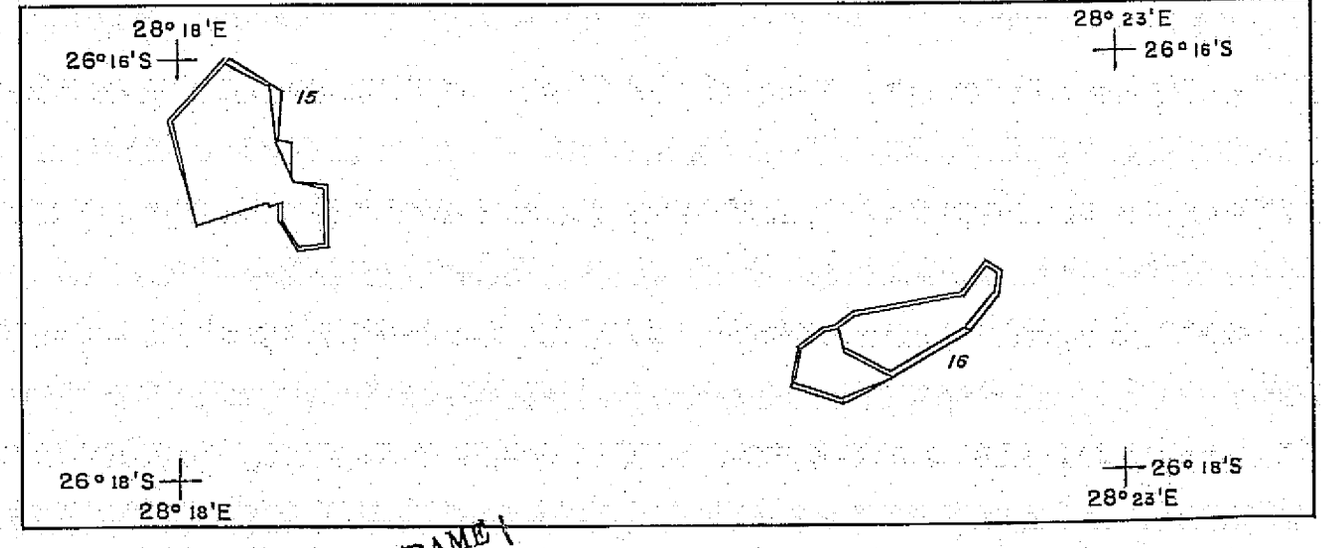

JOB No;
CAMERA;
LENS/ES;
FOCAL LEN
FILTER/S;
FILMS;
SCALES &
STRIP
IO

FOLDOUT FRAME 1

SCALE 1 : 75 000

OF

ME WITWATERSRAND MINE DUMPS

RELATING TO

ERTS I PROGRAM SR 0577

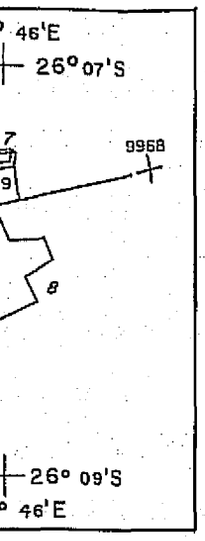

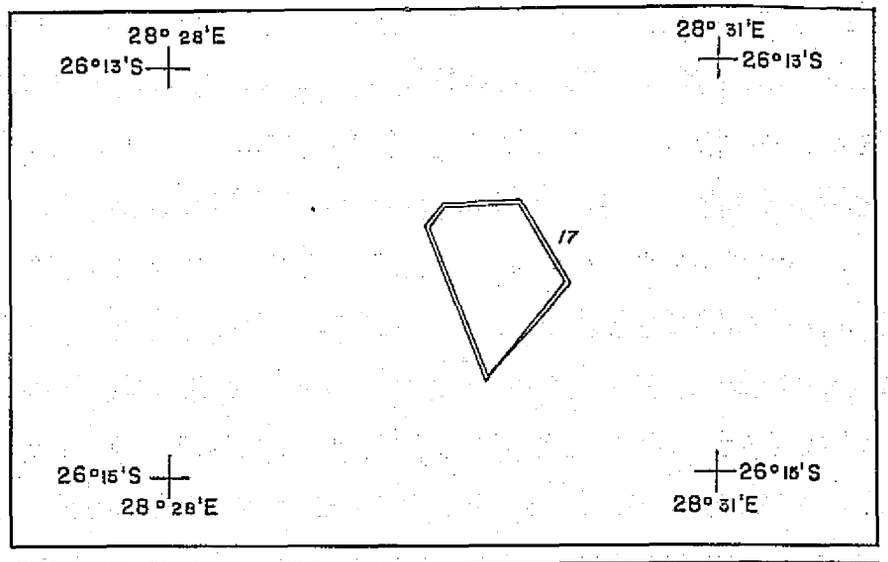

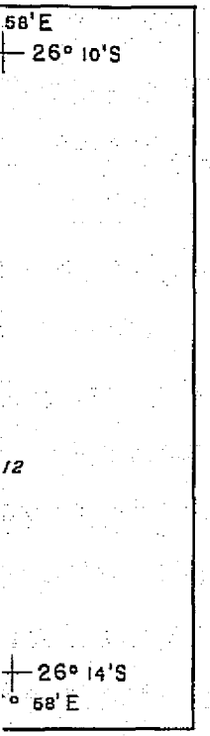

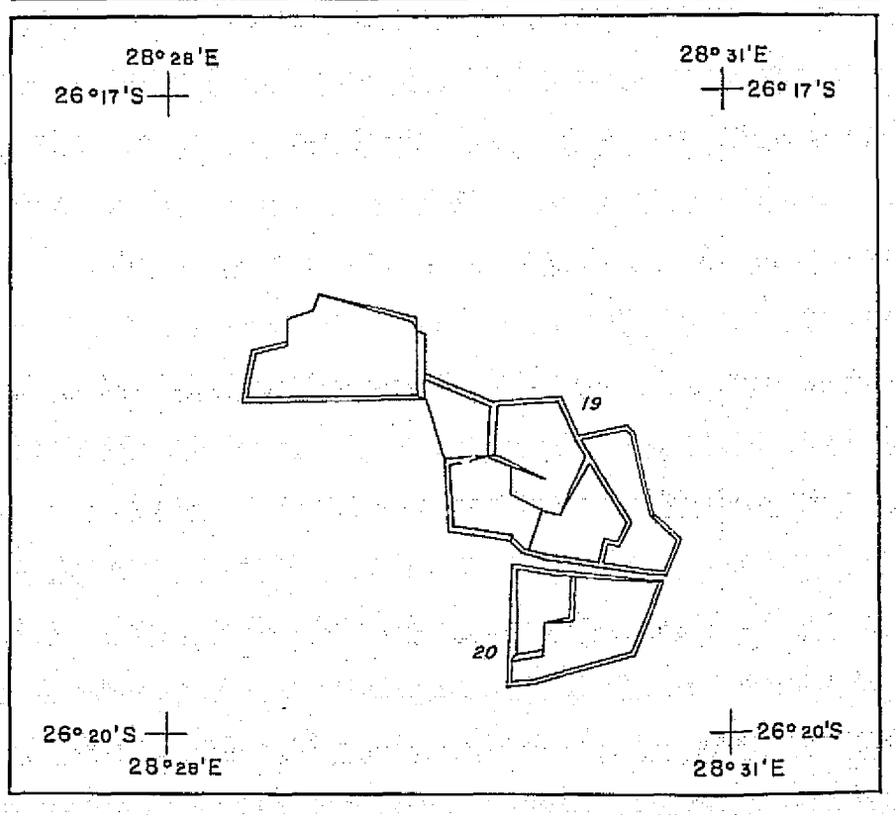

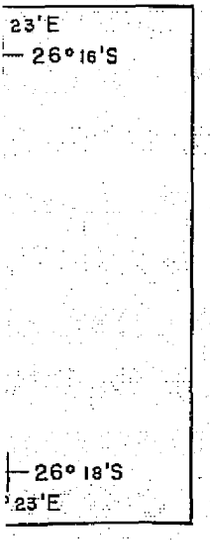

JOB No;	71 / 14
CAMERA;	WILD RC10, No 1346
LENS/ES;	SAg II, No 2029
FOCAL LENGTH;	87,28 mm.
FILTER/S;	RODANISED.
FILMS;	KODAK AEROGRAPHIC PLUS X.

SCALES & DATES OF PHOTOGRAPHY;

STRIP No.	SCALE	No's	DATE
10	1: 70000 APPROX.	9968 - 9980	10 th. NOV. 73

SPECTRAL AFRICA (PTY.) LTD.
P.O. BOX 2, RANDFONTEIN.
TEL. 663 3687
TELEX. J/ 7614

SCALE 1 : 75 000

RJ.S. 26. 1. 74

FOLDOUT FRAME 2

SOME WITWATERSRAND MINE DU
RELATING TO
ERTS I PROGRAM SR 0577

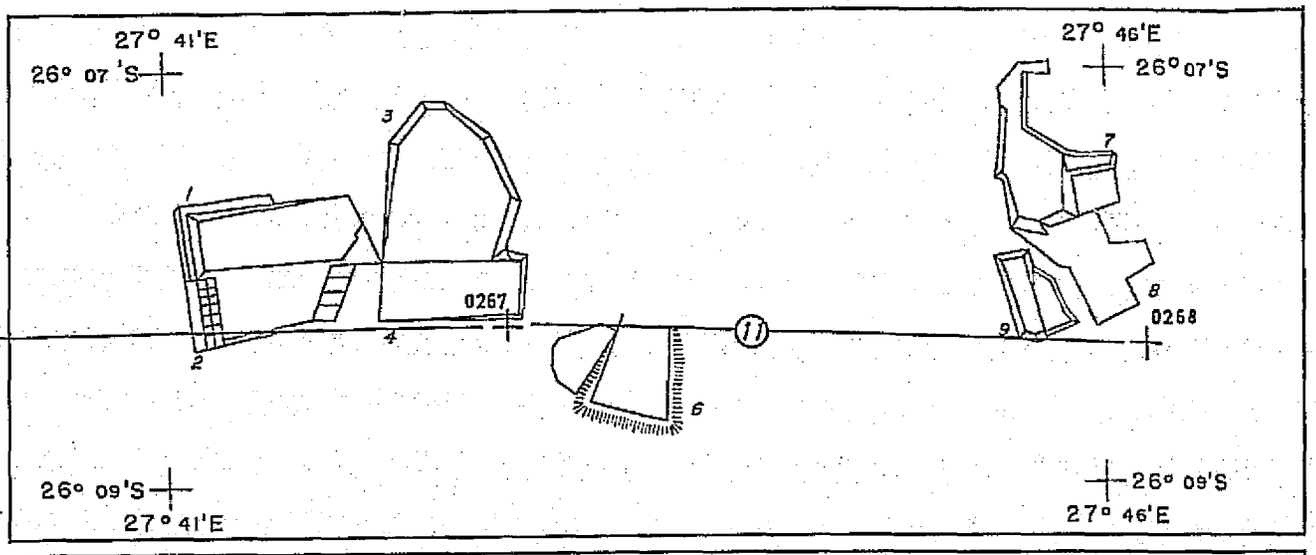

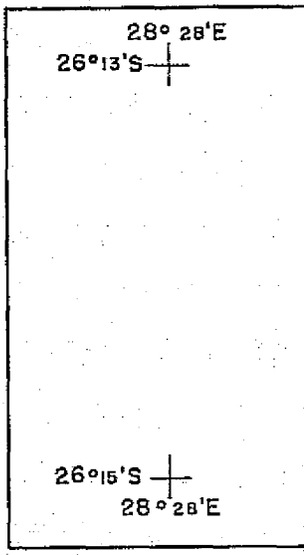

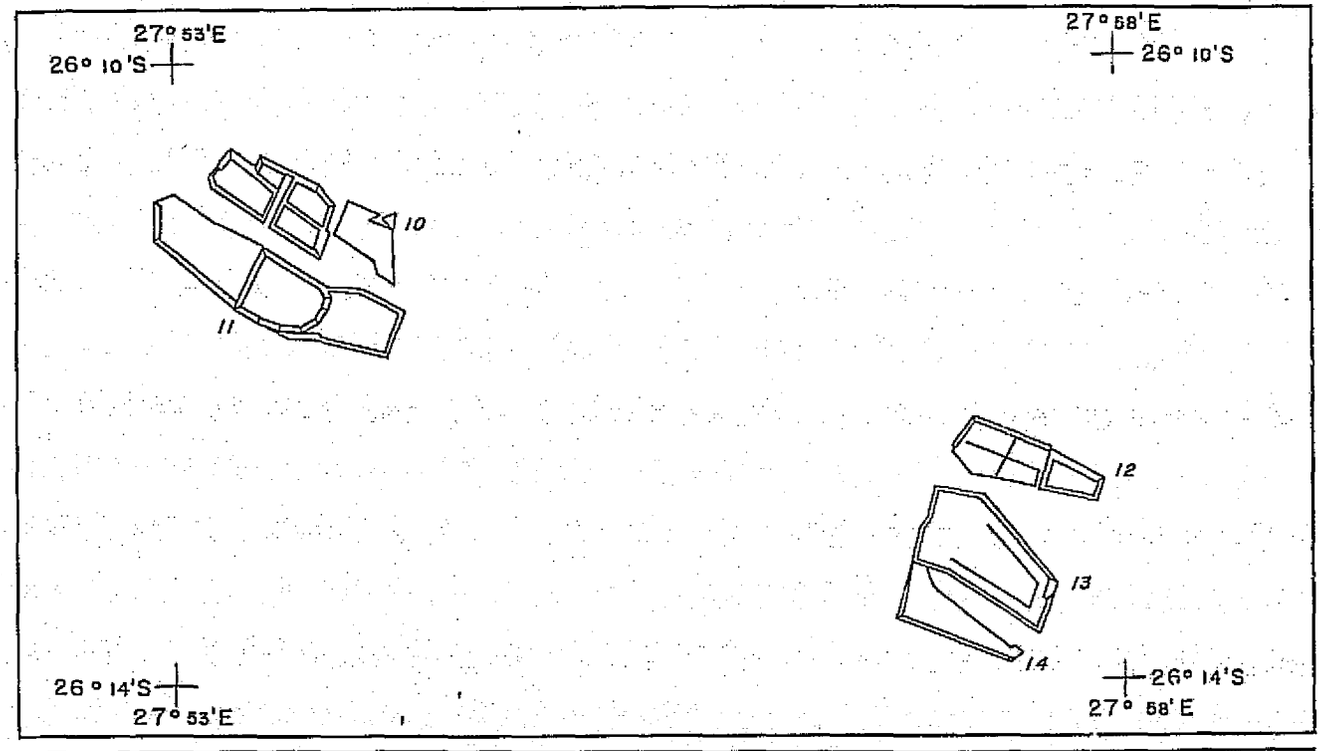

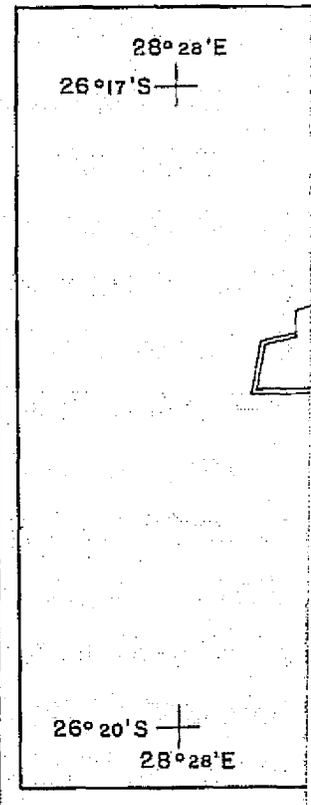

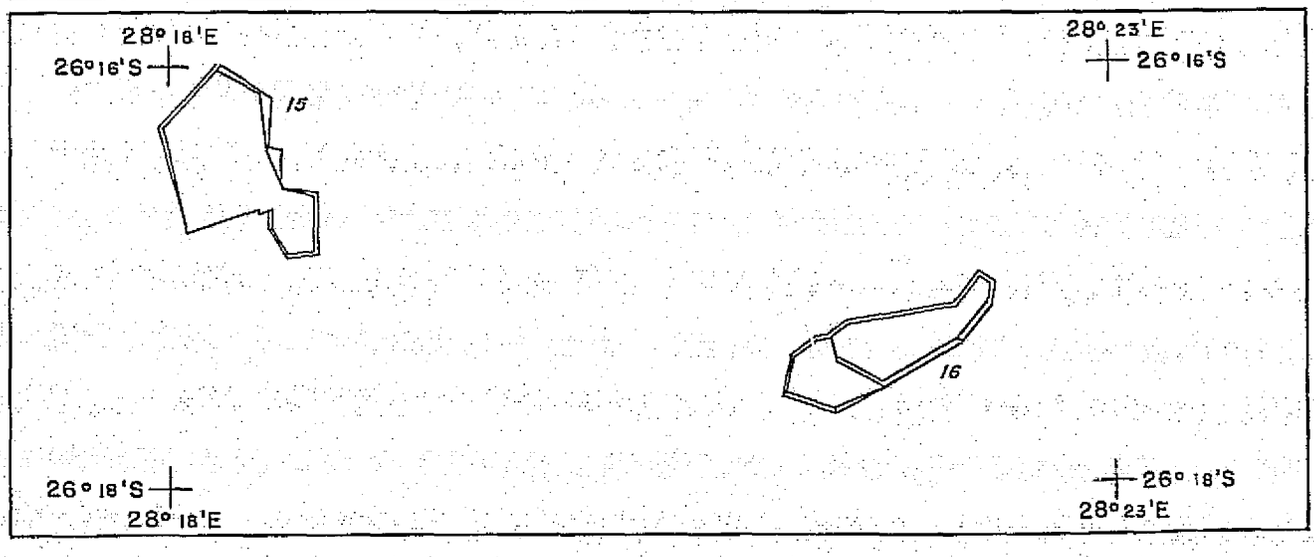

JOB No;
CAMERA;
LENS/ES;
FOCAL LENG
FILTER/S;
FILMS;
SCALES &
STRIP
"

SCALE 1 : 75 000

FULL OUT FRAME !

OF

WITWATERSRAND MINE DUMPS
RELATING TO

RTS I PROGRAM SR 0577

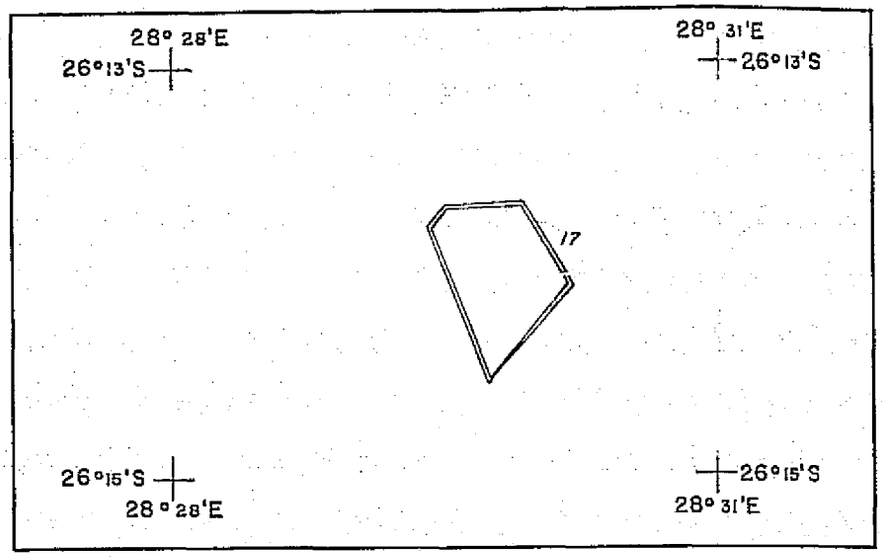

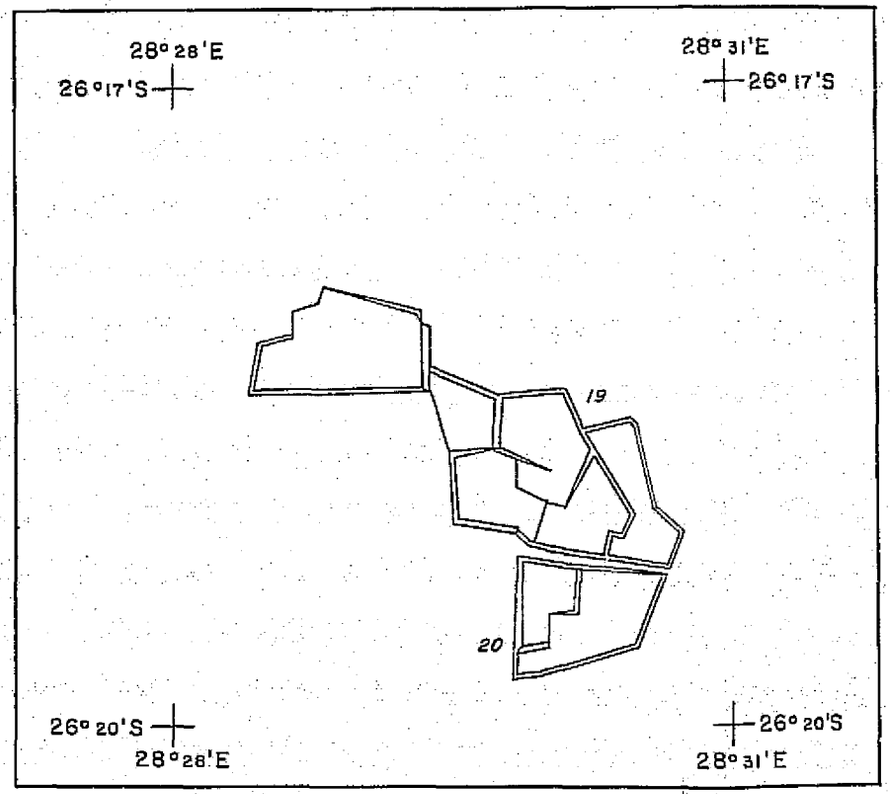

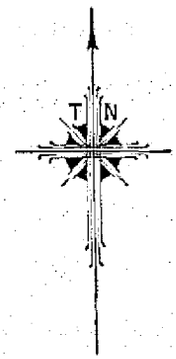

JOB No;	71 / 14
CAMERA;	WILD RC 10 No 1346
LENS/ES;	UAg No 1016
FOCAL LENGTH;	151,45 m.m.
FILTER/S;	BLUE RODANISED 2B SANDWICH
FILMS;	KODAK AEROCOLOUR 2445 (NEG)

SCALES & DATES OF PHOTOGRAPHY;

STRIP No.	SCALE	No's	DATE
"	1:70 000 APPROX.	0266 0268	10th. NOV. '72.

SPECTRAL AFRICA (PTY.) LTD.
P.O. BOX 2, RANDFONTEIN.
TEL. 663 3687
TELEX. J/7614

SCALE 1 : 75 000

R.J.S. 26.1.74

FOLDOUT FRAME 2

FLIGHT INDEX
OF
SOME WITWATERSRAND MINE DUM
RELATING TO
ERTS I PROGRAM SR 0577

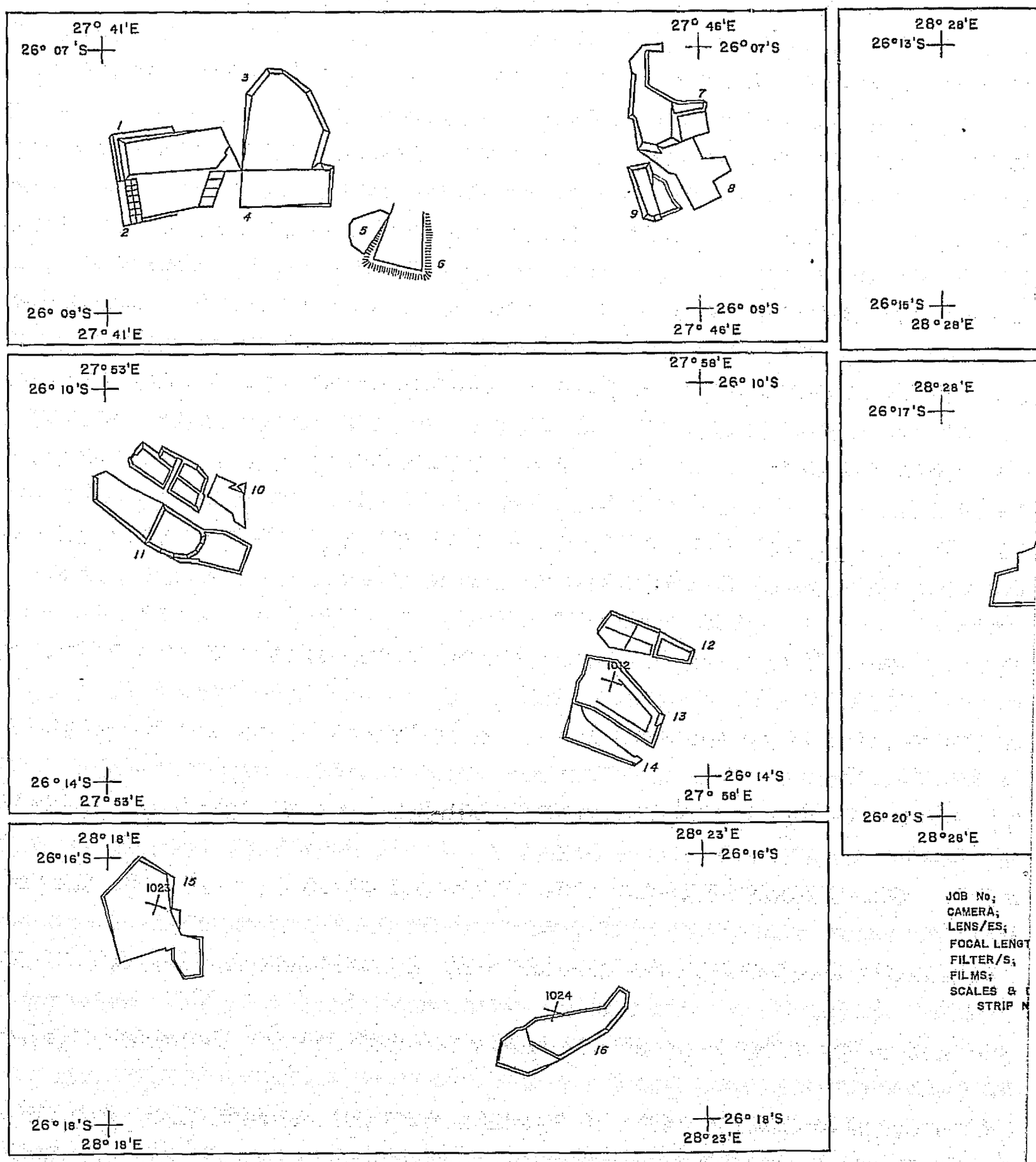

JOB No;
CAMERA;
LENS/ES;
FOCAL LENGT
FILTER/S;
FILMS;
SCALES &
STRIP N

FOLDOUT FRAME

SCALE 1 : 75 000

FLIGHT INDEX
OF
WITWATERSRAND MINE DUMPS
RELATING TO
RTS I PROGRAM SR 0577

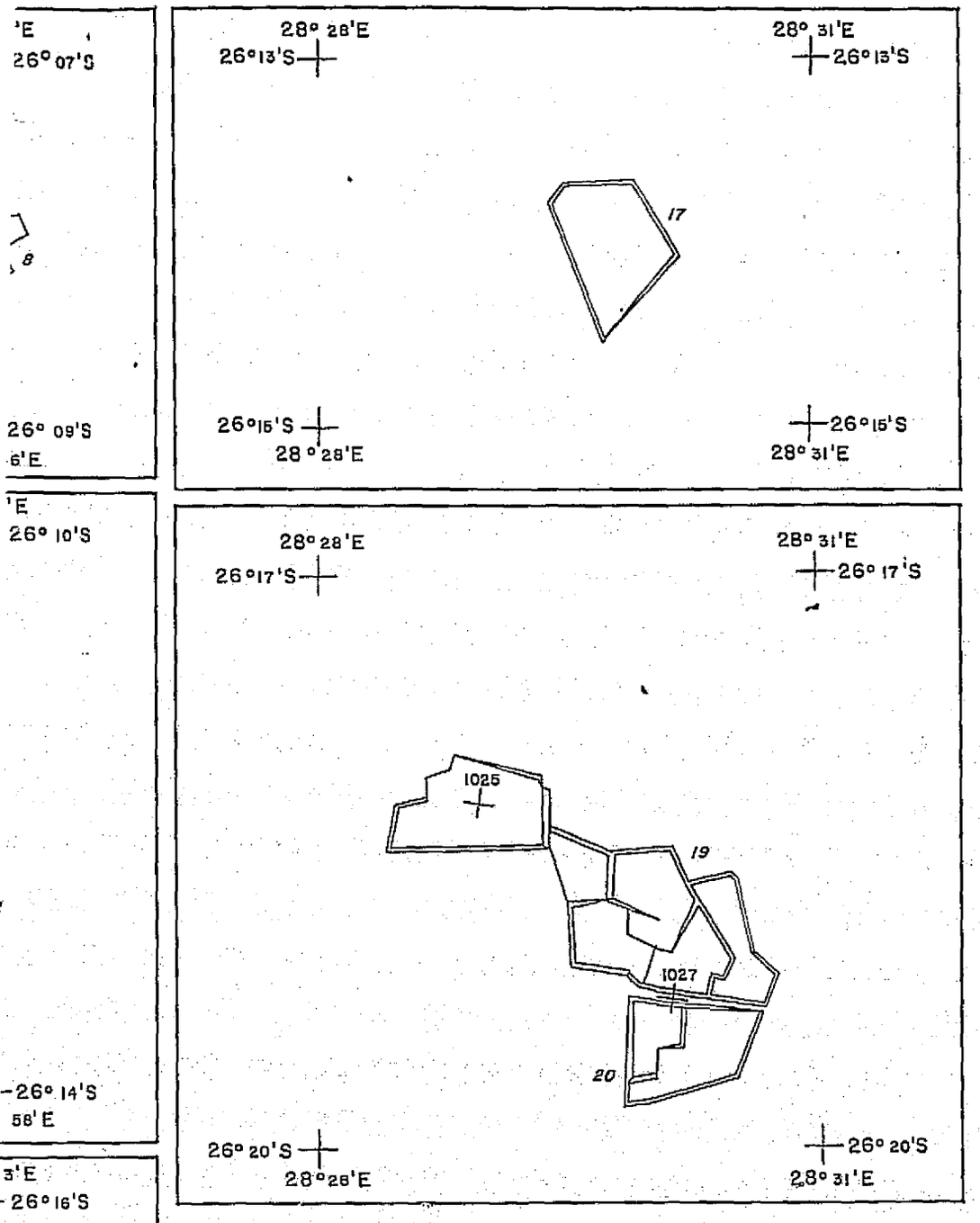

JOB No;	71 / 14
CAMERA;	WILD RC10 No 1346
LENS/ES;	UAg. No 1016
FOCAL LENGTH;	151.45 mm
FILTER/S;	SANDWICH, WRATTEN 15/80c & CC 30 M.
FILMS;	KODAK AEROCHROME 2443 (INFRA RED POS.)

SCALES & DATES OF PHOTOGRAPHY;

STRIP No.	SCALE	No's	DATE
	1: 20,000 APPROX.	1012	11 th.NOV. 72
	" "	1025	12 th.NOV. 72
	" "	1024	" "
	" "	1025	" "
	" "	1027	" "

SPECTRAL AFRICA (PTY.) LTD.
PO.BOX 2, RANDFONTEIN.
TEL. 663 3687
TELEX J / 7614

FOLDOUT FRAME 2

SCALE 1 : 75 000

R.J.S. 26.1.74

SOME WITWATERSRAND MINE DU
RELATING TO
ERTS I PROGRAM SR 0577

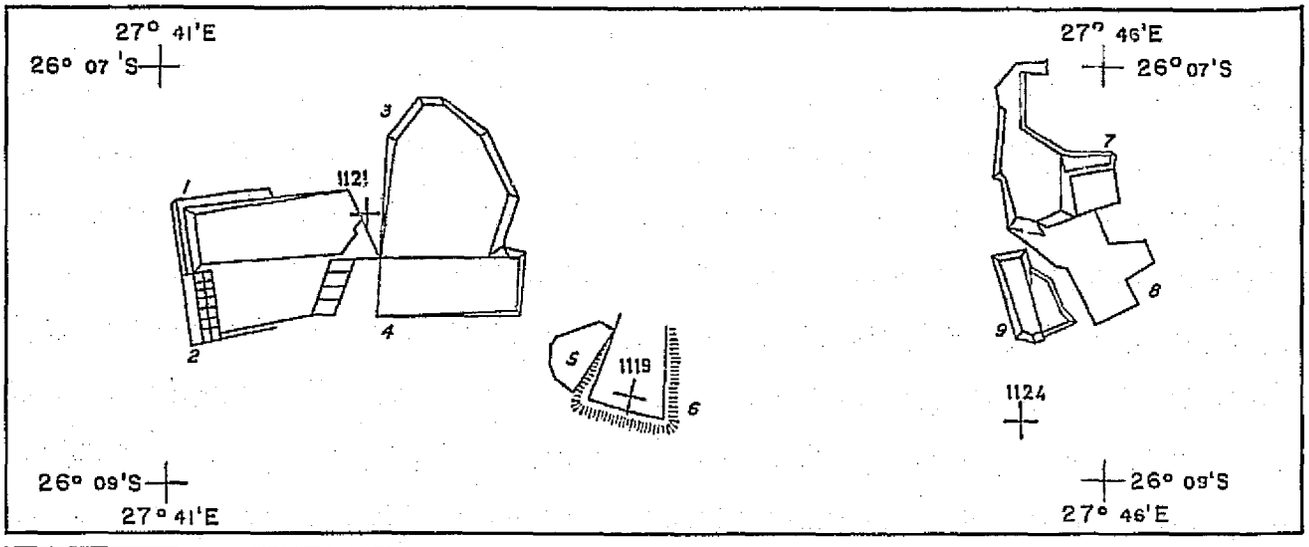

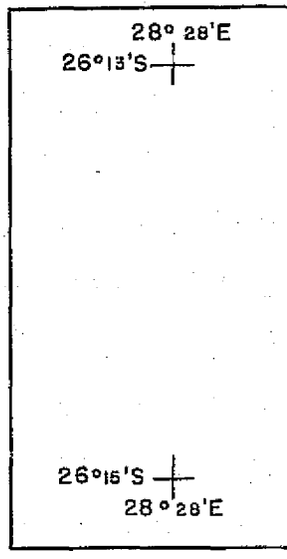

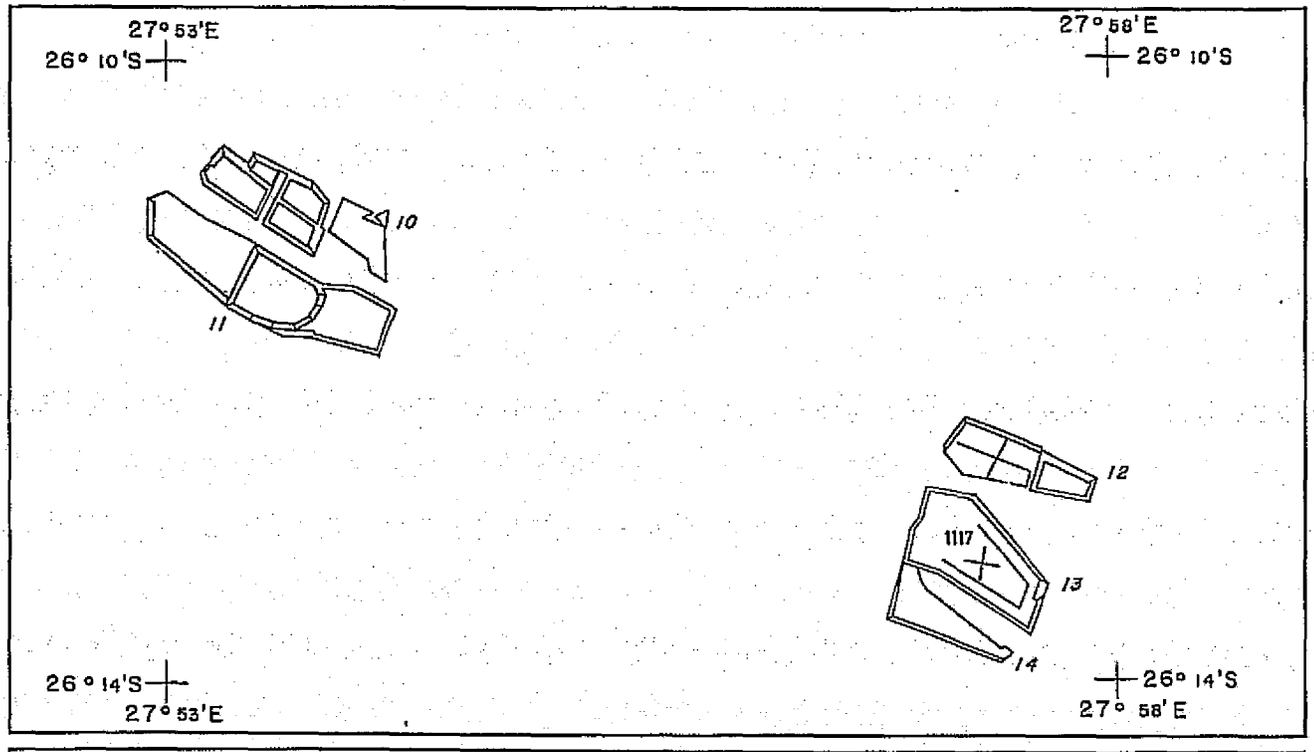

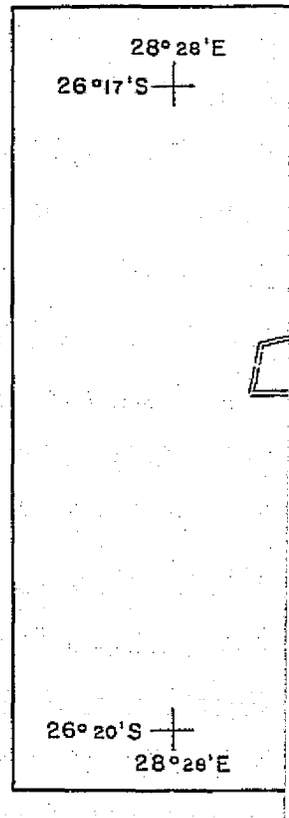

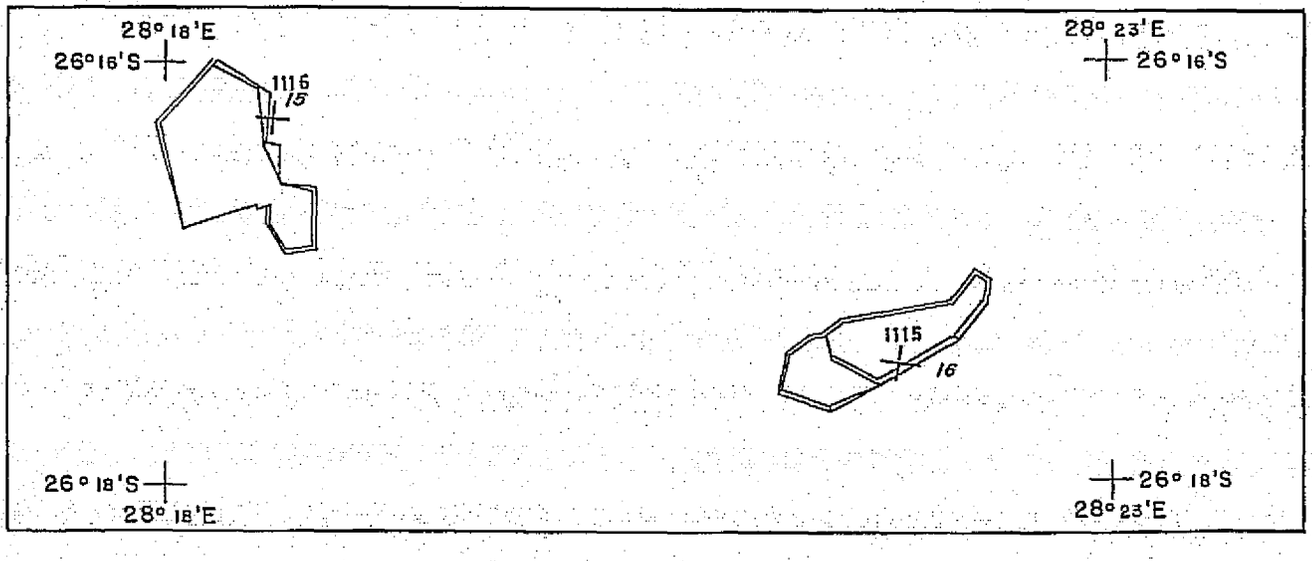

JOB No;
CAMERA;
LENS/ES;
FOCAL LEN
FILTER/S
FILMS;
SCALES
STRIP

SCALE 1 : 75 000

ABOUT FRAME

OF

OME WITWATERSRAND MINE DUMPS
RELATING TO
ERTS I PROGRAM SR 0577

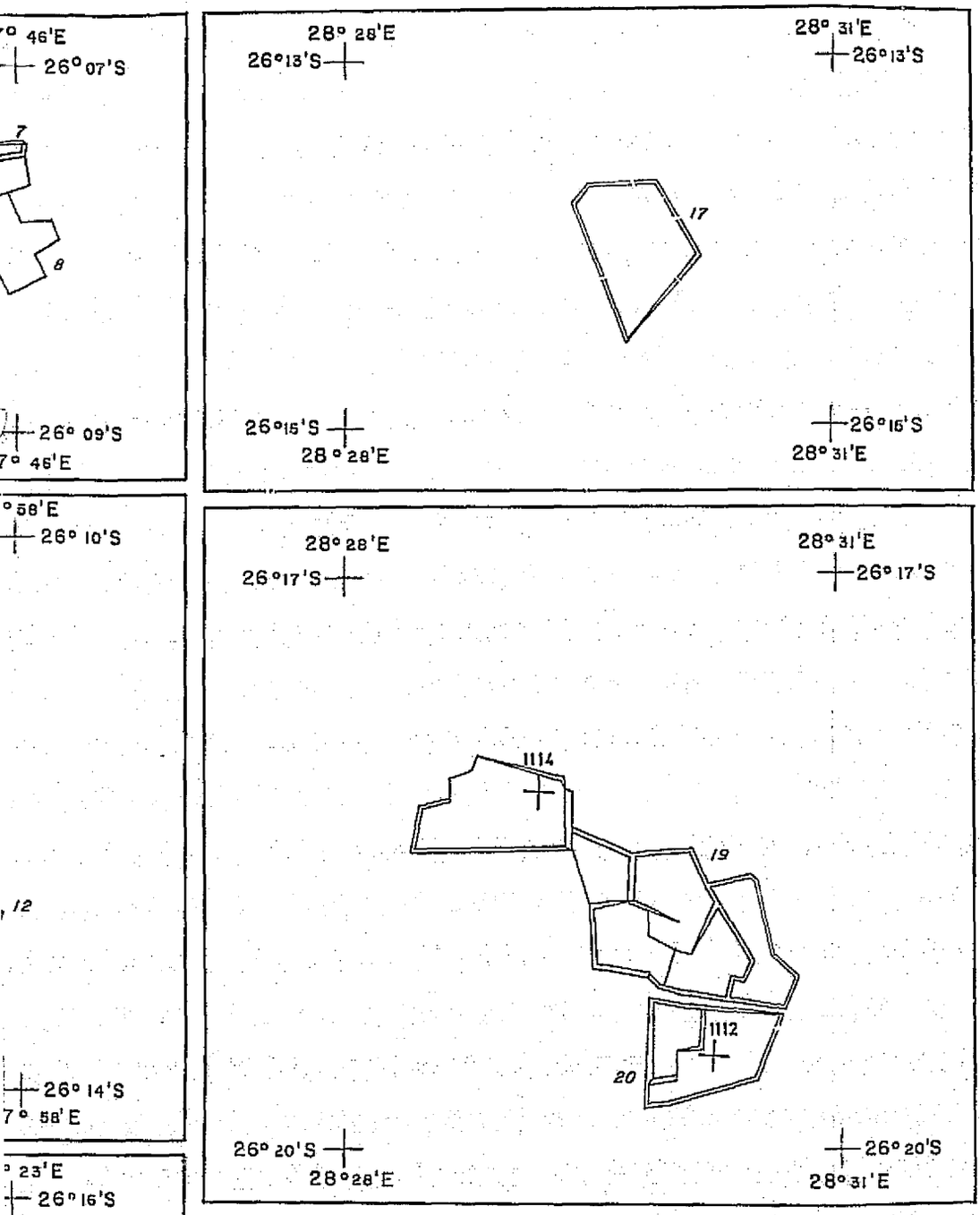

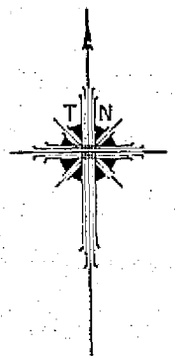

JOB No;	71 / 14
CAMERA;	WILD RC 10 No 1346
LENS/ES;	UAg No 1016
FOCAL LENGTH;	151,45 m.m.
FILTER/S;	
FILMS;	KODAK AEROCOLOUR 2448 (NEG)

SCALES & DATES OF PHOTOGRAPHY;

STRIP No.	SCALE	No's	DATE
	1:20 000 APPROX	1112	12th NOV 72
	" "	1114	"
	" "	1115	"
	" "	1116	"
	" "	1117	"
	" "	1119	"
	" "	1121	"
	" "	1124	"

SPECTRAL AFRICA (PTY.) LTD.
P.O.BOX 2, RANDFONTEIN.
TEL. 663 3687
TELEX. J/7614

RJ.S. 26.1.74

SCALE 1 : 75 000

FOLDOUT FRAME 2

FLIGHT INDEX
OF
SOME WITWATERSRAND MINE DUM
RELATING TO
ERTS I PROGRAM SR 0577

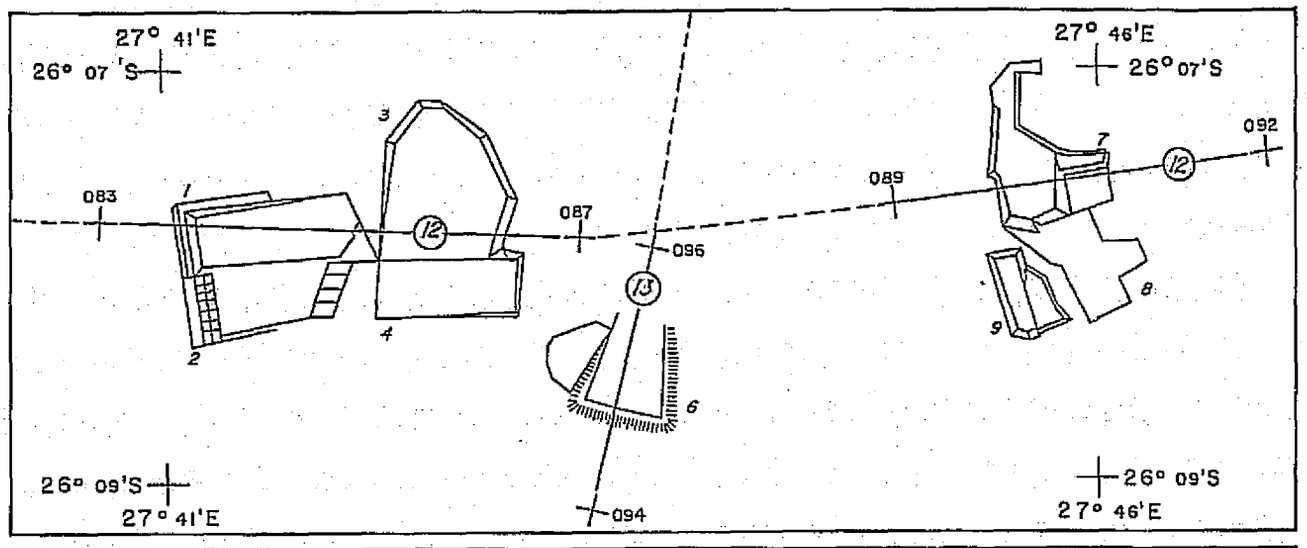

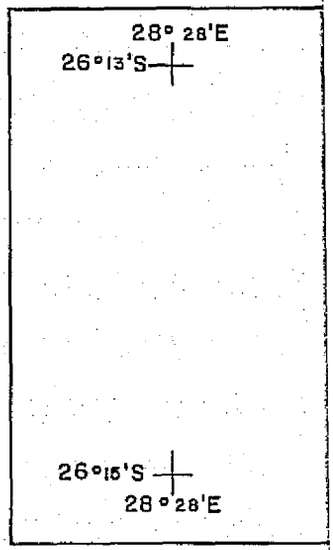

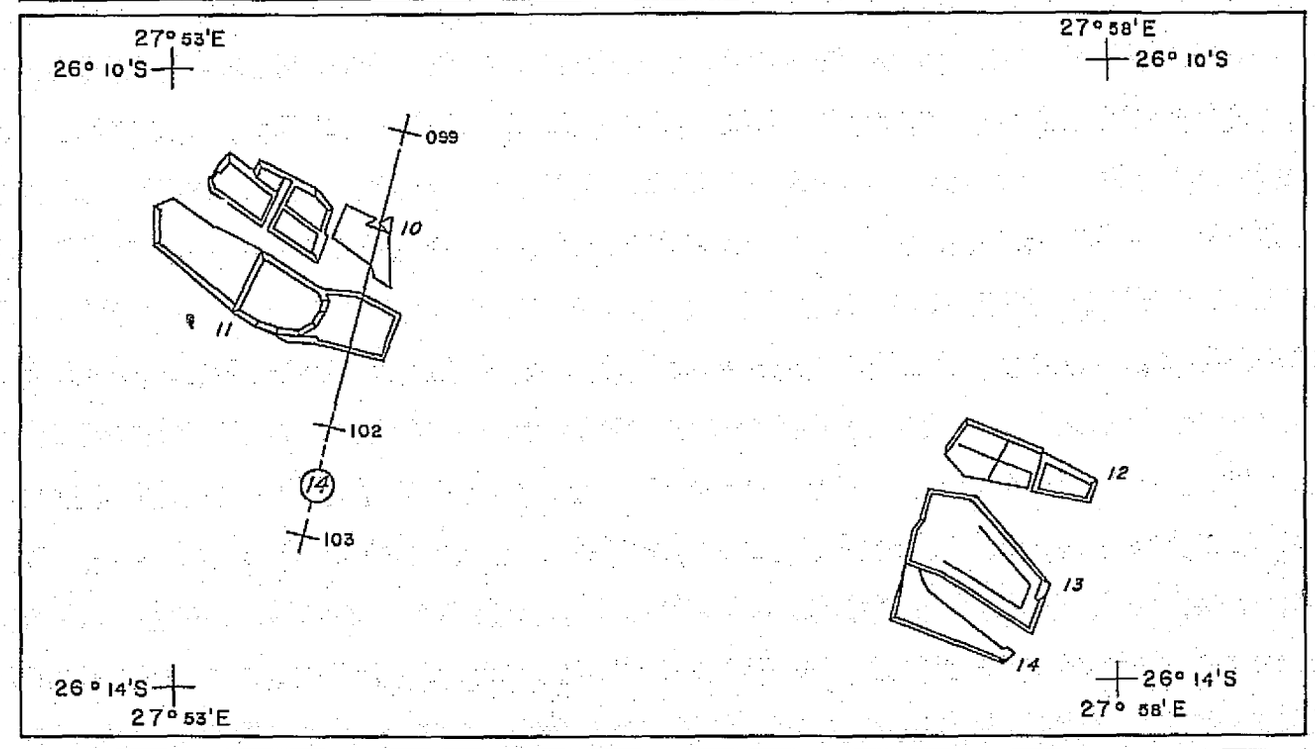

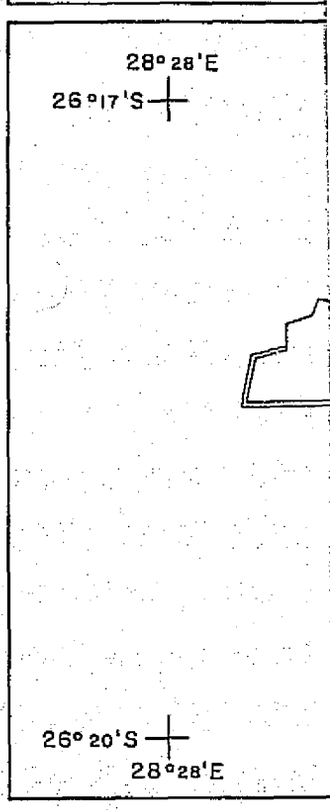

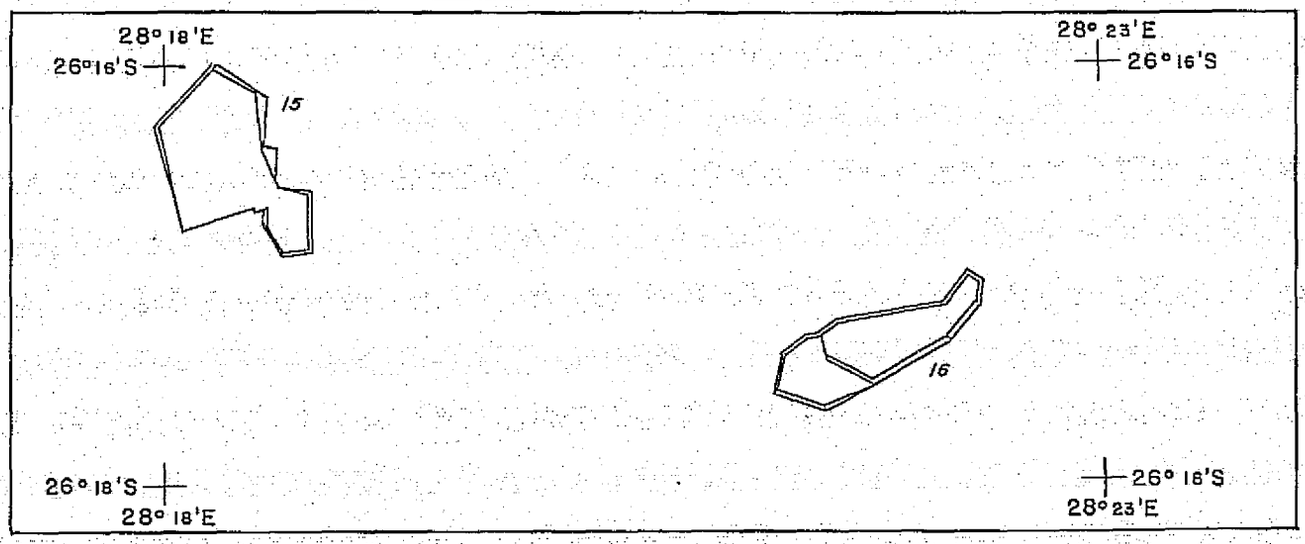

JOB No;
CAMERA;
LENS/ES;
FOCAL LENGTH;
...ER/S;
...MS;
SCALES & DAT
STRIP No.
12
13
14

SCALE 1 : 75 000

FLIGHT INDEX
OF
ME WITWATERSRAND MINE DUMPS
RELATING TO
ERTS I PROGRAM SR 0577

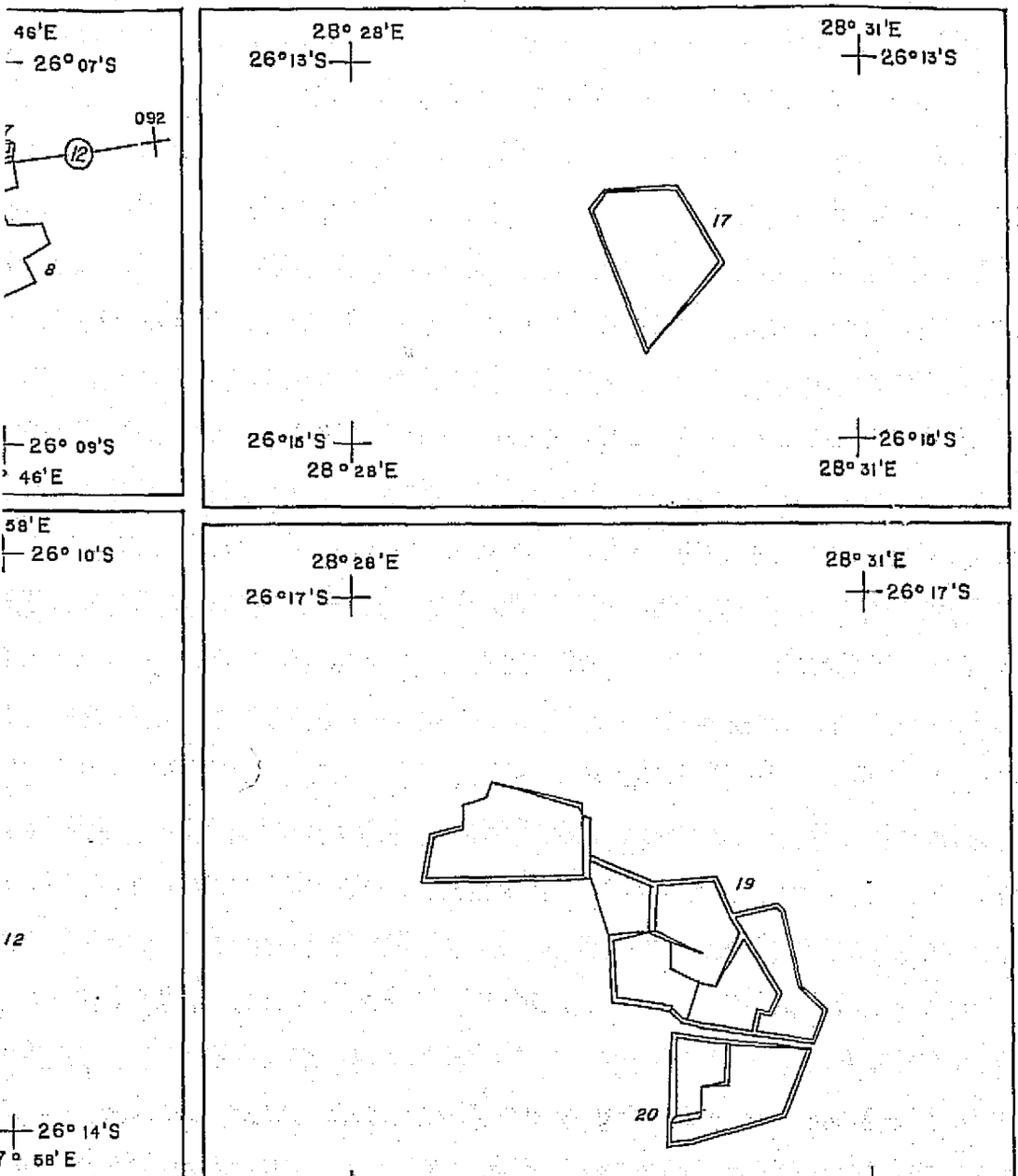

JOB No; 71 / 14
CAMERA; S.D.C. MULTI-SPECTRAL (TYPE 22 MODIFIED)
LENS/ES; 4 x SCHNEIDER KREUZNACH XENTOR 1:2,8
FOCAL LENGTH; 150 mm, No 1, 10-801-925 ; No 2, 10-801-912, No 3, 10-801-899; No 4, 10-801-913
FILTER/S; Q N G F
FILMS; KODAK 2424 (B & W I-R NEG.)
SCALES & DATES OF PHOTOGRAPHY;

STRIP No.	SCALE	No's	DATE
12	1:40 000 APPROX	083 - 092	21 st NOV. 72
13	" "	094 - 096	"
14	" "	099 - 102	"

SPECTRAL AFRICA (PTY.) LTD.
PO. BOX 2, RANDFONTEIN.
TEL. 663 3687
TELEX. J /7614

SCALE 1 : 75 000

FOLDOUT FRAME 2

R.J.S. 26.1.74

OF

SOME WITWATERSRAND MINE D

RELATING TO

ERTS I PROGRAM SR 0577

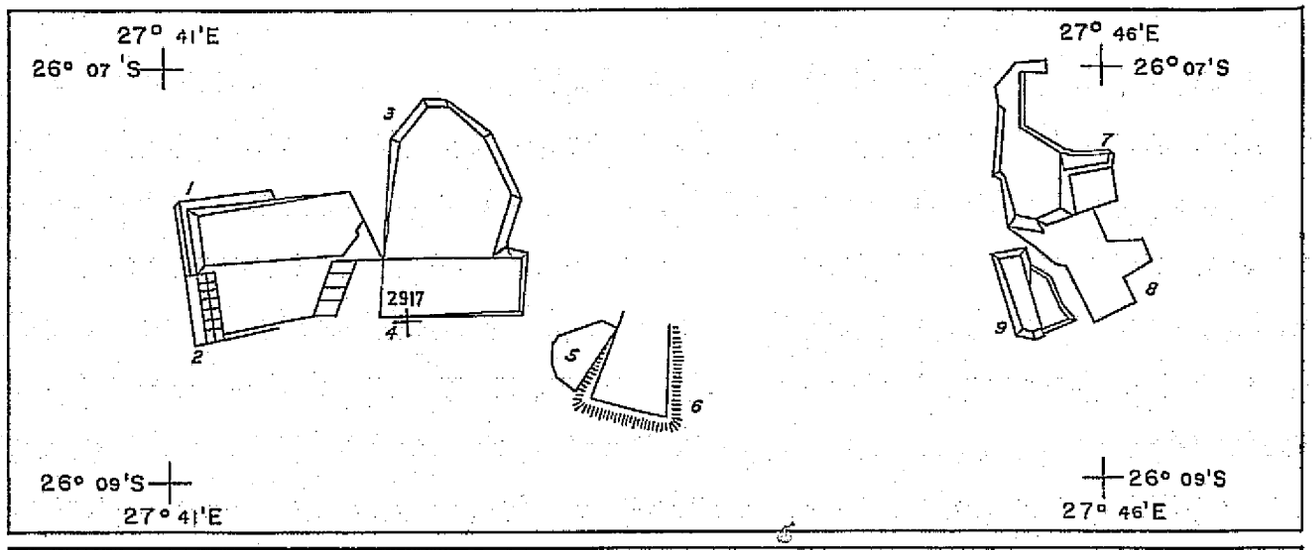

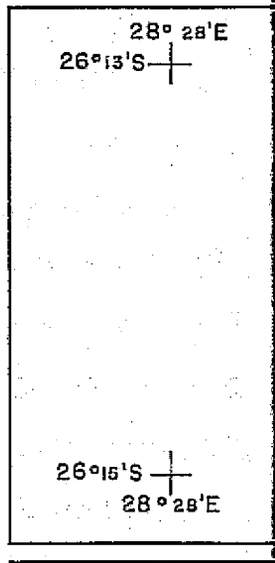

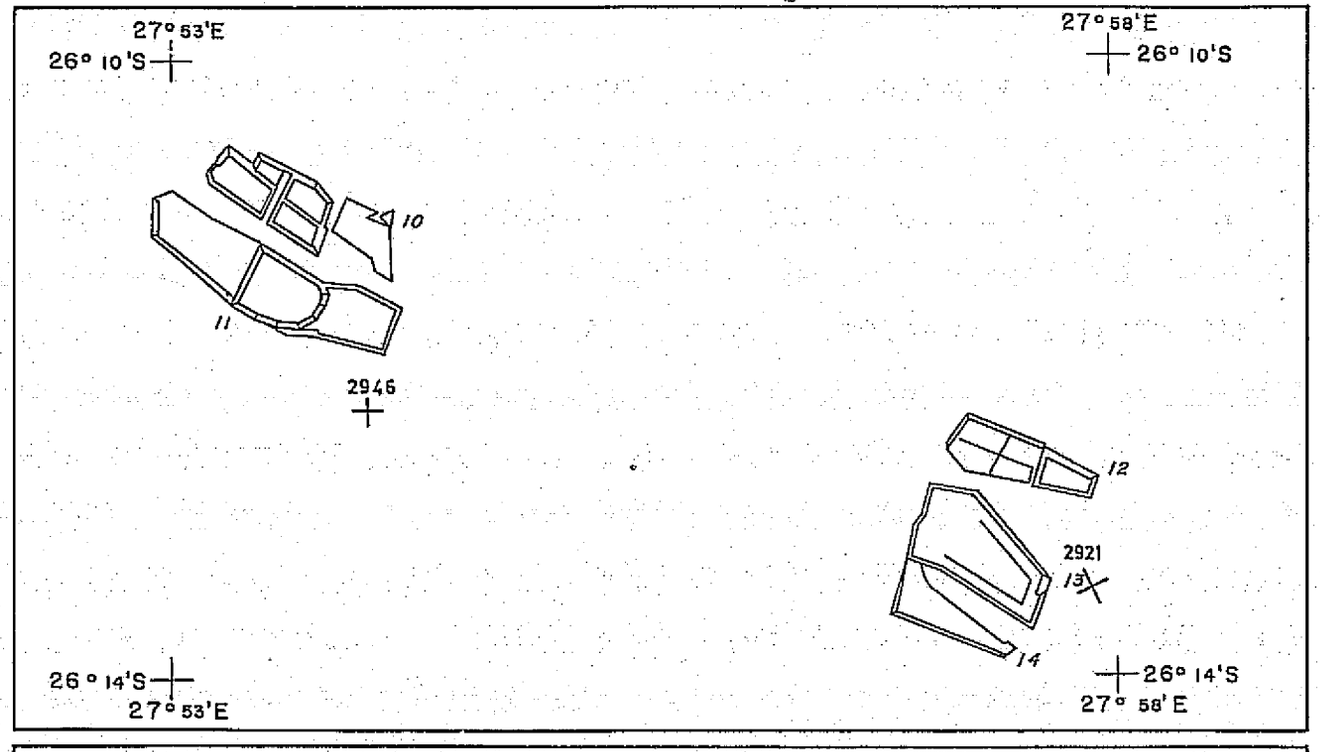

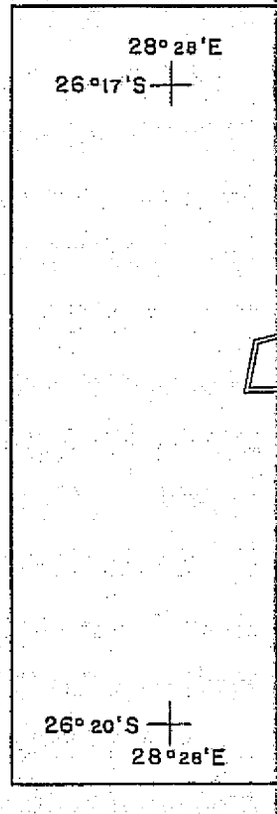

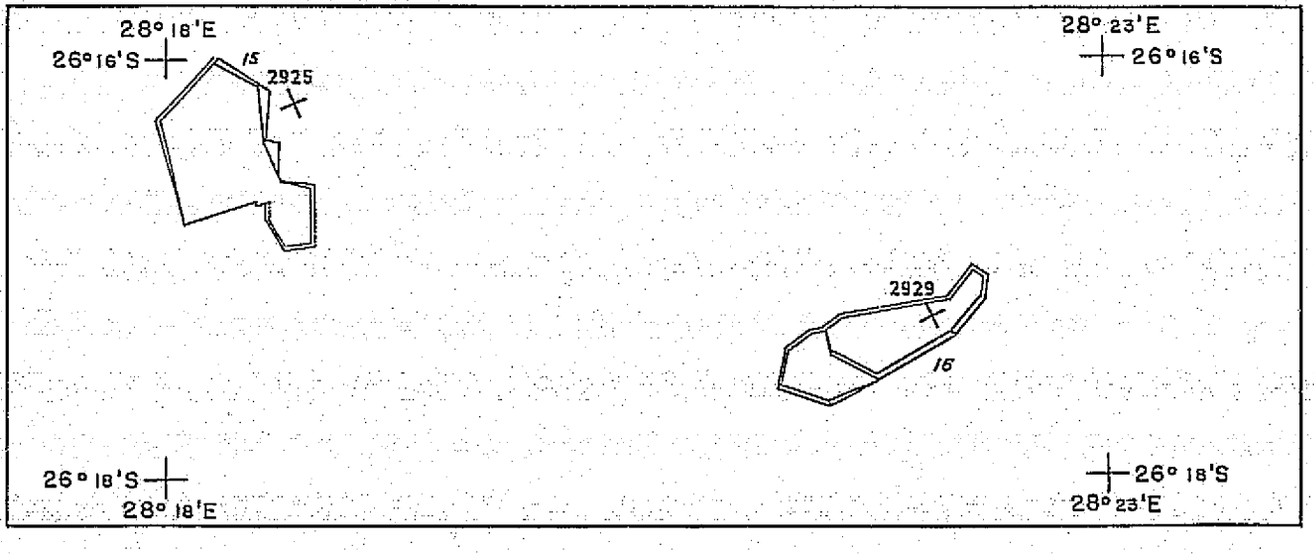

JOB No;
CAMERA;
LENS/ES;
FOCAL LE
FILTER/S
FILMS;
SCALES
STRI

SCALE 1 : 75 000

FOLDOUT FRAME 1

OF

E WITWATERSRAND MINE DUMPS
RELATING TO

ERTS I PROGRAM SR 0577

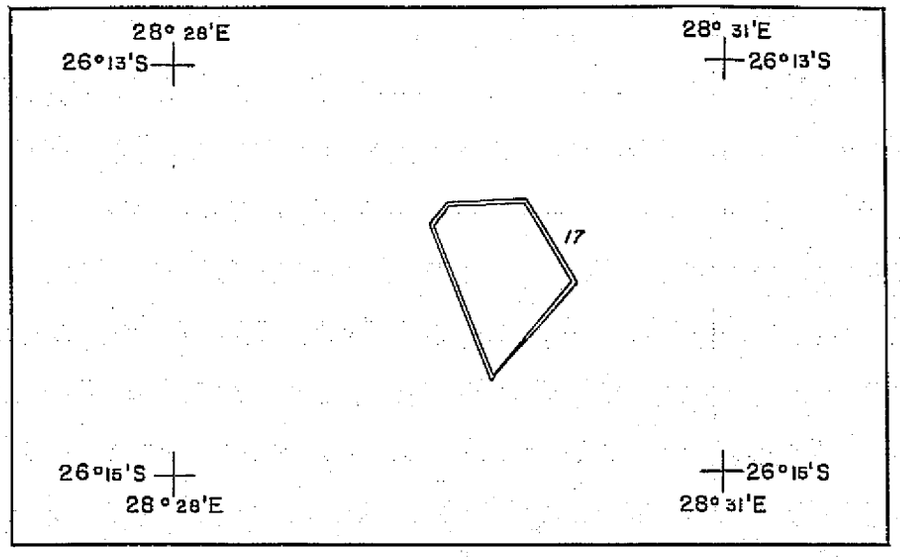

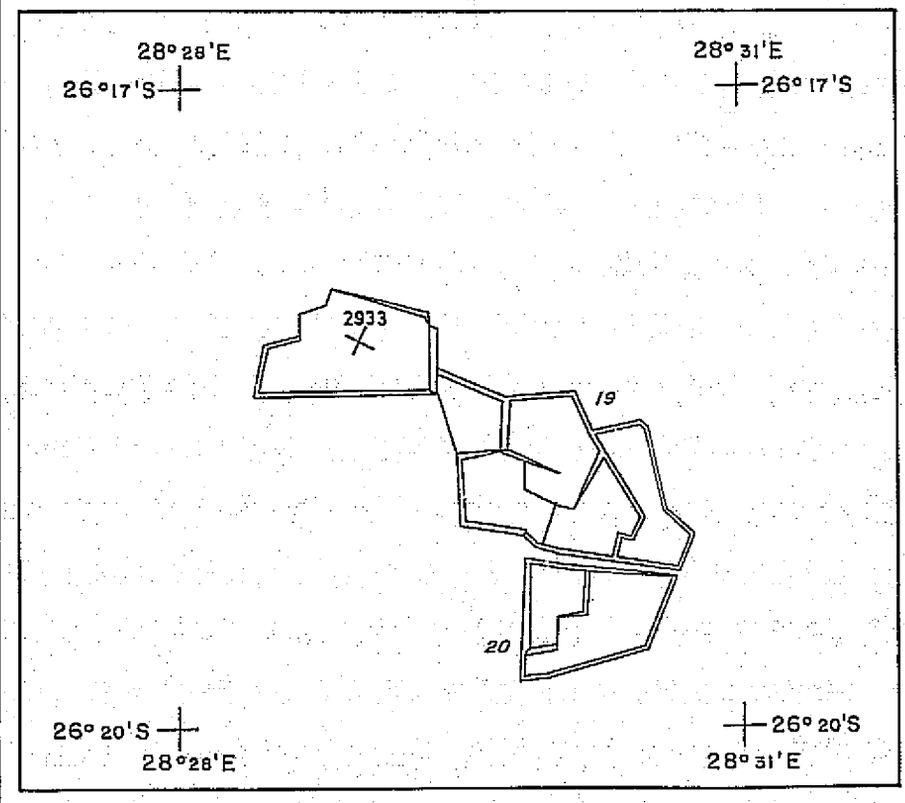

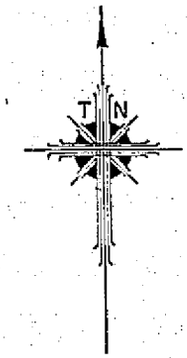

JOB No;	71 / 14
CAMERA;	WILD RC10 No 1346
LENS/ES;	SAg II No 2029
FOCAL LENGTH;	87,28 m.m.
FILTER/S;	HAZE
FILMS;	KODAK AEROCOLOUR 2445 (NEG)

SCALES & DATES OF PHOTOGRAPHY;

STRIP No.	SCALE	No's	DATE
	1:70 000 APPROX.	2917	8th MAY '73
	" "	2921	"
	" "	2925	"
	" "	2929	"
	" "	2933	"
*	" "	2946	"

* NB THIS STRIP COVERS MINE DUMPS 1 TO 9 BUT CANNOT BE RECOVERED TO SCALE ON THIS INDEX.

SPECTRAL AFRICA (PTY.) LTD
P.O.BOX 2, RANDFONTEIN.
TEL. 663 3687
TELEX. J/7614

SCALE 1 : 75 000

RJ.S. 26.1.74

FOLDOUT FRAME 2

FLIGHT INDEX
OF
SOME WITWATERSRAND MIN
RELATING TO
ERTS I PROGRAM SR O

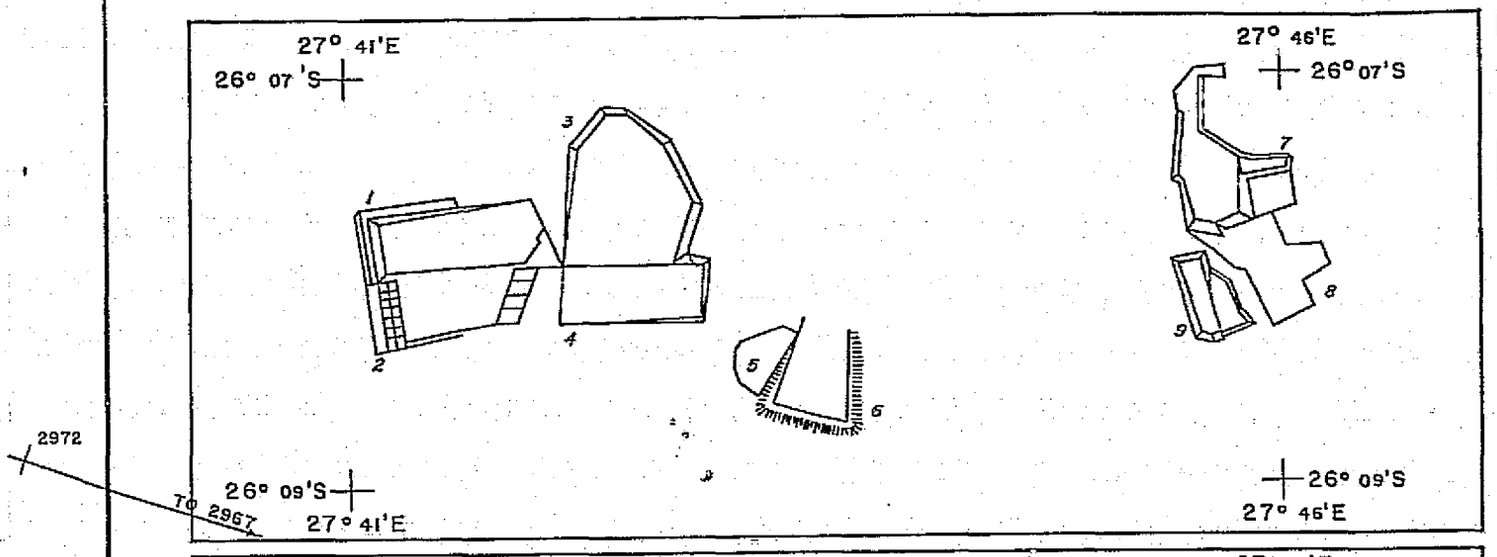

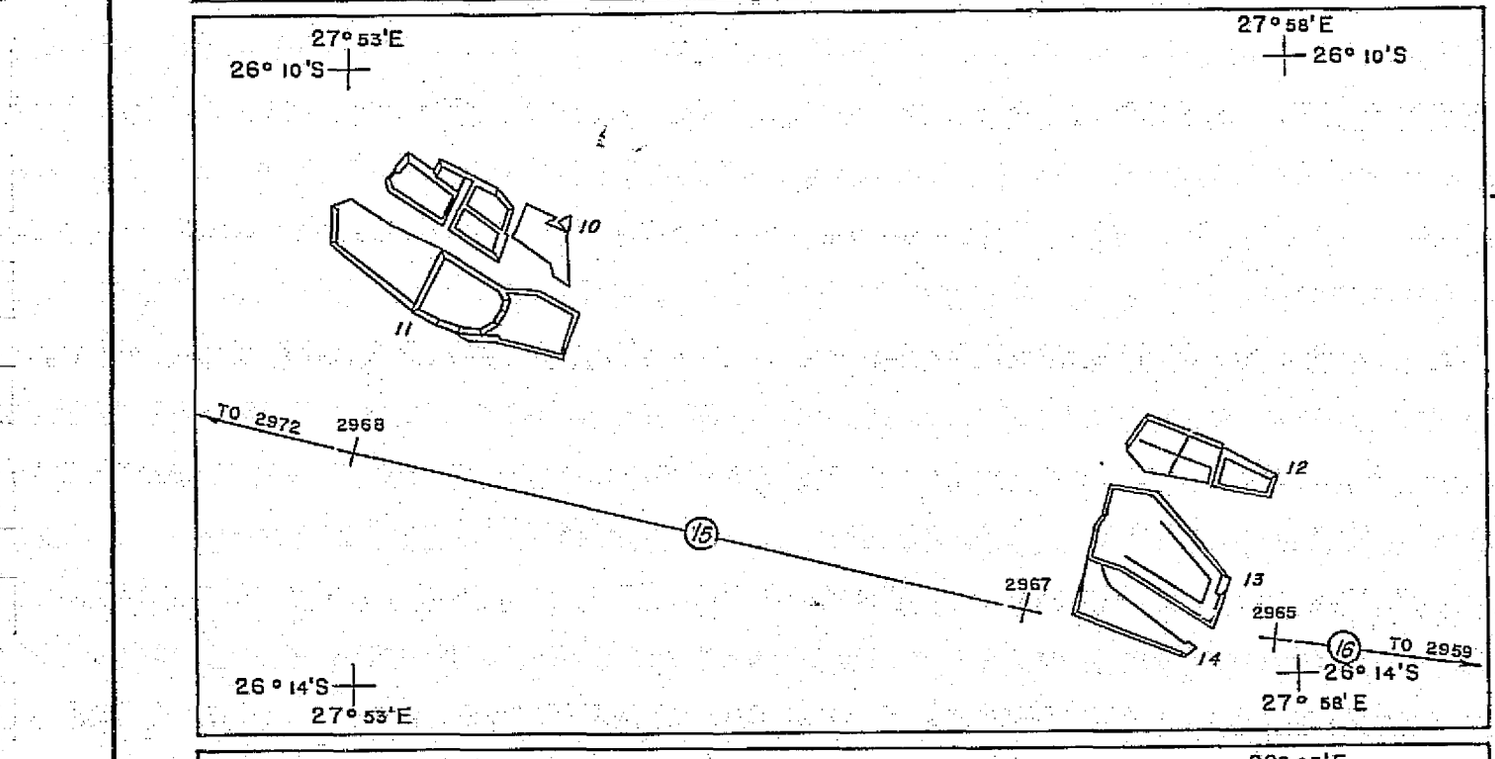

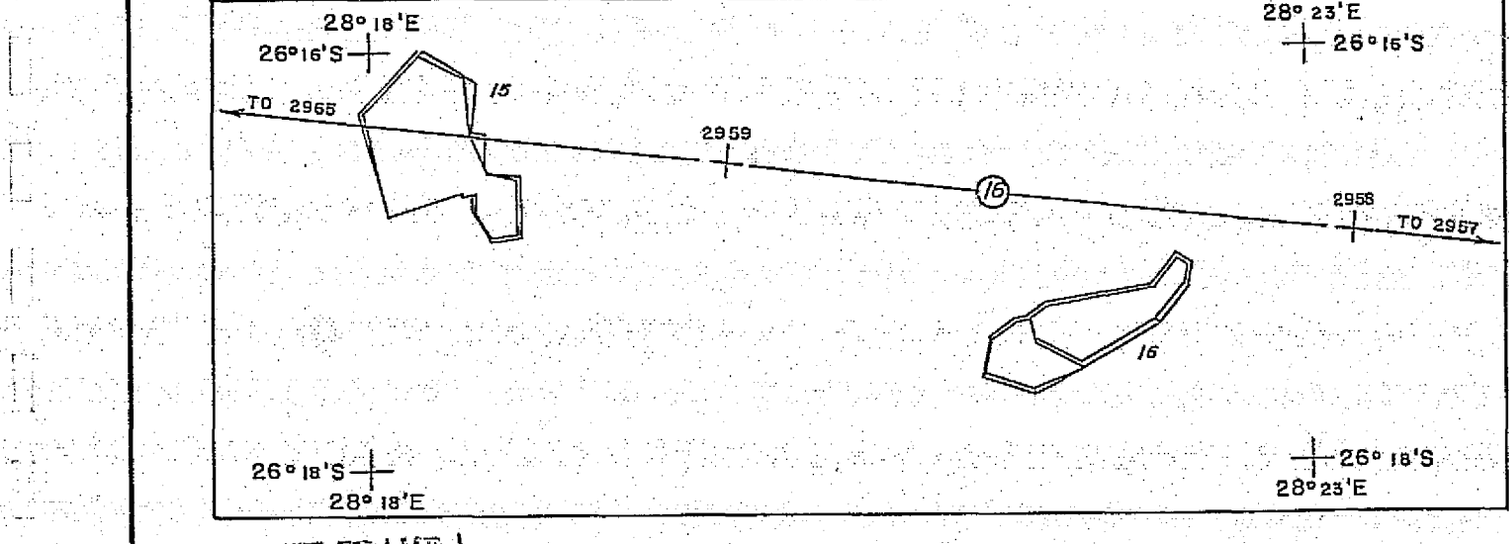

FOLDOUT FRAME 1

SCALE 1 : 75 00

FLIGHT INDEX
OF
SOME WITWATERSRAND MINE DUMPS
RELATING TO
ERTS I PROGRAM SR 0577

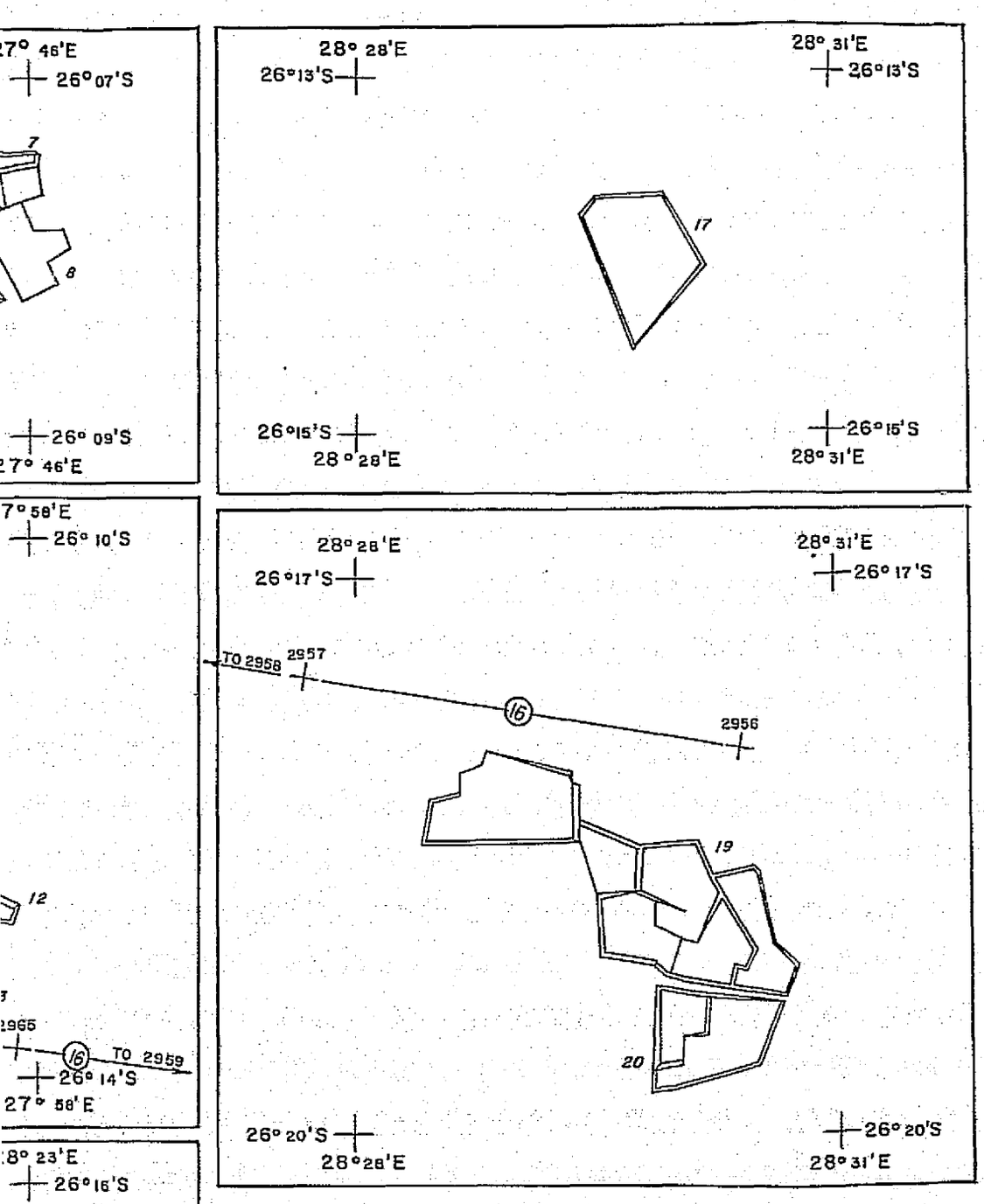

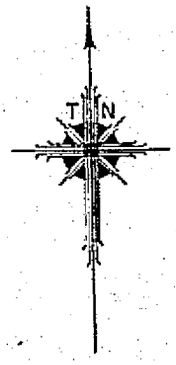

JOB No; 71 / 14
CAMERA; WILD RC10 No 1346
LENS/ES; SAg II, No 2029
FOCAL LENGTH; 87,28 mm.
FILTER/S; WR 15/80 B.
FILMS; KODAK AEROCHROME 2443 (INFRA RED POS.)
SCALES & DATES OF PHOTOGRAPHY;

STRIP No.	SCALE	No's	DATE
15	1:70 000 APPROX..	2965 - 2956	10th MAY 73
* 16	"	2972 - 2967	"

* NB. THIS STRIP COVERS MINE DUMP 17 BUT CANNOT BE RECOVERED TO SCALE ON THIS INDEX.

SPECTRAL AFRICA (PTY.) LTD.
P.O.BOX 2, RANDFONTEIN.
TEL. 663 3687
TELEX. J/7614

FOLDOUT FRAME 2

SCALE 1: 75 000

R.J.S. 26.1.74

APPENDIX 'E'

APPENDIX E

SPECTRAL AFRICA (PTY) LIMITED

INDEX OF ERTS-1 IMAGERY FOR SOUTHERN AFRICA

NASA CODE			NEG OR POS	IMAGE QUALITY		CLOUD COVER	REMARKS
FRAME I/D NO.	DATE	FORMAT CENTRE		RBV	MSS		
DAY TIME		LAT LONG		1 2 3	4 5 6 7	IN %	
CYCLE 1							
1010-07131	02AUG72	C S27-21/E032-30	N	G G G		10	
1011-07172	03AUG72	C S21-34/E032-36	N	G G G		0	
1011-07174	03AUG72	C S23-00/E032-14	N	G G G		0	
1011-07181	03AUG72	C S24-26/E031-51	N	G G G		0	
1011-07183	03AUG72	C S25-52/E031-28	N	G G G		0	
1011-07190	03AUG72	C S27-18/E031-05	N	G G G		0	
CYCLE 3							
1049-07290	10SEP72	C S21-39/E029-43	N		G G G G	0	
1049-07292	10SEP72	C S23-05/E029-20	N		G G G G	0	
1049-07295	10SEP72	C S24-31/E028-57	N		G G G G	0	
1049-07301	10SEP72	C S25-58/E028-33	N		G G G G	0	
1049-07304	10SEP72	C S27-24/E028-10	N		G G G G	0	
CYCLE 4							
1068-07353	29SEP72	C S24-23/E027-33	N		G G G G	20	
1068-07355	29SEP72	C S25-49/E027-11	N		G G G G	10	
1068-07362	29SEP72	C S27-15/E026-48	N		G G G G	0	
1068-07364	29SEP72	C S28-41/E026-24	N		G G G G	0	
1069-07405	30SEP72	C S23-00/E026-29	N		G G G G	0	
1069-07411	30SEP72	C S24-25/E026-07	N		G G G P	0	
1069-07414	30SEP72	C S25-52/E025-43	N		G G G P	0	
1069-07420	30SEP72	C S27-17/E025-20	N		G G G P	0	
1069-07423	30SEP72	C S28-43/E024-56	N		G G G G	0	
CYCLE 5							
1084-07253	15OCT72	C S28-45/E029-12	N		G G G G	10	
1085-07300	16OCT72	C S24-27/E028-56	N		G G G G	10	
1085-07303	16OCT72	C S25-52/E028-33	N		G G G G	10	
1085-07305	16OCT72	C S27-18/E028-09	N		G G G G	0	
1087-07420	18OCT72	C S25-53/E025-40	N		G G G G	0	
CYCLE 9							
1156-07255	26DEC72	C S28-47/E029-09	P		G G G G	50	
1157-07293	27DEC72	C S21-36/E029-43	P		G G G G	0	
1157-07300	27DEC72	C S23-01/E029-20	P		G G G G	0	
1157-07302	27DEC72	C S24-27/E028-57	P		G G G G	10	
1157-07305	27DEC72	C S25-53/E028-32	P		G G G G	40	
1157-07314	27DEC72	C S28-45/E027-43	P		G G G G	50	

ORIGINAL PAGE IS
OF POOR QUALITY

SPECTRAL AFRICA (PTY) LIMITED

INDEX OF ERTS-1 IMAGERY FOR SOUTHERN AFRICA

NASA CODE				NEG OR POS	IMAGE QUALITY		CLOUD COVER	REMARKS
FRAME I/D NO.	DATE	FORMAT	CENTRE LAT LONG		RBV	MSS		
DAY TIME					1 2 3	4 5 6 7	IN %	
1158-07352	28DEC72	C	S21-37/E028-16	P		P P P P	10	
1158-07354	28DEC72	C	S23-03/E027-53	P		P P P P	0	
1158-07361	28DEC72	C	S24-28/E027-30	P		P P P P	10	
1158-07363	28DEC72	C	S25-53/E027-07	P		P P P P	0	
1158-07370	28DEC72	C	S27-18/E026-43	P		P P P P	0	
1158-07372	28DEC72	C	S28-45/E026-19	P		P P P P	0	
1159-07415	29DEC72	C	S24-31/E026-01	P		G G G G	0	
1159-07422	29DEC72	C	S25-56/E025-38	P		G G G G	0	
1159-07424	29DEC72	C	S27-23/E025-14	P		G G G G	0	
1159-07431	29DEC72	C	S28-49/E024-51	P		G G G G	20	
CYCLE 10								
1175-07294	14JAN73	C	S22-58/E029-23	P		G G G G	40	
1175-07301	14JAN73	C	S24-24/E029-01	P		G G G G	10	
1175-07303	14JAN73	C	S25-51/E028-38	P		G G G G	20	
1175-07310	14JAN73	C	S27-17/E028-15	P		G G G G	10	
1175-07312	14JAN73	C	S28-43/E027-50	P		P P G P	10	
1176-07361	15JAN73	C	S25-42/E027-12	P		P P P P	40	
1176-07364	15JAN73	C	S27-09/E026-48	P		G G G G	10	
1176-07370	15JAN73	C	S28-34/E026-24	P		G G G G	10	
1177-07413	16JAN73	C	S23-59/E026-15	P		G G G G	20	
1177-07420	16JAN73	C	S25-26/E025-51	P		G G G G	10	
1177-07422	16JAN73	C	S26-53/E025-26	P		G G G G	0	
1177-07425	16JAN73	C	S28-19/E025-02	P		G G G G	0	
1177-07431	16JAN73	C	S29-45/E024-37	P		G G G G	0	
1178-07483	17JAN73	C	S28-09/E023-39	P		G G G G	0	
1178-07485	17JAN73	C	S29-35/E023-15	P		G G G G	0	
CYCLE 14								
1246-07242	26MAR73	C	S21-25/E030-58	P		G G G G	20	
1246-07245	26MAR73	C	S22-52/E030-36	P		G G G G	30	
1246-07251	26MAR73	C	S24-17/E030-13	P		G G G G	40	
1247-07301	27MAR73	C	S21-31/E029-32	P		G G G G	10	
1247-07303	27MAR73	C	S22-58/E029-10	P		G G G G	20	
1247-07310	27MAR73	C	S24-21/E028-47	P		G G G G	70	
1247-07312	27MAR73	C	S25-47/E028-24	P		G G G G	20	
1248-07355	28MAR73	C	S21-30/E028-05	N		G G G G	0	
1248-07362	28MAR73	C	S22-55/E027-43	N		G G G G	0	
1248-07364	28MAR73	C	S24-19/E027-20	N		G G G G	20	
1248-07371	28MAR73	C	S25-46/E026-57	N		G G G G	10	
1248-07380	28MAR73	C	S28-39/E026-09	N		G G G G	20	

ORIGINAL PAGE IS
OF POOR QUALITY

APPENDIX 'F'

M. H. KREITZER
Spectral Africa (Pty), Ltd.
Randfontein, South Africa

Direct Additive Printing

. . . is a viable technique for producing color composite imagery from multispectral separations (such as ERTS imagery) using only conventional darkroom equipment.

ABSTRACT: *The simultaneous gathering of imagery in more than one independent spectral channel has led to increasing demands for systems of data analysis capable of fully exploiting and displaying the available information content of ERTS-type of imagery. This paper discusses techniques of direct additive photographic printing with particular emphasis on the ERTS-1 system.*

INTRODUCTION

THE SIMULTANEOUS gathering of imagery in more than one independent spectral channel has led to increasing demands for systems of data analysis capable of fully exploiting and displaying the available information content of this type of imagery. It is generally accepted that significant advantages can be gained by presenting such multispectral data in a single analog color combination mode as opposed to sequentially viewing the individual band images. Very often the potential users of this type of imagery do not have access to additive viewing equipment and therefore the availability of additive multispectral photographic prints and transparencies is desirable. Specifically the advent of the ERTS-1 project has led to a need for the production and supply of high-quality additive color imagery. One convenient method of doing this is via direct additive printing. As the method requires only conventional darkroom equipment it should be of particular interest to many data users who have access to such facilities.

Direct additive printing refers to the sequential formation of a color composite photograph from multispectral separations. This is as opposed to the use of additive viewers, video systems or various types of digital readouts and displays. The technique of direct additive printing has significant technical characteristics which are discussed in this paper.

TECHNIQUE

Five basic techniques of direct additive printing are illustrated in the flow diagrams in Figure 1. The alternative appropriate to a given situation depends on the initial mode and the desired system contrast. The individual steps are as follows:

STEP 1. ENLARGEMENT

The initial stage is to enlarge the first generation separations to the desired final size. This is a straightforward procedure but care should be taken to use a long focal-length enlarger lens to avoid significant fall-off in irradiance at the extremities of the enlarged format. A 300-mm lens can be used for the ERTS-1 70-mm separations, thus achieving an irradiance that is uniform to about 3 percent. If the imagery is enlarged carefully, the band-to-band scale changes introduced by this step should be limited only by the differential size changes due to processing.

The exposure should be such as to place all the densities of the first-generation separations on the straight-line portions of the characteristic curve of the printing material. In working from ERTS-1 separations, it is desirable that this step should result in a positive image because the corner crosses supplied for registration purposes are then dark against a light background. The following materials have proved suitable for the production of the enlarged separations.

- *Kodak 2422 Direct Duplicating.* This material, which is used if working from NASA positives, has a limited straight-line characteristic but it is usually adequate for the ERTS imagery. However, wedge densities will be distorted.
- *Kodak 2420 or Ilford FP3.* This material is used if working from NASA negatives. The

PLATE 1. NASA ERTS image using Technique 4 shown in Figure 1. The area is in Southern Rhodesia and includes part of the Great Dyke.

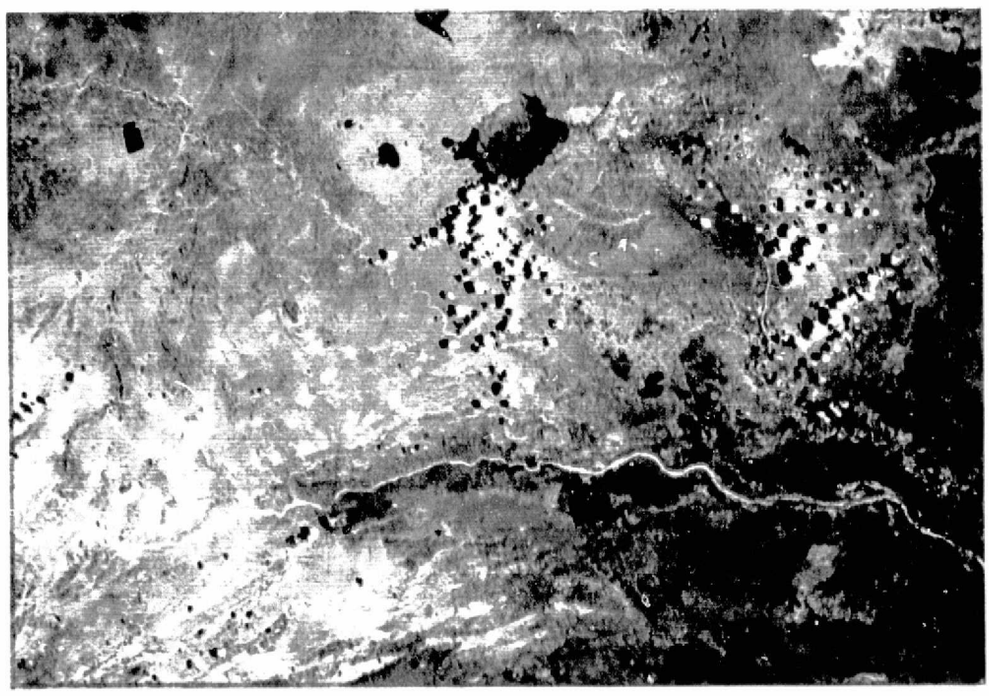

PLATE 2. NASA ERTS image using Technique 2 of Figure 1. The area shows the Limpopo River that forms the border between Rhodesia and South Africa.

Significant aspects of this additive printing technique in general are:

- ★ Only one optical system is required to produce all the enlarged separations;
- ★ Registration can be achieved at the final desired degree of enlargement;
- ★ The color printing is a contact stage, thus avoiding the use of lenses and making the use of narrow band printing filters practicable; and
- ★ In order to expand the relatively small density range of the ERTS-1 multispectral separations to utilize fully the available range of the final color material, a photographic system gamma of about 5 is usual. This system gamma can be varied particularly at the enlarged separation stage, by suitable choice of materials, processing and multiple printing at $\gamma > 1$.

System Performance

In evaluating the limitations and advantages of this direct additive printing technique the following system variables should be considered.

Dynamic range of the end product.

This is represented by the characteristic curves of either color paper or color print film, depending on the desired final product. These ranges are typically 1.7 density units for color paper and 2.6 density units for print film.

Accuracy and precision of multiple-band registration and the effect on system resolution

It is clear that any spatial misregistration of the bands is undesirable. Because the amount of misregistration is independent of the degree of enlargement of the images to be registered, it is desirable to enlarge these images to the point where the amount of unavoidable misregistration is significantly less than that distance on the picture area corresponding to the limiting ground resolution of the system as a whole. In the technique employed for the illustrations, unavoidable misregistration is usually of the order of 0.07 mm although it can be as low as 0.03 mm. If the ERTS-1 imagery is enlarged to a scale of 1:500,000, limiting ground resolution corresponds roughly to 0.1 mm on the picture.

In practice however, slight misregistration gives an effect similar to bas-relief and good registration seems to yield superadditive enhancement possibly due to increase in the signal-to-noise ratio. Therefore, the effect of registering spatially identical, spectrally different images is complex and further work is required to understand it fully.

Examples

Two color images prepared via direct additive printing from ERTS-1 separations are shown in Plates 1 and 2.

Plate 1 was prepared from NASA ERTS-1 image 1103-07291 using Technique 4 of Figure 1. ERTS bands 4, 5, and 7 were exposed through Wratten 98, 99 and 29 filters respectively to yield the "conventional false color" presentation with its characteristic red vegetation. This image, which is remarkable for its clear display of geological features, covers part of the southern sector of the Rhodesian craton and portion of the linear north marginal zone of the Limpopo mobile belt. The Great Dyke traverses the central part of the image and is the most clearly defined feature.

Plate 2 was prepared from NASA ERTS-1 image 1138-07240 using Technique 2 of Figure 1. The same color combination as for Plate 1 was used. The image covers the southeastern part of Rhodesia, and the Limpopo River, which forms the border between Rhodesia and South Africa, can be clearly seen.

The registration accuracy of Plates 1 and 2 are very nearly equal. However, the contrast of Plate 1 is considerably higher than that of Plate 2, as can be seen from the greater color range in the image areas.

Conclusions

Direct additive color printing is a viable technique for producing color composite imagery from multispectral separations using only conventional darkroom equipment. The end product is characterized by a large dynamic range and color gamut together with generally better band-to-band registration than is possible with conventional multiple-projection systems.

New Sustaining Member

The Sidwell Company

THE SIDWELL COMPANY was founded in 1927 toservice the mapping needs of the growing Midwest real estate industry. Since that time it has developed into one of the most diversified photogrammetric mapping companies in the country.

Located in beautiful Sidwell Park 28 miles west of Chicago, it offers convenient access to all parts of the country via O'Hare International Airport and the Interstate Highway System.

DuPage County Airport, the second busiest in Illinois, is located only minutes away from our facilities. As the base for our flight operations it insures quick, efficient service.

Staffed with professional photogrammetrists, Sidwell offers a multi-service organization fully versed in the requirements of aerial photography, photogrammetric mapping, tax mapping and digital data acquisition.

The company maintains its own flight department with three survey aircraft equipped with first order Zeiss cameras, in a choice of focal lengths. Complete aerial photographic facilities include precision rectifying enlargers, Kodak Versamat and Du Pont sheet film automatic film processors and all supporting equipment. Photogrammetric requirements are handled by Kelsh analog stereoplotters and Kern PG-2 analytical stereoplotters equipped with H. Dell Foster three-axis quantizer with grid rotation, scalers and Teletype, Wild PUG-4 point transfer device, aerotriangulation computer software and two-axis H. Dell Foster and Auto-trol digitizers for data acquisition. Final map preparation is accomplished by our drafting department using ink or negative scribing techniques.

In line with today's need for effective management tools, Sidwell has available a staff of professionals who have been providing tax mapping services to local and regional governments for more than two decades. These services, which can be furnished on a local or regional basis, provide the assessing official with a comprehensive, flexible system of assessment.

For those clients who require general property information, Sidwell has a full line of multi-purpose maps in a wide choice of formats. Being off-the-shelf items, they provide the user with immediate map information.

To keep pace with our continuing growth Sidwell has just added a new section to its present headquarters building. This increase in production and administrative facilities is a continuing commitment to our clients to provide the most up-to-date services possible.

Membership Application

I hereby apply for Corporate Membership in the American Society of Photogrammetry and enclose $15.00 ☐ dues for _____ (year), or $7.50 ☐ for period 1 July to 31 December, and $_____ for a _____ Society emblem and/or membership certificate. (Send to ASP, 105 N. Virginia Ave., Falls Church, Va. 22046.)

First Name | Middle Initial | Last Name | Title

Mailing Address (Street and No., City, State, Zip Code and Nation) | County

Profession or Occupation | Present Employment

☐ Reg. Prof. Engineer
☐ Reg. Land Surveyor
☐ Other Societies (List)

Position or Title

(Please print or type on the lines above)

Date | Signature of Applicant

Date | Endorsing Member
(Endorsement desired but not necessary)

APPENDIX 'G'

Computerised Interpretation of ERTS-1 Data in South Africa

T. G. LONGSHAW and B. GILBERTSON

Spectral Africa (Pty) Limited, P.O. Box 2, Randfontein, South Africa.

The article describes concepts and methods for the computerised analysis of digital images from NASA's first Earth Resources Technology Satellite.

One of the most significant events in the field of earth resources reconnaissance was the launching of the first Earth Resources Technology Satellite (ERTS-1). This satellite gathers high resolution, photograph-like imagery of the earth's surface in different spectral bands. The National Aeronautics and Space Administration (NASA) makes these images available to data users either as photographic products, or as digital computer tapes (CCTs). The applications of the photographic images are widely recognized. However, many users are unfamiliar with the potential uses of the computerised information.

This paper discusses the motivation for using ERTS-1 CCTs and describes some computerised pattern recognition techniques being employed in South Africa for their processing. Examples of recognition maps are presented and the potential of automatic interpretation of CCT images is discussed.

The ERTS-1 project

ERTS-1 was launched by NASA on July 23, 1972, and now revolves about the earth at an altitude of 900 km in a circular sun-synchronous orbit. On board the satellite are two sensing systems that acquire multispectral images of the earth's surface. The sensors are a Return Beam Vidicon (RBV) system and a Multispectral Scanner (MSS) system.

The RBV system (Fig. 1) contains three vidicon cameras with individual spectral responses covering the blue-green, yellow-red, and red-infrared regions of the electromagnetic spectrum. The three systems are aligned to view the same ground area (approximately 185 km by 185 km), and when the cameras are shuttered, the images are stored on the RBV photosensitive surfaces. These are then scanned to produce video outputs.

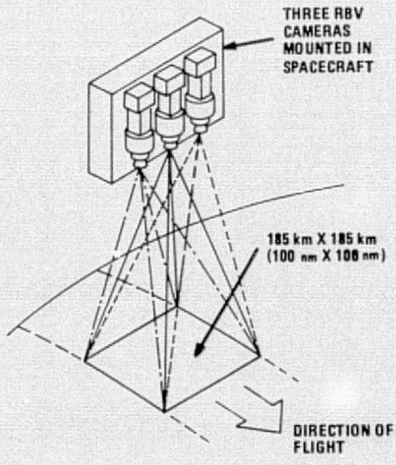

Fig. 1 Return beam vidicon system. (Source: NASA[7]).

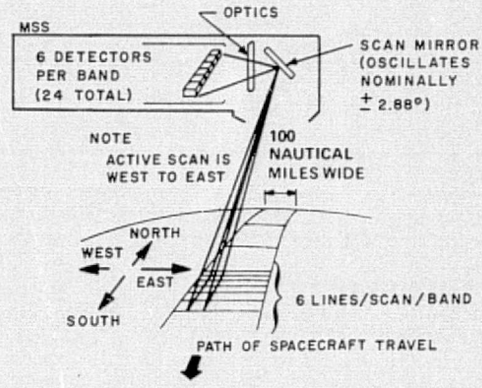

Fig. 2 Multispectral scanner system. (Source: NASA[7]).

The MSS system (Fig. 2) gathers data by imaging the surface of the earth in four spectral bands simultaneously through the same optical system. The bands are 0.5–0.6 μm, 0.6–0.7 μm, 0.7–0.8 μm and 0.8–1.1 μm. The MSS scans crosstrack swaths 185 km wide and twenty-four detectors (6 for each spectral band) convert the incident radiation into a video signal. This signal is immediately converted into a digital bit steam.

The RBV and MSS data are telemetered in analogue and digital mode, respectively, over two S-band links to one of three ground stations, and are then sent to the NASA Data Processing Facility (NDPF) at Goddard Space Flight Centre. This facility corrects the data for various distortions and converts them into film imagery using an electron beam recorder. Additionally the RBV data are digitised.

Two types of final product are thus generated, namely computer compatible tapes and film imagery. An example of an ERTS-1 MSS photographic image is shown in Fig. 3.

Three key data parameters are resolution, radiometric fidelity and registration accuracy. The specifications provided by NASA in this regard are reproduced in Table I.

It should be noted that the parameters of the photographic products generally deteriorate in subsequent generations, and that the photographic products available to most data-users are unavoidably of late-generation (typically post-5th). There is of course no degradation of the digital products.

It is therefore apparent that potentially more accurate data are available from the CCT format than from the photographic product. We shall now consider techniques whereby this advantage can be exploited.

Spectral pattern recognition

The role of computerised image analysis has become a controversial subject, with basically two schools of thought. One

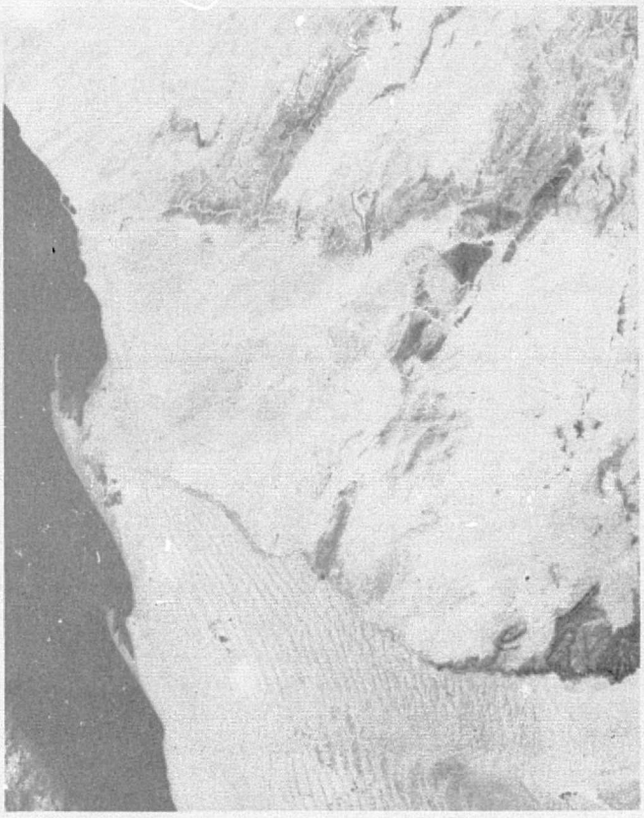

Fig. 3 Band 7 of MSS image 1095-08271, showing the Walvis Bay areas of South West Africa. The sand dunes of the Namib Desert are clearly visible south of the Kuiseb River.

maintains that any image in a photographic format presents data in such a disorganized form that meaningful analysis can only be achieved by visual inspection. The other argues conversely that the necessary thought processes employed by a subjective analyst can be simulated satisfactorily in machine processing[1]. Thus each feature in the imaged scene may be assessed by computer classification on the basis of its size, shape, tone, texture and/or other characteristics. It is apparent, however, that neither standpoint provides a complete solution and that interpretational efficiency can be increased by integration of the two approaches.

ERTS-1 images, because of their multispectral nature, are well suited to interpretation via computerised spectral pattern recognition techniques[2–4]. These techniques involve the application of statistical decision theory to discrimination problems. Consider the radiant power measured in one spectral band when a given

Table I Key performance specifications for ERTS data*

	CCT	Photographic
System resolution for high contrast scene, yellow-green band (m bar ^{1})		
MSS	44	54
RBV	44	45
Radiometric error as percentage of full-scale sensor count or voltage		
MSS	2	5
RBV	30	9
Band to band registration accuracy. Residual errors (rms)		
MSS	15m	159
RBV	?	336m

* These data are based on the May 4, 1972 and July 18, 1972 revisions of NASA[7]. 'Photographic' refers to first-generation 70 mm positive transparencies.

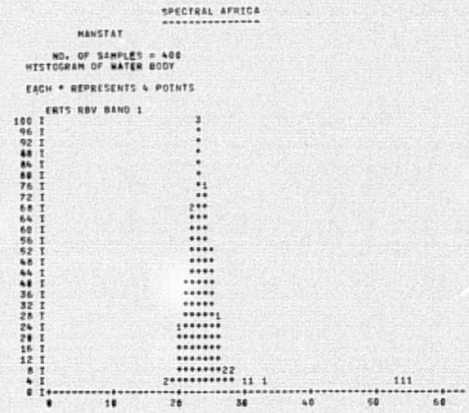

Fig. 4 Histogram of 400 radiance measurements on water body.

class of ground object is observed. Repeated radiance measurements on samples selected from this object class constitute a random experiment. If measurements are made using n spectral bands at a time, the random variables will define a multi-variate probability function, and may be represented as a n-dimensional scatter diagram. This situation is illustrated in Figs. 4 and 5. Fig. 4 shows a histogram obtained from radiance measurements in a single spectral channel on 400 resolution elements covering a water body. Fig. 5 shows the two-dimensional scatter diagram obtained when two spectral channels are used.

Because of differences in the average spectral reflectance properties of different classes of ground object, it is found that such classes tend to cluster in different parts of the scatter diagram. The multi-dimensional scatter diagram can thus be partitioned into disjoint regions corresponding to different object classes by using partition functions such as AA. Therefore if the cluster of radiances observed after a set of measurements on an unknown object is found to fall in a given region, it can be decided that the object belongs to the appropriate object class. Unfortunately the separation of the clusters is not always clearcut. Different spectral bands, or more than two bands at a time, may achieve the desired separation. If not, statistical decision rules, usually based on likelihood ratios, must be used to generate the optimum partition function.

It should be noted here that computer processing of CCTs allows the construction of multi-dimensional scatter diagrams. This is an advantage over photographic composite colour presentations where only 3 bands can be handled at a time. Normally all 4 (MSS) bands contain information and accordingly are best handled as 4-dimensional clusters.

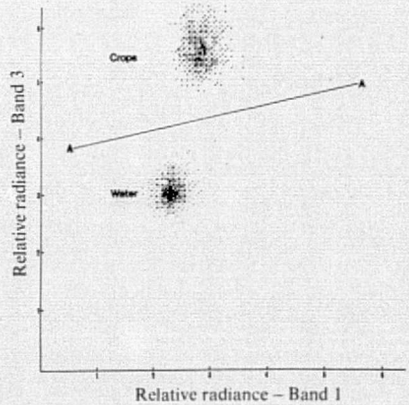

Fig. 5 Two-dimensional diagram of 400 radiance measurements each on a water body and on crops.

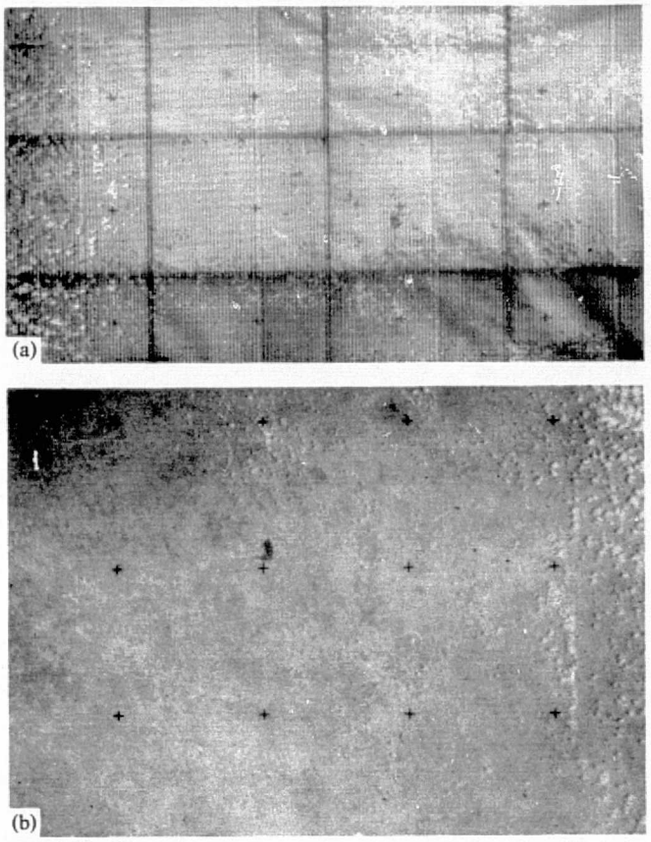

Fig. 6 (a) Photographic reduction of 12 sheets of PROPIC print out; (b) photographic image of (a).

We shall now consider computer programs that were written for this purpose.

Computer programs for ERTS CCTs

A set of 7 basic computer programs are listed in Table II. These are used to manipulate the CCT data, to carry out the data processing required to generate recognition maps, and to effect the necessary print-out routines.

PROPIC is the basic program and is used to edit the image, i.e. to select specific areas for more detailed analysis. This program generates a semi-pictorial printout of one complete band by overprinting line printer characters so that "dark" overprinted characters correspond to low radiance areas of the ground scene. Five pairs of overprinted characters are used to achieve this gross image density correlation, namely bb, b-, bM, MX and TH. The actual sensor spatial resolution is artificially degraded by averaging a 4×4 matrix of resolution elements into a single line printer character. In this manner a print-out of reasonable proportions (256 standard sized pages of computer printout) is obtained for investigation. Fig. 6a shows a photographic reduction of 12 sheets of a PROPIC printout, and should be compared with the actual photographic image of Fig. 6b.

Table II Function of basic computer programs

Program Name	Program function
MANFORM	Converts data format of CCTs.
MANSTAT	Prints radiance values of preselected resolution elements.
PROPIC	Pictorial overprint of entire image, single band.
PRODEC	Generates decision matrix from preselected input ranges.
PLOTLIN	Interwoven print-out of several decision matrices as alphabetic characters on line plotter.
PLOTCAL	Sequential print-out of several decision matrices as colours on Calcomp plotter.
PLOTOUT	Plots outline only of area selected by PRODEC.

PRODEC is the key data processing program. It accepts a 512×512 matrix of resolution elements (i.e. 1/64 of the entire frame), and calculates for a given band whether or not the radiances of individual resolution elements have certain preselected properties. This process is repeated for each of the spectral bands. If the radiances in all of the spectral bands have the necessary characteristics, unity is registered for that particular resolution element; if not, zero is registered. In this manner a recognition map is generated as a binary (unity and zero) 512×512 matrix. It will be clear that this program can generate in 3 (for RBV) or 4 (for MSS) dimensions the disjoint regions corresponding to object category clusters.

PLOTLIN, PLOTCAL and PLOTOUT allow the recognition matrix generated by PRODEC to be plotted out in different forms for visual inspection. Considerations of computing cost and speed cause PLOTLIN to be used for general applications. PLOTLIN prints out on a line printer a pre-selected alphabetic character, A,B,C . . . etc., for each value of unity appearing in PRODEC's binary matrix. No character will be printed where a zero has been recorded. PLOTLIN can handle a number of binary matrices at a time, each corresponding to a different set of radiance specifications, and consequently to different ground object categories. Multiple matrices are all handled in a single print-out run. Fig. 7 shows a printout from PLOTLIN, in which 3 alphabetic characters (A, B and C) have been used to represent 3 different ground object categories.

PLOTCAL performs essentially the same task as PLOTLIN, except that the output is made on a Calcomp Plotter. PLOTCAL can handle only one binary decision matrix at a time. Multiple matrices must be handled sequentially. Presentation can be enhanced by using different coloured inks in the plotter pen for the different decision matrices. Because of its high resolution, PLOTCAL generates the most pleasing visual presentation; however, it contains no more information than the PLOTLIN printout. An example of a PLOTCAL print-out is shown in Fig. 8a, and may be compared with the PLOTLIN print-out of Fig. 8b.

PLOTOUT is an outline routine used to plot the boundaries of large areas. Thus only the contact region between unity and zero levels in the binary decision matrix is produced.

Partitioning of scatter diagrams

The major decision required in utilising PRODEC is the in-

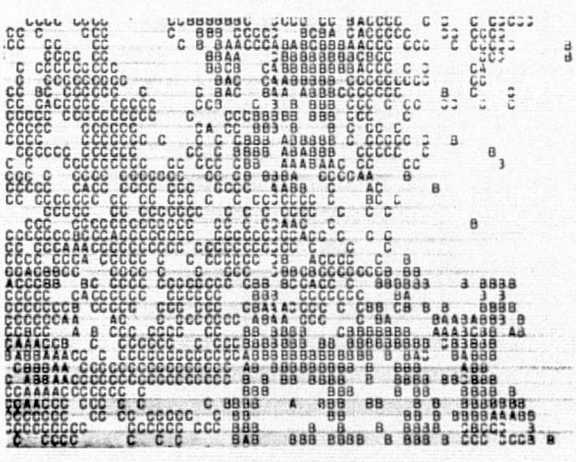

Fig. 7 PLOTLIN print-out.

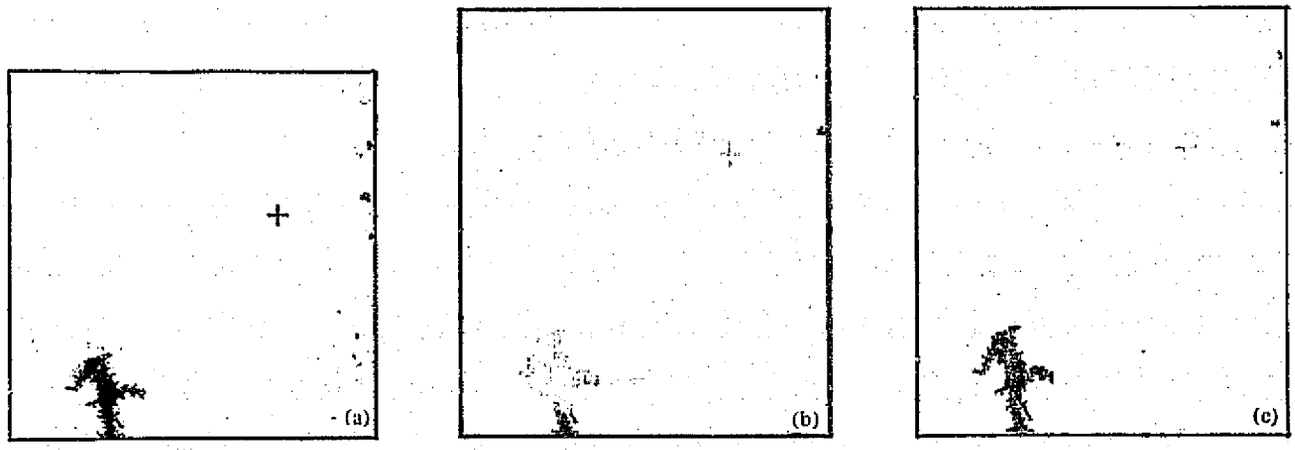

Fig. 8 (a) PLOTCAL print-out of a water body. (b) PLOTLIN print-out of water body using first approach (see text). (c) PLOTLIN print-out of water body using training-set approach.

put radiance characteristics of the object categories. Three approaches are commonly followed:

The *first* approach selects for each band a set of equal radiance intervals (or similar arbitrary choice) between minimum and maximum. These intervals are successively narrowed until the ground objects of interest are being recognised. This method has the disadvantages that it is inefficient from the point of view of computer time, and, since it does not take object statistics into account, is unlikely to achieve optimum discrimination. Fig. 8b illustrates a recognition map generated via this procedure for the recognition of a water body. A number of recognition errors occurred where shadows and a grid-cross were incorrectly identified as water.

In the *second* approach, actual radiance statistics are calculated from *in situ* ground spectral reflectance measurements on the objects of interest[5] and then used as input to PRODEC. This procedure is complicated by the intervening atmosphere between the ground objects and the ERTS sensors.

The *third* approach, conceptually the most exciting, utilises "training sets" to generate radiance statistics. According to this method, a number of geographical locations are selected where the ground objects of interest are known to exist. The coordinates are entered into a computer via program MANSTAT, and the radiance values in each spectral band of each resolution element in that geographical area is obtained. Providing that the area contains a sufficiently large number of resolution elements (and this is generally the case) reliable spectral radiance statistics can be generated. These statistics are used to select the input parameters for program PRODEC, which proceeds to seek further ground objects having these spectral characteristics. Thus ground truth information from a known area can be used to generate search requirements in different unknown geographical locations. An example of this training set approach is shown in Fig. 8c. Here 400 resolution elements covering the water body were used as training set, and the resultant statistics (see Figs. 4 and 5) were used to search the rest of the block for more water. On comparing Figs. 8b and 8c, it will be noted that many of the incorrect classifications have been eliminated.

Future prospects

We have explained how automatic pattern recognition techniques can be applied to ERTS CCT data, and have described a number of computer programs that have been established for this purpose. Simple examples of target recognition using the different techniques were presented.

Techniques such as these open new and challenging fields of study. Researchers throughout the world are investigating applications in diverse disciplines such as agriculture, hydrology, ecology and geology.

It has been speculated that the greatest short-term benefits from the ERTS project will be in the field of mineral exploration[6]. If this is so, then two applications of computerised CCT interpretation would be of particular interest.

The first involves the preparation of geological maps on which to base mineral exploration programmes. These would be particularly valuable in areas that are geologically unknown. Potentially at least, the computer could be instructed to classify rocks and soils over vast areas for which CCTs were available. The main anticipated advantage over photo-interpretation of ERTS photographic products in this application is that all 4 bands can be used simultaneously. Thus the probability of correct classification is, hopefully, increased.

The second application lies in the search for important small surface colorations (such as gossans) that sometimes reveal directly the presence of certain mineral deposits. It is anticipated that in this application the main advantage will be the superior resolution of CCTs over the photographic product. As in the first application, this search can be made, resolution element by resolution element, over vast areas, or even entire countries. The cost of using conventional exploration methods over such large areas would be prohibitive.

Complex technical problems need to be solved if such applications are to be successfully implemented. However, if these solutions exist and are found, a significant contribution to exploration techniques will have been made.

We wish to acknowledge the assistance of the Computer Division of the Johannesburg Consolidated Investment Company in preparing and running the programs.

[1] Colwell, R.N. (1966). Uses and limitations of multispectral remote sensing. *Proc. of the 4th Symp. Remote Sensing of the Environment.* (University of Michigan, Ann Arbor, Mich.).
[2] Nagy, G. (1968). State of the art in pattern recognition. *Proc. IEEE*, 56, 836-862.
[3] Lowe, J.S., Braithwaite, J., Larrowe, V.L., (1966). An investigative study of a spectrum-matching imagery system. Final report prepared under contract No. NAS 8-2111. (The Institute of Science and Technology, University of Michigan, Ann Arbor, Mich.).
[4] Laboratory for Agricultural RemoteSensing, Purdue University. Remote multispectral sensing in agriculture. Annual Report. *Res. Bull.* No. 844, Vol. 3 (September). Also: Remote multispectral sensing in Agruculture, I, 4.
[5] Longshaw, T. G. (1974). Field spectroscopy for multispectral remote sensing : an analytical approach. *Appl. Opt.* (In press).
[6] Carter, W. D. (1971). ERTS-A. A new apogee for mineral finding. *Mining Engineering*, 32, 51-53.
[7] *Earth Resources Technology Satellite Data Users Handbook*, (NASA, Goddard Space Flight Center, Greenbelt, Md.).

APPENDIX 'H'

AN AFFINE TRANSFORMATION TO RELATE ERTS-1 CCT PIXEL MATRICES TO THE SOUTH AFRICAN NATIONAL CO-ORDINATE SYSTEM

T.G. Longshaw

Spectral Africa (Pty) Limited
P.O. Box 2
Randfontein

ABSTRACT

In order to correlate ground truth with ERTS-1 MSS CCT data it is necessary to accurately relate map references in the South African National Co-ordinate System to MSS sample elements within the CCT pixel matrix. To accomplish this, an Affine Transformation may be used which takes the form of two polynomial equations of the same order which express the co-ordinates of one system in terms of the co-ordinates of the other. For relatively small areas, a linear transformation may be used to maintain a rms correlation accuracy of less than one pixel. To maintain the required location accuracy over a full frame, however, a second order transformation is required. For both transformations, control points need to be located by which the transformation co efficients can be evaluated. A computer program was written to carry out this evaluation and apply the transformation to search for data within the CCT matrix from ground location data expressed in the S.A. National Co-ordinate System. The results showed that the uncertainty involved in determining CCT pix . co-ordinates for control points limited the location accuracy of the linear transformation to 40 meters rms. The location accuracy of the second order transformation was 120 meters rms over the full frame. This accuracy was a substantial improvement on the 700 meters rms (NASA, 1972) available from NASA Bulk MSS image annotation.

INTRODUCTION

ERTS-1 MSS Computer Compatible Tapes (CCT's) present earth imagery in a form suitable for automatic interpretation techniques. These allow the user to take advantage of the resolution and radiometric qualities inherent in the CCT's which are superior to that of the NASA 70mm film product issued to investigators (Longshaw and Gilbertson, 1974). Of the automatic interpretation techniques that have been developed (Lars, 1970), spectral recognition programs have been used extensively for the recognition of objects by way of their spectral reflectance characteristics. An important aspect of the recognition of spectral features from the CCT data is accurate spatial correlation of digital picture elements (pixels) with ground truth. The accuracy with which a point on the ground can be located as its corresponding CCT pixel determines the minimum size of objects whose spectral characteristics can be studied via their appropriate CCT pixel values. This location accuracy is dependent on the degree to which sensor attitude and positional errors are corrected within the NDPF Processing Subsystems. For Bulk imagery, these errors are only partially corrected and positional mapping accuracy is of the order of 700 meters. This inaccuracy is expressed as a root mean square average deviation of a point on the ground from the calculated projected location of its imaged pixel. This location data is given as "tick marks" on the edge of NASA 70mm transparencies and included as supplementary data in the CCT's.

Location accuracy can be improved, however, by relating tonal features within an image to corresponding ground features. These features common to both the ground scene and its MSS image can be used as control points to set up transformation equations whereby pixels corresponding to specific ground points can be located within the CCT matrix. An Affine Transformation can be used to establish this mathematical correspondence (Peet et al, 1973) and its use in improving MSS image location accuracy effectively performs the functions of geometric image correction for systematic earth modelling errors and spacecraft positional uncertainty. Using this method, an rms location accuracy of 41 meters in the byte advance direction and 36 meters in the scan advance direction (Longshaw, 1974) was achieved for an area of the order of 500 km^2. For a Bulk MSS full frame (area greater than 34 000 km^2) an rms location accuracy of 138 meters in the byte advance direction and 111 meters in the scan advance direction was achieved. The frame number 1049-07301 covering the Johannesburg and Pretoria area was used in this study.

THE AFFINE TRANSFORMATION

The property of the Affine Transformation relevant to this application is that it relates a point on a surface as expressed by co-ordinates in one projection of that surface to co-ordinates in another projection of that surface. Expressing these co-ordinates as (x,y) and (u,v) respectively, the general affine transformation is of the form

$$x = f_1 (u,v)$$
$$y = f_2 (u,v) \qquad (1)$$

Where f_1 and f_2 are polynomials of the same order.

In the case of the linescan image recorded by the MSS, the Bulk product is corrected to a flat earth projection in the along-scan direction while retaining a linear projection in the scan advance direction. The Bulk MSS image could therefore be described as a pseudo-perspective projection. This can be concluded from

ORIGINAL PAGE IS
OF POOR QUALITY

the corrections applied to Bulk MSS imagery at NDPF as shown in figure 1 in which the familiar effects of panaramic linescan and earth rotation "skew" are shown

FIGURE 1 : MSS GEOMETRIC CORRECTIONS (SOURCE : NASA, 1972)

> "In South Africa, as in most other countries, the national maps are based on a conformal projection. A conformal projection is defined as one in which the scale of the projection is the same in all directions around any arbitrarily chosen point. From this, it may be proved that the projection has the angle-true property. The projection used in South Africa is the Gauss Conform Projection which is a conformal transformation from an ellipsoidal earth to the plane of the projection. The equator and an arbitrarily chosen meridian project as a pair of perpendicular straight lines. The remaining meridians are curved lines having their concave sides facing the central meridian while the remaining paralels are curves having their concave sides facing the geographical south pole. From the definition of this projection it is clear that meridians and parallels intersect orthogonally" (Lauf, 1974).

In this study, the first order (linear) and second order transformations were used for a small area correlation (the West Rand, Transvaal) and a full frame correlation (frame ID 1049-07301), respectively,

$$\left.\begin{aligned} x &= a_o + a_1 + a_2 v \\ y &= b_o + b_1 + b_2 v \end{aligned}\right\} \qquad (2)$$

and

$$\left.\begin{aligned} x &= a_o + a_1 u + a_2 v + a_3 u^2 + a_4 v^2 + a_5 uv \\ y &= b_o + b_1 u + b_2 v + b_3 u^2 + b_4 v^2 + b_5 uv \end{aligned}\right\} \qquad (3)$$

Where (u,v) are the S.A. National Co-ordinates in units of 10 000 feet and (x,y) are the transformed equivalent CCT pixel matrix co-ordinates. Where the x co-ordinate is the sample element in the byte advance direction and the y co-ordinate is the scan line number in the scan advance direction. The co-efficients a_n and b_n (n = 1,2,..5) thus relate (u,v) co-ordinates and (x,y) co-orainates. In order to use the transformations it is necessary to evaluate these co-efficients using a set of control points for which both their (u,v) and equivalent (x,y) co-ordinates are known.

ORIGINAL PAGE IS
OF POOR QUALITY

USING THE TRANSFORMATIONS

In choosing a set of control points to evaluate the co-efficients of equations (3) and (4), objects which produced high-contrast features in the MSS image were identified on 1:50 000 Topographical maps. As the NASA 70mm transparency did not display exactly the same features as were present on the CCT, a Digital-to-Analogue CCT image (Longshaw, 1974) was used to identify prominent high-contrast features represented in the CCT pixel matrix. The matrix co-ordinates (x,y) of the pixels corresponding to the boundary of these contrasting features were then noted from a computer printout of the appropriate area. The corresponding features were then identified on the topographic maps (assisted by aerial photographs) and their interpolated S.A. National Co-ordinates (u,v) were recorded. Using such features as road intersections, vertices of prominent mine dumps, and boundaries of urban communities, sets of control points were obtained. As high contrast boundaries were used in this analysis, the appropriate (x,y) co-ordinates were identified as boundaries between high and low pixel values. In this respect, the accuracy of the

method was limited by the fact that the (x,y) co-ordinates were integer. This sequence of identifying control points is illustrated in figure 2.

FIGURE 2 : DATA USED FOR IDENTIFYING CONTROL POINTS

ORIGINAL PAGE IS
OF POOR QUALITY

RESULTS

For the 500 km^2 area over the West Rand, the first order transformation (equation 2) was evaluated using fourteen control points to calculate a_n, b_n (n = 1,2,3) with (u,v) co-ordinates referred to the $27^{o}E$ meridian. This was done using a least squares method in which the deterministic expression (equation 4) was evaluated using a computer program Affine Transformation - 1st order (AFFTR1). An expression similar to (4) with b_n replacing a_n and y replacing x was evaluated for the b_n co-efficients.

$$\begin{vmatrix} a_0 \\ a_1 \\ a_2 \end{vmatrix} \quad \begin{vmatrix} N & \Sigma u_2 & \Sigma v \\ \Sigma u & \Sigma u & \Sigma uv \\ \Sigma v & \Sigma uv & \Sigma v^2 \end{vmatrix} = \begin{vmatrix} \Sigma x \\ \Sigma ux \\ \Sigma vx \end{vmatrix} \qquad (4)$$

From this calculation equation 2 became

$$\begin{aligned} x &= 13427.8 - 51.547.\ u + 13.1519\ v \\ y &= 34047.1 + 7.2798\ \ u + 37.7599\ v \end{aligned} \qquad (5)$$

To estimate the accuracy of the transformation, (x,y) control points were compared to (x,y) calculated points using equation (5). The differences or "residuals" are shown in figure 3. The rms of these residuals is shown in table 1.

FIGURE 3 : CONTROL POINT RESIDUAL HISTOGRAM - 1st ORDER (500 km^2 AREA)

The full frame correlation was performed in the same manner as described above. Control points were chosen which could be commonly identified on both 1:50 000 topographic maps and CCT pixel printout. These points were input to the computer program AFFTR1 which calculated the appropriate co efficients using equation (4). The residuals are shown in figure 4. The rms of these residuals is shown in table 1.

FIGURE 4 : CONTROL POINT RESIDUAL HISTOGRAM - 1st ORDER (FULL FRAME)

Using equation (3), a least squares approximation was calculated for the second order transformation with (u,v) co-ordinates referred to the $29^{o}E$ meridian. The appropriate deterministic expression (equation 6), was then evaluated using a computer program AFFine TRansformation 2nd order, (AFFTR2). From this evaluation, the co-efficients of equation (3) were calculated. An expression similar to (6) with b_n replacing a_n and y replacing x was evaluated for the b_n co-efficients.

$$\begin{vmatrix} a_0 \\ a_1 \\ a_2 \\ a_3 \\ a_4 \\ a_5 \end{vmatrix} \quad \begin{vmatrix} N & \Sigma u & \Sigma v & \Sigma u^2 & \Sigma v^2 & \Sigma uv \\ \Sigma u & \Sigma u^2 & \Sigma uv & \Sigma u^3 & \Sigma uv^2 & \Sigma u^2v \\ \Sigma v & \Sigma uv & \Sigma v^2 & \Sigma u^2v & \Sigma v^3 & \Sigma uv^2 \\ \Sigma u^2 & \Sigma u^3 & \Sigma u^2v & \Sigma u^4 & \Sigma u^2v^2 & \Sigma u^3v \\ \Sigma v^2 & \Sigma uv^2 & \Sigma v^3 & \Sigma u^2v^2 & \Sigma v^4 & \Sigma uv^3 \\ \Sigma uv & \Sigma u^2v & \Sigma uv^2 & \Sigma u^3v & \Sigma uv^3 & \Sigma u^2v^2 \end{vmatrix} = \begin{vmatrix} \Sigma x \\ \Sigma ux \\ \Sigma vx \\ \Sigma u^2x \\ \Sigma v^2x \\ \Sigma uvx \end{vmatrix} \qquad (6)$$

Using the calculated co efficients for the second order transformation measure of the accuracy of the second order transformation. These residuals are shown in figure 5 and their rms location accuracy shown in table 1.

FIGURE 5 : CONTROL POINT RESIDUALS HISTOGRAM - 2nd ORDER (FULL FRAME)

Two subroutines were then written to use the transformation equations for retrieving appropriate pixels from the CCT's for objects whose outline could be identified by S.A. National Co-ordinates.

TABLE 1

	Root-mean-square location accuracy calculated from transformation residuals	
	Byte advance direction (x) in meters	Scan advance direction (y) in meters
West Rand 500 km^2 area	41	36
Full frame 1049-07301 1st Order Transformation	185	172
Full frame 1049-07301 2nd Order Transformation	138	111
Location accuracy of CCT Bulk images from NASA	700	700
Bulk Processing Subsystem (NASA, 1972)		

SUMMARY

The accuracy of the image-annotated location data and geometric corrections for Bulk MSS imagery limits the minimum size of objects that can be analysed by spectral recognition techniques. This location data has an accuracy of 700 meters rms. A method has been described in which affine transformations was applied to improve CCT image location accuracy to the order of 40 meters rms for small areas (500 km^2) and 120 meters rms for the full frame 1049-07301 (area >25 000 km^2). In a 500 km^2 area covering the West Rand of the Witwatersrand, accuracy was limited by the integer values of the control points (x,y) co-ordinates. This limitation was also present in the full frame transformation. The second order transformation was seen to improve the location accuracy for the full frame beyond that attainable using the first order transformation. The rms location accuracies of the transformations are shown in table 1. A computer subroutine was subsequently written to use the transformations to access appropriate pixels for application programs.

REFERENCES

Laboratory for Agricultural Remote Sensing, Purdue University,
West Lafayette (1970)
"Remote Multispectral Sensing in Agriculture"
Annual Report, Vol. 4, pp. 11-41.

Lauf, G.B.,
Private Communication (1974).

Longshaw, T.G. and B. Dilbertson
"Computerized Interpretation of ERTS-1 Data in South Africa"
S.A. Journal of Science, 70, (1974).

Longshaw, T.G.
"Photographic Imaging of ERTS-1 Data for High Resolution Display"
This symposium.

NASA, Data Users Handbook ERTS-1, 1972.

Peet, F.G; Mack, A.R and L.S. Crosson
"Affine Transformations from Aerial Photos to Computer Compatible Tapes"
Third ERTS Symposium 1973.
NASA/Goddard Space Flight Centre, Greenbelt, Maryland.

ACKNOWLEDGEMENTS

The author wishes to thank Prof. G.B. Lauf of the Department of Land Survey, University of the Witwatersrand, for his advice regarding earth modelling projections and Mrs. J. Trollip of Spectral Africa for invaluable computational assistance.